UM-HSRI-PF-74-1-2

COPY NO._____

INFLUENCE OF COMBINED HIGHWAY GRADE
AND HORIZONTAL ALIGNMENT
ON SKIDDING

FINAL REPORT

VOLUME 2 OF 2

PREPARED FOR

TRANSPORTATION RESEARCH BOARD
NATIONAL COOPERATIVE HIGHWAY RESEARCH PROGRAM
NATIONAL ACADEMY OF SCIENCES

BY

DUANE F. DUNLAP
PAUL S. FANCHER
ROBERT E. SCOTT
CHARLES C. MACADAM
LEONARD SEGEL

SEPTEMBER 1974

TABLE OF CONTENTS

PART II - APPENDICES

APPENDIX A

ACCIDENT DATA ANALYSIS

A.1 DATA

A.1.1 EXPOSURE AND GEOMETRIC DATA. Exposure and geometric information was obtained from both the Ohio and Pennsylvania Turnpike Commissions. A description of this data is necessary for an understanding of the analysis task.

The exposure information is in the form of screen counts between interchanges by toll class. From this data it was possible to compute the number of vehicles which crossed each one-tenth mile segment of the highway during the period represented by the accident data.

The Ohio Turnpike consists of two pavements which are each two-lane, 24 feet wide, separated by a median, with 80 feet between the centerline of each pavement. The inside and outside shoulders are each 10 feet wide.

The cross-section of each pavement is triangular on the tangents, with a crown of 3/16 inch per foot. On curves, the crown is removed and the cross-section is then a straight line.

The superelevation on curves is given below as a function of the degree of curve.

SUPERELEVATION ON OHIO TURNPIKE

Degree of Curve	Superelevation in in./ft.
0-1°14'	3/16
1°15'-1°29'	5/16
1°30'-1°44'	7/16
1°45'-1°59'	9/16
2°00'-2°14'	3/4
2°15'-2°30'	1 (max. superelevation)

The superelevation is accomplished by rotating each pavement about the median edge. Thus the two inside edges always remain the same elevation. Spiral transitions are used on curves of 1° or more.

Although the length of the spiral transitions is available, the analysis has been based on the value of the degree of curvature of the simple curve, and this value has been assumed for all points on a curve, including the transitions. This was done for convenience but does not introduce a serious problem. The length of the transitions is typically from 200 to 400 feet, while the resolution on accident location is one-tenth mile or 528 feet. Thus the resolution is not sufficient to locate an accident within a transition as opposed to the simple curve.

The Pennsylvania Turnpike has two lanes, each 12 feet wide in each direction. Thus, the eastbound and westbound traffic-ways are each 24 feet wide. The transverse profile of each traffic-way is a straight line; i.e., there is no crown. Instead, there is some superelevation of the inside edge, even on tangents. The two inside edges (adjacent to the median) are at the same elevation. When a curve is encountered, the outside edge of the traffic-way on the inside of the curve is lowered to achieve superelevation, and the outside edge of the traffic-way on the outside of the curve is raised.

The superelevation for each traffic-way as a function of the degree of curve is given in the following list.

SUPERELEVATION ON THE PENNSYLVANIA TURNPIKE

Degree of Curve (cord definition)	Superelevation in in./ft.
0 (Tangents) to 1°15'	1/6
1°30'	1/4
1°45'	5/16
2°	3/8
2°15'	7/16
2°30'	9/16
2°45'	11/16
3°	3/4
3°15'	13/16

SUPERELEVATION ON THE PENNSYLVANIA TURNPIKE (Cont.)

Degree of Curve (cord definition)	Superelevation in in./ft.
3°30'	7/8
3°45'	15/16
4°00' to 5°30'	1
6°	1 (upgrade) 1 3/16 (downgrade)*

Horizontal alignment data was obtained for each turn-pike, giving the degree and direction of curvature at each one-tenth mile of the highways. Vertical alignment was similarly obtained, giving the grade to the nearest 0.1%.**

A "highway file" was generated for each turnpike, including exposure, superelevation, and horizontal and vertical alignment data for each one-tenth mile. The curvature is given in arc minutes (using the arc definition of curvature), and grade is given in tenths of a percent. These files allow computation of exposure (vehicle-miles) for varying combinations of grade and curvature.

---

*For curves of 6°, a superelevation of 1 3/16 in/ft was used in the analysis regardless of grade.

**The range of grades on the highways are -3.0% to + 2.0% in Ohio and -3.5% to + 3.5% in Pennsylvania. The maximum curvatures are 2°30' in Ohio and 6° in Pennsylvania.

A.1.2 ACCIDENT DATA. The accident data used in
the accident data analysis task consists of information
taken from police reports of accidents on the Ohio and
Pennsylvania Turnpikes. The data was obtained in digitally
coded form and an accident file was created on magnetic
tape for each turnpike in the format of the Statistical
Research System of HSRI. The Ohio file contains 6,189
accidents which occurred from January 1966 through
June 1970—four and one-half years.

The Pennsylvania file contains 11,492 accidents that
occurred between June 1967 and June 1969, inclusive—two
and one-half years—on both the main route and the North-
east Extension. Several accidents in these files occurred
in toll plazas, service areas, etc., and do not represent
the class of accidents pertinent to this study. Only
accidents on the main line were included. The numbers of
accidents used in the study are 5,553 in Ohio and 9,822 in
Pennsylvania. The highway curvature, superelevation, and
grade from the "highway file" were merged with the accident
file so that each accident record also contained the
alignment data at each accident site.

With files of accident and exposure data, both con-
taining geometric information, it is possible to compute
either accident frequency or accident rate (accidents/
vehicle mile) for combinations of horizontal and vertical

125

alignment. Much of the analysis to be described in this appendix is based on accident experience by grade and curvature, using six or seven levels (intervals) of grade and eight levels of curvature. These levels constitute matrices of 48 and 56 possible cells. The matrices of vehicle miles over the period of accident data are given in Tables* A-1 and A-2. The corresponding matrices of the number of accidents are given in Tables A-3 and A-4.

The accident rates for the two highways over the respective data collection periods in accidents per 100 million vehicle miles are 95.9 in Ohio and 148.1 in Pennsylvania. The higher rate in Pennsylvania has not yet been explained, except possibly by the older design and narrow median. It is interesting to note in this regard that the average traffic is nearly equal on both. The average number of vehicle miles per mile of length per day (or average ADT) is 15,496 vehicles per day in Ohio and 14,621 in Pennsylvania.

---

*All tables pertinent to this appendix are included at the end of this appendix.

A.2 REGRESSION MODEL

The numbers of accidents by each condition of horizontal and vertical alignment shown in Tables A-3 and A-4 vary greatly. Most of the variation is explained simply by the similarly great variation in exposure or the vehicle miles traveled at each geometric condition. The strong dependence of accidents on exposure is shown by a linear regression of the number of accidents against vehicle miles. The regression equation for each turnpike is:

Ohio
$$Y_a = 18.3 + 0.00820V_m$$
$$\rho^2 = 0.987 \quad n = 44$$
(A.1)

Pennsylvania
$$Y_a = 48.2 + 0.01110V_m$$
$$\rho^2 = 0.919 \quad n = 51$$
(A.2)

where Y_a is the number of accidents, V_m is vehicle miles x 10^{-4}, and n is the number of data cells. The slope of Y_a is the mean accident rate for each turnpike in accidents per 10^4 vehicle miles. The proportion of the variation from cell to cell explained by the regression is given by the square of the correlation ρ. Thus exposure explains 99% of the variation in Ohio and 92% of the variation in Pennsylvania.

127

Both the constant and slope of the regression for Pennsylvania are higher than for Ohio. This is consistent with the observation that the Pennsylvania Turnpike has a generally higher accident rate.

Since much of the variability is explained by exposure, the unexplained variation, including effects of alignment, can best be studied by examining accident rate. A generalized dummy variable multiple regression model approach was used. The model is of the form

$$Y_a = F(\vec{X}_1, \vec{X}_2) \pm \varepsilon \qquad (A.3)$$

Y_a = accident rate observed in highway sections defined by a specific grade and curvature in accidents per 10^4 vehicle miles

$\vec{X}_1$ = vector defining highway grade for discrete intervals

$\vec{X}_2$ = vector defining highway curvature for discrete intervals

ε = error

The error ε is variability in crash rate that is not explained by the model for independent effects of grade and curvature. The errors may arise from any source not

represented in the model, including interaction of grade and curvature or factors not related to highway geometry. The regression model is fitted with the objective of minimizing the sum of squares of this residual variability and assures that the mean ε across all cells is zero.

The alignment vectors are expressed as a set of dummy (0 or 1) variables which allow an analysis of variance to be performed over discrete levels by using least squares multiple regression. Specifically, the variables used for Ohio are:

OHIO

DUMMY VARIABLE SPECIFICATION

	Grade (%)	X_{11}	X_{12}	X_{13}	X_{14}	X_{15}
1.	-3.5 to -2.5	1	0	0	0	0
2.	-2.4 to -1.5	0	1	0	0	0
3.	-1.4 to -0.7	0	0	1	0	0
4.	-0.6 to +0.6	0	0	0	0	0
5.	+0.7 to +1.4	0	0	0	1	0
6.	+1.5 to +2.4	0	0	0	0	1

Curvature		X_{21}	X_{22}	X_{23}	X_{24}	X_{25}	X_{26}	X_{27}
1.	0°0'	0	0	0	0	0	0	0
2.	0°1' - 0°21'	1	0	0	0	0	0	0
3.	0°22' - 0°43'	0	1	0	0	0	0	0
4.	0°44' - 1°5'	0	0	1	0	0	0	0
5.	1°6' - 1°27'	0	0	0	1	0	0	0
6.	1°28' - 1°49'	0	0	0	0	1	0	0
7.	1°50' - 2°11'	0	0	0	0	0	1	0
8.	2°12' - 2°33'	0	0	0	0	0	0	1

All five grade variables are zero for cases in the grade interval of 0 ± 0.6%. Thus the interval representing level road becomes the "reference" interval. Similarly, curvatures of 0°0' (straight road) become the "reference" curvature interval.

The multiple regression analysis was performed using the Michigan Interactive Data Analysis System (MIDAS). A summary of the output of the regression is shown in Table A-5 for the Ohio Turnpike and Table A-6 for the Pennsylvania Turnpike, using eight levels of curvature for both. The model fitted to the Ohio data explains 65% of the variability in accident rate. Similarly, the Pennsylvania model explains 60% of the variability.

The regression model provides an expected value for each cell of curvature by grade. The model for expected value is

$$\hat{Y}_{ij} = \mu + \Delta G_i + \Delta D_j \qquad\qquad (A.4)$$

where

$\hat{Y}_{ij}$ = the expected accident rate for the cell defined by grade G_i (i=1,...7) and curvature D_j (j=1,...8)

μ = common contribution to accident rate for all cells

ΔG_i = incremental contribution to accident rate that is common to all cells with grade G_i

ΔD_j = incremental contribution to accident rate that is common to all cells with curvature D_j.

Thus each cell is composed of additive components that depend on grade and curvature. The model used assumes that the difference between expected and observed (actual) rates (ε) is a random variable whose mean over all cells is zero and whose variance is the same over all cells.

The results of the regression indicate substantial variation in the contribution of grade and curvature to accident rate as is indicated by the variation in ΔG_i and ΔD_j for both turnpikes. However, not all contributions

are statistically significant at the 5% confidence level.*
In the Ohio data, only the higher accident rates on down-
grades of -2.5 to -3.5% and on curves of from 0°44' to
1°5' are statistically significant. The effects of
curvature in Pennsylvania were only significant at curves
over 1°50'; none of the grade intervals was statistically
significant in Pennsylvania.

The differences between the observed (actual) rates
and the expected rates are also the residuals, or

$$Observed - Expected = Residual$$

Tables A-26 and A-29 give the observed rates, the expected
rates based on the multiple regression, and the residuals
for each cell defined by grade and curvature on the two
turnpikes. Also shown in the tables are the 95%
confidence intervals for the expected rates.

Since random error from causal factors unrelated to
geometry will produce residual differences, only those
cells with residuals with absolute values greater than
the confidence intervals indicate noteworthy failure of

_____

*Statistical significance at the 5% confidence level means
 that the probability that an observed variation could
 have occurred by chance from random error rather than
 from a true variation is 0.05.

the regression model to explain the observed rates. Five
cells for the Ohio Turnpike are outside the 95% confidence
interval. These are indicated by asterisks and are found
on -2.5% to -3.5% downgrades and on curves of 0°44' to
1°5'. Only one, however, is problematical, i.e., with
an observed rate greater than the expected rate. Table
A-29 indicates seven cells with observed rates outside the
confidence intervals, all at curvatures greater than 3°23'.
Only three are problematical and only one (-2.5 to -3.5%
grade and 3°23' to 4°12' curvature) includes a substantial
number of accidents.

The effects of grade and curvature on the expected
accident rate is shown more conveniently in Figures A-1
through A-4.* Figures A-1 and A-3 show the effects of
curvature. The data plotted in these figures are for level
highway (grades of 0 ± 0.6%). The plots of expected rates
for other grade intervals would be identical in shape but
displaced vertically. Figures A-2 and A-4 give the
expected rates by grade for tangents (D = 0°0').
Similarly, the plots for other curvatures would be simple
vertical displacements of the curve shown.

---

*The figures for this appendix are given after the end of
  the text and before the tables.

The figures for Pennsylvania indicate a gradually increasing accident rate with increasing curvature, with no significant dependence on grade. Contrastingly, the Ohio data show high peaks at grades of -2.5 to -3.5% and curves of 0°44' to 1°5', with no significant effects of other grades or curvatures.

Since the Pennsylvania Turnpike has much sharper curves than encountered in Ohio, the intervals used for the eight levels of curvature are much wider in the Pennsylvania analysis. This makes direct comparison between the two difficult. All curvatures found in Ohio are contained in the first four levels in Pennsylvania. The high peak at curves of about 1° in Ohio could be masked by the much wider interval including such curves in Pennsylvania.

The regression was repeated for Pennsylvania using eleven levels of curvature, the first eight of which are identical to those used for the Ohio data. The results of the regression are given in Tables A-11 and A-32 and Figures A-5 and A-6. Except for the two high peaks in Ohio, the plots reflect the generally higher accident rates in Pennsylvania. Using eleven levels of curvature in Pennsylvania rather than eight raises the proportion of explained variation from 60% to 67% and reduces the standard error of the regression.

The expected rate in Pennsylvania appears to have two steps with curvature in the eleven-level model rather than a gradual increase as in the eight-level model. The first step occurs at curvatures of from 1°6' to 1°27', and the second at the highest curvatures of 4°13' to 6°. There is not a peak at 0°44'-1°5', however, as in Ohio. Furthermore, the first step occurs at curvatures for which no dependence with curvature is evident in Ohio. The eleven-curvature model shows no significant dependence on grade.

A.3 SINGLE-VEHICLE AND WET-PAVEMENT ACCIDENTS

The above discussion of the regression model relates to all accidents on the mainline of the two turnpikes. The regression was repeated for single-vehicle accidents and for accidents on wet pavement.

These two subgroups were examined for two reasons. Firstly, wet-pavement and single-vehicle accidents could be expected to be common under conditions conducive to skidding. Secondly, the high peaks in the Ohio data at downgrades and at 1° curves were found to have relatively high proportions of such accidents.

Exposure data was not available for wet-pavement conditions. That is, we do not know what fraction of the mileage is accumulated on wet highway. Thus, computation of accident rates for wet roads was not possible. However,

it seems reasonable to assume that local differences in climatology are minor on both turnpikes, and therefore that the proportion of travel on wet pavement is independent of grade and curvature. Based on this assumption an accident rate was computed for wet-surface conditions by dividing the number of such accidents by the total vehicle miles traveled under all conditions.

The results of the regression for wet pavement are given in Tables A-7, A-10, and A-13, while the tables of observed, expected, residual rates, and 95% confidence intervals are given in Tables A-28, A-31, and A-34. Plots of the expected rates for wet road are indicated by "w" in Figures A-1 through A-6.

The absolute height of the curves for wet-surface conditions has no meaning other than representing the relative proportion of accidents that were on wet road. The shape of the curves, i.e., changes in the height of the wet curve relative to the total, does indicate the influence of wet pavement on the propensity for accidents on grades or curves.

The regression tables indicate a significant contribution to wet pavement accidents at the same levels of grade and curvature that were significant for all accidents. Furthermore, the "wet" accidents represent a higher proportion of the total on the steeper downgrades and 1°

curves on the Ohio Turnpike. This indicates that a wet surface may be an important contributing factor to accidents at these geometries. A similar phenomena is not observed in the Pennsylvania data.

Treatment of single-vehicle accidents does not involve a similar exposure problem. These accidents, which are often "loss-of-control" events, can occur under all travel conditions. Thus the total vehicle miles in each level of grade and curvature is appropriate for computing single-vehicle accident rates. Although the absolute height of the single-vehicle accident curves (s) in Figures A-1 through A-6 have meaning, the interpretation of the curves is identical to that for the wet-pavement curves. The results are similar to those for wet pavement, with a high incidence at 1° curves and downgrades in Ohio, but less striking.

A.4 SUPERELEVATION AND SIDE FORCE FACTOR

The Pennsylvania Turnpike has a higher overall accident rate than the Ohio Turnpike (148 and 96 accidents per 100 million vehicle miles, respectively). More relevant to the objectives of this study, the regressions against curvature indicate that the effects of curvature on accident rate are quite different for the two highways.

The superelevation rates are quite different on the two highways, and thus the apparent effects of curvature might be dependent on superelevation policy. To investigate this possibility, the regression model was repeated for two independent variables other than curvature. One was simply superelevation. The second was a derived "side force factor" model incorporating both superelevation and curvature.

The results of the models using superelevation (in inches/foot) are given in Tables A-14 through A-19 and A-35 through A-40, and Figures A-7 through A-14. The superelevation model is less satisfactory and less revealing than the curvature models. The explained variability is only 32% in Ohio and 35% in Pennsylvania—approximately half that of the curvature models. Thus superelevation alone does not explain the variation with geometry as well as curvature.

The high peak in Ohio is not apparent with superelevation, probably because other curvatures have the same superelevation and dilute the effect. None of the incremental contributions of grade or superelevation are statistically significant in the Ohio data.

The expected accident rate increases nonuniformly with superelevation in Pennsylvania, but is only

statistically significant at superelevations of 7/8
in/ft and 1 in/ft.

Superelevation alone does not satisfactorily explain
the variability in accident rate on either highway, nor
the differences between them. Since superelevation is
uniquely determined by curvature on each highway, the use
of superelevation as the independent variable of regression
is equivalent to rebracketing curvature. Similar results
would be obtained on each highway using the curvature model
if curvature intervals were redefined such that each
interval contained curves of one superelevation rate. The
lower correlations achieved with the superelevation model
suggest, however, that such a bracketing of curvature
would be less satisfactory than the intervals that were
used here.

Skidding or loss of control on a curve will occur
only when the equivalent side force factor* demanded by
a turn or maneuver exceeds the capabilities of the tire-
highway interface. The side force factor, f, (which will
be referred to simply as side force) is given by ($\underline{2}$, $\underline{3}$):

$$f = \frac{V^2}{15R} - e \qquad\qquad (A.5)$$

---

*The equivalent side force is the imbalance between centri-
fugal force and the horizontal component of force provided
by superelevation.

where

e = superelevation rate in feet/foot

V = vehicle speed in mph

R = radius of curve in feet

Superelevation rates (e) and curvature (D) are given in sixteenths of an inch per foot and arc minutes, respectively, in the data used for this study.* The above equation then reduces to

$$f = \frac{DV^2}{85944} - \frac{e}{192} \tag{A.6}$$

where

e = superelevation rate in sixteenths of an inch per foot

V = vehicle speed in mph

D = curvature in arc minutes

---

*The curvatures for the turnpikes are based on the arc definition of curvature, but the difference between the arc and cord definitions are trivial for the curvatures encountered on the turnpikes.

Side force was computed from curvature and super-elevation for each accident location and added to the file of accidents. It was similarly computed for each tenth mile of the highway, thus allowing derivation of exposure by side force.

The actual traveling speed before the collision would be appropriate for the side force computation. The speed given with accident data is subjective and not reliable. Furthermore, speed is not associated with the exposure data. Therefore, side force was computed for the posted speed limits. These speeds provide reasonable representation of the traffic on both limited-access highways. The speeds used in the side force computations are:

Ohio: V = 70 mph

Pennsylvania: 55 mph at milepost 47.6-48.4,

                    245.4-247, 333.1-334.8

                    65 mph elsewhere

A matrix of accidents per vehicle mile ($X10^4$) was generated for each cell of side force (f) and grade, using eight levels of f. The side force level intervals in the multiple regressions are:

Side Force Factor

Level	Ohio	Pennsylvania
1 (tangents)	-0.15625	0.0138
2	-0.00517 to 0.00338	0.00979 to 0.0107
3	0.00813 to 0.0129	0.0148 to 0.0230
4	0.0176 to 0.0224	0.0304 to 0.0361
5	0.0271 to 0.0319	0.0418 to 0.0476
6	0.04139	0.0600 to 0.0780
7	0.0491 to 0.0509	0.08498
8	0.0515 to 0.0592	0.0921 to 0.196

Side force factors not included in the above intervals were not encountered on the highways.

The results of dummy variable multiple regressions of accident rate (in accidents/10^4 vehicle mi.) are given in Tables A-20 through A-25. The side force model explains about 68% of the cell-to-cell variability on the Ohio Turnpike and about 74% on the Pennsylvania, and is superior in this regard to the curvature models. The standard errors of regression are also correspondingly smaller. Tabulations of observed and expected rates, residuals, and confidence intervals are given in Tables A-41 through A-46. Plots of the expected rates with curvature and with grade are given in Figures A-11 through A-14. The results strongly resemble the results using the curvature. A high peak occurs in both the grade and

side force curves and tables for Ohio. The peak with
side force is at f = 0.04139, which occurs on 1° curves
and is thus the same peak observed in the curvature model.
The Pennsylvania data does not indicate a dependence on
grade, but does have an increasing accident rate with
increasing f.

A.5   GENERAL DISCUSSION OF REGRESSION MODEL RESULTS

The regression models are additive models. Expected
rates at particular combinations of grade and curvature
(or side force, etc.) are the sum of the contributions of
grade and curvature. Differences between expected rates
and observed rates are failures of the additive model to
precisely "predict" accident experience because of random
"error" in the data. The term "error" is used in the
general sense here to include any effects not examined by
the model. These include factors other than highway
geometry that might contribute to accident causation and
incidence, such as mechanical defects, driver factors,
weather, etc. Additionally, geometric influences that
cannot be represented by an additive model contribute to
the error. These would consist primarily of cross-product
terms or interaction effects.

The 95% confidence intervals—about the expected
rates—define a range within which the observed rates can
be expected to fall with a probability of 0.95. Thus,

observed rates outside the interval are normally inter-
preted as "real" failures of the model, rather than "by
chance" consequences of random error.

Interaction between grade and curvature could also
result in residuals of absolute value greater than the
confidence interval, and could result in observed values
either greater or lower than the expected results. Such
an effect could be expected to be manifest by a pattern,
with increasing effects at higher curvatures and steeper
grades. Only effects which contribute to increased acci-
dent rates are problematical. Any interaction which tends
to reduce accident experience is desirable.

The points discussed above assist in interpretation
of the results of the regression models. The regressions
against grade and curvature on the Ohio Turnpike are
presented in Tables A-5 to A-7 and A-26 to A-28 and in
Figures A-1, A-2. Considering all accidents, the regres-
sions indicate that only grades of 0°44'-1°5' have
incremental contributions to expected accident rate that
are statistically significant (Table A-5). The effects
are very marked at these points, but have little depen-
dence on other grades and curvatures (Figures A-1, A-2).
The offending grade and curvature have one common cell in
which the additive effects result in a very high expected
accident rate. The cell is striking since the observed

accident rate is 665 accidents/10^8 vehicle miles, nearly seven times the average for the highway and nearly 2.5 times as great as the next highest cell.

Five cells of the matrix have observed rates which are outside the confidence interval. We cannot conclude, however, that all five are not the result of chance. With a probability of 0.05, the residuals could be outside the confidence intervals of individual cells because of random error. Since there are 44 cells in the Ohio curvature model, 5% or 2.2 could be expected to fall outside the confidence interval by "chance" alone. The number out- side the confidence interval has a binomial distribution, and the probability of finding 5 out of 44 such cases is 0.07. This is a low probability, so we may conclude that the residuals in some of the five cells represent real differences. However, we cannot identify which.

The cell of curvatures of about 1° at steep down- grades is the only cell with residuals greater than the confidence interval and represents the only evidence of problematical geometry. There are 34 accidents in this cell, and all occurred in the westbound lanes at mileposts 166.4-166.6.

Accidents on wet pavement and single-vehicle accidents have a high incidence in the high-accident-rate curvature and grade, as indicated in Figures A-1 and A-2. They are

both over-represented in the high-rate cell where wet-pavement involvements constitute 74% of all involvements, compared with 25% for the entire highway, and 79% for single-vehicle accidents, compared with 67% overall. The regression coefficients are also statistically significant for both types of accidents in both geometry categories.

The results in Pennsylvania are quite different. Grade has no statistically significant contribution. Accident rate increases with increased curvature and all incremental terms for curvatures above 1°50' are significant. Wet-pavement accidents follow a similar pattern without the over-involvement seen in Ohio. However, one modest curvature (0°44'-1°49') does have a significant over-representation of "wet" accidents. In general, the Pennsylvania data have a higher accident rate than Ohio at all curvatures and grades except for the notably high cell in Ohio.

The Pennsylvania regression with eleven levels of curvature permits a more direct comparison between the two highways. This regression, Tables A-11 to 13 and A-32 to 34 and Figures A-5 and 6, indicates a step in rate at curvatures of 1°6' and a second step at 4°13'. Neither wet pavement nor single-vehicle accidents appear to be consistently over-represented at these curvatures.

The superelevation models explain only 32-35% of the variability in accident rate and are not, in general, successful models. The general increase with super-elevation in Pennsylvania is consistent with the curvature model, but the results in Ohio mask the high accident experience at 1° curves.

The side force factor models have the highest R^2 and thus explain the greatest proportion of variability of the three models: 68% in Ohio and 74% in Pennsylvania. They reinforce the observation from the curvature models, but still fail to illuminate the differences between the two highways. The single peaks in Ohio occur at f = 0.0414, which is equivalent to a 1° curve, and at downgrades of 2.5-3.5%. Both peaks arise from the same highway segment noted in the curvature model. The Pennsylvania f data indicate the generally increasing rate, with increasing f equivalent to increasing curvature. Comparisons between highways at similar side force values show that Pennsylvania has consistently higher accident rates at all values, and does not have a spike at 0.04 as does Ohio. Ohio does not show the higher rates at f values of 0.05 and 0.06 as does Pennsylvania.

All of the regressions resulted in a greater number of cells with observed rates outside the 95% confidence interval than could be expected from random error, i.e., error not correlated with grade or curvature. However,

there are no patterns indicating that substantive interactive effects are present.

A.6 CRITIQUE OF AN ALTERNATIVE ANALYTIC TECHNIQUE

The regression technique employed to obtain expected accident rates uses the data for all geometric combinations to compute the expected rates. Specifically, the expected rates for tangent sections are based on accident experience on curves as well as on tangent sections, and the estimated rate on level sections includes use of data on grades.

Readers not familiar with regression techniques or methods of estimation may wonder why estimates of the effect of grade alone should include use of data confounded by the effects of curvature. Indeed, we might be inclined to base such an estimate only on data from tangent sections. An alternate technique using such an approach was investigated.

Specifically, this technique assumes that the observed crash rates (i.e., crashes/mile) at either zero grade or zero curvature do not have an error component. A further assumption is that the crash rate differences between cells defined by different grade levels for those cells with zero curvature are the actual incremental effects on crash-rate differences between grade level.

Similarly, crash-rate differences between cells defined
by different curvature levels for those cells with zero
grade are the actual incremental effects on crash rate
of differences between curvature levels.

That is, a prediction model of the following form
is proposed:

$$\hat{C}_{ij} = \mu + \delta G_i + \delta D_j \qquad (A.7)$$

where

$\hat{C}_{ij}$ = predicted crash rate for the cell defined
by the ith grade level and the jth
curvature level.

μ = the observed crash rate, C_{iojo}, under
the conditions in which the ith grade
level defined as io implies a zero grade
and the jth curvature level defined as
jo implies a zero curvature.

δG_i = the difference between the observed crash
rate, C_{ijo} and μ. This is the difference
between the observed crash rate for grade
i when curvature is zero and the observed
crash rate when both grade and curvature
are zero.

δD_j = the difference between the observed crash rate and μ. This is the difference between the crash rate for curvature j when grade is zero and the observed crash rate when both grade and curvature are zero.

This method was applied to the data from the Pennsylvania Turnpike shown with eleven levels of curvature. For this data the values of δG_i were determined as follows:

j	Grade	C_{ijo}	μ	δG_i
1	(-4.0% to -2.5%)	0.0160	0.0111	+0.0049
2	(-2.4% to -1.5%)	0.0119	0.0111	+0.0008
3˙	(-1.5% to -0.7%)	0.0107	0.0111	-0.0004
4	(-0.6% to +0.6%)	0.0111	0.0111	0.0000
5	(+0.7% to +1.5%)	0.0101	0.0111	-0.0010
6	(+1.5% to 2.4%)	0.0112	0.0111	+0.0001
7	(+2.5% to 3.5%)	0.0165	0.0111	+0.0054

Similarly, the values of δD_j were determined as follows:

i	Curvature	C_{ioj}	μ	δD_j
1	(0°0')	0.0111	0.0111	0.0
2	(0°1' - 0°21')	0.0054	0.0111	-0.0057
3	(0°22' - 0°43')	0.0076	0.0111	-0.0035
4	(0°44' - 1°5')	0.0138	0.0111	+0.0027
5	(1°6' - 1°27')	0.0280	0.0111	+0.0169
6	(1°28' - 1°49')	0.0223	0.0111	+0.0112
7	(1°50' - 2°11')	0.0247	0.0111	+0.0136
8	(2°12' - 2°33')	0.0217	0.0111	+0.0106
9	(2°34' - 3°22')	0.0216	0.0111	+0.0105
10	(3°23' - 4°12')	0.0143	0.0111	+0.0032
11	(4°13' - 6°00')	0.0648	0.0111	+0.0537

These values of μ, δG_i and δD_j were then used to compute predicted crash rates, C_{ij}. These predicted crash rates and the difference between observed and predicted crash rates are also shown in Table A-47 for each grade and curvature cell defined by i, j.

The differences between observed and predicted crash rates were then used to rank the individual cells from largest to smallest difference. Those cells having the largest difference were then suggested as candidates for further investigation. The assumption was that there may be an interaction effect between grade and curvature in those cells which leads to the larger than expected

crash rates—given the contributions from grade and curvature. This is analogous to the excess crash cell identification procedure used with the residuals from the dummy variable multiple regression model.

The ranking of the cells from largest difference to smallest difference is presented in Table A-48. Also included for reference is the ranking that resulted from the use of the residuals from the dummy variable multiple regression model. Visual comparison of the two rankings indicates considerable disagreement between the two procedures. The cell with the highest rank—Grade 1 and Curvature 10—using the difference method was ranked fifth highest, using the regression model residual method. More importantly, the cell with the largest regression model residual—Grade 4 and Curvature 11—was ranked in the range 24 to 40 by the difference method, merely because Grade 4 is a level road.

Spearman's rank correlation coefficient, r_s, was computed to estimate the degree of relationship between the two rankings. Using the computed value, $r_s = 0.58$, the null hypothesis that no relationship exists between the two ranks is rejected with an $\alpha = 0.01$ probability of a Type-I error. Thus there is some relationship between the rankings. However, as indicated, the conclusions of the analysis would have been quite different if the

difference method had been used to identify grade by curvature cells which have larger than expected crash rates.

The difference method also has some more fundamental shortcomings. The average of the differences is -0.2305, indicating that they are not symmetric about zero. By definition, the regression model residuals are symmetric about zero. However, there is no reason why the differences should sum to zero, since there are unexplained variations in all of the observed crash rates. The difference method ignores these unexplained variations and hence leads to results that are not consistent with the multiple regression model residual approach.

The standard error of the estimate using this technique is 0.0120. The standard error of the regression model is only .006, or half as great. While both methods provide a linear model of accident rate by curvature and grade, the regression model provides a more reliable estimate. In essence, the effects of curvature or grade can be estimated "better" using all the data. This results from the fact that none of the observations are free of random error, including those of level or tangent sections. Since the use of dummy variable multiple regression to identify cells which have larger than

expected crash rates is based upon a more rigorous
approach, its conclusions are more readily acceptable.
Thus, since the difference method leads to different and
less reliable conclusions, its use is not considered
acceptable.

Figure A-1

Curvature Model
Expected Relationship Between Curvature and
Crash Rate using Ohio Turnpike Data

t = total crashes
s = single vehicle crashes
w = wet pavement crashes

Degree of Curvature
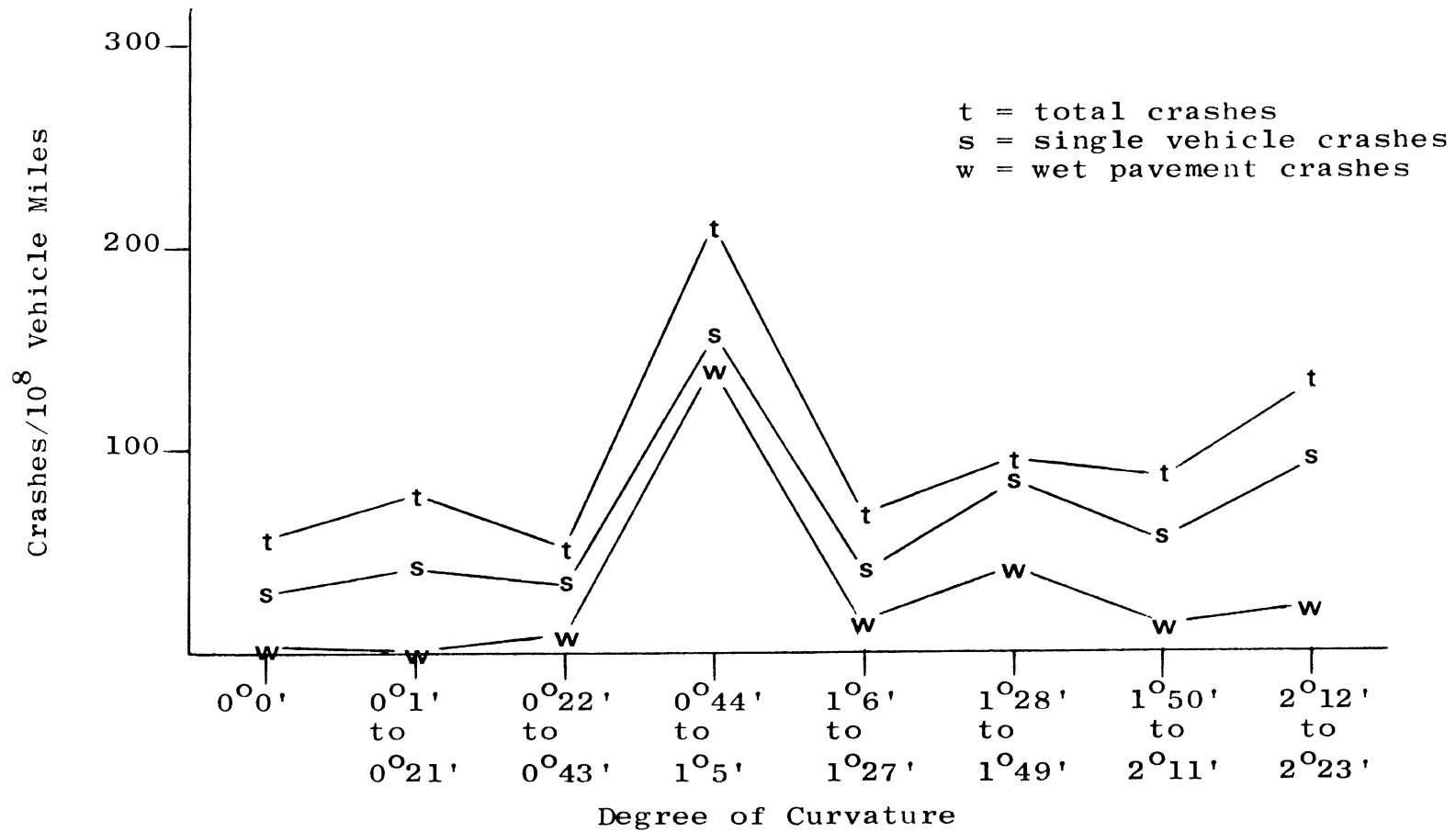
Figure A-2

Curvature Model

Expected Relationship Between Grade and Crash
Rate using Ohio Turnpike Data

t = total crashes
s = single vehicle crashes
w = wet pavement crashes

Crashes/10⁸ Vehicle Miles

Grade in Percent
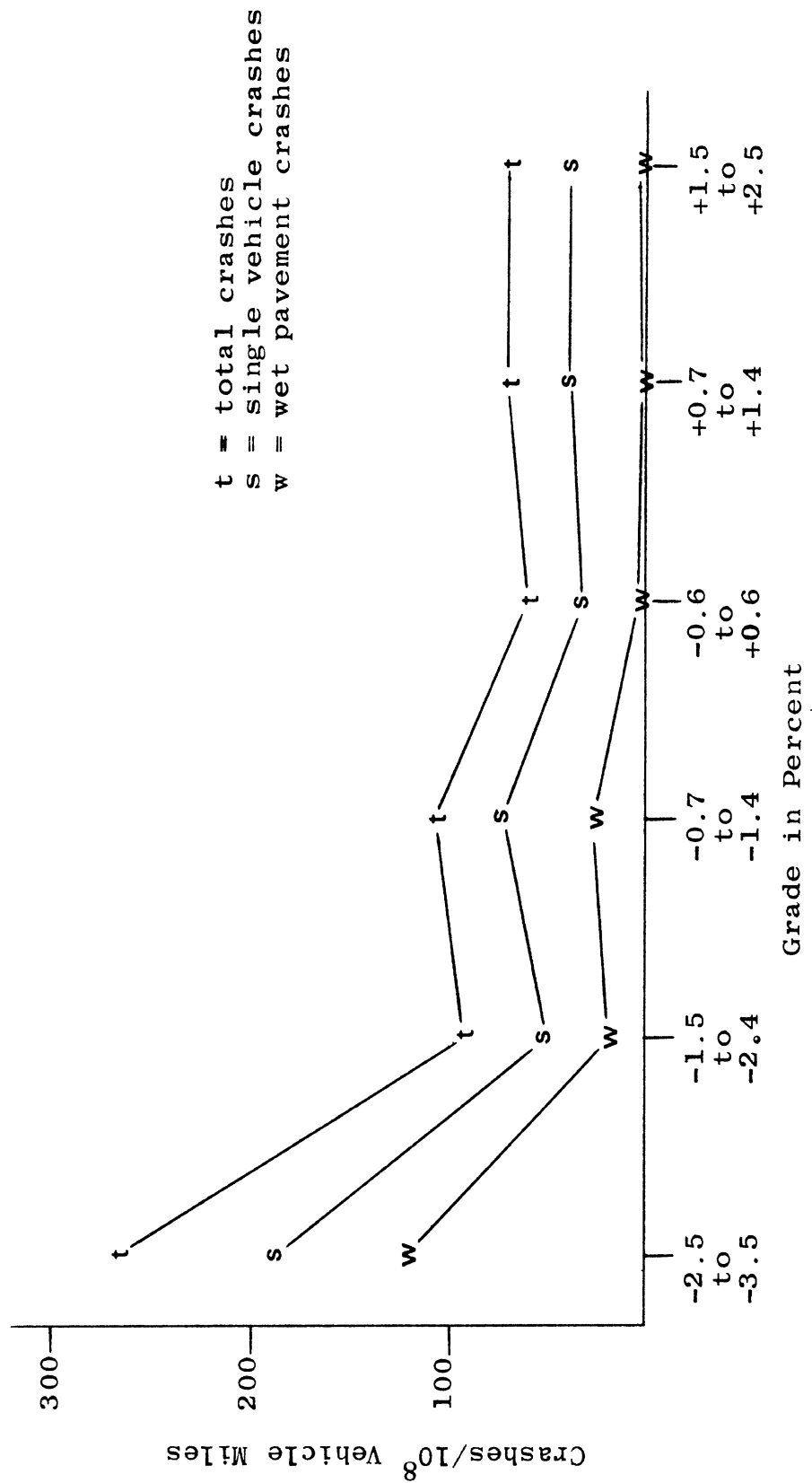
Figure A-3

Curvature Model
Expected Relationship Between Curvature and Crash
Rate Using Pennsylvania Turnpike Data
(8 Levels of Curvature)

t = total crashes
s = single vehicle crashes
w = wet pavement crashes

Crashes/10^8 Vehicle Miles

Degree of Curvature

157
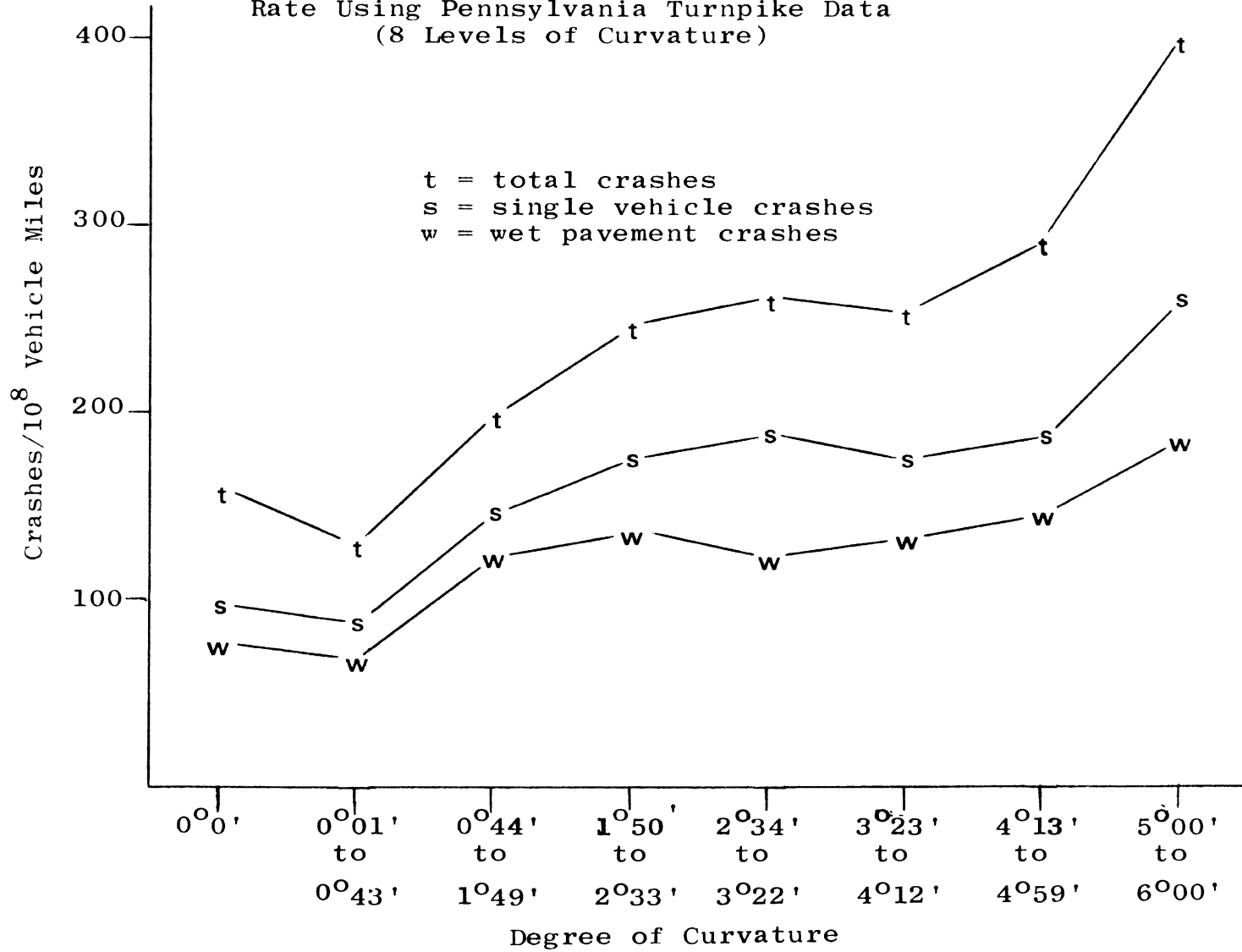
Figure A-4

Curvature Model
Expected Relationship Between Grade and Crash
Rate using Pennsylvania Turnpike Data
(8 Levels of Curvature)

158
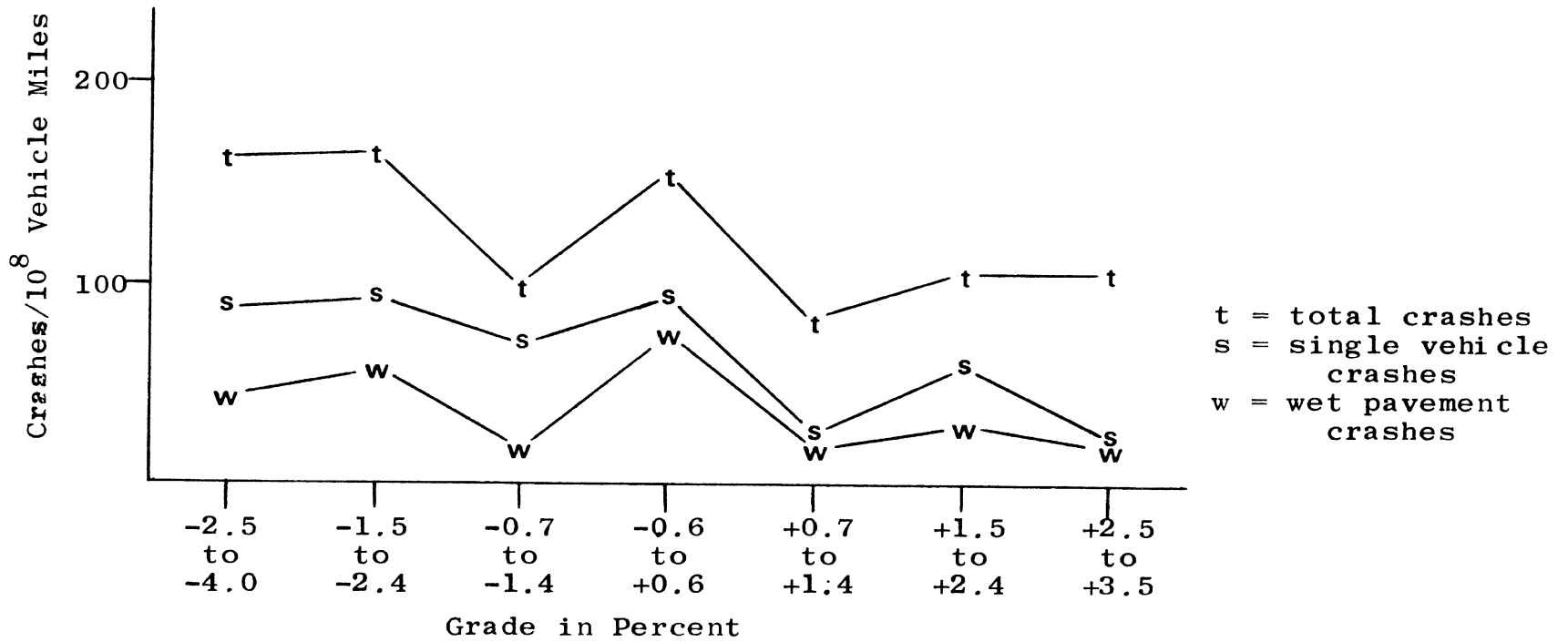
Figure A-5

Curvature Model
Expected Relationship Between Curvature and Crash
Rate using Pennslyvania Turnpike Data
(11 Levels of Curvature)

t = total crashes
s = single vehicle crashes
w = wet pavement crashes

Degree of Curvature
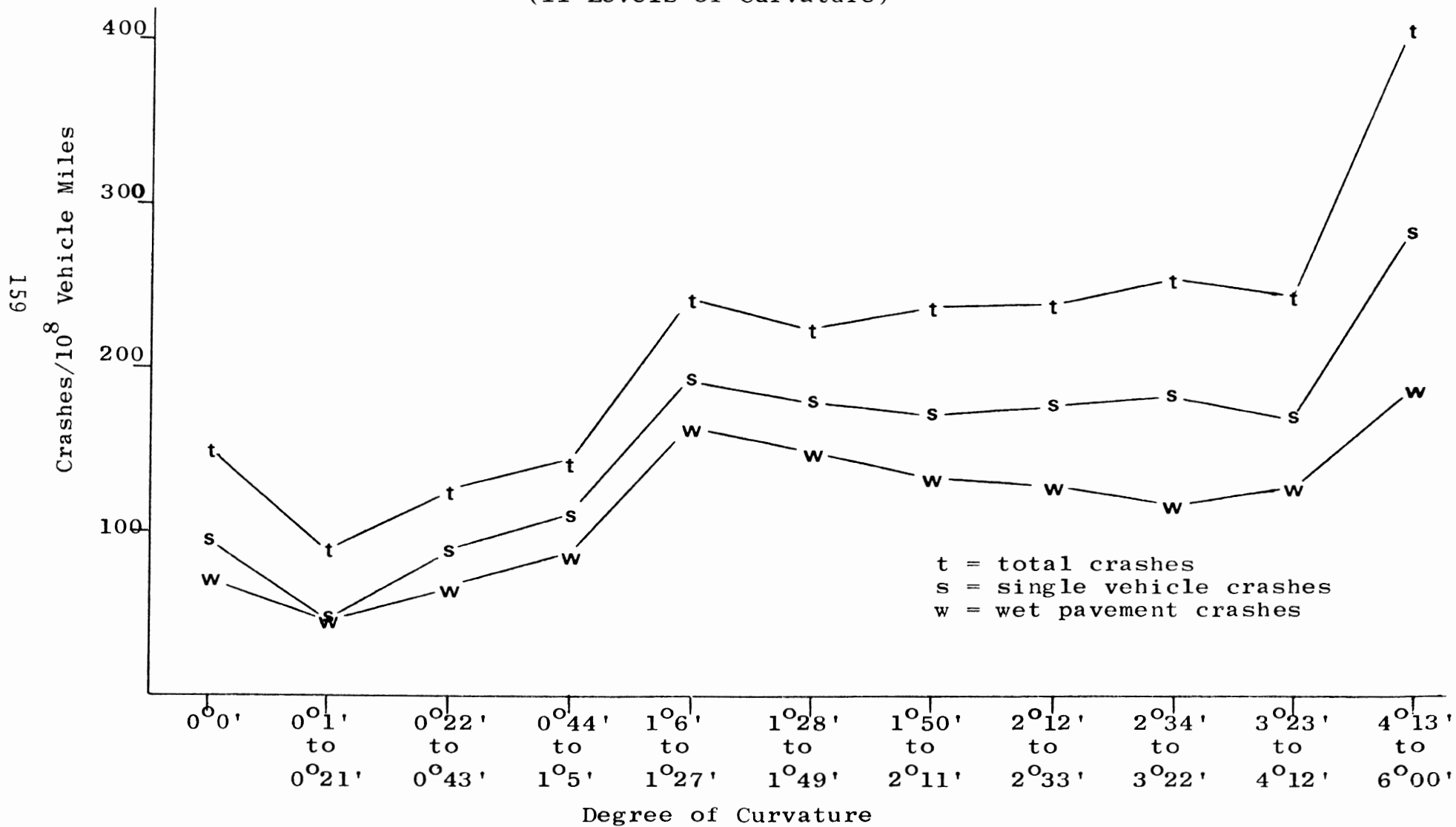
Figure A-6

Curvature Model
Expected Relationship Between Grade and Crash
Rate Using Pennsylvania Turnpike Data
(11 Levels of Curvature)

t = total crashes
s = single vehicle crashes
w = wet pavement crashes

Grade in Percent
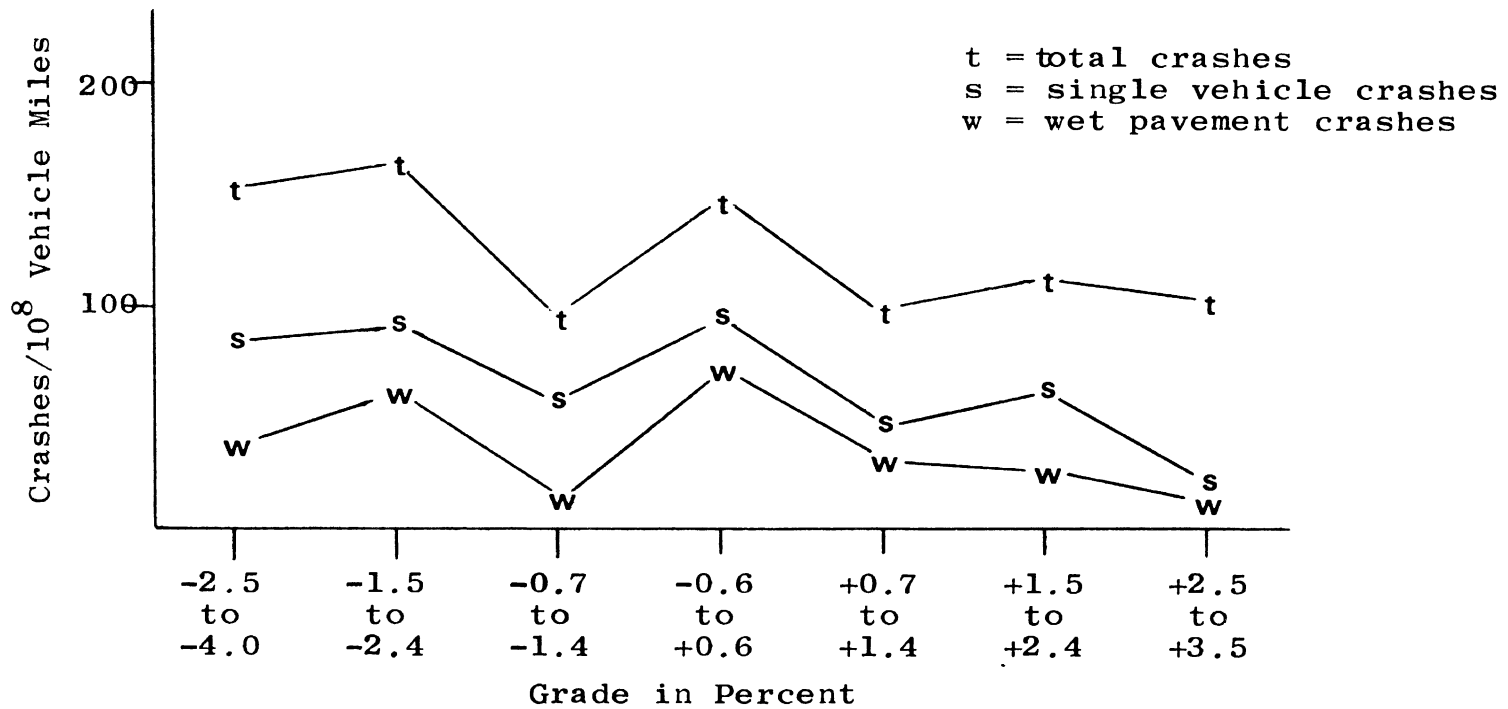
Figure A-7

Superelevation Model
Expected Relationship Between Superelevation and
Crash Rate Using Ohio Turnpike Data

t = total crashes
s = single vehicle
      crashes
w = wet pavement
      crashes

Crashes/10^8 Vehicle Miles

Superelevation in Sixteenths of an inch/foot

(Tangents)
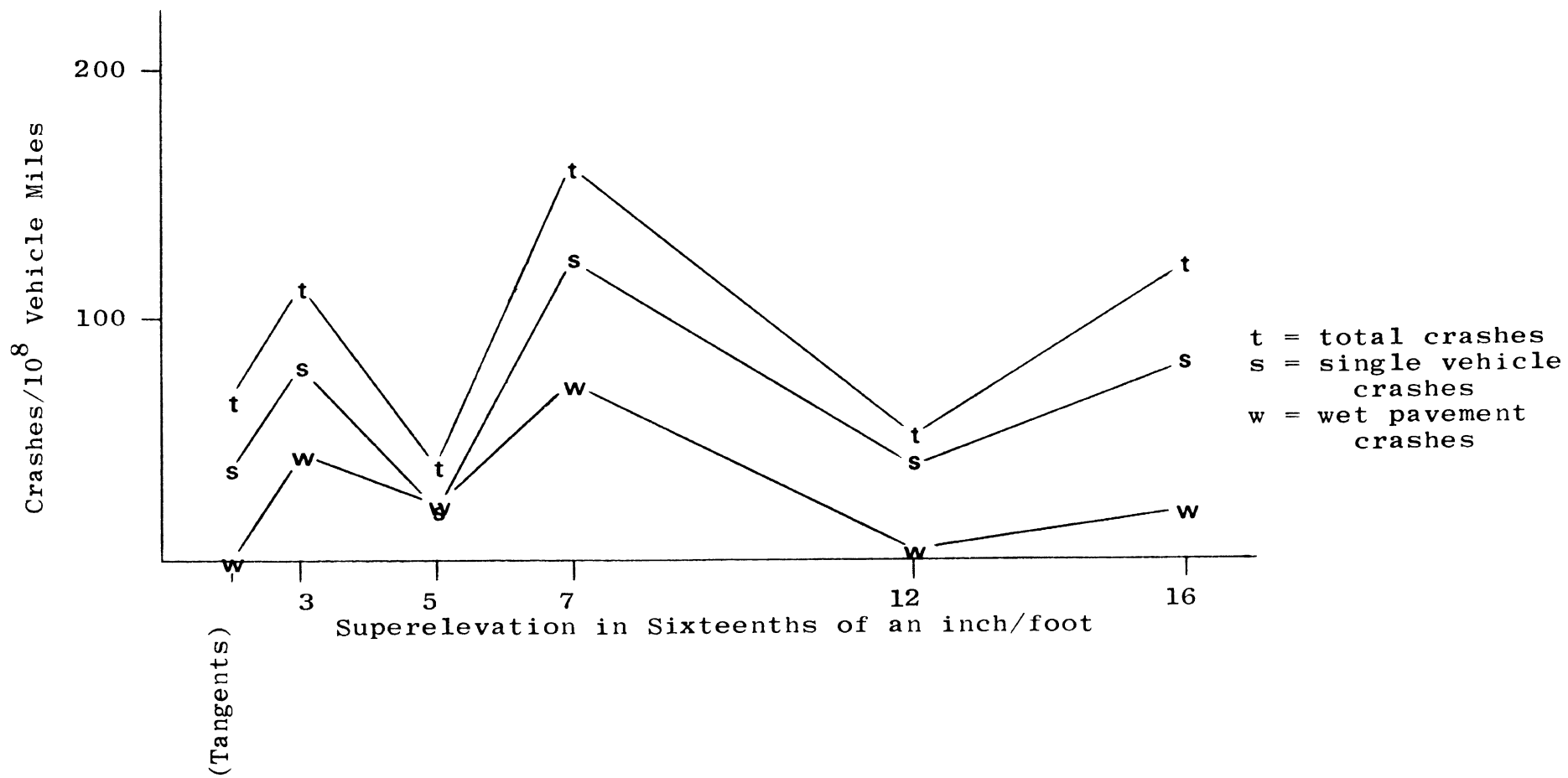
Figure A-8

Superelevation Model
Expected Relationship Between Grade and
Crash Rate Using Ohio Turnpike Data

162

Crashes/10^8 Vehicle Miles

200 —

100 —

t
t
s
w
s
t   t
s
w
s   s
t
w
t
s
w
w
w

-2.5   -1.5   -0.7   -0.6   +0.7   +1.5
to   to   to   to   to   to
-4.0   -2.4   -1.4   +0.6   +1.4   +2.4

Grade in Percent

t = total crashes
s = single vehicle crashes
w = wet pavement crashes
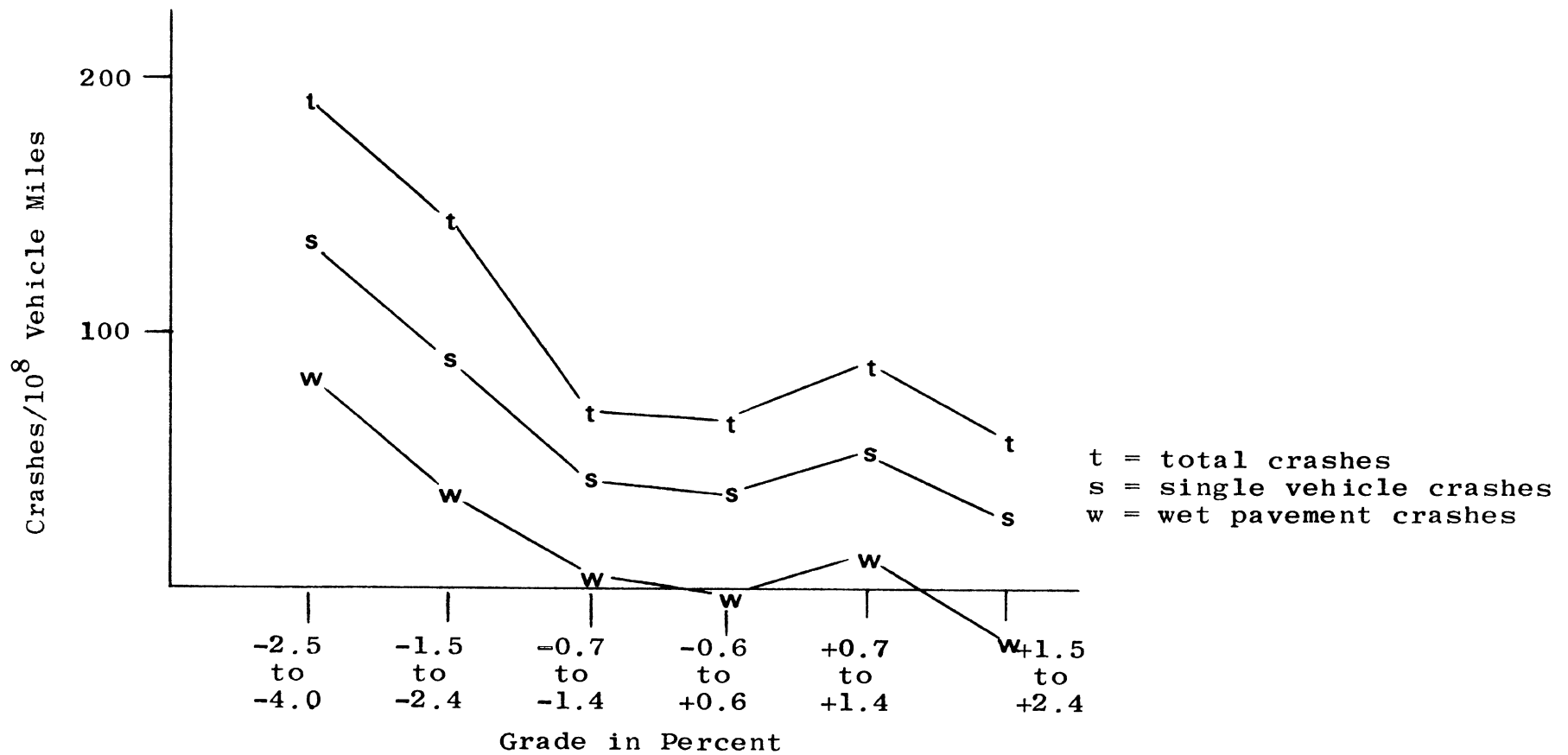
Figure A-9

Superelevation Model
Expected Relationship Between Superelevation and
Crash Rate using Pennsylvania Turnpike Data

t = total crashes
s = single vehicle crashes
w = wet pavement crashes
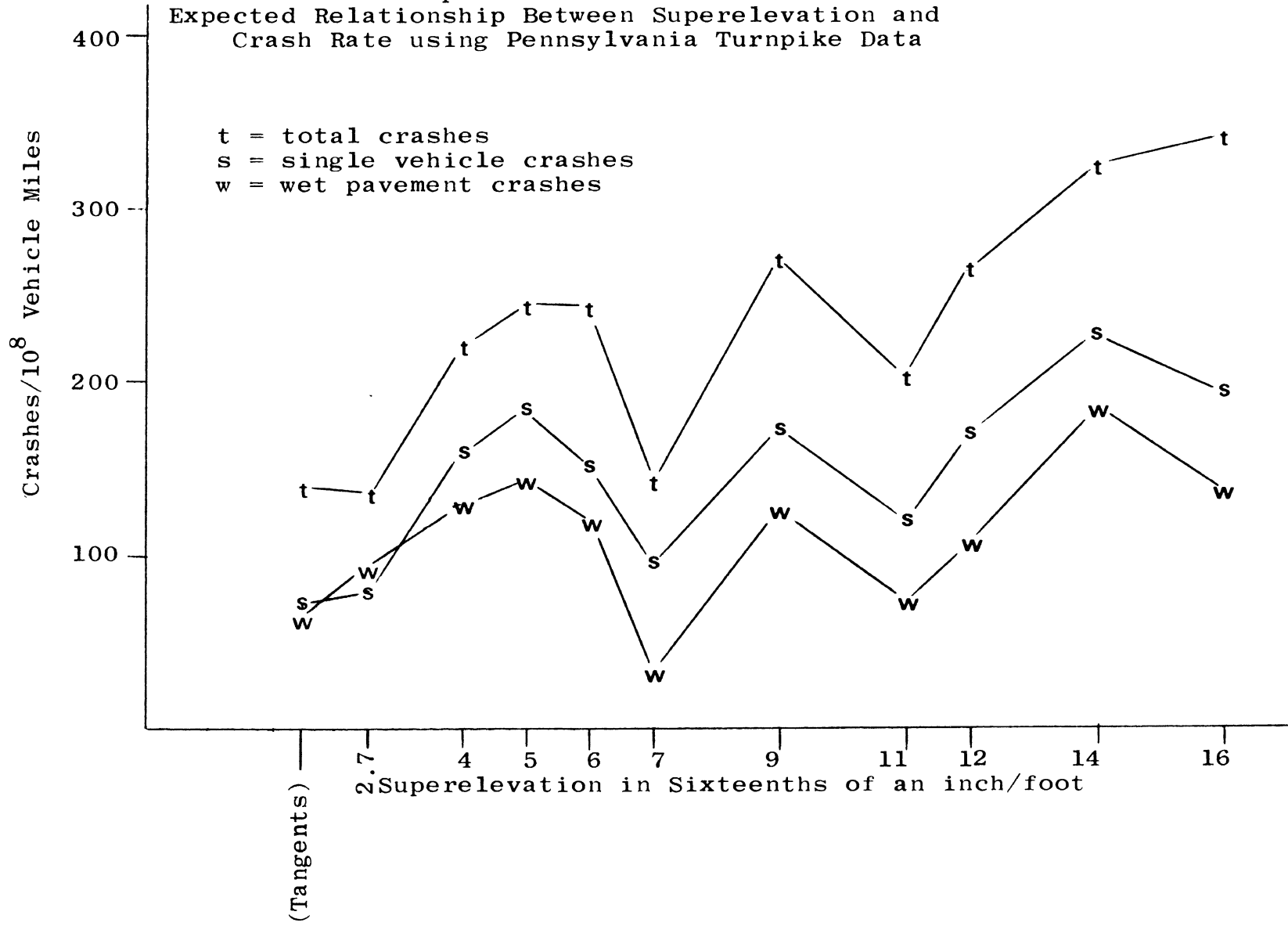
Figure A-10

Superelevation Model
Expected Relationship Between Grade and
Crash Rate Using Pennsylvania Turnpike Data

164
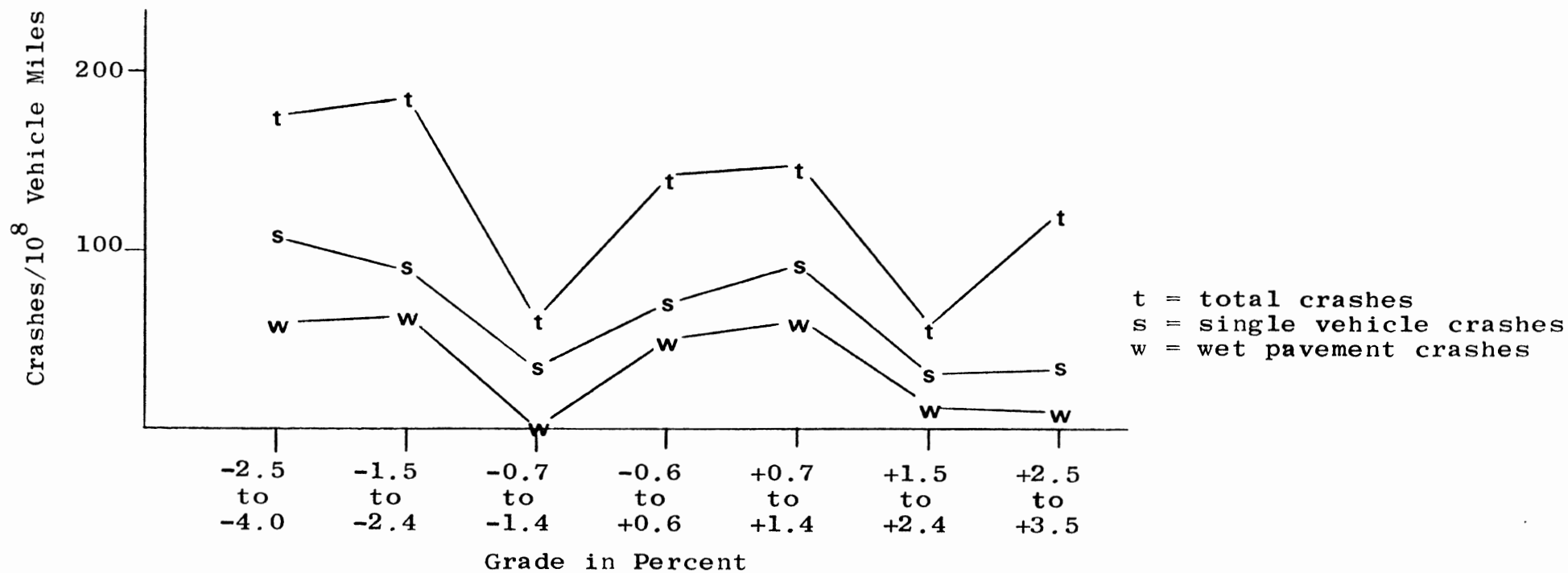
Figure A-11

Side Force Factor Model
Expected Relationship Between Friction and
Crash Rate Using Ohio Turnpike Data

t = total crashes
s = single vehicle
crashes
w = wet pavement
crashes

165
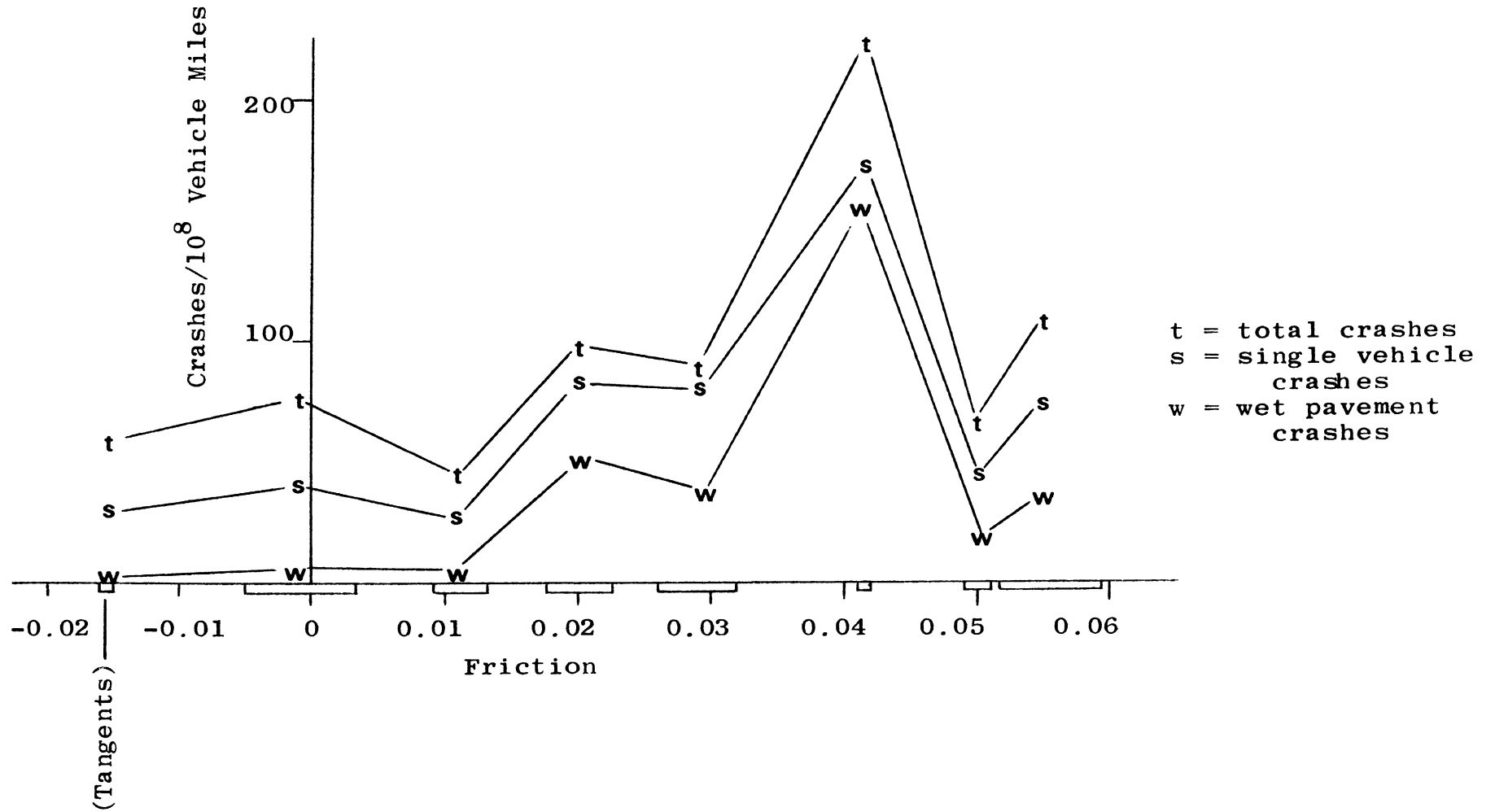
Figure A-12

Side Force Factor Model
Expected Relationship Between Grade and
Crash Rate Using Ohio Turnpike Data

t = total crashes
s = single vehicle crashes
w = wet pavement crashes

Crashes/10^8 Vehicle Miles

Grade in Percent

-2.5 to -4.0
-1.5 to -2.4
-0.7 to -1.4
-0.6 to +0.6
+0.7 to +1.4
+1.5 to +2.4
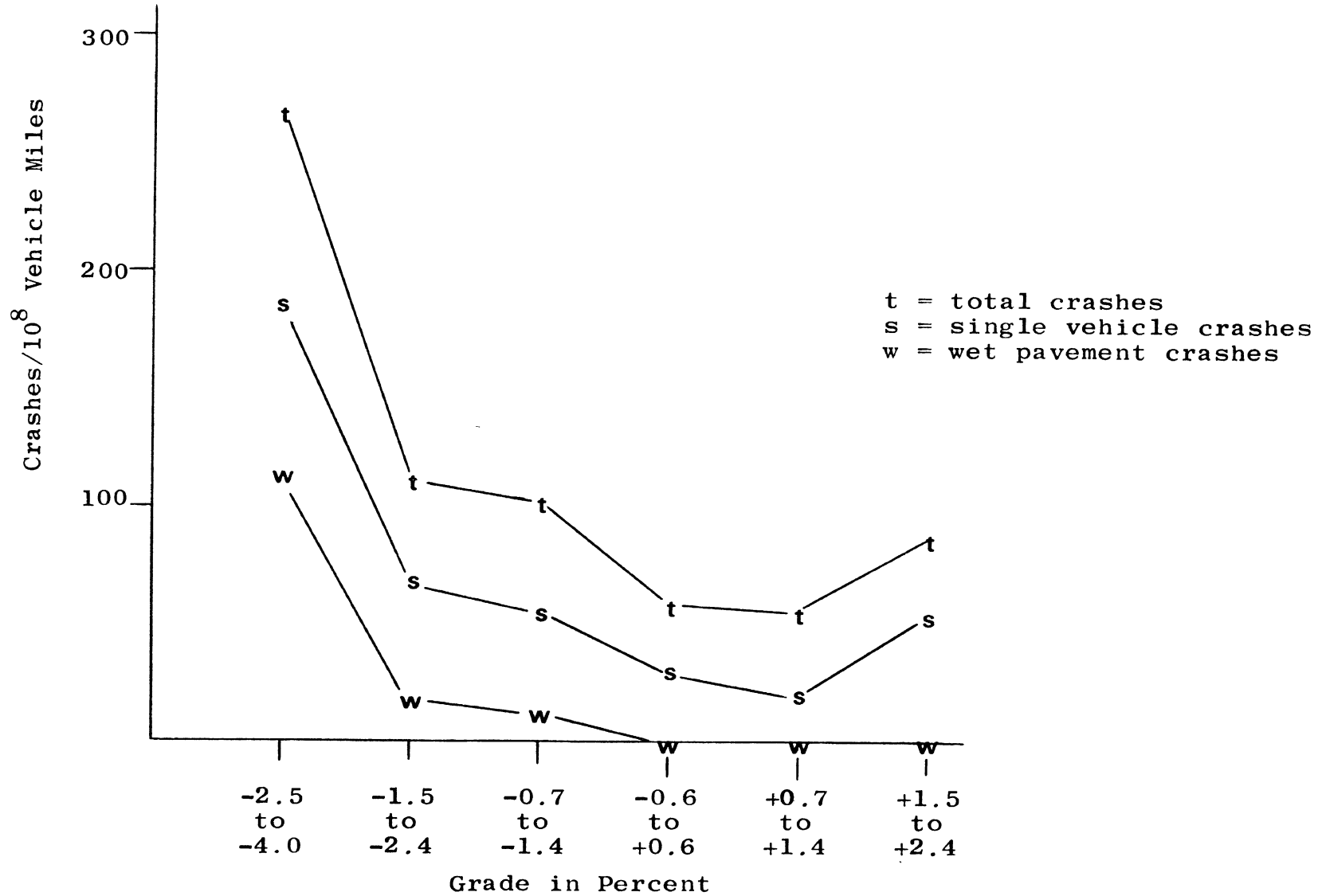
Figure A-13

Side Force Factor Model
Expected Relationship Between Friction and
Crash Rate Using Pennsylvania Turnpike Data

t = total crashes
s = single vehicle crashes
w = wet pavement crashes

200

100

(Tangents)

-0.02   0.00   0.02   0.04   0.06   0.08   0.1   0.12   0.14   0.16   0.18   0.20

167
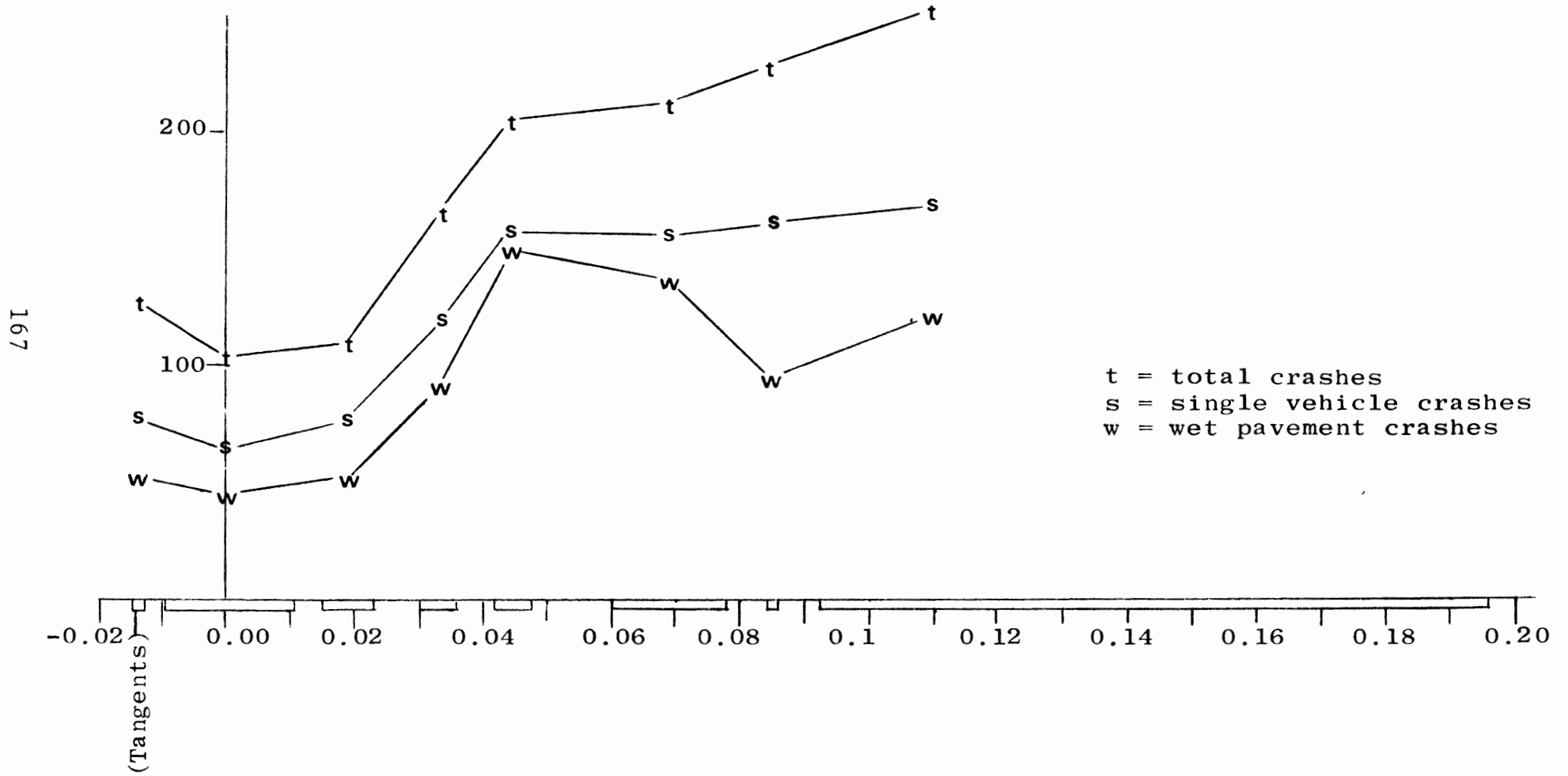
Figure A-14

Side Force Factor Model
Expected Relationship Between Grade and
Crash Rate Using Pennsylvania Turnpike Data

t = total crashes
s = single vehicle
      crashes
w = wet pavement
      crashes
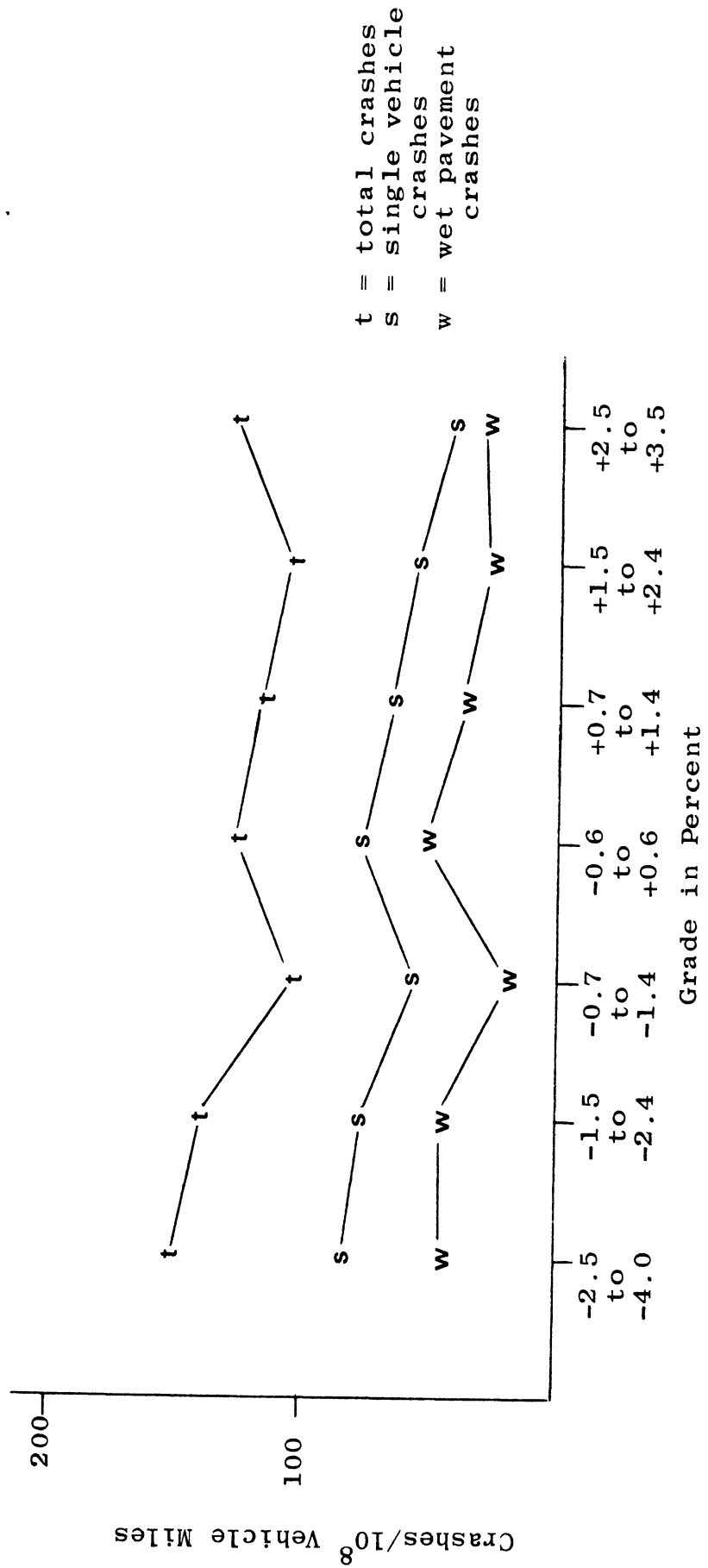
TABLE A-1

OHIO TURNPIKE VEHICLE MILES BY HIGHWAY ALIGNMENT

Degree of Curvature - Simple Curve

Grade in Percent	0°0'	0°1' to 0°21'	0°22' to 0°43'	0°44' to 1°5'	1°6' to 1°27'	0°28' to 1°49'	1°50' to 2°11'	2°12' to 2°33'
+2.4 to +1.5	29,527	6,404	10,490	7,246	1,420.9	650.4	1,249	751.5
+1.4 to +0.7	37,751	6,716	8,065	2,996	1,394.3	69.5	433.1	1,292.3
+0.6 to -0.6	229,890	51,309	28,809	16,123	6,671	7,296	4,203	4,053
-0.7 to -1.4	36,531	6,872	8,207	3,620	1,031.6	69.7	430.7	1,287.8
-1.5 to -2.4	29,152	4,721	8,258	6,101	1,417.3	655.7	1,253	746.9
-2.5 to -3.5	-1,019.0	314	2,033	511.2				
Total	363,870	76,336	65,812	36,597.2	11,935	8,741.3	7,568.8	8,131.5

Vehicle miles x 10^{-4} for all vehicle classes in both directions.

Total vehicle miles = 578,992 x 10^4

TABLE A-2

PENNSYLVANIA TURNPIKE VEHICLE MILES BY HIGHWAY ALIGNMENT

Degree of Curvature - Simple Curve

Grade in Percent	0°0'	0°1' to 0°43'	0°44' to 1°49'	1°50' to 2°33'	2°34' to 3°22'	3°23' to 4°12'	4°13' to 4°59'	5°00' to 6°00'
+4.0 to +2.5	38,373.4	3,530.2	13,424.4	12,345.6	11,698.7	6,163.5	1,051.6	2,580.0
+2.4 to +1.5	40,180.8	8,797.2	13,083.4	6,261.7	6,541.0	809.8	0	0
+1.4 to +0.7	52,017.0	10,552.2	10,693.7	5,193.4	3,428.0	1,065.4	271.8	168.6
+0.6 to -0.6	109,563.3	17,008.5	20,349.6	11,894.4	6,332.8	1,191.4	0	509.1
-0.7 to -1.4	52,715.7	10,609.3	10,979.3	5,039.5	3,413.1	1,063.6	246.9	170.8
-1.5 to -2.4	39,941.6	8,800.7	13,023.0	6,289.5	6,374.2	886.7	0	0
-2.5 to -4.0	38,365.9	3,632.0	13,273.1	12,252.1	11,598.3	5,947.1	1,004.0	2,543.6
Total	371,157.7	62,930.1	94,896.5	59,276.2	49,386.1	17,127.5	2,574.3	5,972.1

Vehicle miles x 10^{-4} for all vehicle classes, in both directions

Total vehicle miles = 663,321 x 10^4

TABLE A-3

OHIO TURNPIKE, NUMBER OF ACCIDENTS BY HIGHWAY ALIGNMENT

Degree of Curvature - Simple Curve

Grade	0°0'	0°1' to 0°21'	0°22' to 0°43'	0°44' to 1°5'	1°6' to 1°27'	1°28' to 1°49'	1°50' to 2°11'	2°12' to 2°33'
+2.4 to +1.5	347	74	121	122	7	6	6	11
+1.4 to +0.7	350	59	66	41	12	1	5	13
+0.6 to -0.6	1,888	349	240	177	51	58	44	72
-0.7 to -1.4	355	72	74	93	15	1	5	27
-1.5 to -2.4	362	56	95	149	11	7	18	10
-2.5 to -3.5	15	9	25	34	0	0	0	0
Total	3,317	619	621	616	96	73	78	133

Total Number = 5,553

TABLE A-4

PENNSYLVANIA TURNPIKE, NUMBER OF ACCIDENTS BY HIGHWAY ALIGNMENT
DEGREE OF CURVATURE - SIMPLE CURVE

Grade	0°0'	0°1' to 0°43'	0°44' to 1°49'	1°50' to 2°35'	2°34' to 3°22'	3°23' to 4°12'	4°13' to 4°59'	5°00' to 6°00'
+3.3 to +2.5	632	43	204	261	235	134	26	80
+2.4 to +1.5	451	103	209	115	122	16	0	0
+1.4 to +0.7	523	81	207	75	90	22	5	4
+0.6 to -0.6	1,221	121	351	276	137	17	0	35
-0.7 to -1.4	562	95	175	82	63	17	12	3
-1.5 to -2.4	476	75	214	208	200	25	0	0
-2.5 to -3.5	614	51	235	293	289	203	32	102
Total	4,479	569	1,595	1,310	1,136	434	75	224

Total Number = 9,822

172

Table A-5
Multiple Regression Analysis for the
Ohio Turnpike Accident Rate
Curvature - 8 Levels
All Accidents

ρ^2 = 0.6488   Std. error of regression = 0.0067

μ = 0.00594   Std. error (SE_μ) = 0.0035

Incremental Grade Adjustment

i	Grade (%)	δG_i	Std. Error $(SE_{\delta G_i})$
1	-3.5 to -2.5	0.02050	0.0042*
2	-2.4 to -1.5	0.00353	0.0034
3	-1.4 to -0.7	0.00477	0.0034
4	-0.6 to +0.6	0.0	------
5	0.7 to 1.4	0.00078	0.0033
6	1.5 to 2.4	0.00090	0.0033

Incremental Curvature Adjustment

j	Curvature	δD_j	Std. Error $(SE_{\delta D_j})$
1	0°0'	0.0	---
2	0°1' to 0°21'	0.00201	0.0039
3	0°22' to 0°43'	-0.00086	0.0039
4	0°44' to 1°5'	0.01534	0.0039*
5	1°6' to 1°27'	0.00076	0.0041
6	1°28' to 1°49'	0.00335	0.0041
7	1°50' to 2°11'	0.00263	0.0041
8	2°12' to 2°33'	0.00743	0.0041

*The value of δ is significantly different from zero
at the 5% confidence level (α = 0.05).

Table A-6

Multiple Regression Analysis for the
Ohio Turnpike Accident Rate
Curvature - 8 Levels
Single-Vehicle Accidents

ρ^2 = 0.6225   Std. error of regression = 0.0056

μ = 0.00309   Std. error (SE_μ) = 0.0029

Incremental Grade Adjustment

i	Grade (%)	δG_i	Std. Error $(SE_{\delta G_i}$
1	-3.5 to -2.5	0.01570	0.0036*
2	-2.4 to -1.5	0.00187	0.0028
3	-1.4 to -0.7	0.00402	0.0028
4	-0.6 to +0.6	0.0	------
5	0.7 to 1.4	0.00050	0.0028
6	1.5 to 2.4	0.00052	0.0028

Incremental Curvature Adjustment

j	Curvature	δD_j	Std. Error $(SE_{\delta D_j})$
1	0°0'	0.0	---
2	0°1' to 0°21'	0.00116	0.0033
3	0°22' to 0°43'	0.00032	0.0033
4	0°44' to 1°5'	0.01301	0.0033*
5	1°6' to 1°27'	0.00091	0.0034
6	1°28' to 1°49'	0.00546	0.0034
7	1°50' to 2°11'	0.00288	0.0034
8	2°12' to 2°33'	0.00609	0.0034

*The value of δ is significantly different from zero
at the 5% confidence level (α = 0.05).

Table A-7

Multiple Regression Analysis for the Ohio Turnpike Accident Rate Curvature - 8 Levels

Wet Road Accidents

$\rho^2 = 0.5895$ Std. error of regression = 0.0057

$\mu = 0.00017$ Std. error $(SE_\mu) = 0.0030$

Incremental Grade Adjustment

i	Grade (%)	δG_i	Std. Error $(SE_{\delta G_i})$
1	-3.5 to -2.5	0.01172	0.0036*
2	-2.4 to -1.5	0.00142	0.0029
3	-1.4 to -0.7	0.00264	0.0029
4	-0.6 to +0.6	0.0	------
5	0.7 to 1.4	-0.00089	0.0029
6	1.5 to 2.4	-0.00077	0.0029

Incremental Curvature Adjustment

j	Curvature	δD_j	Std. Error $(SE_{\delta D_j})$
1	0°0'	0.0	---
2	0°1' to 0°21'	0.00044	0.0033
3	0°22' to 0°43'	0.00124	0.0033
4	0°44' to 1°5'	0.01405	0.0033*
5	1°6' to 1°27'	0.00124	0.0035
6	1°28' to 1°49'	0.00401	0.0035
7	1°50' to 2°11'	0.00159	0.0035
8	2°12' to 2°33'	0.00305	0.0035

*The value of δ is significantly different from zero at the 5% confidence level ($\alpha = 0.05$).

Table A-8

Multiple Regression Analysis for the
Pennsylvania Turnpike Accident Rate
Curvature - 8 Levels

All Accidents

ρ^2 = 0.5989   Std. error of regression = 0.0080

μ = 0.01545   Std. error (SE_μ) = 0.0041

Incremental Grade Adjustment

i	Grade (%)	δG_i	Std. Error $(SE_{\delta G_i})$
1	-3.5 to -2.5	0.00052	0.0042
2	-2.4 to -1.5	0.00096	0.0045
3	-1.4 to -0.7	-0.00576	0.0042
4	-0.6 to +0.6	0.0	------
5	0.7 to 1.4	-0.00724	0.0042
6	1.5 to 2.4	-0.00468	0.0045
7	2.5 to 3.5	-0.00450	0.0042

Incremental Curvature Adjustment

j	Curvature	δD_j	Std. Error $(SE_{\delta D_j})$
1	0°0'	0.0	---
2	0°1' to 0°43'	-0.00247	0.0043
3	0°44' to 1°49'	0.00433	0.0043
4	1°50' to 2°33'	0.00899	0.0043*
5	2°34' to 3°22'	0.01056	0.0043*
6	3°23' to 4°12'	0.00961	0.0043*
7	4°13' to 4°59'	0.01969	0.0051*
8	5°00' to 6°00'	0.02417	0.0048*

*The value of δ is significantly different from zero
at the 5% confidence level $(\alpha = 0.05)$.

Table A-9

Multiple Regression Analysis for the Pennsylvania Turnpike Accident Rate
Curvature - 8 Levels
Single Vehicle Accidents

ρ^2 = 0.4763   Std. error of regression = 0.0072

μ = 0.00963   Std. error (SE_μ) = 0.0037

Incremental Grade Adjustment

i	Grade (%)	δG_i	Std. Error $(SE_{\delta G_i})$
1	-3.5 to -2.5	-0.00083	0.0038
2	-2.4 to -1.5	-0.00051	0.0040
3	-1.4 to -0.7	-0.00272	0.0038
4	-0.6 to +0.6	0.0	------
5	0.7 to 1.4	-0.00683	0.0038
6	1.5 to 2.4	-0.00360	0.0040
7	2.5 to 3.5	-0.00720	0.0038

Incremental Curvature Adjustment

j	Curvature	δD_j	Std. Error $(SE_{\delta D_j})$
1	0°0'	0.0	---
2	0°1' to 0°43'	-0.00107	0.0039
3	0°44' to 1°49'	0.00517	0.0039
4	1°50' to 2°33'	0.00788	0.0039
5	2°34' to 3°22'	0.00887	0.0039
6	3°23' to 4°12'	0.00748	0.0039
7	4°13' to 4°59'	0.01368	0.0046*
8	5°00' to 6°00'	0.01640	0.0043*

*The value of δ is significantly different from zero at the 5% confidence level (α = 0.05).

Table A-10

Multiple Regression Analysis for the
Pennsylvania Turnpike Accident Rate
Curvature - 8 Levels
Wet Road Accidents

ρ^2 = 0.4590   Std. error of regression = 0.0049

μ = 0.00749   Std. error (SE_μ) = 0.0026

Incremental Grade Adjustment

i	Grade (%)	δG_i	Std. Error $(SE_{\delta G_i})$
1	-3.5 to -2.5	-0.00355	0.0026
2	-2.4 to -1.5	-0.00173	0.0028
3	-1.4 to -0.7	-0.00590	0.0026
4	-0.6 to +0.6	0.0	------
5	0.7 to 1.4	-0.00600	0.0026
6	1.5 to 2.4	-0.00451	0.0028
7	2.5 to 3.5	-0.00542	0.0026

Incremental Curvature Adjustment

i	Curvature	δD_j	Std. Error $(SE_{\delta D_j})$
1	0°0'	0.0	0.0026
2	0°1' to 0°43'	0.00066	0.0026
3	0°44' to 1°49'	0.00500	0.0026*
4	1°50' to 2°33'	0.00596	0.0026
5	2°34' to 3°22'	0.00479	0.0026*
6	3°23' to 4°12'	0.00576	0.0026*
7	4°13' to 4°59'	0.00709	0.0032*
8	5°00' to 6°00'	0.01095	0.0029*

*The value of δ is significantly different from zero

at the 5% confidence level (α = 0.05).

Table A-11

Multiple Regression Analysis for the Pennsylvania Turnpike Accident Rate Curvature - 11 Levels

All Accidents

ρ^2 = 0.6731   Std. error of regression = 0.0063

μ = 0.01482   Std. error (SE_μ) = 0.0030

Incremental Grade Adjustment

i	Grade (%)	δG_i	Std. Error $(SE_{\delta G_i})$
1	-3.5 to -2.5	0.00071	0.0027
2	-2.4 to -1.5	0.00160	0.0028
3	-1.4 to -0.7	-0.00521	0.0027
4	-0.6 to +0.6	0.00000	------
5	0.7 to 1.4	-0.00510	0.0027
6	1.5 to 2.4	-0.00355	0.0028
7	2.5 to 3.5	-0.00472	0.0027

Incremental Curvature Adjustment

j	Curvature	δD_j	Std. Error $(SE_{\delta D_j})$
1	0°0'	0.0	0.0034
2	0°1' to 0°21'	-0.00569	0.0034
3	0°22' to 0°43'	-0.00232	0.0034
4	0°44' to 1°5'	-0.00064	0.0034
5	1°6' to 1°27'	0.00945	0.0034*
6	1°28' to 1°49'	0.00759	0.0034*
7	1°50' to 2°11'	0.00901	0.0034*
8	2°12' to 2°33'	0.00904	0.0034*
9	2°34' to 3°22'	0.01056	0.0034*
10	3°23' to 4°12'	0.00961	0.0034*
11	4°13' to 6°00'	0.02567	0.0038*

*The value of δ is significantly different from zero at the 5% confidence level (α = 0.05).

Table A-12

Multiple Regression Analysis for the Pennsylvania Turnpike Accident Rate Curvature - 11 Levels

Single Vehicle Accidents

ρ^2 = 0.6593   Std. error of regression = 0.0052

μ = 0.00958   Std. error (SE_μ) = 0.0024

Incremental Grade Adjustment

i	Grade (%)	δG_i	Std. Error $(SE_{\delta G_i})$
1	-3.5 to -2.5	-0.00121	0.0022
2	-2.4 to -1.5	-0.00031	0.0023
3	-1.4 to -0.7	-0.00388	0.0022
4	-0.6 to +0.6	0.0	------
5	0.7 to 1.4	-0.00495	0.0022*
6	1.5 to 2.4	-0.00341	0.0023
7	2.5 to 3.5	-0.00758	0.0022*

Incremental Curvature Adjustment

j	Curvature	δD_j	Std. Error $(SE_{\delta D_j})$
1	0°0'	0.0	0.0028
2	0°1' to 0°21'	-0.00481	0.0028
3	0°22' to 0°43'	-0.00078	0.0028
4	0°44' to 1°5'	0.00127	0.0028
5	1°6' to 1°27'	0.01006	0.0028*
6	1°28' to 1°49'	0.00852	0.0028*
7	1°50' to 2°11'	0.00763	0.0028*
8	2°12' to 2°33'	0.00822	0.0028*
9	2°34' to 3°22'	0.00884	0.0028*
10	3°23' to 4°12'	0.00748	0.0028*
11	4°13' to 6°00'	0.01850	0.0031*

*The value of δ is significantly different from zero at the 5% confidence level (α = 0.05).

Table A-13

Multiple Regression Analysis for the
Pennsylvania Turnpike Accident Rate
Curvature - 11 Levels

Wet Road Accidents

ρ^2 = 0.5874   Std. error of regression = 0.0044

μ = 0.00710   Std. error (SE_μ) = 0.0021

Incremental Grade Adjustment

i	Grade (%)	δG_i	Std. Error $(SE_{\delta G_i})$
1	-3.5 to -2.5	-0.00319	0.0019
2	-2.4 to -1.5	-0.00105	0.0019
3	-1.4 to -0.7	-0.00567	0.0019
4	-0.6 to +0.6	0.0	------
5	0.7 to 1.4	-0.00392	0.0019
6	1.5 to 2.4	-0.00443	0.0019
7	2.5 to 3.5	-0.00612	0.0019

Incremental Curvature Adjustment

j	Curvature	δD_j	Std. Error $(SE_{\delta D_j})$
1	0°0'	0.0	-------
2	0°1' to 0°21'	-0.00242	0.0023
3	0°22' to 0°43'	-0.00054	0.0023
4	0°44' to 1°5'	0.00156	0.0023
5	1°6' to 1°27'	0.00938	0.0023*
6	1°28' to 1°49'	0.00770	0.0023*
7	1°50' to 2°11'	0.00621	0.0023*
8	2°12' to 2°33'	0.00578	0.0023*
9	2°34' to 3°22'	0.00479	0.0023*
10	3°23' to 4°12'	0.00576	0.0023*
11	4°13' to 6°00'	0.01174	0.0026*

*The value of δ is significantly different from zero
at the 5% confidence level (α = 0.05).

Table A-14
Multiple Regression Analysis for the
Ohio Turnpike Accident Rate
Superelevation
All Accidents

$\rho^2 = 0.32394$ Std. error of regression = 0.0111

$\mu = 0.00658$ Std. error $(SE_\mu) = 0.0066$

Incremental Grade Adjustment

i	Grade (%)	δG_i	Std. Error $(SE_{\delta G_i})$
1	-3.5 to -2.5	0.01326	0.0097
2	-2.4 to -1.5	0.00780	0.0070
3	-1.4 to -0.7	0.00027	0.0070
4	-0.6 to +0.6	0.00	------
5	0.7 to 1.4	0.00215	0.0084
6	1.5 to 2.4	-0.00082	0.0084

Incremental Superelevation Adjustment

j	Superelevation	δe_j	Std. Error $(SE_{\delta e_j})$
1	3/16 on tangents	0.00	-----
2	3/16 on curves	0.00466	0.0064
3	7/16	-0.00264	0.0129
4	9/16	0.00925	0.0074
5	12/16	-0.00145	0.0083
6	16/16	0.00542	0.0074

Table A-15
Multiple Regression Analysis for the
Ohio Turnpike Accident Rate
Superelevation
Single Vehicle Accidents

ρ^2 = 0.3366   Std. error of regression = 0.0082

μ = 0.00369   Std. error (SE_μ) = 0.0049

Incremental Grade Adjustment

i	Grade (%)	δG_i	Std. Error $(SE_{\delta G_i})$
1	-3.5 to -2.5	0.00994	0.0072
2	-2.4 to -1.5	0.00519	0.0052
3	-1.4 to -0.7	0.00054	0.0052
4	-0.6 to +0.6	0.00	-------
5	0.7 to 1.4	0.00157	0.0062
6	1.5 to 2.4	-0.00091	0.0062

Incremental Superelevation Adjustment

j	Superelevation	δe_j	Std. Error $(SE_{\delta e_j})$
1	3/16 on tangents	0.00	------
2	3/16 on curves	0.00431	0.0047
3	7/16	-0.00172	0.0095
4	9/16	0.00839	0.0055
5	12/16	0.00013	0.0061
6	16/16	0.00422	0.0055

Table A-16
Multiple Regression Analysis for the Ohio Turnpike Accident Rate Superelevation Wet Road Accidents

$\rho^2 = 0.5015$ Std. error of regression = 0.0049

$\mu = -0.00026$ Std. error $(SE_\mu) = 0.0029$

Incremental Grade Adjustment

i	Grade (%)	δG_i	Std. Error $(SE_{\delta G_i})$
1	-3.5 to -2.5	0.00878	0.0043
2	-2.4 to -1.5	0.00393	0.0031
3	-1.4 to -0.7	0.00074	0.0031
4	-0.6 to +0.6	0.00	------
5	0.7 to 1.4	0.00141	0.0037
6	1.5 to 2.4	-0.00174	0.0037

Incremental Superelevation Adjustment

j	Superelevation	δe_j	Std. Error $(SE_{\delta e_j})$
1	3/16 on tangents	0.00	-----
2	3/16 on curves	0.00460	0.0028
3	7/16	0.00223	0.0057
4	9/16	0.00739	0.0033*
5	12/16	0.00068	0.0037
6	16/16	0.00204	0.0033

*The value of δ is significantly different from zero at the 5% confidence level ($\alpha = 0.05$).

Table A-17

Multiple Regression Analysis for the
Pennsylvania Turnpike Accident Rate
Superelevation
All Accidents

ρ^2 = 0.3540   Std. error of regression = 0.0132

μ = 0.0140   Std. error (SE_μ) = 0.0062

Incremental Grade Adjustment

i	Grade (%)	δG_i	Std. Error $(SE_{\delta G_i})$
1	-3.5 to -2.5	0.00346	0.0056
2	-2.4 to -1.5	0.00454	0.0059
3	-1.4 to -1.5	-0.00801	0.0050
4	-0.6 to +0.6	0.0	------
5	0.7 to 1.4	0.00058	0.0060
6	1.5 to 2.4	-0.00861	0.0056
7	2.5 to 3.5	-0.00197	0.0056

Incremental Superelevation Adjustment

j	Superelevation	δe_j	Std. Error $(SE_{\delta e_j})$
1	1/6 on tangents	0.00	-----
2	1/6 on curves	-0.00025	0.0070
3	4/16	0.00811	0.0070
4	5/16	0.01036	0.0070
5	6/16	0.01019	0.0070
6	7/16	0.00028	0.0084
7	9/16	0.01294	0.0070
8	11/16	0.00630	0.0084
9	12/16	0.01241	0.0070
10	13/16	0.00645	0.0108
11	14/16	0.01850	0.0074*
12	15/16	-0.00917	0.0109
13	16/16	0.01984	0.0070*

*The value of δ is significantly different from zero

at the 5% confidence level (α = 0.05).

Table A-18

Multiple Regression Analysis for the Pennsylvania Turnpike Accident Rate Superelevation Single Vehicle Accidents

$\rho^2 = 0.3753$ Std. error of regression = 0.0091

$\mu = 0.00712$ Std. error $(SE_\mu) = 0.0043$

Incremental Grade Adjustment

i	Grade (%)	δG_i	Std. Error $(SE_{\delta G_i})$
1	-3.5 to -2.5	0.00373	0.0039
2	-2.4 to -1.5	0.00189	0.0041
3	-1.4 to -1.5	-0.00376	0.0041
4	-0.6 to +0.6	0.0	------
5	0.7 to 1.4	0.00210	0.0041
6	1.5 to 2.4	-0.00415	0.0038
7	2.5 to 3.5	-0.00375	0.0039

Incremental Superelevation Adjustment

j	Superelevation	δe_j	Std. Error $(SE_{\delta e_j})$
1	1/6 on tangents	0.C	-----
2	1/6 on curves	0.00103	0.0049
3	4/16	0.00885	0.0049
4	5/16	0.01164	0.0049*
5	6/16	0.00824	0.0049
6	7/16	0.00247	0.0058
7	9/16	0.01013	0.0049
8	11/16	0.00478	0.0058
9	12/16	0.00994	0.0049*
10	13/16	0.00045	0.0075
11	14/16	0.01580	0.0051*
12	15/16	-0.00466	0.0075
13	16/16	0.01198	0.0049*

*The value of δ is significantly different from zero

at the 5% confidence level ($\alpha = 0.05$).

Table A-19

Multiple Regression Analysis for the Pennsylvania Turnpike Accident Rate
Superelevation
Wet Road Accidents

$\rho^2 = 0.3754$ Std. error of regression = 0.0074

$\mu = 0.00484$ Std. error $(SE_\mu) = 0.0034$

Incremental Grade Adjustment

i	Grade (%)	δG_i	Std. Error $(SE_{\delta G_i})$
1	-3.5 to -2.5	0.00116	0.0031
2	-2.4 to -1.5	0.00158	0.0033
3	-1.4 to -1.5	-0.00484	0.0033
4	-0.6 to +0.6	0.0	------
5	0.7 to 1.4	0.00118	0.0033
6	1.5 to 2.4	-0.00371	0.0031
7	2.5 to 3.5	-0.00397	0.0032

Incremental Superelevation Adjustment

j	Superelevation	δe_j	Std. Error $(SE_{\delta e_j})$
1	1/6 on tangents	0.0	-----
2	1/6 on curves	0.00126	0.0039
3	4/16	0.00826	0.0039*
4	5/16	0.00938	0.0039*
5	6/16	0.00666	0.0039
6	7/16	-0.00167	0.0047
7	9/16	0.00772	0.0039
8	11/16	0.00198	0.0047
9	12/16	0.00535	0.0039
10	13/16	0.00189	0.0061
11	14/16	0.01344	0.0041*
12	15/16	-0.00058	0.0061
13	16/16	0.00852	0.0039*

*The value of δ is significantly different from zero

at the 5% confidence level ($\alpha = 0.05$).

Table A-20
Multiple Regression Analysis for the
Ohio Turnpike Accident Rate
Side Force Factor
All Accidents

$\rho^2 = 0.6825$ .... Std. error of regression = 0.0065

$\mu = 0.00585$ .... Std. error $(SE_\mu) = 0.0034$

Incremental Grade Adjustment

i	Grade (%)	δG_i	Std. Error $(SE_{\delta G_i})$
1	-3.5 to -2.5	0.02107	0.0041*
2	-2.4 to -1.5	0.00509	0.0033
3	-1.4 to -0.7	0.00427	0.0033
4	-0.6 to +0.6	0.00	------
5	0.7 to 1.4	-0.00022	0.0033
6	1.5 to 2.4	0.00278	0.0033

Incremental Side Force Factor Adjustment

j	Side Force Factor	δf_j	Std. Error $(SE_{\delta f_j})$
1	-0.015625 on tang.	0.0	--------
2	-0.00517 to 0.00338	0.00173	0.0038
3	0.00813 to 0.01288	-0.00165	0.0038
4	0.01763 to 0.02238	0.00394	0.0040
5	0.02714 to 0.03189	0.00301	0.0040
6	0.04139	0.01642	0.0038*
7	0.04906 to 0.05089	0.00060	0.0040
8	0.05153 to 0.05920	0.00510	0.0040

*The value of δ is significantly different from zero
at the 5% confidence level ($\alpha = 0.05$).

Table A-21

Multiple Regression Analysis for the
Ohio Turnpike Accident Rate
Side Force Factor
Single Vehicle Accidents

ρ^2 = 0.6424   Std. error of regression = 0.0056

μ = 0.00298   Std. error (SE_μ) = 0.0029

Incremental Grade Adjustment

i	Grade (%)	δG_i	Std. Error $(SE_{\delta G_i})$
1	-3.5 to -2.5	0.01565	0.0036*
2	-2.4 to -1.5	0.00382	0.0028
3	-1.4 to -0.7	0.00256	0.0028
4	-0.6 to +0.6	0.0	------
5	0.7 to 1.4	-0.00096	0.0028
6	1.5 to 2.4	0.00220	0.0028

Incremental Side Force Factor Adjustment

j	Side Force Factor	δf_j	Std. Error $(SE_{\delta f_j})$
1	-0.015625 on tang.	0.00	------
2	-0.00517 to 0.00338	0.00114	0.0032
3	0.00813 to 0.01288	-0.00023	0.0032
4	0.01763 to 0.02238	0.00536	0.0034
5	0.02714 to 0.03189	0.00488	0.0034
6	0.04139	0.01420	0.0032*
7	0.04906 to 0.05089	0.00136	0.0034
8	0.05153 to 0.05920	0.00442	0.0034

*The value of δ is significantly different from zero
at the 5% confidence level (α = 0.05).

Table A-22

Multiple Regression Analysis for the
Ohio Turnpike Accident Rate
Side Force Factor
Wet Road Accidents

ρ^2 = 0.6535   Std. error of regression = 0.0053

μ = -0.00009   Std. error (SE_μ) = 0.0028

Incremental Grade Adjustment

i	Grade (%)	δG_i	Std. Error $(SE_{\delta G_i})$
1	-3.5 to -2.5	0.01137	0.0033*
2	-2.4 to -1.5	0.00176	0.0026
3	-1.4 to -0.7	0.00137	0.0026
4	-0.6 to +0.6	0.0	------
5	0.7 to 1.4	-0.00075	0.0026
6	1.5 to 2.4	-0.00013	0.0026

Incremental Side Force Factor Adjustment

j	Side Force Factor	δf_j	Std. Error $(SE_{\delta f_j})$
1	-0.015625 on tang.	0.0	------
2	-0.00517 to 0.00338	0.00044	0.0030
3	0.00813 to 0.01288	0.00067	0.0030
4	0.01763 to 0.02238	0.00513	0.0032
5	0.02714 to 0.03189	0.00354	0.0032
6	0.04139	0.01566	0.0030*
7	0.04906 to 0.05089	0.00166	0.0032
8	0.05153 to 0.05920	0.00222	0.0032

*The value of δ is significantly different from zero
at the 5% confidence level (α = 0.05).

Table A-23
Multiple Regression Analysis for the
Pennsylvania Turnpike Accident Rate
Side Force Factor
All Accidents

$\rho^2 = 0.7445$ Std. error of regression = 0.0038

$\mu = 0.01276$ Std. error $(SE_\mu) = 0.0019$

Incremental Grade Adjustment

i	Grade (%)	δG_i	Std. Error $(SE_{\delta G_i})$
1	-3.5 to -2.5	0.00243	0.0019
2	-2.4 to -1.5	0.00140	0.0019
3	-1.4 to -0.7	-0.00254	0.0019
4	-0.6 to +0.6	0.0	------
5	0.7 to 1.4	-0.00109	0.0019
6	1.5 to 2.4	-0.00225	0.0019
7	2.5 to 3.5	0.00008	0.0019

Incremental Side Force Factor Adjustment

j	Side Force Factor	δf_j	Std. Error $(SE_{\delta f_j})$
1	-0.0139 on Tangents	0.0	------
2	-0.0979 to 0.0107	-0.00233	0.0020
3	0.0148 to 0.0230	-0.00172	0.0020
4	0.0304 to 0.0361	0.00407	0.0020
5	0.0418 to 0.0476	0.00754	0.0020*
6	0.05999 to 0.07790	0.00861	0.0020*
7	0.084980	0.01017	0.0020*
8	0.092070 to 0.19601	0.01285	0.0020*

*The value of δ is significantly different from zero

at the 5% confidence level ($\alpha = 0.05$).

Table A-24

Multiple Regression Analysis for the
Pennsylvania Turnpike Accident Rate
Side Force Factor
Single Vehicle Accidents

ρ^2 = 0.7169   Std. error of regression = 0.0032

μ = 0.00772   Std. error (SE_μ) = 0.0016

Incremental Grade Adjustment

i	Grade (%)	δG_i	Std. Error $(SE_{\delta G_i})$
1	-3.5 to -2.5	0.00072	0.0016
2	-2.4 to -1.5	0.00004	0.0016
3	-1.4 to -0.7	-0.00189	0.0016
4	-0.6 to +0.6	0.0	------
5	0.7 to 1.4	-0.00135	0.0016
6	1.5 to 2.4	-0.00225	0.0016
7	2.5 to 3.5	-0.00359	0.0016*

Incremental Side Force Factor Adjustment

j	Side Force Factor	δf_j	Std. Error $(SE_{\delta f_j})$
1	-0.0139 on tangents	0.0	-----
2	-0.00979 to 0.0107	-0.00106	0.0017
3	0.0148 to 0.0230	-0.00010	0.0017
4	0.0304 to 0.0361	0.00434	0.0017*
5	0.0418 to 0.0476	0.00801	0.0017*
6	0.05999 to 0.07790	0.00798	0.0017*
7	0.084980	0.00857	0.0017*
8	0.092070 to 0.19601	0.00919	0.0017*

*The value of δ is significantly different from zero

at the 5% confidence level (α = 0.05).

Table A-25
Multiple Regression Analysis for the
Pennsylvania Turnpike Accident Rate
Side Force Factor
Wet Road Accidents

ρ^2 = 0.6511   Std. error of regression = 0.0027

μ = 0.00518   Std. error (SE_μ) = 0.0013

Incremental Grade Adjustment

i	Grade (%)	δG_i	Std. Error $(SE_{\delta G_i})$
1	-3.5 to -2.5	-0.00078	0.0013
2	-2.4 to -1.5	-0.00060	0.0013
3	-1.4 to -0.7	-0.00329	0.0013*
4	-0.6 to +0.6	0.0	------
5	0.7 to 1.4	-0.00139	0.0013
6	1.5 to 2.4	-0.00256	0.0013
7	2.5 to 3.5	-0.00236	0.0013

Incremental Side Factor Force Adjustment

j	Side Factor Force	δf_j	Std. Error $(SE_{\delta f_j})$
1	-0.0139 on tangents	0.0	-----
2	-0.00979 to 0.0107	-0.00068	0.0014
3	0.0418 to 0.0230	0.00126	0.0014
4	0.0304 to 0.0361	0.00396	0.0014*
5	0.0418 to 0.0476	0.00761	0.0014*
6	0.05999 to 0.07790	0.00604	0.0014*
7	0.084980	0.00440	0.0014*
8	0.092070 to 0.19601	0.00672	0.0014*

*The value of δ is significantly different from zero

at the 5% confidence level (α = 0.05).

Table A-26

OHIO TURNPIKE CURVE & GRADE ANALYSIS

(All Crashes)

Grade in Percent

Curvatures		-2.5 to -3.5	-1.5 to -2.4	-0.7 to -1.4	-0.6 to +0.6	+0.7 to +1.4	+1.5 to +2.4
0°0'	Obs	.0147	.0124	.0097	.0082	.0093	.0118
	Exp	.0264	.0095	.0107	.0059	.0067	.0068
	CI	.0080	.0069	.0069	.0069	.0069	.0069
	Res	-.0117 *	.0030	-.0010	.0023	.0026	.0049
0°1' to 0°21'	Obs	.0287	.0119	.0105	.0068	.0088	.0116
	Exp	.0284	.0115	.0127	.0079	.0087	.0088
	CI	.0080	.0069	.0069	.0069	.0069	.0069
	Res	.0002	.0004	-.0022	-.0011	.0001	.0027
0°22' to 0°43'	Obs	.0123	.0115	.0090	.0083	.0082	.0116
	Exp	.0256	.0086	.0098	.0051	.0059	.0060
	CI	.0080	.0069	.0069	.0069	.0069	.0069
	Res	-.0133 *	.0029	-.0008	.0033	.0023	.0056
0°44' to 1°5'	Obs	.0665	.0244	.0757	.0110	.0137	.0168
	Exp	.0418	.0248	.0760	.0215	.0221	.0222
	CI	.0080	.0069	.0069	.0069	.0069	.0069
	Res	.0248 *	-.0004	-.0004	-.0103 *	-.0084 *	-.0053 *
1°6' to 1°27'	Obs		.0078	.0145	.0076	.0086	.0049
	Exp		.0102	.0115	.0057	.0075	.0076
	CI		.0072	.0072	.0072	.0072	.0072
	Res		-.0025	.0031	.0009	.0011	-.0027
1°28' to 1°49'	Obs		.0107	.0143	.0079	.0143	.0092
	Exp		.0128	.0141	.0093	.0101	.0102
	CI		.0072	.0072	.0072	.0072	.0072
	Res		-.0021	.0002	-.0013	.0042	-.0010
1°50' to 2°11'	Obs		.0144	.0116	.0105	.0115	.0048
	Exp		.0121	.0133	.0086	.0093	.0095
	CI		.0072	.0072	.0072	.0072	.0072
	Res		.0023	-.0017	.0019	.0022	-.0047
2°12' to 2°23'	Obs		.0134	.0210	.0178	.0101	.0146
	Exp		.0169	.0181	.0134	.0141	.0143
	CI		.0072	.0072	.0072	.0072	.0072
	Res		-.0035	.0028	.0044	-.0041	.0004

* Statistically significant @ .95 level.

194

Table A-27

OHIO TURNPIKE CURVE & GRADE ANALYSIS
(Single-Vehicle Relative Crash Rate)

Grade in Percent

Curvatures		-2.5 to -3.5	-1.5 to -2.4	-0.7 to -1.4	-0.6 to +0.6	+0.7 to +1.4	+1.5 to +2.4
0°0'	Obs	.0079	.0079	.0062	.0056	.0064	.0072
	Exp	.0188	.0050	.0071	.0031	.0036	.0036
	CI	.0067	.0058	.0058	.0058	.0058	.0058
	Res	-.0109 *	.0030	-.0009	.0025	.0027	.0036
0°1' to 0°21'	Obs	.0191	.0064	.0071	.0045	.0042	.0069
	Exp	.0199	.0061	.0083	.0042	.0047	.0048
	CI	.0067	.0058	.0058	.0058	.0058	.0058
	Res	-.0008	.0002	-.0011	.0002	-.0006	.0021
0°22' to 0°43'	Obs	.0098	.0084	.0060	.0059	.0057	.0073
	Exp	.0191	.0053	.0074	.0034	.0039	.0039
	CI	.0067	.0058	.0058	.0058	.0058	.0058
	Res	-.0093 *	.0031	-.0015	.0025	.0018	.0033
0°44' to 1°5'	Obs	.0528	.0197	.0163	.0086	.0090	.0128
	Exp	.0317	.0180	.0201	.0161	.0166	.0166
	CI	.0007	.0058	.0058	.0058	.0058	.0058
	Res	.0210 *	.0017	-.0033	-.0075 *	-.0075 *	-.0038
1°6' to 1°27'	Obs		.0035	.0097	.0058	.0043	.0035
	Exp		.0059	.0080	.0040	.0045	.0045
	CI		.0060	.0060	.0060	.0060	.0060
	Res		-.0023	.0017	.0018	.0002	.0010
1°28' to 1°49'	Obs		.0076	.0143	.0058	.0143	.0077
	Exp		.0104	.0126	.0085	.0090	.0091
	CI		.0060	.0060	.0060	.0060	.0060
	Res		-.0028	.0017	-.0028	.0052	-.0014
1°50' to 2°11'	Obs		.0079	.0093	.0086	.0069	.0040
	Exp		.0078	.0100	.0060	.0065	.0065
	CI		.0060	.0060	.0060	.0060	.0060
	Res		.0001	-.0007	.0026	.0005	-.0025
2°12' to 2°23'	Obs		.0080	.0179	.0099	.0077	.0093
	Exp		.0110	.0133	.0092	.0097	.0097
	CI		.0060	.0060	.0060	.0060	.0060
	Res		-.0030	.0046	.0007	-.0019	-.0004

* Statistically significant at .95 level.

195

Table A-28

OHIO TURNPIKE CURVE & GRADE ANALYSIS

(Wet-Road Relative Crash Rate)

Grade in Percent

Curvatures		-2.5 to -3.5	-1.5 to -2.4	-0.7 to -1.4	-0.6 to +0.6	+0.7 to +1.4	+1.5 to +2.4
0°0'	Obs	.0039	.0025	.0015	.0016	.0017	.0018
	Exp	.0116	.0013	.0025	0	0	0
	CI	.0068	.0059	.0059	.0059	.0059	.0059
	Res	-.0076 *	.0013	-.0009	.0017	.0028	.0027
0°1' to 0°21'	Obs	.0032	.0032	.0028	.0021	.0019	.0027
	Exp	.0120	.0017	.0029	.0003	0	0
	CI	.0068	.0059	.0059	.0059	.0059	.0059
	Res	-.0088 *	.0015	-.0002	.0018	.0026	.0031
0°22' to 0°43'	Obs	.0059	.0030	.0035	.0031	.0030	.0020
	Exp	.0128	.0025	.0037	.0011	.0002	.0003
	CI	.0068	.0059	.0059	.0059	.0059	.0059
	Res	-.0069 *	.0053	-.0002	.0020	.0028	.0017
0°44' to 1°5'	Obs	.0489	.0128	.0144	.0057	.0073	.0083
	Exp	.0256	.0153	.0165	.0139	.0130	.0131
	CI	.0068	.0059	.005`	.0059	.0059	.0059
	Res	.0233 *	-.0025	-.0022	-.0082 *	-.0056	-.0048
1°6' to 1°27'	Obs		.0021	.0019	.0030	0	.0007
	Exp		.0025	.0037	.0011	.0062	.0003
	CI		.0061	.0061	.0061	.0061	.0061
	Res		-.0004	-.0018	.0019	-.0002	.0004
1°28' to 1°49'	Obs		.0046	.0143	.0027	.0029	0
	Exp		.0052	.0065	.0038	.0029	.0031
	CI		.0061	.0061	.0061	.0061	.0061
	Res		-.0007	.0078 *	-.0011	-.0029	-.0031
1°50' to 2°11'	Obs		.0048	.0023	.0024	0	0
	Exp		.0028	.0041	.0014	.0005	.0006
	CI		.0061	.0061	.0061	.0061	.0061
	Res		.0019	-.0017	-.0010	-.0005	-.0006
2°12' to 2°23'	Obs		.0027	.0047	.0037	.003-	.0027
	Exp		.0043	.0055	.0029	.0020	.0021
	CI		.0061	.0061	.0061	.0061	.0061
	Res		-.0016	-.0009	.0008	.0011	.0006

196

Table A-29

PENNSYLVANIA TURNPIKE CURVE & GRADE ANALYSIS

(All Crashes)

Grade in Percent

Curvatures		-2.5 to -4.0	-1.5 to -2.4	-0.7 to -1.4	-0.6 to +0.6	+0.7 to +1.4	+1.5 to +2.4	+2.5 to +3.5
0°0'	Obs	.0160	.0119	.0107	.0111	.0101	.0112	.0164
	Exp	.0160	.0164	.0097	.0155	.0082	.0108	.0109
	CI	.0079	.0084	.0079	.0081	.0079	.0084	.0079
	Res	.0000	.0045	.0010	-.0043	.0018	.0004	.0055
0°1' to 0°43'	Obs	.0140	.0085	.0090	.0071	.0077	.0117	.0122
	Exp	.0135	.0139	.0072	.0130	.0057	.0083	.0085
	CI	.0079	.0084	.0079	.0081	.0079	.0084	.0079
	Res	.0005	-.0054	.0017	-.0059	.0019	.0034	.0037
0°44' to 1°49'	Obs	.0177	.0164	.0159	.0172	.0194	.0160	.0151
	Exp	.0203	.0207	.0140	.0198	.0125	.0151	.0153
	CI	.0079	.0084	.0079	.0081	.0079	.0084	.0079
	Res	-.0026	-.0043	.0019	-.0025	.0068	.0009	-.0001
1°50' to 2°33'	Obs	.0249	.0314	.0135	.0216	.0263	.0187	.0201
	Exp	.0250	.0254	.0127	.0244	.0172	.0198	.0199
	CI	.0079	.0084	.0079	.0067	.0079	.0084	.0079
	Res	-.0011	.0077	-.0024	-.0012	.0028	-.0014	.0012
2°34' to 3°22'	Obs	.0249	.0314	.0185	.0216	.0263	.0187	.0201
	Exp	.0265	.0270	.0203	.0260	.0188	.0213	.0215
	CI	.0079	.0084	.0079	.0081	.0079	.0084	.0079
	Res	-.0016	.0044	-.0018	-.0044	.0075	-.0027	-.0014
3°23' to 4°12'	Obs	.0341	.0282	.0180	.0143	.0207	.0198	.0217
	Exp	.0256	.0270	.0203	.0260	.0188	.0213	.0215
	CI	.0079	.0084	.0079	.0081	.0079	.0084	.0079
	Res	.0086 *	.0022	-.0033	-.0198 *	.0028	-.0006	.0012
4°13' to 4°59'	Obs	.0319		.0486		.0184		.0247
	Exp	.0357		.0294		.0279		.0306
	CI	.0092		.0092		.0092		.0092
	Res	.0038		.0192 *		-.0095		-.0059
5°00' to 6°00'	Obs	.0401		.0176	.0687	.0237		.0310
	Exp	.0401		.0339	.0396	.0324		.0351
	CI	.0086		.0086	.0088	.0086		.0086
	Res	-.0000		-.0163 *	.0291 *	-.0087 *		-.0041

197

Table A-30

PENNSYLVANIA TURNPIKE CURVE & GRADE ANALYSIS

(Single-Vehicle Relative Crash Rate)

Grade in Percent

Curvatures		-2.5 to -4.0	-1.5 to -2.4	-0.7 to -1.4	-0.6 to +0.6	+0.7 to +1.4	+1.5 to +2.4	+2.5 to +3.5
0°0'	Obs	.0088	.0063	.0061	.0061	.0052	.0063	.0069
	Exp	.0088	.0091	.0069	.0096	.0028	.0060	.0025
	CI	.0071	.0075	.0071	.0073	.0071	.0075	.0071
	Res	.0000	-.0028	-.0008	-.0035	.0024	.0003	.0044
0°1' t8 0°43'	Obs	.0072	.0058	.0042	.0042	.0045	.0069	.0054
	Exp	.0078	.0081	.0058	.0085	.0018	.0049	.0014
	CI	.0071	.0075	.0071	.0073	.0071	.0075	.0071
	Res	-.0006	-.0023	-.0016	-.0043	.0027	.0020	.0040
0°44' t8 1°49'	Obs	.0130	.0118	.0115	.0127	.0143	.0102	.0084
	Exp	.0139	.0143	.0121	.0147	.0080	.0112	.0076
	CI	.0071	.0075	.0071	.0073	.0071	.0075	.0071
	Res	-.0009	-.0025	-.0006	-.0020	.0063	-.0010	.0008
1°50' t8 2°33'	Obs	.0158	.0235	.0111	.0164	.0100	.0145	.0096
	Exp	.0167	.0170	.0148	.0175	.0107	.0139	.0104
	CI	.0071	.0075	.0071	.0073	.0071	.0075	.0071
	Res	-.0009	.0065	-.0037	-.0011	-.0007	.0006	-.0008
2°34' t8 3°22'	Obs	.0160	.0232	.0132	.0163	.0172	.0130	.0090
	Exp	.0177	.0182	.0158	.0185	.0117	.0149	.0113
	CI	.0071	.0075	.0071	.0073	.0071	.0075	.0071
	Res	-.0017	.0052	-.0026	-.0022	.0055	-.0019	-.0023
3°23' t8 4°12'	Obs	.0242	.0124	.0113	.0092	.0141	.0136	.0133
	Exp	.0163	.0166	.0144	.0171	.0103	.0136	.0101
	CI	.0071	.0075	.0071	.0073	.0071	.0075	.0071
	Res	.0079 *	-.0042	-.0031 *	-.0079 *	.0038	.0000	.0034
4°13' t8 4°59'	Obs	.0179		.0446		.0037		.0095
	Exp	.0224		.0206		.0165		.0161
	CI	.0083		.0083		.0083		.0071
	Res	.0015		-.0240 *		-.0128 *		-.0066
5°00' t8 6°00'	Obs	.0026		.0117	.0471	.0119		.0159
	Exp	.0018		.0233	.0260	.0192		.0188
	CI	.0077		.0077	.0079	.0077		.0071
	Res	.0008		-.0116 *	-.0211 *	-.0073		-.0029

* Statistically significant @ .95 level.

198

Table A-31

PENNSYLVANIA TURNPIKE CURVE & GRADE ANALYSIS

(Wet-Road Relative Crash Rate)

Grade in Percent

Curvatures		-2.5 to -4.0	-1.5 to -2.4	-0.7 to -1.4	-0.6 to +0.6	+0.7 to +1.4	+1.5 to +2.4	+2.5 to +3.5
0°0'	Obs	.0052	.0028	.0028	.0034	.0026	.0033	.0049
	Exp	.0030	.0058	.0016	.0075	.0015	.0030	.0021
	CI	.0049	.0052	.0049	.0050	.0049	.0052	.0049
	Res	.0012	-.0029	.0012	-.0038	.0011	.0003	.0028
0°1' to 0°43'	Obs	.0033	.0032	.0016	.0020	.0024	.0040	.0042
	Exp	.0033	.0051	.0003	.0068	.0008	.0023	.0014
	CI	.0049	.0052	.0049	.0050	.0049	.0052	.0049
	Res	.0000	-.0019	.0007	-.0048	.0015	.0017	.0028
0°44' to 1°49'	Obs	.0096	.0087	.0072	.0091	.0114	.0079	.0063
	Exp	.0089	.0107	.0066	.0125	.0065	.0080	.0071
	CI	.0049	.0052	.0049	.0050	.0049	.0052	.0049
	Res	.0007	-.0020	.0006	-.0034	.0049	-.0001	-.0007
1°50' to 2°33'	Obs	.0098	.0176*	.0059	.0121	.0073	.0080	.0062
	Exp	.0099	.0117	.0076	.0134	.0075	.0089	.0080
	CI	.0049	.0052	.0043	.0050	.0049	.0052	.0049
	Res	-.0001	.0059	-.0016	-.0013	-.0001	-.0009	-.0018
2°34' to 3°22'	Obs	.0091	.0118	.0073	.0104	.0090	.0057	.0055
	Exp	.0087	.0105	.0064	.0123	.0063	.0078	.0069
	CI	.0049	.0052	.0049	.0050	.0049	.0052	.0049
	Res	.0004	.0012	.0009	-.0019	.0028	-.0021	-.0014
3°23' to 4°12'	Obs	.0151*	.0113	.0047	.0076*	.0084	.0099	.0086
	Exp	.0097	.0115	.0073	.0132	.0072	.0087	.0078
	CI	.0049	.0052	.0049	.0050	.0049	.0052	.0049
	Res	.0054	-.0002	-.0026	-.0057	.0012	.0011	.0008
4°13' to 4°59'	Obs	.0100		.0162*		.0037		.0076
	Exp	.0110		.0087		.0086		.0092
	CI	.0057		.0057		.0057		.0057
	Res	.0010		.0075		-.0049		-.0015
5°00' to 6°00'	Obs	.0083*		.0059*	.0393*	.0059*		.0120
	Exp	.0149		.0125	.0184	.0124		.0130
	CI	.0053		.0053	.0054	.0053		.0053
	Res	-.0066		-.0067	.0208	-.0065		-.0010

199

Table A-32

PENNSYLVANIA TURNPIKE CURVE & GRADE ANALYSIS

(All Crashes)

Grade in Percent

Curvatures		-2.5 to -4.0	-1.5 to -2.4	-0.7 to -1.4	-0.6 to +0.6	+0.7 to +1.4	+1.5 to +2.4	+2.5 to +3.5
0°0'	Obs	.0160	.0119	.0107	.0111	.0101	.0112	.0165
	Exp	.0155	.0164	.0096	.0148	.0097	.0113	.0101
	CI	.0060	.0059	.0060	.0059	.0060	.0060	.0059
	Res	.0005	-.0045	.0011	-.0037	.0003	-.0001	.0064 *
0°1' to 0°21'	Obs	.0136	.0090	.0000	.0054	.0000	.0034	.0162
	Exp	.0099	.0107	.0039	.0091	.0040	.0056	.0044
	CI	.0060	.0059	.0060	.0059	.0060	.0060	.0059
	Res	.0038	-.0017	-.0039	-.0038	-.0040	-.0022	.0118
0°22' to 0°43'	Obs	.0141	.0085	.0091	.0076	.0078	.0123	.0118
	Exp	.0132	.0141	.0073	.0125	.0074	.0090	.0078
	CI	.0060	.0059	.0060	.0059	.0060	.0060	.0059
	Res	.0009	-.0056	.0019	-.0049	.0004	.0034	.0040
0°44' to 1°5'	Obs	.0146	.0163	.0124	.0138	.0130	.0112	.0016
	Exp	.0149	.0158	.0090	.0142	.0091	.0106	.0095
	CI	.0060	.0059	.0060	.0059	.0060	.0060	.0059
	Res	-.0003	.0005	.0035	-.0004	.0039	.0006	-.0079 *
1°6' to 1°27'	Obs	.0190	.0239	.0239	.0280	.0230	.0269	.0089
	Exp	.0250	.0259	.0191	.0243	.0192	.0207	.0196
	CI	.0060	.0059	.0060	.0059	.0060	.0060	.0059
	Res	-.0060 *	-.0020	.0049	.0038	.0038	.0062 *	-.0107 *
1°28' to 1°49'	Obs	.0201	.0156	.0190	.0223	.0291	.0189	.0156
	Exp	.0231	.0240	.0172	.0224	.0173	.0189	.0177
	CI	.0060	.0059	.0060	.0059	.0060	.0060	.0059
	Res	-.0030	-.0084 *	.0018	-.0002	.0118 *	.0000	-.0021
1°50' to 2°11'	Obs	.0206	.0300	.0148	.0247	.0159	.0219	.0228
	Exp	.0246	.0254	.0186	.0238	.0187	.0203	.0191
	CI	.0060	.0059	.0060	.0059	.0060	.0060	.0059
	Res	-.0040	.0045	-.0038	.0008	-.0028	.0016	.0036

Table A-32   (Continued)

Pennsylvania Turnpike Curve & Grade Analysis - All Crashes

Curvatures		-2.5 to -4.0	-1.5 to -2.4	-0.7 to 1.4	-0.6 to +0.6	+0.7 to +1.4	+1.5 to +2.4	+2.5 to +3.5
2°12' to 2°33'	Obs	.0283	.0361	.0176	.0217	.0130	.0150	.0190
	Exp	.0246	.0255	.0187	.0239	.0188	.0203	.0191
	CI	.0060	.0059	.0060	.0059	.0060	.0060	.0059
	Res	.0037	.0106	-.0010	-.0022	-.0058	-.0053	-.0001
2°34' to 3°22'	Obs	.0249	.0314	.0185	.0216	.0263	.0187	.0201
	Exp	.0261	.0270	.0202	.0254	.0203	.0218	.0201
	CI	.0060	.0059	.0060	.0059	.0060	.0060	.0059
	Res	-.0012	.0044	-.0017	-.0038	.0060 *	-.0032	-.0000
3°23' to 4°12'	Obs	.0341	.0282	.0160	.0143	.0207	.0198	.0217
	Exp	.0251	.0260	.0192	.0244	.0193	.0209	.0197
	CI	.0060	.0059	.0060	.0059	.0060	.0060	.0059
	Res	.0090 *	.0022	-.0032	-.0102 *	.0013	-.0011	.0020
4°13' to 6°00'	Obs	.0378		.0359	.0548	.0204		.0292
	Exp	.0412		.0353	.0405	.0354		.0358
	CI	.0066	.0071	.0071	.0065	.0066		.0071
	Res	-.0034	.0006	.0006	.0243 *	-.0150 *		-.0066

* Statistically significant @ .95 level.

201

Table A-33

PENNSYLVANIA TURNPIKE CURVE & GRADE ANALYSIS
(Single-Vehicle Relative Crash Rate)
Grade in Percent

Curvatures		-2.5 to -4.0	-1.5 to -2.4	-0.7 to -1.4	-0.6 to +0.6	+0.7 to +1.4	+1.5 to +2.4	+2.5 to +3.5
0°0'	Obs	.0088	.0063	.0061	.0061	.0052	.0063	.0069
	Exp	.0084	.0093	.0057	.0096	.0046	.0062	.0020
	CI	.0049	.0048	.0049	.0048	.0049	.0049	.0048
	Res	.0004	-.0030	.0004	-.0035	.0006	.0001	.0049
0°1' to 0°21'	Obs	.0034	.0036	0.0	.0018	0.0	0.0	.0032
	Exp	.0036	.0045	.0009	.0048	-.0002	.0014	-.0028
	CI	.0049	.0048	.0049	.0048	.0049	.0049	.0048
	Res	-.0002	-.0009	-.0009	-.0030	.0002	-.0014	.0060 *
0°22' to 0°43'	Obs	.0075	.0059	.0043	.0050	.0045	.0074	.0056
	Exp	.0076	.0085	.0049	.0088	.0039	.0054	.0012
	CI	.0049	.0048	.0049	.0048	.0049	.0049	.0048
	Res	-.0001	-.0026	-.0006	-.0038	.0006	.0020	.0044
0°44' to 1°5'	Obs	.0100	.0117	.0079	.0090	.0087	.0066	.0008
	Exp	.0096	.0105	.0070	.0109	.0059	.0074	.0033
	CI	.0049	.0048	.0049	.0048	.0049	.0049	.0048
	Res	.0003	.0012	.0009	-.0019	.0028	-.0008	-.0025
1°6' to 1°27'	Obs	.0164	.0179	.0154	.0252	.0156	.0199	.0057
	Exp	.0184	.0193	.0158	.0196	.0147	.0162	.0121
	CI	.0046	.0048	.0049	.0048	.0049	.0049	.0048
	Res	-.0020	-.0014	-.0004	-.0056	.0009	.0037	-.0064
1°28' to 1°49'	Obs	.0151	.0111	.0162	.0179	.0237	.0121	.0092
	Exp	.0169	.0178	.0142	.0181	.0131	.0147	.0105
	CI	.0049	.0048	.0049	.0048	.0049	.0049	.0048
	Res	-.0018	-.0067 *	.0020	-.0002	.0105 *	-.0026	-.0013
1°50' to 2°11'	Obs	.0141	.0193	.0099	.0195	.0109	.0167	.0087
	Exp	.0160	.0166	.0132	.0172	.0123	.0138	.0096
	CI	.0049	.0048	.0049	.0048	.0049	.0049	.0048
	Res	-.0019	.0024	-.0034	.0023	-.0014	.0029	-.0009

Table A-33 (Continued)

Pennsylvania Turnpike Curve & Grade Analysis – Single-Vehicle Relative Crash Rate

Curvatures		-2.5 to -4.0	-1.5 to -2.4	-0.7 to -1.4	-0.6 to +0.6	+0.7 to +1.4	+1.5 to +2.4	+2.5 to +3.5
2°12' to 2°33'	Obs	.0179	.0276	.0123	.0132	.0092	.0125	.0106
	Exp	.0166	.0175	.0139	.0178	.0129	.0144	.0102
	CI	.0049	.0048	.0049	.0048	.0049	.0049	.0048
	Res	.0013	.0101 *	-.0016	-.0046	-.0037	-.0019	.0004
2°34' t8 3°22'	Obs.	.0160	.0232	.0132	.0163	.0172	.0130	.0088
	Exp	.0172	.0181	.0146	.0184	.0135	.0150	.0108
	CI	.0049	.0048	.0049	.0048	.0049	.0049	.0048
	Res	-.0013	.0051 *	-.0014	-.0022	.0037	-.0020	-.0020
3°23' t8 4°12'	Obs	.0242	.0124	.0113	.0092	.0141	.0136	.0133
	Exp	.0159	.0168	.0132	.0171	.0121	.0137	.0095
	CI	.0049	.0048	.0049	.0048	.0049	.0049	.0048
	Res	.0083 *	-.0044	-.0019	-.0079 *	.0020	-.0001	.0038
4°13' t8 6°00'	Obs	.0237		.0311	.0471	.0068	.0140	.0140
	Exp	.0269		.0247	.0281	.0231	.0205	.0205
	CI	.0054		.0058	.0053	.0054	.0053	.0053
	Res	-.0032		.0069 *	.0190 *	-.0163 *	-.0065 *	-.0065 *

* Statistically significant @ .95 level.

203

Table A-34

PENNSYLVANIA TURNPIKE CURVE & GRADE ANALYSIS

(Wet-Road Relative Crash Rate)

Grade in Percent

Curvatures		-2.5 to -4.0	-1.5 to -2.4	-0.7 to -1.4	-0.6 to +0.6	+0.7 to +1.4	+1.5 to +2.4	+2.5 to +3.5
0°0'	Obs	.0052	.0028	.0028	.0037	.0026	.0033	.0049
	Exp	.0039	.0061	.0014	.0071	.0032	.0026	.0010
	CI	.0041	.0040	.0041	.0040	.0041	.0041	.0040
	Res	.0013	-.0033	.0014	-.0034	-.0006	.0007	.0039
0°1' to 0°21'	Obs	0.0	.0036	0.0	.0015	0.0	0.0	.0032
	Exp	.0015	.0036	-.0010	.0047	.0008	.0003	-.0014
	CI	.0041	.0040	.0041	.0040	.0041	.0041	.0040
	Res	-.0015	.0000	.0010	-.0032	-.0008	-.0003	.0046 *
0°22' to 0°43'	Obs	.0036	.0032	.0016	.0021	.0024	.0043	.0044
	Exp	.0034	.0055	.0009	.0066	.0026	.0021	.0004
	CI	.0041	.0040	.0041	.0040	.0041	.0041	.0040
	Res	.0002	-.0023	.0007	-.0045 *	-.0002	.0022	.0040 *
0°44' to 1°5'	Obs	.0062	.0078	.0044	.0061	.0058	.0051	.0007
	Exp	.0055	.0076	.0030	.0087	.0047	.0042	.0025
	CI	.0041	.0040	.0041	.0040	.0041	.0041	.0040
	Res	.0007	.0002	.0014	-.0026	.0011	.0009	-.0018
1°6' to 1°27'	Obs	.0130	.0143	.0100	.0202	.0189	.0105	.0040
	Exp	.0133	.0154	.0108	.0165	.0126	.0120	.0104
	CI	.0041	.0040	.0041	.0040	.0041	.0041	.0040
	Res	-.0003	-.0011	-.0008	.0037	.0063 *	-.0015	-.0064 *
1°28' to 1°49'	Obs.	.0120	.0087	.0109	.0130	.0185	.0101	.0061
	Exp	.0116	.0138	.0091	.0148	.0109	.0104	.0087
	CI	.0041	.0040	.0041	.0040	.0041	.0041	.0040
	Res	.0004	-.0051 *	.0018	-.0018	.0076 *	-.0003	-.0026
1°50' to 2°11'	Obs	.0086	.0155	.0058	.0144	.0086	.0101	.0059
	Exp	.0101	.0123	.0076	.0133	.0094	.0089	.0072
	CI	.0041	.0040	.0041	.0040	.0041	.0041	.0040
	Res	-.0015	.0032	-.0018	.0011	-.0008	.0012	-.0013

Table A-34 (Continued)

Pennsylvania Turnpike Curve & Grade Analysis – Wet-Road Relative Crash Rate

Curvature		-2.5 to -4.0	-.15 to -2.4	-0.7 to -1.4	-0.6 to +0.6	+0.7 to +1.4	+1.5 to +2.4	+2.5 to +3.5
2°12' to 2°33'	Obs	.0113	.0198	.0061	.0097	.0061	.0059	.0067
	Exp	.0097	.0118	.0072	.0129	.0090	.0084	.0068
	CI	.0041	.0040	.0041	.0040	.0041	.0041	.0040
	Res	.0016	.0080 *	-.0011	-.0032	-.0029	-.0025	-.0001
2°34' to 3°22'	Obs	.0091	.0118	.0073	.0104	.0090	.0057	.0055
	Exp	.0087	.0108	.0062	.0119	.0080	.0075	.0058
	CI	.0041	.0040	.0041	.0040	.0041	.0041	.0040
	Res	.0004	.0010	.0011	-.0015	.0010	-.0018	-.0003
3°23' to 4°12'	Obs	.0151	.0113	.0047	.0076	.0085	.0099	.0086
	Exp	.0097	.0118	.0072	.0129	.0089	.0084	.0067
	CI	.0041 *	.0040	.0041	.0040	.0041	.0041	.0040
	Res	.0054	-.0005	-.0025	-.0053 *	-.0004	.0015	.0019
4°13' to 6°00'	Obs	.0087		.0120	.0393	.0045		.0107
	Exp	.0156		.0132	.0188	.0149		.0127
	CI	.0045		.0048	.0044	.0045		.0040
	Res	-.0069		-.0012	.0205	-.0104		-.0020

* Statistically significant @ .95 level.

Table A-35

OHIO TURNPIKE SUPERELEVATION & GRADE ANALYSIS

(All Crashes)

Grade in Percent

Superelevation in inches/foot		-2.5 to -3.5	-1.5 to -2.4	-0.7 to -1.4	-0.6 to +0.6	+0.7 to +1.4	+1.4 to +2.5
3/16 on tangents	Obs	.0097	.0119	.0115	.0082	.0081	.0128
	Exp	.0189	.0144	.0068	.0066	.0087	.0058
	CI	.0130	.0166	.0130	.0130	.0147	.0147
	Res	-.0102	-.0024	.0047	.0016	-.0006	.0070
3/16 on curves	Obs	.0347	.0137	.0085	.0081	.0118	.0133
	Exp	.0245	.0190	.0115	.0112	.0134	.0104
	CI	.0130	.0166	.0130	.0130	.0147	.0147
	Res	.0102	-.0053	-.0030	-.0031	-.0016	.0029
5/16	Obs				.0039		
	Exp				.0039		
	CI				.0257		
	Res				.0000		
7/16	Obs		.0503	.0072	.0079		.0051
	Exp		.0236	.0161	.0158		.0150
	CI		.0203	.0139	.0139		.0153
	Res		.0276*	-.0089	-.0079		-.0099
12/16	Obs		.0072	.0058	.0105		
	Exp		.0129	.0054	.0051		
	CI		.0205	.0149	.0149		
	Res		-.0057	.0004	.0053		
16/16	Obs		.0067	.0191	.0160	.0164	
	Exp		.0198	.0123	.0120	.0142	
	CI		.0203	.0139	.0139	.0153	
	Res		-.0131	.0068	.0040	.0022	

* Statistically significant @ .95 level.

206

Table A-36

OHIO TURNPIKE SUPERELEVATION & GRADE ANALYSIS
(Single Vehicle Relative Crash Rate)

Grade in Percent

Superelevation in inches/foot		-2.5 to -3.5	-1.5 to -2.4	-0.7 to -1.4	-0.6 to -0.6	+1.4 to +0.7	+2.5 to +1.5
3/16 on tangent	Obs	.0046	.0076	.0073	.0056	.0055	.0078
	Exp	.0136	.0089	.0042	.0037	.0053	.0028
	CI	.0123	.0096	.0096	.0096	.0109	.0109
	Res	-.0091	-.0012	.0031	.0019	.0003	.0050
3/16 on curve	Obs	.0270	.0099	.0057	.0057	.0071	.0089
	Exp	.0179	.0132	.0085	.0080	.0096	.0071
	CI	.0123	.0096	.0096	.0096	.0109	.0109
	Res	.0091	-.0033	-.0028	-.0023	-.0025	.0018
5/16	Obs				.0020		
	Exp				.0020		
	CI				.0161		
	Res				.0000		
7/16	Obs		.0359	.0072	.0058		.0043
	Exp		.0173	.0125	.0121		.0112
	CI		.0103	.0103	.0103		.0113
	Res		.0187 *	-.0054	-.0063		-.0069
12/16	Obs		.0040	.0046	.0086		
	Exp		.0090	.0043	.0038		
	CI		.0110	.0110	.0110		
	Res		-.0050	.0003	.0047		
16/16	Obs		.0040	.0133	.0099	.0117	
	Exp		.0131	.0084	.0079	.0095	
	CI		.0103	.0103	.0103	.0113	
	Res		-.0091	.0049	.0020	.0022	

* Statistically significant @ .95 level.

Table A-37

OHIO TURNPIKE SUPERELEVATION & GRADE ANALYSIS
(Wet-Road Relative Crash Rate)

Grade in Percent

Superelevation in inches/foot		-2.5 to -3.5	-1.5 to -2.4	-0.7 to -1.4	-0.6 to +0.6	+0.7 to +1.4	+1.4 to +2.5
3/16 on tangent	Obs	.0023	.0024	.0018	.0016	.0015	.0019
	Exp	.0085	.0037	.0005	-.0003	.0011	-.0020
	CI	.0073	.0057	.0057	.0057	.0065	.0065
	Res	-.0062	-.0012	.0013	.0018	.0004	.0039
3/16 on curve	Obs	.0193	.0053	.0035	.0030	.0039	.0041
	Exp	.0131	.0083	.0051	.0043	.0058	.0026
	CI	.0073	.0057	.0057	.0057	.0064	.0065
	Res	.0062	-.0029	-.0016	-.0013	-.0019	.0015
5/16	Obs				.0020		
	Exp				.0020		
	CI				.0096		
	Res				.0000		
7/16	Obs		.0216	.0072	.0027		.0000
	Exp		.0110	.0079	.0071		.0054
	CI		.0062	.0062	.0062		.0068
	Res		.0105 *	-.0007	-.0044		-.0054
12/16	Obs		.0024	.0012	.0024		
	Exp		.0044	.0012	.0004		
	CI		.0066	.0066	.0066		
	Res		-.0020	.0000	.0020		
16/16	Obs		.0013	.0035	.0037	.0047	
	Exp		.0057	.0025	.0018	.0032	
	CI		.0062	.0062	.0062	.0068	
	Res		-.0044	.0010	.0019	.0015	

* Statistically significant @ .95 level,

208

Table A-58

PENNSYLVANIA TURNPIKE SUPERELEVATION & GRADE ANALYSIS
(All Crashes)

Grade in Percent

Superelevation in inches/foot		-2.5 to -4.0	-1.5 to -2.4	-0.7 to -1.4	-0.6 to +0.6	+0.7 to +1.4	+1.5 to +2.4	+2.5 to +3.5
1/6 on tangents	Obs	.0150	.0136	.0109	.0111	.0098	.0100	.0176
	Exp	.0175	.0186	.0060	.0140	.0146	.0054	.0120
	CI	.0122	.0125	.0126	.0122	.0127	.0121	.0122
	Res	-.0025	-.0049	.0049	-.0029	-.0048	.0046	.0055
1/6 on curves	Obs	.0162	.0120	.0092	.0108	.0135	.0119	.0128
	Exp	.0173	.0183	.0058	.0138	.0144	.0051	.0118
	CI	.0122	.0125	.0126	.0122	.0127	.0121	.0122
	Res	-.0109	-.0063	.0035	-.0030	-.0087	.0068	.0010
4/16	Obs	.0164	.0246	.0277	.0228	.0194	.0166	.0174
	Exp	.0256	.0267	.0141	.0221	.0227	.0135	.0202
	CI	.0122	.0125	.0126	.0122	.0127	.0121	.0122
	Res	-.0092	-.0021	.0135 *	.0007	-.0033	.0031	-.0027
5/16	Obs	.0254	.0101	.0114	.0227	.0599	.0173	.0138
	Exp	.0279	.0289	.0164	.0244	.0250	.0158	.0224
	CI	.0122	.0125	.0126	.0122	.0127	.0121	.0122
	Res	-.0025	-.0189 *	-.0050	-.0016	.0349 *	.0016	-.0086
6/16	Obs	.0165	.0252	.0107	.0247	.0253	.0270	.0301
	Exp	.0277	.0287	.0162	.0242	.0248	.0156	.0222
	CI	.0122	.0125	.0126	.0122	.0127	.0121	.0122
	Res	-.0112	-.0035	-.0055	.0005	.0005	.0114	.0079
7/16	Obs	.0145			.0201	.0092	.0049	
	Exp	.0178			.0143	.0149	.0057	
	CI	.0146			.0146	.0149	.0146	
	Res	-.0033			.0058	-.0057	.0032	
9/16	Obs	.0196	.0636	.0166	.0218	.0124	.0096	.0352
	Exp	.0304	.0315	.0189	.0270	.0275	.0183	.0250
	CI	.0122	.0125	.0126	.0122	.0127	.0121	.0122
	Res	-.0109	.0321 *	-.0024	-.0052	-.0152 *	-.0088	.0102

209

Table A-38 (Continued)

Pennsylvania Turnpike Superelevation & Grade Analysis - All Crashes

Superelevation in inches/foot		-2.5 to -4.0	-1.5 to -2.4	-0.7 to -1.4	-0.6 to +0.6	+0.7 to +1.4	+1.5 to +2.4	+2.5 to +3.5
11/16	Obs	.0322			.0150		.0037	.0233
	Exp	.0238			.0203		.0117	.0183
	CI	.0146			.0146		.0145	.0146
	Res	.0083			-.0053		-.0080	.0050
12/16	Obs	.0206	.0386	.0139	.0218	.0389	.0164	.0248
	Exp	.0299	.0310	.0184	.0264	.0270	.0178	.0245
	CI	.0122	.0125	.0126	.0122	.0127	.0121	.0122
	Res	-.0094	.0077	-.0045	-.0046	.0119	-.0014	.0003
13/16	Obs						.0058	.0246
	Exp						.0119	.0185
	CI						.0191	.0191
	Res						-.0061	.0061
14/16	Obs	.0706	.0037	.0205	.0534		.0235	.0128
	Exp	.0360	.0371	.0245	.0325		.0239	.0305
	CI	.0128	.0130	.0132	.0128		.0127	.0127
	Res	.0346 *	-.0333 *	-.0040	.0209 *		-.0004	-.0177 *
15/16	Obs		.0061					.0061
	Exp		.0094					.0029
	CI		.0191					.0191
	Res		-.0033					.0033
16/16 to 19/16	Obs	.0444	.0709	.0253	.0287	.0169	.0193	.0215
	Exp	.0373	.0384	.0258	.0338	.0344	.0252	.0319
	CI	.0122	.0125	.0126	.0122	.0127	.0121	.0122
	Res	.0071	.0325 *	-.0006	-.0052	-.0175 *	-.0060	-.0103

* Statistically significant @ .95 level.

210

Table A-39

PENNSYLVANIA TURNPIKE SUPERELEVATION & GRADE ANALYSIS
(Wet-Road Relative Crash Rate)

Superelevation in inches/foot		Grade in Percent						
		-2.5 to -4.0	-1.5 to -2.4	-0.7 to -1.4	-0.6 to +0.6	+0.7 to +1.4	+1.5 to +2.4	+2.5 to +3.5
1/6 on tangent	Obs	.0049	.0032	.0023	.0037	.0025	.0029	.0052
	Exp	.0060	.0064	.0000	.0048	.0060	.0011	.0009
	CI	.0068	.0070	.0071	.0068	.0071	.0068	.0068
	Res	-.0011	-.0032	.0028	-.0012	-.0035	.0018	.0043
1/6 on curve	Obs	.0065	.0052	.0026	.0045	.0060	.0042	.0053
	Exp	.0073	.0077	.0013	.0061	.0073	.0024	.0021
	CI	.0068	.0070	.0071	.0068	.0071	.0068	.0068
	Res	-.0008	-.0025	.0013	-.0016	-.0013	.0018	.0031
4/16	Obs	.0090	.0147	.0170	.0132	.0127	.0095	.0071
	Exp	.0143	.0147	.0083	.0131	.0143	.0094	.0091
	CI	.0068	.0070	.0071	.0068	.0071	.0068	.0068
	Res	-.0052	-.0000	.0087 *	.0001	-.0016	.0001	-.0020
5/16	Obs	.0169	.0053	.0054	.0149	.0365	.0082	.0038
	Exp	.0154	.0158	.0094	.0142	.0154	.0105	.0102
	CI	.0068	.0070 *	.0071	.0068	.0071 *	.0068	.0068
	Res	.0016	-.0105	-.0040	.0007	.0211	-.0023	-.0065
6/16	Obs	.0069	.0130	.0041	.0144	.0136	.0121	.0078
	Exp	.0127	.0131	.0067	.0115	.0127	.0078	.0075
	CI	.0068	.0070	.0071	.0068	.0071	.0068	.0068
	Res	-.0057	-.0001	-.0025	.0029	.0009	.0043	.0002
7/16	Obs	0			.0034	.0020	.0059	
	Exp	.0043			.0032	.0043	.0005	
	CI	.0082			.0082	.0084	.0082	
	Res	-.0043			.0002	-.0023	.0064	
9/16	Obs	.0080	.0334	.0054	.0101	.0069	.0032	.0124
	Exp	.0137	.0141	.0077	.0126	.0137	.0089	.0086
	CI	.0068	.0070 *	.0071	.0068	.0071	.0068	.0068
	Res	-.0058	.0192	-.0023	-.0025	-.0068	-.0056	.0038

211

Pennsylvania Turnpike Superelevation & Grade Analysis - Wet-Road Relative Crash Rate

Superelevation in inches/foot		-2.5 to -4.0	-1.5 to -2.4	-0.7 to -1.4	-0.6 to +0.6	+0.7 to +1.4	+1.5 to +2.4	+2.5 to +3.5
11/16	Obs	.0133			.000		.000	.0075
	Exp	.0080			.0068		.0031	.0028
	CI	.0082			.0082		.0081	.0082
	Res	.0053			-.0068		-.0031	.0046
12/16	Obs	.0074	.0144	.0055	.0106	.0134	.0051	.0064
	Exp	.0114	.0118	.0054	.0102	.0114	.0065	.0062
	CI	.0068	.0070	.0071	.0068	.0071	.0068	.0068
	Res	-.0040	.0026	.0002	.0005	.0020	-.0014	.0001
13/16	Obs						.0000	.0058
	Exp						.0030	.0028
	CI						.0107	.0107
	Res						-.0030	.0030
14/16	Obs	.0429	.0000	.0117	.0229		.0176	.0048
	Exp	.0194	.0199	.0134	.0183		.0146	.0143
	CI	.0072	.0073	.0074	.0072		.0071	.0071
	Res	.0235 *	-.0199 *	-.0017	.0046		.0030	-.0095 *
15/16	Obs		.0061					.0000
	Exp		.0058					.0003
	CI		.0107					.0107
	Res		.0003					-.0003
16/16 to 19/16	Obs	.0112	.0290	.0061	.0166	.0060	.0077	.0084
	Exp	.0145	.0149	.0085	.0134	.0145	.0097	.0094
	CI	.0068	.0070	.0071	.0068	.0071	.0068	.0068
	Res	-.0034	.0141 *	-.0025	.0032	-.0085 *	-.0019	-.0010

* Statistically significant @ .95 level.

Table A-40

PENNSYLVANIA TURNPIKE SUPERELEVATION & GRADE ANALYSIS
(Single-Vehicle Relative Crash Rate)

Grade in Percent

Superelevation in inches/foot		-2.5 to -4.0	-1.5 to -2.4	-0.7 to -1.4	-0.6 to +0.6	+0.7 to +1.4	+1.5 to +2.4	+2.5 to +3.5
1/6 on tangent	Obs	.0083	.0072	.0062	.0061	.0051	.0056	.0073
	Exp	.0108	.0090	.0034	.0071	.0092	.0030	.0034
	CI	.0084	.0086	.0087	.0084	.0087	.0083	.0084
	Res	-.0026	-.0018	.0029	-.0010	-.0041	.0026	.0040
1/6 on curve	Obs	.0105	.0084	.0052	.0071	.0085	.0071	.0063
	Exp	.0119	.0100	.0044	.0081	.0102	.0040	.0044
	CI	.0084	.0086	.0087	.0084	.0087	.0083	.0084
	Res	-.0013	-.0016	.0008	-.0011	-.0017	.0031	.0019
4/16	Obs	.0121	.0169	.0237	.0188	.0155	.0108	.0099
	Exp	.0197	.0179	.0122	.0160	.0181	.0118	.0122
	CI	.0084	.0086	.0087 *	.0084	.0087	.0083	.0084
	Res	-.0076	-.0009	.0115	.0028	-.0025	-.0010	-.0023
5/16	Obs	.0194	.0085	.0096	.0182	.0495	.0128	.0094
	Exp	.0225	.0206	.0150	.0163	.0209	.0146	.0150
	CI	.0084	.0086 *	.0087	.0084	.0087 *	.0083	.0084
	Res	-.0031	-.0121	-.0054	-.0058	.0286	-.0018	-.0056
6/16	Obs	.0113	.0163	.0071	.0195	.0173	.0206	.0115
	Exp	.0191	.0173	.0116	.0154	.0175	.0112	.0116
	CI	.0084	.0086	.0087	.0084	.0087	.0083	.0084
	Res	-.0077	-.0010	-.0045	.0041	-.0002	.0094 *	-.0001
7/16	Obs	.0115			.0134	.0071	.0079	
	Exp	.0133			.0096	.0117	.0054	
	CI	.0101			.0101	.0103	.0101	
	Res	-.0018			.0038	-.0045	.0025	
9/16	Obs	.0123	.0412	.0112	.0132	.0084	.0078	.0197
	Exp	.0210	.0191	.0135	.0172	.0194	.0131	.0135
	CI	.0084	.0086	.0087	.0084	.0087 *	.0083	.0084
	Res	-.0037	.0251 *	-.0023	-.0041	-.0109 *	-.0053	.0062

Table A-40 (Continued)

Pennsylvania Turnpike Superelevation & Grade Analysis – Single Vehicle Relative Crash Rate

Superelevation in inches/foot		-2.5 to -4.0	-1.5 to -2.4	-0.7 to 1.4	-0.6 to +0.6	+0.7 to +1.4	+1.5 to +2.4	+2.5 to +3.5
11/16	Obs	.0266			.0000		.0037	.0130
	Exp	.0156			.0119		.0077	.0081
	CI	.0101			.0101		.0100	.0101
	Res	.0109 *		-.0119 *		-.0040	.0049	
12/16	Obs	.0127	.0287	.0099	.0166	.0255	.0115	.0105
	Exp	.0208	.0189	.0133	.0171	.0192	.0129	.0133
	CI	.0084	.0086	.0087	.0084	.0087	.0083	.0084
	Res	-.0081	.0098 *	-.0034	-.0004	.0064	-.0014	-.0028
13/16	Obs						.0000	.0072
	Exp						.0034	.0038
	CI						.0131	.0131
	Res						.0034	.0034
14/16	Obs	.0498	.0037	.0147	.0305		.0235	.0093
	Exp	.0266	.0248	.0192	.0229		.0188	.0192
	CI	.0088	.0090	.0091	.0088		.0087	.0088
	Res	.0232 *	-.0211 *	-.0045	.0076		.0047	-.0099
15/16	Obs		.0000					.0031
	Exp		.0044					.0013
	CI		.0132					.0132
	Res		-.0044					.0044
16/16 to 16/19	Obs	.0296	.0290	.0202	.0198	.0103	.0096	.0112
	Exp	.0228	.0210	.0153	.0191	.0212	.0149	.0153
	CI	.0084	.0086	.0087	.0084	.0087	.0083	.0084
	Res	.0068	.0080	.0048	.0007	-.0109 *	-.0053	-.0041

* Statistically significant @ .95 level.

214

Table A-41

OHIO TURNPIKE SIDE FORCE FACTOR - GRADE

All Accidents

Side Force Factor		Grade -2.5 to -3.5	-1.5 to -2.4	-0.7 to -1.4	-0.6 to +0.6	+0.7 to +1.4	+1.5 to +2.4
-0.015625 Tangents	Obs	0.01668*	0.01238	0.00969	0.00820	0.00932	0.01179
	Exp	0.02691	0.01094	0.01012	0.00585	0.00562	0.00863
	CI	0.0068	0.0067	0.0067	0.0068	0.0068	0.0068
	Res	-0.01023	0.00145	-0.00043	0.00235	0.00370	0.00316
-0.00517 to 0.00338	Obs	0.02866	0.01186	0.01091	0.00672	0.00894	0.01138
	Exp	0.02865	0.01267	0.01154	0.00758	0.00736	0.01036
	CI	0.0068	0.0067	0.0067	0.0068	0.0068	0.0068
	Res	0.00001	-0.00081	-0.00094	-0.00086	0.00158	0.00101
0.00813 to 0.01288	Obs	0.01230*	0.01100	0.00840	0.00866	0.00711	0.01067
	Exp	0.02526	0.00928	0.00846	0.00419	0.00397	0.00697
	CI	0.0068	0.0067	0.0067	0.0068	0.0068	0.0068
	Res	-0.01296	0.00171	-0.00007	0.00447	0.00315	0.00370
0.01763 to 0.02238	Obs	-------	0.01392	0.01092	0.00735	0.01138	0.01729
	Exp	-------	0.01488	0.01406	0.00979	0.00956	0.01257
	CI	-------	0.0067	0.0067	0.0068	0.0068	0.0068
	Res	-------	-0.00096	-0.00314	-0.00244	0.00182	0.00472
0.02714 to 0.03189	Obs	-------	0.02048	0.00903	0.00767	0.00304	0.01603
	Exp	-------	0.01396	0.01314	0.00886	0.00864	0.01165
	CI	-------	0.0067	0.0067	0.0068	0.0068	0.0068
	Res	-------	0.00652	-0.00411	-0.00120	-0.00560	0.00438
0.04139	Obs	0.06651*	0.02573	0.02549	0.01679	0.01500*	0.01707*
	Exp	0.04334	0.02736	0.02654	0.02227	0.02204	0.02505
	CI	0.0068	0.0067	0.0067	0.0068	0.0068	0.0068
	Res	0.02318	-0.00163	-0.00104	-0.00548	-0.00704	-0.00798

215

Table A-41 (Continued)

0.04906 to 0.05089	Obs	0.00860	0.01395	0.00810	0.00774	0.00576
	Exp	0.01154	0.01072	0.00644	0.00622	0.00923
	CI	0.0067	0.0067	0.0068	0.0068	0.0068
	Res	-0.00294	0.00323	0.00166	0.00152	-0.00347
0.05153 to 0.05920	Obs	0.01270	0.01272	0.01244	0.01160	0.00820
	Exp	0.01604	0.01522	0.01095	0.01072	0.01373
	CI	0.0096	0.0096	0.0108	0.0108	0.0108
	Res	-0.00334	0.00650	0.00149	0.00088	-0.00553

* Statistically significant @ .95 level.

216

Table A-42

OHIO TURNPIKE SIDE FORCE FACTOR - GRADE

Single-Vehicle Accidents

Side Force Factor		Grade					
		-2.5 to -3.5	-1.5 to -2.4	-0.7 to -1.4	-0.6 to +0.6	+0.7 to +1.4	+1.5 to +2.4
-0.015625 Tangents	Obs	0.00785*	0.00792	0.00619	0.00559	0.00638	0.00721
	Exp	0.01863	0.00680	0.00554	0.00298	0.00202	0.00518
	CI	0.0059	0.0058	0.0058	0.0059	0.0059	0.0059
	Res	-0.01078	0.00113	0.00064	0.00260	0.00437	0.00204
-0.00517 to 0.00338	Obs	0.01911	0.00635	0.00713	0.00446	0.00417	0.00677
	Exp	0.01977	0.00794	0.00668	0.00412	0.00316	0.00632
	CI	0.0059	0.0058	0.0058	0.0059	0.0059	0.0059
	Res	-0.00066	-0.00158	0.00045	0.00034	0.00101	0.00045
0.00813 to 0.01288	Obs	0.00984*	0.00718	0.00533	0.00593	0.00546	0.00600
	Exp	0.01839	0.00656	0.00531	0.00275	0.00178	0.00494
	CI	0.0059	0.0058	0.0058	0.0059	0.0059	0.0059
	Res	-0.00855	0.00062	0.00002	0.00318	0.00368	0.00106
0.01763 to 0.02238	Obs	-------	0.01392	0.00794	0.00583	0.00643	0.01522
	Exp	-------	0.01216	0.01091	0.00835	0.00738	0.01054
	CI	-------	0.0058	0.0058	0.0059	0.0059	0.0059
	Res	-------	0.00176	-0.00296	-0.00252	-0.00095	0.00468
0.02714 to 0.03189	Obs	-------	0.01718	0.00677	0.00511	0.00304	0.01480
	Exp	-------	0.01167	0.01042	0.00786	0.00689	0.01005
	CI	-------	0.0058	0.0058	0.0059	0.0059	0.0059
	Res	-------	0.00550	-0.00365	-0.00275	-0.00385	-0.00474
0.04139	Obs	0.05282*	0.02049	0.01763	0.01337	0.00975*	0.01227*
	Exp	0.03283	0.02100	0.01974	0.01718	0.01622	0.01938
	CI	0.0059	0.0058	0.0058	0.0059	0.0059	0.0059
	Res	0.01200	-0.00050	-0.00211	-0.00381	-0.00646	-0.00711

217

Table A-42 (Continued)

0.04906 to 0.05089	Obs	0.00573	0.00858	0.00602	0.00464	0.00432
	Exp	0.00816	0.00690	0.00434	0.00337	0.00653
	CI	0.0058	0.0058	0.0059	0.0059	0.0059
	Res	-0.00242	0.00169	0.00168	0.00129	-0.00222
0.05153 to 0.005920	Obs	0.00672	0.01589	0.00867	0.00738	0.00597
	Exp	0.01122	0.00997	0.00741	0.00644	0.00960
	CI	0.0083	0.0083	0.0093	0.0093	0.0093
	Res	-0.00498	0.00593	0.00127	0.00094	-0.00364

* Statistically significant at .95 level.

Table A-43

OHIO TURNPIKE SIDE FORCE FACTOR - GRADE

Wet-Road Accidents

Side Force Factor		Grade					
		-2.5 to -3.5	-1.5 to -2.4	-0.7 to -1.4	-0.6 to +0.6	+0.7 to +1.4	+1.5 to +2.4
-0.015625 Tangents	Obs	0.00393*	0.00254	0.00153	0.00157	0.00175	0.00180
	Exp	0.01129	0.00167	0.00129	-0.00009	-0.00084	-0.00021
	CI	0.0055	0.0054	0.0054	0.0055	0.0055	0.0055
	Res	-0.00736	0.00087	0.00024	0.00166	0.00259	0.00201
-0.00517 to 0.00338	Obs	0.00318*	0.00318	0.00276	0.00207	0.00194	0.00261
	Exp	0.01173	0.00211	0.00173	0.00035	0.00040	0.00023
	CI	0.0055	0.0054	0.0054	0.0055	0.0055	0.0055
	Res	-0.00854	0.00107	0.00104	0.00171	0.00233	0.00239
0.00813 to 0.01288	Obs	0.00590*	0.00220	0.00275	0.00296	0.00165	0.00167
	Exp	0.01196	0.00234	0.00196	0.00058	-0.00017	0.00046
	CI	0.0055	0.0054	0.0054	0.0055	0.0055	0.0055
	Res	-0.00605	-0.00014	0.00079	0.00238	0.00182	0.00121
0.01763 to 0.02238	Obs	-------	0.00696	0.00596	0.00347	0.00693	0.00415
	Exp	-------	0.00680	0.00642	0.00504	0.00429	0.00491
	CI	-------	0.0054	0.0054	0.0055	0.0055	0.0055
	Res	-------	0.00016	-0.00046	-0.00157	0.00264	-0.00076
0.02714 to 0.03189	Obs	-------	0.00528	0.00451	0.00234	0.0	0.00740
	Exp	-------	0.00522	0.00483	0.00356	0.00271	0.00333
	CI	-------	0.0054	0.0054	0.0055	0.0055	0.0055
	Res	-------	0.00007	-0.00032	-0.00111	-0.00271	0.00407
0.04139	Obs	0.04891*	0.01526	0.01574	0.01040	0.08250*	0.00854*
	Exp	0.02695	0.01734	0.01695	0.01558	0.01483	0.01545
	CI	0.0055	0.0054	0.0054	0.0055	0.0055	0.0055
	Res	0.02196	-0.00207	-0.00121	-0.00518	-0.00658	-0.00691

Table A-43 (Continued)

0.04906 to 0.05089	Obs	0.00430	0.00215	0.00297	0.0	0.00072
	Exp	0.00334	0.00295	0.00158	0.00083	0.00145
	CI	0.0054	0.0054	0.0055	0.0055	0.0055
	Res	-0.00096	-0.00081	0.00140	-0.00083	-0.00073
0.05153 to 0.05920	Obs	0.00299	0.00424	0.00285	0.00211	0.00075
	Exp	0.00389	0.00351	0.00214	0.00138	0.00201
	CI	0.0077	0.0077	0.0087	0.0087	0.0087
	Res	-0.00091	0.00028	0.00072	0.00073	-0.00126

* Statistically significant at .95 level.

Table A-44

PENNSYLVANIA TURNPIKE SIDE FORCE FACTOR - GRADE

All Accidents

Side Force Factor		Grade						
		-2.5 to -3.5	-1.5 to -2.4	-0.7 to -1.4	-0.6 to +0.6	+0.7 to +1.4	+1.5 to +2.4	+2.5 to +3.5
-0.0139 (Tangents)	Obs	0.01600	0.01192	0.01066	0.01114	0.01005	0.01122	0.01647
	Exp	0.01520	0.01416	0.01031	0.01276	0.01168	0.01052	0.01285
	CI	0.0037	0.0037	0.0037	0.0037	0.0037	0.0037	0.0037
	Res	0.00081	-0.00224	0.00035	-0.00162	-0.00162	0.00071	0.00362
-0.00979 to 0.0107	Obs	0.01478	0.00857	0.00873	0.00734	0.00828	0.01186	0.01164
	Exp	0.01288	0.01184	0.00799	0.01044	0.00935	0.00819	0.01052
	CI	0.0037	0.0037	0.0037	0.0037	0.0037	0.0037	0.0037
	Res	0.00191	-0.00327	0.00074	-0.00310	-0.00107	0.00367	0.00112
0.0148 to 0.0230	Obs	0.01179	0.00800*	0.01015	0.00855	0.00673	0.01106	0.01916*
	Exp	0.01348	0.01240	0.00859	0.01104	0.00996	0.00879	0.01113
	CI	0.0037	0.0037	0.0037	0.0037	0.0037	0.0037	0.0037
	Res	-0.00169	-0.00444	0.00155	-0.00249	-0.00323	0.00226	0.00803
0.0304 to 0.0361	Obs	0.01668	0.02157	0.01498	0.01592	0.01639	0.01514	0.01526
	Exp	0.01926	0.01823	0.01438	0.01683	0.01574	0.01458	0.01691
	CI	0.0037	0.0037	0.0037	0.0037	0.0037	0.0037	0.0037
	Res	-0.00259	0.00334	0.00060	-0.00091	0.00065	0.00056	-0.00166
0.0418 to 0.0476	Obs	0.01739*	0.01712*	0.02119	0.02168	0.02684*	0.02080	0.01521*
	Exp	0.02273	0.02170	0.01785	0.02030	0.01921	0.01805	0.02038
	CI	0.0037	0.0037	0.0037	0.0037	0.0037	0.0037	0.0037
	Res	-0.00534	-0.00457	0.00334	0.00138	0.00762	0.00275	-0.00518
0.05999 to 0.07790	Obs	0.02454	0.02864*	0.01635	0.02380	0.01697	0.01714	0.02028
	Exp	0.02380	0.02277	0.01892	0.02137	0.02028	0.01912	0.02145
	CI	0.0037	0.0037	0.0037	0.0037	0.0037	0.0037	0.0037
	Res	0.00074	0.00587	-0.00256	0.00243	-0.00331	-0.00198	-0.00118

221

Table A-44   (Continued)

0.084980	Obs	0.02499	0.03005*	0.01801	0.02228	0.02674*	0.01703	0.01955
	Exp	0.02537(	0.02433	0.02048	0.02293	0.02184	0.02068	0.02301
	CI	0.0037	0.0037	0.0037	0.0037	0.0037	0.0037	0.0037
	Res	-0.00038	0.00572	-0.00247	-0.00065	0.00490	-0.00365	-0.00347
0.092070 to 0.19601	Obs	0.03460*	0.02660	0.02160	0.03058*	0.02059*	0.01906*	0.02440
	Exp	0.02805	0.02701	0.02316	0.02561	0.02453	0.02337	0.02570
	CI	0.0037	0.0037	0.0037	0.0037	0.0037	0.0037	0.0037
	Res	0.00655	-0.00041	-0.00156	0.00497	-0.00394	-0.00431	-0.00130

Table A-45

PENNSYLVANIA TURNPIKE SIDE FORCE FACTOR - GRADE

Single-Vehicle Accidents

Side Force Factor		Grade						
		-2.5 to -3.5	-1.5 to -2.4	-0.7 to -1.4	-0.6 to +0.6	+0.7 to +1.4	+1.5 to +2.4	+2.5 to +3.5
-0.0139 (Tangents)	Obs	0.00878	0.00628	0.00611	0.00613	0.00523	0.00630	0.00688
	Exp	0.00844	0.00776	0.00583	0.00772	0.00637	0.00547	0.00413
	CI	0.0031	0.0031	0.0031	0.0031	0.0031	0.0031	0.0031
	Res	0.00035	-0.00148	0.00028	-0.00159	-0.00114	0.00083	0.00275
-0.00979 to 0.0107	Obs	0.00739	0.00601	0.00399	0.00427	0.00484	0.00701	0.00477
	Exp	0.00737	0.00670	0.00476	0.00666	0.00531	0.00441	0.00307
	CI	0.0031	0.0031	0.0031	0.0031	0.0031	0.0031	0.0031
	Res	0.00002	-0.00069	-0.00078	-0.00239	-0.00047	0.00260	0.00170
0.0148 to 0.0230	Obs	0.00769	0.00500	0.00643	0.00386	0.00492	0.00704	0.01011*
	Exp	0.00834	0.00766	0.00573	0.00762	0.00627	0.00537	0.00404
	CI	0.0031	0.0031	0.0031	0.0031	0.0031	0.0031	0.0031
	Res	-0.00065	-0.00266	0.00070	-0.00377	-0.00136	0.00166	0.00607
0.0304 to 0.0361	Obs	0.01153	0.01543*	0.00961	0.01164	0.01017	0.00972	0.00799
	Exp	0.01278	0.01210	0.01017	0.01206	0.01071	0.00981	0.00847
	CI	0.0031	0.0031	0.0031	0.0031	0.0031	0.0031	0.0031
	Res	-0.00125	0.00333	-0.00056	-0.00042	-0.00054	-0.00009	-0.00048
0.0418 to 0.0476	Obs	0.01330*	0.01185*	0.01634	0.01780	0.02087*	0.01288	0.00876*
	Exp	0.01645	0.01577	0.01384	0.01573	0.01438	0.01348	0.01215
	CI	0.0031	0.0031	0.0031	0.0031	0.0031	0.0031	0.0031
	Res	-0.00315	-0.00392	0.00250	0.00207	0.00649	-0.00060	-0.00339
0.05999 to 0.07790	Obs	0.01688	0.02069*	0.01168	0.01702	0.01228	0.01346	0.00957
	Exp	0.01642	0.01574	0.01381	0.01570	0.01435	0.01345	0.01211
	CI	0.0031	0.0031	0.0031	0.0031	0.0031	0.0031	0.0031
	Res	0.00046	0.00495	-0.00213	0.00132	-0.00207	0.00001	-0.00254

Table A-45   (Continued)

0.084980	Obs	0.01542	0.02250*	0.01252	0.01738	0.01763	0.01195	0.00828*
	Exp	0.01700	0.01633	0.01439	0.01629	0.01494	0.01404	0.01270
	CI	0.0031	0.0031	0.0031	0.0031	0.0031	0.0031	0.0031
	Res	-0.00158	0.00617	-0.00188	0.00110	0.00269	-0.00208	-0.00442
0.092070 to	Obs	0.02344*	0.01126*	0.01688	0.02058*	0.01195*	0.01233	0.01363
0.19601	Exp	0.01763	0.01685	0.01502	0.01691	0.01556	0.01466	0.01333
	CI	0.0031	0.0031	0.0031	0.0031	0.0031	0.0031	0.0031
	Res	0.00581	-0.00570	0.00186	0.00367	-0.00361	-0.00233	0.00031

* Statistically significant @ .95 level

Table A-46

PENNSYLVANIA TURNPIKE SIDE FORCE FACTOR - GRADE
Wet Road Accidents

Side Force Factor		Grade						
		-2.5 to -3.5	-1.5 to -2.4	-0.7 to -1.4	-0.6 to +0.6	+0.7 to +1.4	+1.5 to +2.4	+2.5 to +3.5
-0.0139 (Tangents)	Obs	0.00519	0.00280	0.00279	0.00369	0.00260	0.00331	0.00487
	Exp	0.00439	0.00457	0.00189	0.00518	0.00378	0.00261	0.00282
	CI	0.0026	0.0026	0.0026	0.0026	0.0026	0.0026	0.0026
	Res	0.00079	-0.00177	0.00090	-0.00149	-0.00119	0.00070	0.00205
-0.00979 to 0.0107	Obs	0.00355	0.00307	0.00151	0.00187	0.00258	0.00433	0.00358
	Exp	0.00372	0.00389	0.00121	0.00450	0.00310	0.00193	0.00214
	CI	0.0026	0.0026	0.0026	0.0026	0.0026	0.0026	0.0026
	Res	-0.00017	-0.00082	0.00030	-0.00263	-0.00052	0.00240	0.00144
0.0148 to 0.0230	Obs	0.00769	0.00300 *	0.00198	0.00469	0.00259	0.00402	0.01011 *
	Exp	0.00566	0.00583	0.00315	0.00644	0.00504	0.00388	0.00408
	CI	0.0026	0.0026	0.0026	0.0026	0.0026	0.0026	0.0026
	Res	0.00203	-0.00283	-0.00117	-0.00174	-0.00246	0.00015	0.00603
0.0304 to 0.0361	Obs	0.00564*	0.01153*	0.00650	0.00706	0.00763	0.00795	0.00678
	Exp	0.00836	0.00854	0.00585	0.00914	0.00775	0.00658	0.00678
	CI	0.0026	0.0026	0.0026	0.0026	0.0026	0.0026	0.0026
	Res	-0.00272	0.00299	0.00065	-0.00208	-0.00012	0.00127	-0.00000
0.0418 to 0.0476	Obs	0.01006	0.00941*	0.01124	0.01269	0.01870*	0.01012	0.00628 *
	Exp	0.01200	0.01218	0.00950	0.01278	0.01139	0.01022	0.01043
	CI	0.0026	0.0026	0.0026	0.0026	0.0026	0.0026	0.0026
	Res	-0.00194	-0.00277	0.00174	-0.00009	0.00731	-0.00010	-0.00415
0.05999 to 0.07790	Obs	0.01089	0.01526*	0.00634	0.01286	0.00905	0.00736	0.00575*
	Exp	0.01044	0.01061	0.00793	0.01122	0.00982	0.00865	0.00886
	CI	0.0026	0.0026	0.0026	0.0026	0.0026	0.0026	0.0026
	Res	0.00046	0.00465	-0.00159	0.00165	-0.00077	-0.00129	-0.00311

225

Table A-46 (Continued)

0.084980							
Obs	0.00898	0.01058	0.00733	0.01080*	0.00912	0.00426	0.00501
Exp	0.00880	0.00897	0.00629	0.00958	0.00818	0.00702	0.00722
CI	0.0026	0.0026	0.0026	0.0026	0.0026	0.0026	0.0026
Res	0.00018	0.00160	0.00103	0.00122	0.00093	-0.00276	-0.00221

0.092070 to 0.19601							
Obs	0.01248	0.01023	0.00675	0.01705*	0.00731	0.00897	0.00948
Exp	0.01111	0.01129	0.00861	0.01189	0.01050	0.00933	0.00954
CI	0.0026	0.0026	0.0026	0.0026	0.0026	0.0026	0.0026
Res	0.00137	-0.00106	-0.00186	0.00516	-0.00319	-0.00036	-0.00005

* Statistically significant @ .95 level

Table A-47. Pennsylvania Turnpike Crash Rate by Grade and Curvature with Prediction Model $R_2=0.0111 + \Delta C_i + \Delta G_i$

	Grade						
	1 $\Delta G_1=$ 0.0049	2 $\Delta G_2=$ 0.0008	3 $\Delta G_3=$ 0.0004	4 0.0000	5 -0.0010	6 +0.0001	7 +0.0054
1 $\Delta C_1=0.0$							
Observed	0.0160	0.0119	0.0107	0.0111	0.0101	0.0112	0.0165
Predicted	0.0160	0.0119	0.0107	0.0111	0.0101	0.0112	0.0165
Difference	0.0	0.0	0.0	0.0	0.0	0.0	0.0
2 $\Delta C_2=-0.0057$							
Observed	0.0136	0.0090	0.0	0.0054	0.0	0.0034	0.0162
Predicted	0.0103	0.0062	0.0050	0.0054	0.0044	0.0053	0.0108
Difference	+0.0033	+0.0028	-0.0050	0.0	-0.0044	-0.0019	+0.0054
3 $\Delta C_3=-0.0035$							
Observed	0.0141	0.0085	0.0091	0.0076	0.0078	0.0123	0.0118
Predicted	0.0125	0.0084	0.0076	0.0076	0.0066	0.0077	0.0130
Difference	+0.0016	+0.0001	+0.0015	0.0	+0.0012	+0.0046	-0.0012
4 $\Delta C_4=0.0027$							
Observed	0.0146	0.0163	0.0124	0.0138	0.0130	0.0112	0.0016
Predicted	0.0187	0.0146	0.0134	0.0138	0.0128	0.0139	0.0192
Difference	-0.0041	+0.0017	-0.0010	0.0	+0.0002	-0.0027	-0.0176
5 $\Delta C_5=0.0169$							
Observed	0.0190	0.0239	0.0239	0.0280	0.0230	0.0269	0.0089
Predicted	0.0329	0.0288	0.0276	0.0280	0.0220	0.0281	0.0334
Difference	-0.0139	-0.0049	-0.0037	0.0	+0.0010	-0.0012	-0.0245

227

Table A-47 (Continued)

6 $\triangle c_6 = 0.0112$							
Observed	0.0201	0.0156	0.0190	0.0223	0.0291	0.0189	0.0156
Predicted	0.0272	0.0231	0.0219	0.0223	0.0213	0.0224	0.0277
Difference	-0.0071	-0.0075	-0.0029	0.0	+0.0078	-0.0035	-0.0121
7 $\triangle c_7 = 0.0136$							
Observed	0.0206	0.0300	0.0148	0.0247	0.0159	0.0219	0.0228
Predicted	0.0296	0.0255	0.0243	0.0247	0.0237	0.0248	0.0301
Difference	-0.0090	+0.0045	-0.0095	0.0	-0.0078	-0.0029	-0.0083
8 $\triangle c_8 = 0.0106$							
Observed	0.0283	0.0361	0.0176	0.0217	0.0130	0.0150	0.0190
Predicted	0.0266	0.0225	0.0213	0.0217	0.0207	0.0218	0.0271
Difference	+0.0017	+0.0146	-0.0037	0.0	-0.0077	-0.0068	-0.0081
9 $\triangle c_9 = 0.0105$							
Observed	0.0249	0.0314	0.0185	0.0216	0.0263	0.0187	0.0201
Predicted	0.0265	0.0224	0.0212	0.0216	0.0206	0.0217	0.0270
Difference	-0.0016	0.0090	-0.0027	0.0	+0.0057	-0.0030	-0.0069
10 $\triangle c_{10} = 0.0032$							
Observed	0.0341	0.0282	0.0160	0.0143	0.0207	0.0198	0.0217
Predicted	0.0192	0.0151	0.0139	0.0143	0.0133	0.0144	0.0197
Difference	+0.0149	+0.0131	+0.0021	0.0	+0.0074	+0.0054	+0.0020
11 $\triangle c_{11} = 0.0537$							
Observed	0.0378	--	0.0359	0.0648	0.0204	--	0.0292
Predicted	0.0697	--	0.0644	0.0648	0.0638	--	0.0702
Difference	-0.0319	--	-0.0285	0.0	-0.0434	--	-0.0410

Table A-48. Ranking of Grade by Curvature Cells Using
Differences Between Observed and Predicted Crash Rates

Rank	Grade (j)	Curvature (i)	Difference	Rank Obtained from Regression Model Residuals
1	-2.5 to -4.0 (1)	$3^O23'$ to $4^O12'$ (10)	+0.0149	5
2	-1.5 to -2.4 (2)	$2^O12'$ to $2^O33'$ (8)	+0.0146	4
3	-1.5 to -2.4 (2)	$3^O23'$ to $4^O12'$ (10)	+0.0131	21
4	-1.5 to -2.4 (2)	$2^O34'$ to $3^O22'$ (9)	+0.0090	11
5	+0.2 to +1.4 (5)	$1^O28'$ to $1^O49'$ (6)	+0.0078	3
6	+0.7 to +1.4 (5)	$3^O23'$ to $4^O12'$ (10)	+0.0074	27
7	+0.7 to +1.4 (5)	$2^O34'$ to $3^O22'$ (9)	+0.0057	8
8	+1.5 to +2.4 (6)	$3^O23'$ to $4^O12'$ (10)	+0.0054	45
9	+2.5 to +3.5 (7)	$0^O1'$ to $0^O21'$ (2)	+0.0054	2
10	+1.5 to +2.4 (6)	$0^O22'$ to $0^O43'$ (3)	+0.0046	20
11	=1.5 to -2.4 (2)	$1^O50'$ to $2^O11'$ (7)	+0.0045	10
12	-2.5 to -4.0 (1)	$0^O1'$ to $0^O21'$ (2)	+0.0033	14
13	-1.5 to -2.4 (2)	$0^O1'$ to $0^O21'$ (2)	+0.0028	47
14	-0.7 to -1.4 (3)	$3^O23'$ to $4^O12'$ (10)	+0.0021	55
15	+2.5 to +3.5 (7)	$3^O23'$ to $4^O12'$ (10)	+0.0020	23
16	-2.5 to -4.0 (1)	$2^O12'$ to $2^O33'$ (8)	+0.0017	17
17	-1.5 to -2.4 (2)	$0^O44'$ to $1^O5'$ (4)	+0.0017	34
18	-2.5 to -4.0 (1)	$0^O22'$ to $0^O43'$ (3)	+0.0016	29
19	-0.7 to -1.4 (3)	$0^O22'$ to $0^O43'$ (3)	+0.0015	24
20	+0.7 to +1.4 (5)	$0^O22'$ to $0^O43'$ (3)	+0.0012	35
21	+0.7 to +1.4 (5)	$1^O6'$ to $1^O27'$ (5)	+0.0010	16
22	+0.7 to +1.4 (5)	$0^O44'$ to $1^O5'$ (4)	+0.0002	13
23	-1.5 to -2.4 (2)	$0^O22'$ to $0^O43'$ (3)	+0.0001	67
24	-2.5 to -.40 (1)	$0^O0'$ (1)	0.0	33
25	-1.5 to -.24 (2)	$0^O0'$ (1)	0.0	64

Table A-48 (Continued)

26	-0.7 to -1.4 (3)	$0^{\circ}0'$ (1)	0.0	28
27	-0.6 to +0.6 (4)	$0^{\circ}0'$ (1)	0.0	57
28	+0.7 to +1.4 (5)	$0^{\circ}0'$ (1)	0.0	36
29	+1.5 to +2.4 (6)	$0^{\circ}0'$ (1)	0.0	38
30	+2.5 to +3.5 (7)	$0^{\circ}0'$ (1)	0.0	6
31	-0.6 to +0.6 (4)	$0^{\circ}3'$ to $0^{\circ}21'$ (2)	0.0	59
32	-0.6 to +0.6 (4)	$0^{\circ}22'$ to $0^{\circ}43'$ (3)	0.0	65
33	-0.6 to +0.6 (4)	$0^{\circ}44'$ to $1^{\circ}5'$ (4)	0.0	42
34	-0.6 to +0.6 (4)	$1^{\circ}6'$ to $1^{\circ}27'$ (5)	0.0	15
35	-0.6 to +0.6 (4)	$1^{\circ}28'$ to $1^{\circ}49'$ (6)	0.0	40
36	-0.6 to +0.6 (4)	$1^{\circ}50'$ to $2^{\circ}11'$ (7)	0.0	30
37	-0.6 to +0.6 (4)	$2^{\circ}12'$ to $2^{\circ}33'$ (8)	0.0	51
38	-0.6 to +0.6 (4)	$2^{\circ}34'$ to $3^{\circ}22'$ (9)	0.0	60
39	-0.6 to +0.6 (4)	$3^{\circ}23'$ to $4^{\circ}12'$ (10)	0.0	73
40	-0.6 to +0.6 (4)	$4^{\circ}13'$ to $6^{\circ}00'$ (11)	0.0	1
41	-0.7 to -1.4 (3)	$0^{\circ}44'$ to $1^{\circ}5'$ (4)	-0.0010	19
42	+2.5 to +3.5 (7)	$0^{\circ}22'$ to $0^{\circ}43'$ (3)	-0.0012	12
43	+1.5 to +2.4 (6)	$1^{\circ}6'$ to $1^{\circ}27'$ (5)	-0.0012	7
44	-2.5 to -4.0 (1)	$2^{\circ}34'$ to $2^{\circ}33'$ (9)	-0.0016	46
45	+1.5 to +2.4 (6)	$0^{\circ}1'$ to $0^{\circ}21'$ (2)	-0.0019	22
46	+1.5 to +2.4 (6)	$0^{\circ}44'$ to $1^{\circ}5'$ (4)	-0.0027	31
47	-0.7 to -1.4 (3)	$2^{\circ}34'$ to $3^{\circ}22'$ (9)	-0.0027	48
48	-0.7 to -1.4 (3)	$1^{\circ}28'$ to $1^{\circ}49'$ (6)	-0.0029	25
49	+1.5 to +2.4 (6)	$1^{\circ}50'$ to $2^{\circ}11'$ (7)	-0.0029	26
50	+1.5 to +2.4 (6)	$2^{\circ}34'$ to $3^{\circ}22'$ (9)	-0.0030	54
51	+1.5 to +2.4 (6)	$1^{\circ}28'$ to $1^{\circ}49'$ (6)	-0.0035	37
52	-0.7 to -1.4 (3)	$1^{\circ}6'$ to $1^{\circ}27'$ (5)	-0.0037	9
53	-0.7 to -1.4 (3)	$2^{\circ}12'$ to $2^{\circ}33'$ (8)	-0.0037	44
54	-2.5 to -4.0 (1)	$0^{\circ}44'$ to $1^{\circ}5'$ (4)	-0.0041	41
55	+0.7 to +1.4 (5)	$0^{\circ}1'$ to $0^{\circ}21'$ (2)	-0.0044	63

56	-1.5 to -2.4 (2)	$1^{\circ}6'$ to $1^{\circ}27'$ (5)	-0.0049	49
57	-0.7 to -1.4 (3)	$0^{\circ}1'$ to $0^{\circ}21'$ (2)	-0.0050	61
58	+1.5 to +2.4 (6)	$2^{\circ}21'$ to $2^{\circ}33'$ (8)	-0.0068	66
59	+2.5 to +3.5 (7)	$2^{\circ}34'$ to $3^{\circ}22'$ (9)	-0.0069	43
60	-2.5 to -4.0 (1)	$1^{\circ}28'$ to $1^{\circ}49'$ (6)	-0.0071	53
61	-1.5 to -2.4 (2)	$1^{\circ}28'$ to $1^{\circ}49'$ (6)	-0.0075	72
62	+0.7 to +1.4 (5)	$2^{\circ}12'$ to $2^{\circ}33'$ (8)	-0.0077	68
63	+0.7 to +1.4 (5)	$1^{\circ}50'$ to $2^{\circ}11'$ (7)	-0.0078	52
64	+2.5 to +3.5 (7)	$2^{\circ}12'$ to $2^{\circ}33'$ (8)	-0.0081	39
65	+2.5 to +3.5 (7)	$1^{\circ}50'$ to $2^{\circ}11'$ (7)	-0.0083	18
66	-2.5 to -4.0 (1)	$1^{\circ}50'$ to $2^{\circ}11'$ (7)	-0.0090	62
67	-0.7 to -1.4 (3)	$1^{\circ}50'$ to $2^{\circ}11'$ (7)	-0.0095	58
68	+2.5 to +3.5 (7)	$1^{\circ}28'$ to $1^{\circ}49'$ (6)	-0.0121	50
69	-2.5 to -4.0 (1)	$1^{\circ}6'$ to $1^{\circ}27'$ (5)	-0.0139	69
70	+2.5 to +3.5 (7)	$0^{\circ}44'$ to $1^{\circ}5'$ (4)	-0.0176	71
71	+2.5 to +3.5 (7)	$1^{\circ}6'$ to $1^{\circ}27'$ (5)	-0.0245	74
72	-0.7 to -1.4 (3)	$4^{\circ}13'$ to $6^{\circ}00'$ (11)	-0.0285	32
73	-2.5 to -4.0 (1)	$4^{\circ}13'$ to $6^{\circ}00'$ (11)	-0.0319	56
74	+2.5 to -3.5 (7)	$4^{\circ}13'$ to $6^{\circ}00'$ (11)	-0.0410	70
75	+0.7 to +1.4 (5)	$4^{\circ}13'$ to $6^{\circ}00'$ (11)	-0.0434	75
76	-1.5 to -2.4 (2)	$4^{\circ}13'$ to $6^{\circ}00'$ (11)	Missing Data	76
77	+1.5 to +2.4 (6)	$4^{\circ}13'$ to $6^{\circ}00'$ (11)	Missing Data	77

APPENDIX B

VEHICLE DYNAMICS ON CURVE-GRADE SECTIONS OF HIGHWAY

The purpose of this appendix is to present analyses of the factors which can lead to loss of control on sections of highway with curvature and grade. First, simplified analytical results are described to provide a perspective from which to examine the detailed results obtained by full-scale simulation. Then the simulation results are given.

B.1 SIMPLIFIED ANALYSES OF VEHICLE PROPERTIES INFLUENCING SKIDDING

For purposes of this section, "skidding" is defined to mean vehicle motion which results from a driver losing control of his vehicle because he has operated the vehicle in a manner which exceeds the level of friction available for controlling the vehicle. For example, in braking, a driver can lose control of his vehicle if the front wheels, the rear wheels, or all four wheels lock. If all four wheels lock, the driver cannot achieve greater braking force by pushing harder on the brake pedal. If the front wheels lock, the driver's ability to steer the vehicle is greatly reduced. If the rear wheels lock, the vehicle becomes dynamically unstable and tends to spin around, and, in extreme cases, travel rear-end first. In all three

of these cases, the level of friction available at the tire/road interface has been exceeded at one or both sets of wheels.

Loss of control in cornering can be caused by the front-tire side force saturating (i.e., approaching a maximum level) or by the rear-tire side force saturating. When the front tires saturate and the rear tires do not, the vehicle will not turn any sharper. The driver has lost control of the vehicle because he cannot turn more tightly by increasing the steer angle. If the rear tires are saturated, the front tires may generate a force large enough to produce a yaw moment imbalance, and the vehicle will spin around. In general, the side forces from the rear tires have a stabilizing effect, tending to keep a vehicle directionally stable.

While braking in a turn, a driver must regulate his steering and braking to maintain the desired path without exceeding the upper limits on longitudinal or lateral tire force at the front or rear wheels.

Occasionally, situations occurring on the highway cause drivers to demand more shear force from their tires than the tire/road frictional potential will permit. When this happens, the vehicle can skid and, if the vehicle strikes something while out of control, a skidding accident occurs.

The purpose of the following paragraphs is to present simplified analyses showing how vehicle properties act to influence the possibility of skidding in braking and cornering maneuvers. These computations of braking and cornering capability do not include the efficiency of the driver in using the entire tire/vehicle performance available to him; rather they show the extent to which the vehicle can use the friction potential available to it.

B.1.1 BRAKING. A simplified analysis of the braking process follows. Consider the vehicle as shown in Figure B-1 presented below.
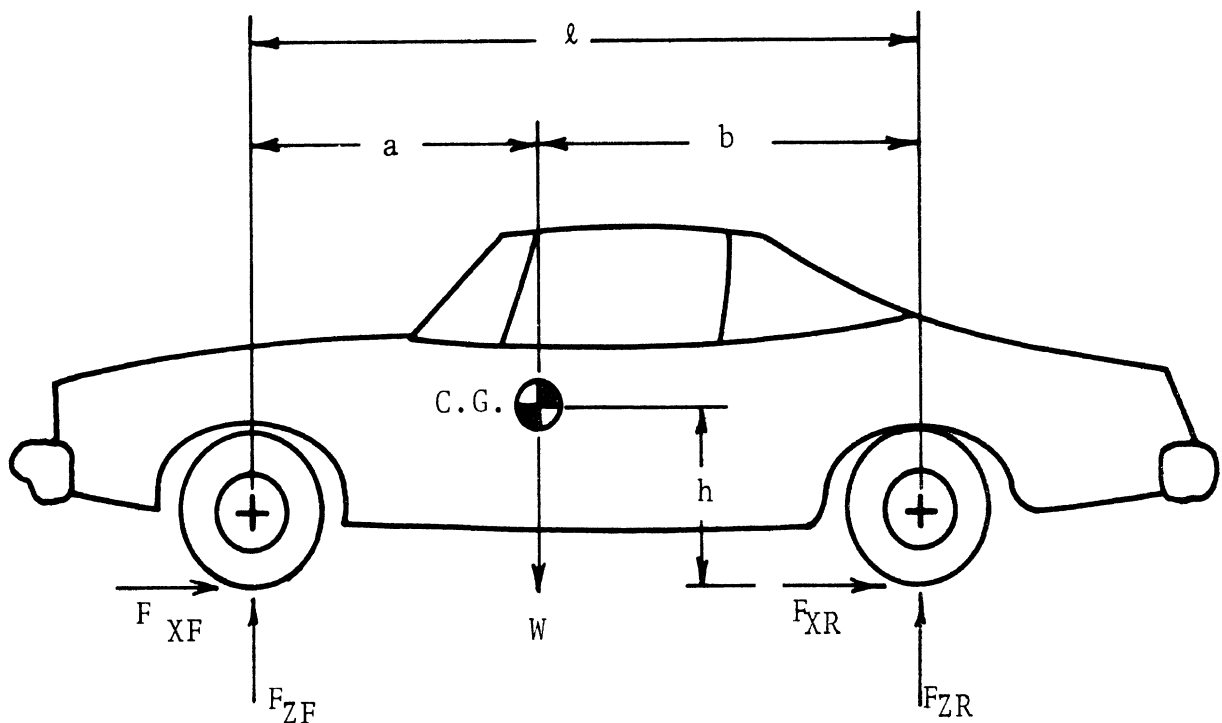
Figure B-1. Nomenclature for Braking Analysis.

Summing the moments about the center of gravity (c.g.) and assuming pitch equilibrium

$$h(F_{XR} + F_{XF}) + F_{ZR}b - F_{ZF}a = 0 \qquad (B.1)$$

Ideally, both the front and rear tires produce maximum braking force. Assuming that μ' represents the maximum normalized force that either the front tires or the rear tires can produce, then under ideal braking

$$\mu'F_{ZF} = F_{XF} \qquad (B.2)$$

and

$$\mu'F_{ZR} = F_{XR} \qquad (B.3)$$

From Equations (B.1), (B.2), and (B.3) it can be shown that

$$F_{ZR} = F_{ZF}\left(\frac{a - h\mu'}{b + h\mu'}\right) \qquad (B.4)$$

for an ideal stop in which

$$F_{XF} + F_{XR} = \mu'W \qquad (B.5)$$

where $\quad W = F_{ZF} + F_{ZR} \qquad (B.6)$

Also, from (B.2), (B.3), and (B.4) it is clear that

$$F_{XR} = F_{XF} \left(\frac{a - h\mu'}{b + h\mu'}\right) \qquad (B.7)$$

Relationships (B.5) and (B.7) are shown on Figure B-2. It can be seen by examining the ideal braking curves presented in the figure that parameters a and b, specifying the fore-aft position of the c.g. have a large influence on the ideal distribution of braking front to rear for a given μ'.

Superimposed on Figure B-2 is a typical example of brake proportioning front to rear for a passenger car. In this example, 62% of the braking takes place at the front wheels and 38% takes place at the rear wheels. For a vehicle with its center of gravity at the middle of the wheelbase (i.e., a = b = 5'), this proportioning does a reasonably good job of fitting the ideal braking curve. Notice that for μ' = 0.6 this proportioning is ideal for the a = b = 5' case. This means that for this case the front and rear tires are operating at maximum force levels simultaneously.

Below μ' = 0.6, the front-tire braking force reaches a maximum before the rear-tire braking force. An example of this is shown in the figure. For F_{XR}/W = .15, the

These lines represent
$F_{XR} + F_{XF} = \mu'W$ for an ideal stop

Example brake
proportioning
$F_{XR} = (\frac{38}{62})F_{XF}$

a = 6', b = 4'   Ideal
                  braking
a = 5', b = 5'   curves
                  h = 2'
                  Eqn. (B7)
a = 4', b = 6'
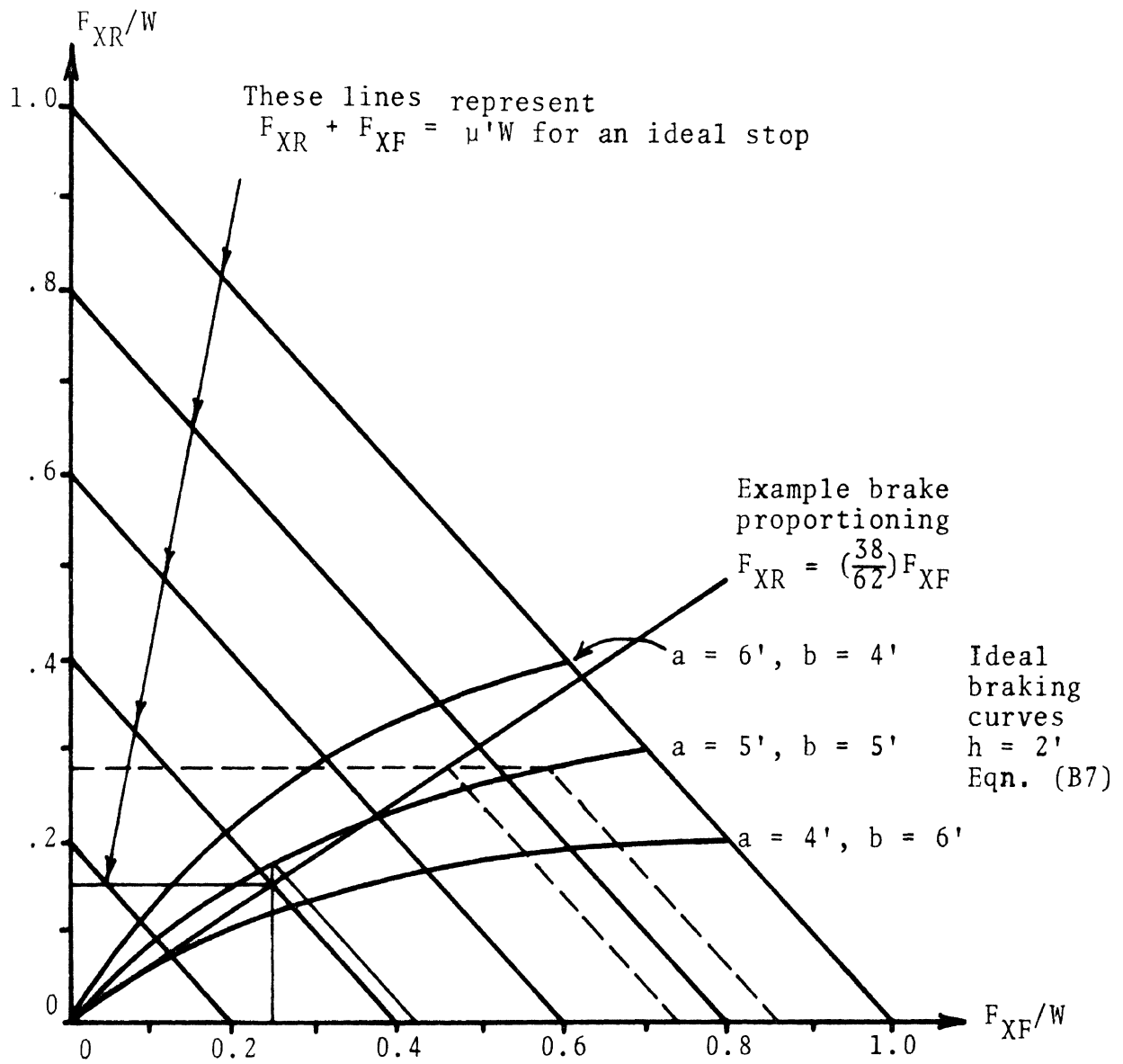
Figure B-2.   The Effect of Brake Proportioning on
              Braking Performance.

238

total braking force determined by the brake proportioning is 0.4W. However, the ideal curve shows that 0.42W could have been obtained with the same level of front-tire normalized braking force (F_{XF}/W). Above $\mu' = 0.6$, the rear-tire brake force reaches a maximum before the front-tire brake force. Consider the case where $F_{XR}/W = 0.28$. The dashed lines in the figure illustrate that, for this level of F_{XR}/W, ideal braking would yield 0.86W total brake force, compared to 0.74W as determined by the brake proportioning.

Clearly, a vehicle with the common type of brake proportioning illustrated here cannot utilize all the friction potential available for stopping. A well-known practice is to compute braking efficiency as a function of μ' for a given brake proportioning. That is, for a proportioning, p, such that $F_{XR} = p\ F_{XF}$, the braking efficiency, η, is given by:

$$\eta = \frac{F_{XR} + F_{XF}}{\mu'W}$$

$$= \frac{(1 + \frac{1}{p})(\frac{a}{\ell})}{(1 + \mu'(1 + \frac{1}{p})(\frac{h}{\ell}))} \qquad \begin{array}{l}\text{for } F_{XR} = \mu'F_{ZR} \\ \text{(i.e., rear tire} \\ \text{maximum force)}\end{array}$$

$$= \frac{(1 + p)(\frac{b}{\ell})}{(1 - \mu'(1 + p)(\frac{h}{\ell}))} \qquad \begin{array}{l}\text{for } F_{XF} = \mu'F_{ZF} \\ \text{(i.e., front tire} \\ \text{maximum force)}\end{array}$$

(B.8)

(These equations can be derived from the simple vehicle
model treated here.) In the example with a = b = 5' and
$p = \frac{38}{62}$, the braking efficiency as a function of μ' is
given in the following table:

μ'	η
0.2	0.863
0.4	0.926
0.6	1.000
0.8	0.926
1.0	0.863

These efficiencies are good. Clearly, the efficiency can
be very poor if the proportioning is not properly matched
to the fore-aft position of the c.g. for some loading
conditions of the vehicle. Also, the influence of a
change in c.g. height, h, is important in evaluating the
efficiency of a given brake proportioning.

Factors such as differences in front-to-rear tire
force capabilities, anti-lock brakes, and variable pro-
portioning systems require a more sophisticated analysis
than has been presented here. Detailed computer simula-
tions have been employed in this project to study the
dynamics of the braking of vehicles under a variety of

complex roadway conditions. Nevertheless, this simplified analysis serves to show the basic problems with regard to efficient braking on all surfaces.

B.1.2 CORNERING. Figure B-3 shows a vehicle in a turn on a downgrade. The three force and three moment equations of equilibrium are given in Equations (B.9) through (B.14) as listed after Figure B-3. Note that small angle approximations have been used wherever possible.

Approximate gravity forces (using small angle assumptions, i.e., G and e $\leq$ 0.1 rad.):

> W   in Z direction
>
> -WG in X direction downhill (G positive
>   for uphill)
>
> We   in Y direction lateral, parallel to
>   road

Approximate Equilibrium Equations:

> Note: i=1 means left front
>
>   i=2 means right front
>
>   i=3 means left rear
>
>   i=4 means right rear

$\dfrac{W}{g} \quad \dfrac{V^2}{R}$

Right Turn
Rear View

e shown > 0

G shown < 0

Figure B-3

242

Normal to Road:

$$W + \frac{W}{g} \frac{V^2}{R} e + \sum_{i=1}^{4} F_{Zi} = 0 \qquad (B.9)$$

Lateral Parallel to Road:

$$\frac{W}{g} \frac{V^2}{R} = We + \sum_{i=1}^{4} F_{Yi} \qquad (B.10)$$

Longitudinal Parallel to Road:

$$0 = -WG + \sum_{i=1}^{4} F_{Xi} \qquad (B.11)$$

Yaw:

$$(F_{Y1} + F_{Y2})a = (F_{Y3} + F_{Y4})b \qquad (B.12)$$

Pitch:

$$(\Sigma F_{Xi})h + (F_{Z3} + F_{Z1})b - (F_{Z1} + F_{Z2})a = 0 \qquad (B.13)$$

Roll:

$$(\Sigma F_{Yi})h + (F_{Z2} + F_{Z4})t - (F_{Z1} + F_{Z3})t = 0 \qquad (B.14)$$

243

Since a simplified analysis applicable to slippery surfaces is intended, the effects of vehicle roll will be neglected and both front tires and both rear tires will be treated together. Solving Equations (B.9) through (B.13) for the front vertical load, F_{ZF}, and the rear vertical load, F_{ZR}, the following results are obtained:

$$F_{ZF} = - \frac{b}{\ell} \left[\frac{mV^2}{R} e + W - \frac{WGh}{b} \right] \qquad (B.15)$$

$$F_{ZR} = - \frac{a}{\ell} \left[\frac{mV^2}{R} e + W + \frac{WGh}{a} \right] \qquad (B.16)$$

where $\ell = a+b =$ wheelbase. Note that grade enters this analysis only because a small amount of load transfer is needed to balance the tire braking force required to maintain constant velocity on a downhill slope. For passenger car operation on highways, the terms $\frac{mV^2}{R} e$, $\frac{WGh}{b}$, and $\frac{WGh}{a}$ in (B.15) and (B.16) are small and they can be neglected. (Since detailed computer simulation has been used to produce quantitatively precise results, a simple analysis can be used for the exemplary purposes of this discussion.) Thus,

$$F_{ZF} \doteq \frac{b}{\ell} W \qquad (B.17)$$

$$F_{ZR} \doteq - \frac{a}{\ell} W \qquad (B.18)$$

244

By neglecting roll and by treating both front wheels and both rear wheels together, the lateral force equation and the yaw moment equation become:

Lateral: $\quad F_{YF} + F_{YR} = \dfrac{W}{g}\ \dfrac{V^2}{R} - We$ $\qquad$ (B.19)

Yaw: $\qquad aF_{YF} - bF_{YR} = 0$ $\qquad\qquad$ (B.20)

As a first approximation under limit conditions (i.e., conditions under which tire side force has reached a maximum or saturated), the maximum possible tire forces are given by

$$F_{YFL} \doteq \pm\mu_F\ |F_{ZF}| \qquad \text{(positive for right turn)} \qquad \text{(B.21)}$$

$$F_{YRL} \doteq \pm\mu_R\ |F_{ZR}| \qquad \text{(positive for right turn)} \qquad \text{(B.22)}$$

Before proceeding further, it is of interest to compare results obtained using Equations (B.17) through (B.22) with results obtained by Zuk (4) for a site on I-95 where I-95 crosses US 1 in Virginia. The parameters of the vehicle and the highway are:

$$G = -0.026 \text{ (downhill)}$$
$$e = 0.0156$$

$$R = 5730 \text{ ft.}$$

$$\mu_F = \mu_R = 0.3$$

$$W = 4000 \text{ lbs.}$$

$$a = 4.5 \text{ ft.}$$

$$b = 5.5 \text{ ft.}$$

$$h = 2.0 \text{ ft. (not needed for the simplified}$$
$$\text{equations)}$$

The maximum velocity at maximum side force predicted by Zuk's analysis was 164.6 mph compared to 165 mph predicted by Equations (B.17) through (B.22). When R was reduced to 1000 ft. (to represent maneuvering conditions in Zuk's analysis), the maximum velocity predicted by Zuk was 68.7 mph and this analysis predicts 69 mph.

Now consider cases where the front and rear tire characteristics are different. Tire-in-use factors such as wear, inflation pressure, and replacement tire differences can lead to different front-to-rear tire shear force characteristics. (See Appendix G.) For the purposes of this section, it is assumed that the maximum friction coefficients, μ_F and μ_R, represent the influence of the multitude of factors which interact at the tire/road interface.

When μ_F differs from μ_R, the yaw moment balance
determines whether the vehicle operates at maximum possible
front-tire side force or at maximum possible rear-tire
side force. A graphical method of solution for Equations
(B.19) through (B.22) is illustrated in Figure B-4. In
this figure, possible values of F_{YF} are plotted versus
corresponding values of F_{YR}. Points satisfying Equation
(B.20), the yaw moment balance, lie on a straight line
through the origin with slope b/a. The maximum possible
rear-tire force, F_{YRL}, determines a vertical line, and
F_{YFL} determines a horizontal line. The "F_{YRL} and F_{YFL}
lines" intersect the line $F_{YF} = \frac{b}{a} F_{YR}$ at two points. The
point closest to the origin (symbolized by P in Figure B-4)
determines the maximum possible total side force ($F_{YF} + F_{YR}$)
while maintaining a yaw moment balance.

Any attempt by the driver to turn "tighter" than
predicted by the analysis will result in either a "plow-out"
or a "spin-out" response, depending upon the front-to-rear
side force characteristics of the vehicle. The vehicle
will plow out if the front-tire side force is maximized.
The vehicle will spin out if the rear-tire side force
reaches a maximum.

Lines of constant total lateral force, $F_{YR} + F_{YR}$,
have a slope of -1.0 in Figure B-4. The line of total
lateral force passing through point P determines the total
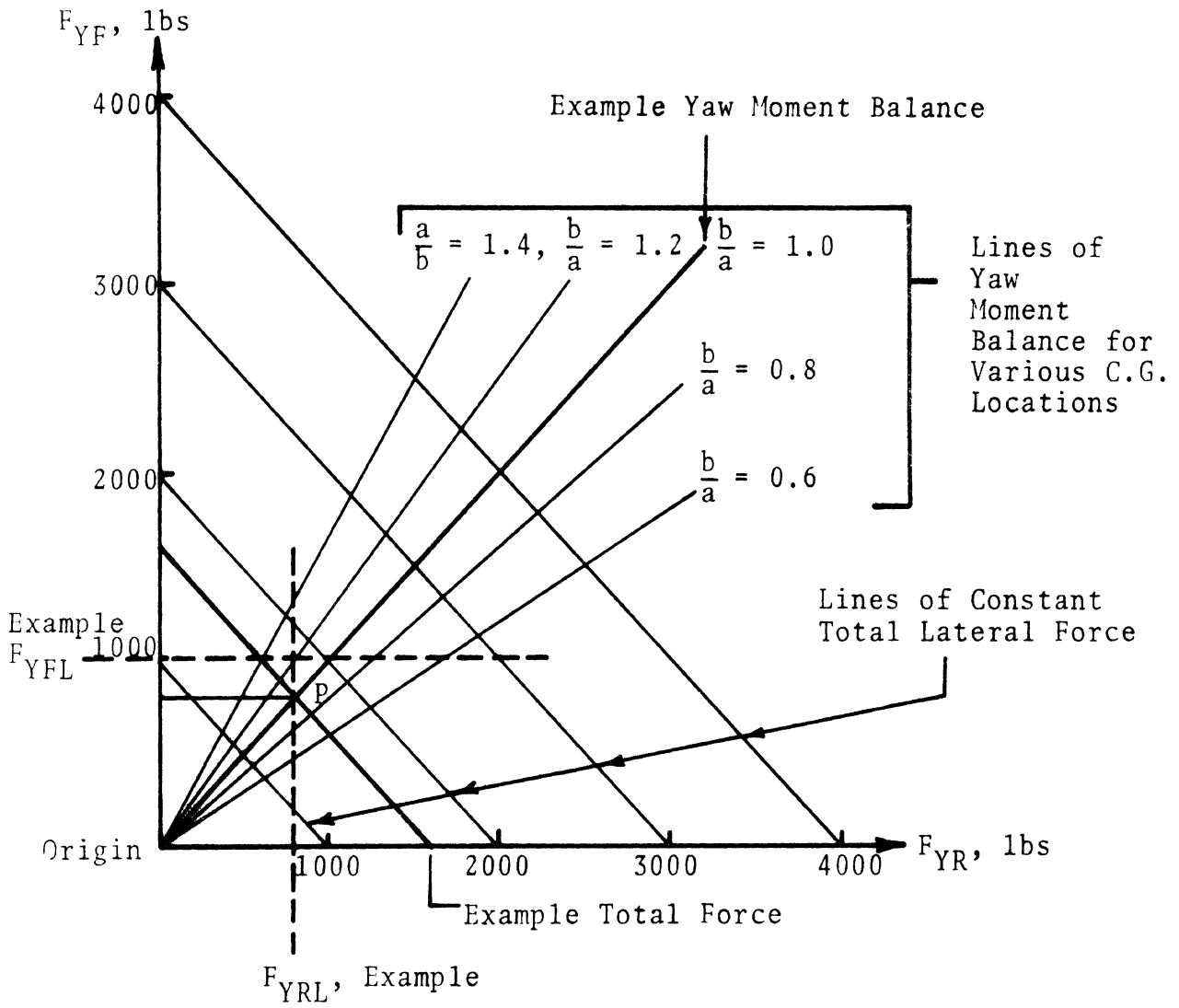
Figure B-4. Graphic Solution of Cornering Equations.

lateral force which can be developed by the vehicle's tires in an equilibrium turn as described by Equations (B.17) through (B.22). Equation (B.19) equates the total lateral force to the speed and weight of the vehicle and to the geometry of the road (i.e., R and e).

For the example illustrated by the heavy lines in Figure B-4, F_{YFL} = 1000 lbs., but for an equilibrium turn, F_{YF} = 800 lbs. in order to maintain a yaw moment balance. In this case, the tires could produce a total of 1800 lbs. force; however, the vehicle can utilize only 1600 lbs. out of the 1800 lbs. available.

A summary of typical calculated results for different values of μ_R and μ_F is presented in Table B-1.*

Table B-1

SITE AND VEHICLE PARAMETERS GIVEN ON PAGES 245 AND 246

μ_F	μ_R	F_{YFL}	F_{YRL}	F_{YF}	F_{YR}	V (maximum)
0.3	0.3	660	540	660	540	242 ft/sec (165 mph)
0.3	0.2	660	360	440	360	200 ft/sec (136 mph)
0.4	0.3	880	540	660	540	242 ft/sec (165 mph)
0.3	0.4	660	720	660	540	242 ft/sec (165 mph)
0.2	0.3	440	540	440	360	200 ft/sec (136 mph)

*Note that a surface with a 30 skid number at 130 mph may have a rather high skid number at 40 mph.

Examination of the results (Table B-1) shows that the smaller coefficient of friction determines the maximum total force attainable. Analytically, this is seen by comparing the yaw moments which would be produced by the maximum front and rear tire forces, viz,

$$aF_{YFL} = \mu_F \; \frac{abW}{\ell}$$

$$bF_{YRL} = -\mu_R \; \frac{abW}{\ell}$$

Thus, the smallest magnitude moment is produced by the tires having the lowest "friction coefficient." If $\mu_R > \mu_F$, the front tires saturate and an increase in steer angle will not produce a greater path curvature $(\frac{1}{R})$; if $\mu_F > \mu_R$, the rear tires saturate and increasing steer angle will cause a yaw moment imbalance which cannot be counteracted by increased rear tire side force, and consequently the vehicle tends to spin out. (During spin-out, the vehicle sideslip angle, β, defined as the angle between the velocity vector and an axis out the front of the vehicle, diverges.)

This analysis provides the background for a working definition of "loss of control" in cornering:

A driver has suffered loss of control when either

    1. an increase in steering angle no longer produces a higher path curvature $(\frac{1}{R})$ (trajectory instability), or

2. an increase in steer angle produces
    an unstable yaw acceleration (directional
    instability).

The first type of loss of control is recognized
easily when it occurs in the simulation. The computed
time histories are characterized by an ever-increasing
steer angle with no corresponding increase in lateral
acceleration, yaw rate, or path curvature. The second
(spin-out) type of loss of control produces a dramatically
divergent sideslip angle. Figures B-5 and B-6 illustrate
the conditions which lead to the two types of loss of
control defined in this section.

In the plow-out example of Figure B-5 it is assumed
that the maximum lateral force, F_{YFL}, from both front
tires is 800 lbs. and, due to tire differences or other
factors, F_{YFL} is equal to the maximum available lateral
force from the rear tires (F_{YRL}), even though the center
of gravity is closer to the front wheels than to the rear
wheels (i.e., b > a). Points satisfying the yaw moment
balance lie along a radial line drawn through the origin
with slope, b/a, in Figure B-5. Lines of constant total
lateral force have a negative slope equal to unity. These
lines represent Equation (B.19) for various steady turning
conditions. The point where loss of control occurs can
be found by proceeding out the yaw moment balance line

251
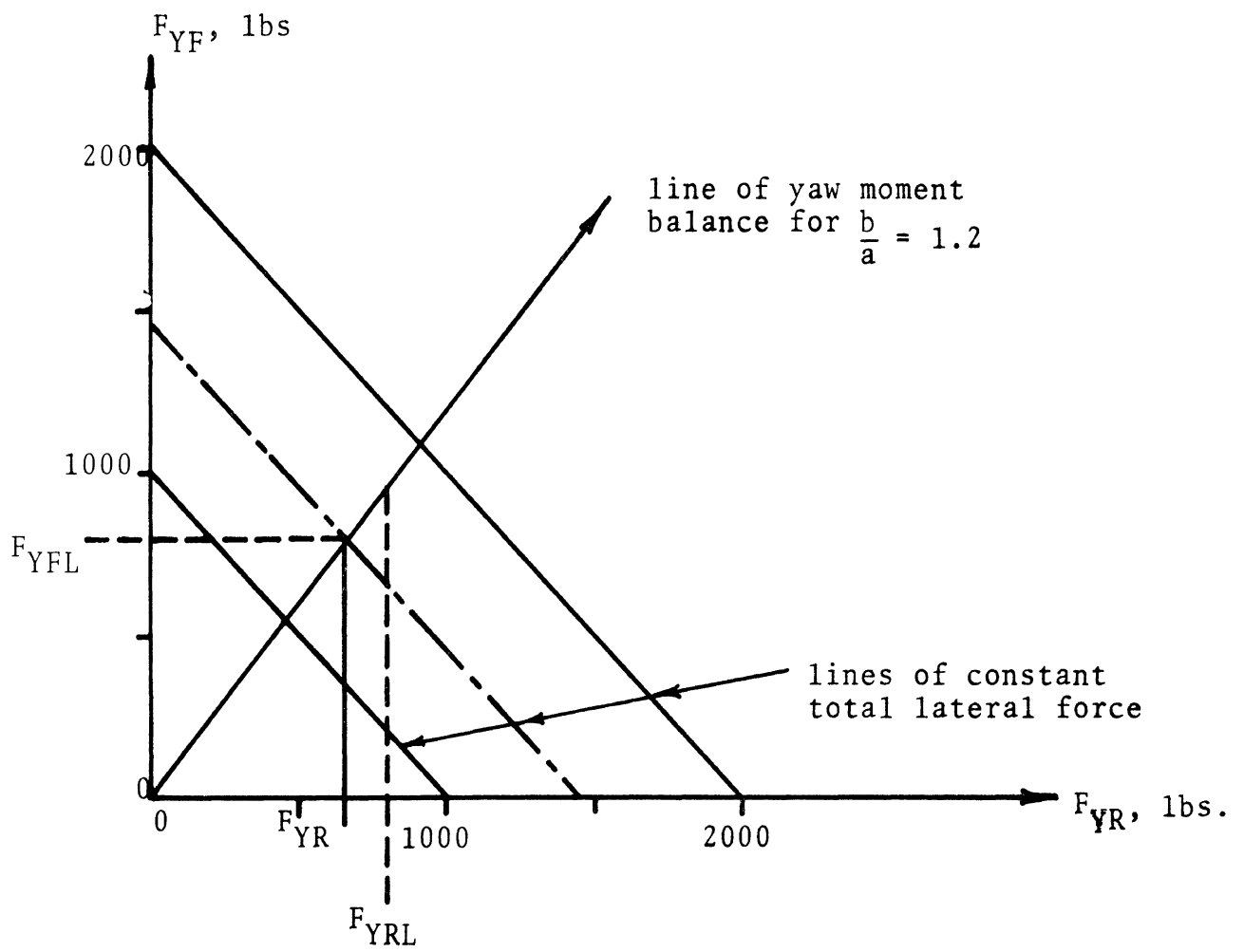
Figure B-5. Front-Tire Saturation (Plow-Out)

252
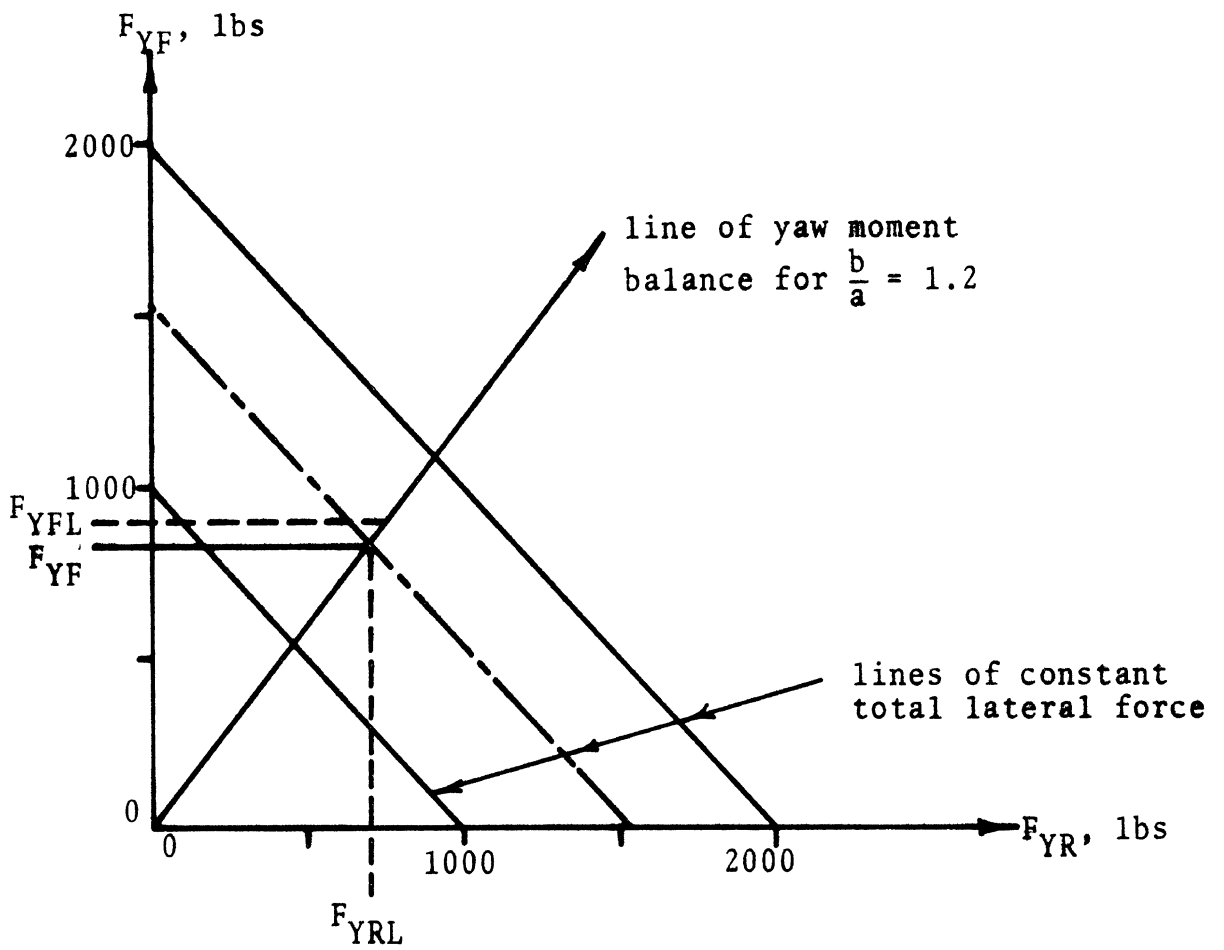
Figure B-6. Rear-Tire Saturation (Spin-Out)

from the origin through higher and higher values of total lateral force up to the point where either F_{YRL} or F_{YFL} is reached. In Figure B-5, F_{YFL} is reached first, indicating that for this example front tire saturation occurs before rear tire saturation. Examination of the figure shows that the maximum total lateral force which can be obtained without loss of control is approximately 1460 lbs. Note that in this case the tires could have produced a 1600-lb. total lateral force if it were not necessary to maintain a yaw moment balance.

Figure B-6 illustrates the spin-out type of loss of control. The limiting values of tire force selected for this example are F_{YFL} = 900 lbs. and F_{YRL} = 700 lbs. Examination of Figure B-6 indicates that F_{YRL} is the limiting factor and that the maximum value of (F_{YF} + F_{YR}) without spin-out is 1540 lbs., which is less than the 1600 lbs. available from the front and rear tires combined if the moment balance is not considered.

These simple examples provide a useful perspective for interpreting the detailed results obtained in the full-scale simulation.

B.1.3 BRAKING AND CORNERING. The simplified analysis (Equations (B.17) through (B.22) can be extended to include the influence of braking on the equilibrium turning performance of the vehicle. For this purpose assume nearly instantaneous fore-aft load transfer and neglect the change in velocity taking place over a short time period. For a desired level of braking force, F_X, the pitch moment equation, is:

$$F_X h + F_{ZR} b - F_{ZF} a = 0 \qquad (B.23)$$

where

$$F_{ZR} + F_{ZF} = -W \qquad (B.24)$$

or, solving (B.23) and (B.24),

$$F_{ZR} = -\frac{a}{\ell} W - \frac{F_X h}{\ell} \qquad (B.25)$$

$$F_{ZF} = -\frac{b}{\ell} W + \frac{F_X h}{\ell} \qquad (B.26)$$

(Note that $F_X < 0$ for braking.) The longitudinal braking force F_X is distributed front to rear according to the brake proportioning of the vehicle.

$$F_{XF} \doteq 1.5 \ F_{XR} \qquad (B.27)$$

where

$$F_X = F_{XF} + F_{XR} \qquad (B.28)$$

A simple means of representing the maximum lateral forces attainable while braking is given by equations of the form:

$$F_{YFL} = \pm \sqrt{(\mu_F F_{ZF})^2 - (F_{XF})^2} \quad \text{(positive sign for right turn)}$$

$$\qquad (B.29)$$

$$F_{YRL} = \pm \sqrt{(\mu_R F_{ZR})^2 - (F_{XR})^2} \quad \text{(positive sign for right turn)}$$

$$\qquad (B.30)$$

Equations (B.29) and (B.30) are reasonable approximations for qualitative results. More exact relations are employed in the simulation. Nevertheless, (B.29) and (B.30) are sufficient for illustrating the influence of braking.

Consider the vehicle and roadway described by the parameters given on pages 245 and 246. Assuming that the desired F_X is -500 lbs., then

$$F_{XR} = -200 \text{ lbs.} \quad (1.5 \ F_{XR} = F_{XF})$$

$$F_{XF} = -300 \text{ lbs.}$$

$$F_{ZR} = -1700 \text{ lbs.}$$

$$F_{ZF} = -2300 \text{ lbs.}$$

256

$$F_{YRL} = 470 \text{ lbs.}$$

$$F_{YFL} = 622 \text{ lbs.}$$

$$F_{YF} = 574 \text{ lbs.}$$

$$V_{(maximum)} = 225 \text{ ft/sec (153 mph)}$$

These calculations are shown graphically in Figure B-7, along with similar results for the non-braked vehicle. It can be seen in this example that the desired braking (equal to $\frac{1}{8}$ g) reduced the maximum attainable lateral force from 1200 lbs. to 1044 lbs. The maximum velocity was reduced from 165 mph to 153 mph.

B.1.4 SUMMARY. The simplified analyses presented in this section indicate that drivers are not likely to lose control of their vehicles at moderate highway speeds unless they are traveling and maneuvering under slippery conditions with poor tires.

B.2 SIMULATION RESULTS

B.2.1 HVOSM SIMULATION. The HVOSM vehicle model consists of four rigid masses with a total of fifteen degrees of freedom (see Figure B-8). The sprung mass is allowed three translatory and three rotational degrees of freedom. The rear axle unsprung mass is allowed one
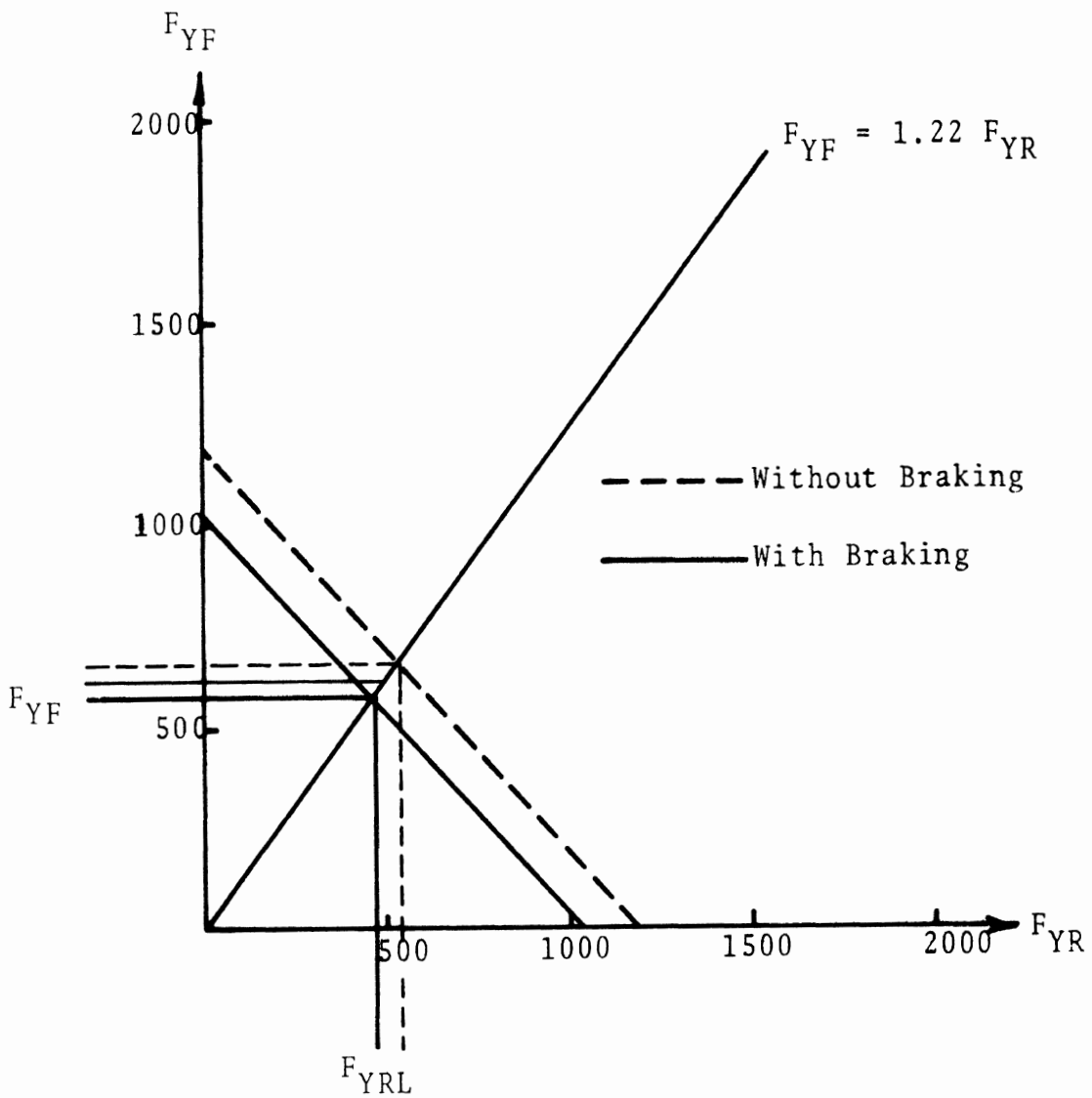
Figure B-7.   Influence of Braking on Cornering
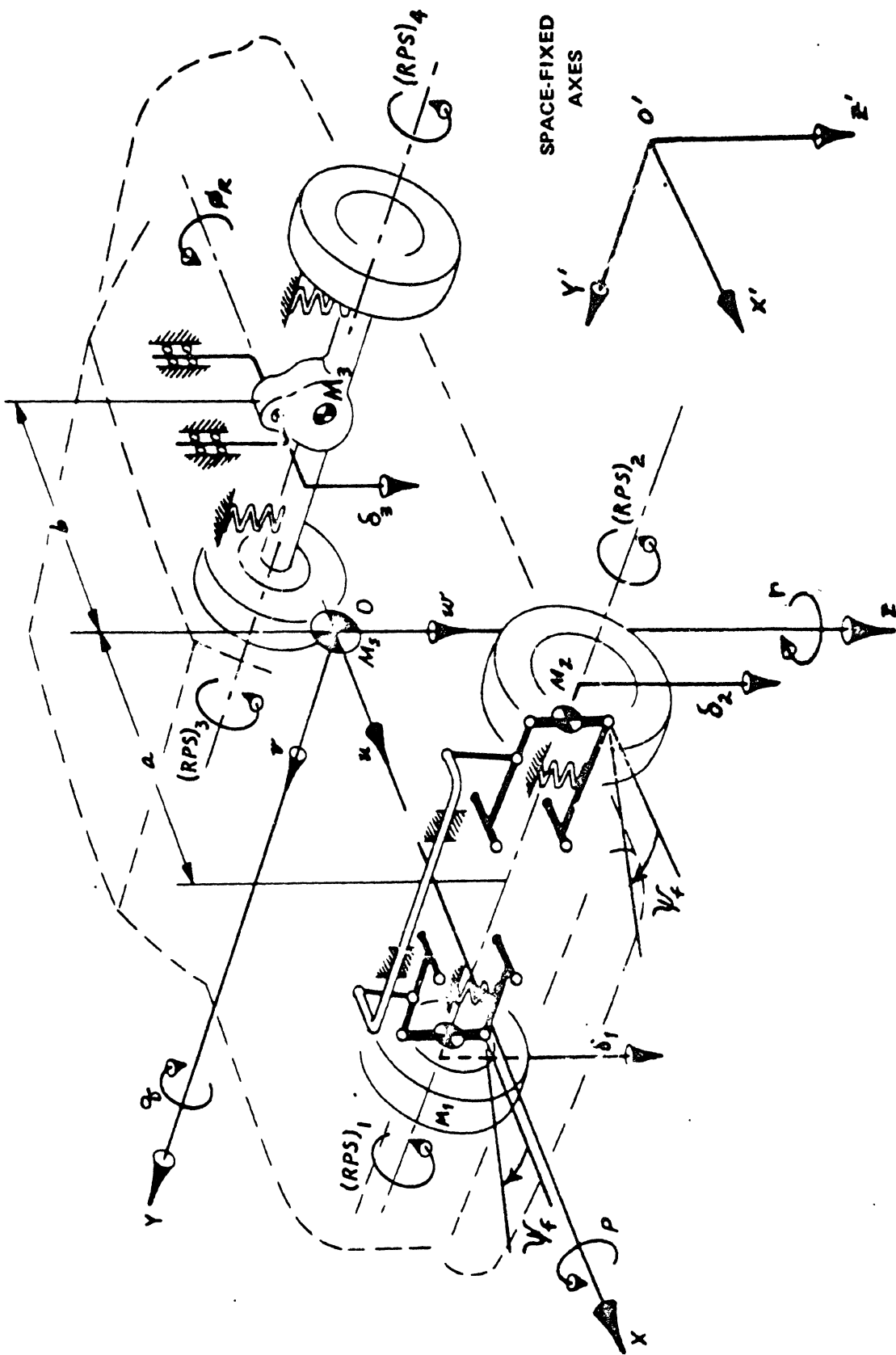
Figure B-8. HVOSM—Vehicle Model

rotational and one translatory degree of freedom. Each of the front unsprung masses is allowed one translatory degree of freedom. The four wheels each have a rotational degree of freedom in addition to one front wheel steer degree of freedom.

The centers of gravity of the front unsprung masses are constrained to deflection paths parallel to the sprung mass Z axis. The center of gravity of the rear unsprung mass is assumed constrained to motion perpendicular to the sprung mass X axis while additionally constrained to remain a fixed distance from the rear axle "roll center." The rear axle roll center is constrained to a path parallel to the sprung mass Z axis. The rotational degrees of freedom of the four wheels allow for the effect of rotational wheel slip on tire forces during braking or traction. The steer degree of freedom is initiated only when rigid obstacles such as curbs are encountered.

The following assumptions define the suspension geometry: (1) the camber angle of each front wheel relative to the vehicle is determined by interpolation of a tabular input of camber angle as a function of suspension deflection; (2) steer angles of the front wheels are assumed equal and front roll steer effects are neglected; (3) rear axle roll steer is treated as a linear function

of the angular degree of freedom of the rear axle; and
(4) anti-pitch effects are approximated by coefficients
tabulated as functions of suspension deflections.

The external forces consist of tire forces, aero-
dynamic forces, and rolling resistance. The tire forces
act within the tire-terrain contact patch, while aero-
dynamic drag and rolling resistance forces are grossly
approximated as acting directly through the sprung mass
center of gravity along the vehicle X axis.

For complete details of the HVOSM simulation, see
Reference (1). A number of auxiliary programs were written
to supplement the HVOSM simulation in generating tire-
surface data, terrain table data, and feedback control of
the vehicle. These programs and models are described in
the next three sections.

B.2.2 TIRE/SURFACE DATA GENERATION. The HVOSM simu-
lation requires tabular input of tire/surface friction
data in a particular form which is inconvenient for the
purposes of this study, since little distinction is allowed
for the separate friction contributions of tire and sur-
face to the total friction. As a result, an auxiliary
program was written by HSRI which accepted separate inputs
of general tire characteristics and general surface
characteristics separately and outputted the total tire/
surface friction tables required by the HVOSM simulation.
See Figure B-9.

```
Tire Characteristics ────────►┌──────────────────┐
                              │  Tire/Surface    │
                              │      Data        │────────►  Friction
                    .         │   Generation     │           Tables
                              │    Program       │           Required
Surface Characteristics ─────►│                  │           by HVOSM
                              └──────────────────┘           Program
```
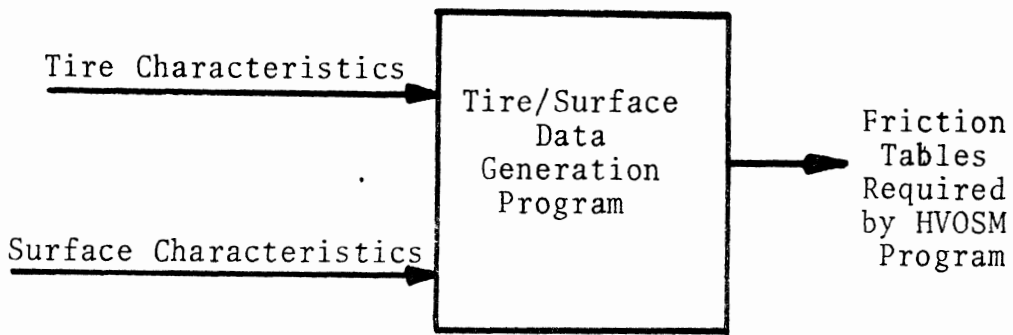
Figure B-9

      The tire and surface interaction of interest in this
study is shown in the surface/tire matrix of Table B-2.
The definitions and descriptions pertaining to Table B-2
are shown in Tables B-3 and B-4.

      The tire properties are characterized by a set of
input parameters chosen to best reflect average friction
variations, with slip and load based on actual tire test
data available at HSRI. Table B-5 summarizes these
assumed parameters for each tire.

<div align="center">

Table B-2

Surface/Tire Matrix

</div>

Tire Surface	A	B	C
1	$\mu_x\big|_{\substack{s=1\\v=40}} = .24$ $\mu_x\big|_{\substack{s=1\\v=80}} = .04$ $\mu_{xp} = .44$	$\mu_x\big|_{\substack{s=1\\v=40}} = .17$ $\mu_x\big|_{\substack{s=1\\v=80}} = 0.0$ $\mu_{xp} = .37$	$\mu_x\big|_{\substack{s=1\\v=40}} = .12$ $\mu_x\big|_{\substack{s=1\\v=80}} = 0.0$ $\mu_{xp} = .32$
2	$\mu_x\big|_{\substack{s=1\\v=40}} = .36$ $\mu_x\big|_{\substack{s=1\\v=80}} = .16$ $\mu_{xp} = .56$	$\mu_x\big|_{\substack{s=1\\v=40}} = .25$ $\mu_x\big|_{\substack{s=1\\v=80}} = .05$ $\mu_{xp} = .45$	$\mu_x\big|_{\substack{s=1\\v=40}} = .18$ $\mu_x\big|_{\substack{s=1\\v=80}} = 0.0$ $\mu_{xp} = .38$
3	Same as 2-A but $\mu_x\big|_{\substack{s=1\\v=80}} = .28$	Same as 2-B but $\mu_x\big|_{\substack{s=1\\v=80}} = .17$	Same as 2-C but $\mu_x\big|_{\substack{s=1\\v=80}} = .10$
4	Same as 5-A but $\mu_x\big|_{\substack{s=1\\v=80}} = .18$	Same as 5-B but $\mu_x\big|_{\substack{s=1\\v=80}} = .04$	Same as 5-C but $\mu_x\big|_{\substack{s=1\\v=80}} = 0.0$
5	$\mu_x\big|_{\substack{s=1\\v=40}} = .48$ $\mu_x\big|_{\substack{s=1\\v=80}} = .28$ $\mu_{xp} = .68$	$\mu_x\big|_{\substack{s=1\\v=40}} = .34$ $\mu_x\big|_{\substack{s=1\\v=80}} = .14$ $\mu_{xp} = .54$	$\mu_x\big|_{\substack{s=1\\v=40}} = .24$ $\mu_x\big|_{\substack{s=1\\v=80}} = .04$ $\mu_{xp} = .44$

where: $\mu_x\big|_{\substack{s=1\\v=40}} \equiv$ locked wheel friction coefficient at 40 mph

$\mu_x\big|_{\substack{s=1\\v=80}} \equiv$ locked wheel friction coefficient at 80 mph

$\mu_{xp} \equiv$ peak longitudinal friction coefficient at 40 mph

Table B-3

Surface Descriptions

Surface	Type	Skid Number @ 40 mph	Skid Number Gradient With Respect to Velocity
1	Smooth	20	$-.5$ $(mph)^{-1}$
2	Fine, Rounded	30	$-.5$ $(mph)^{-1}$
3	Fine, Gritty	30	$-.2$ $(mph)^{-1}$
4	Coarse, Rounded	40	$-.75$ $(mph)^{-1}$
5	Coarse, Gritty	40	$-.5$ $(mph)^{-1}$

Table B-4

Tire Descriptions

Tire	Tread Wear
A	New
B	Half-Worn
C	Fully Worn

Tire Parameters	A (New)	B (Half-Worn)	C (Fully Worn
FXGRAD	- .25	- .25	- .25
T_F	1.2	.85	.6
C_S	15000	15000	15000
S_P	.2	.2	.2
DUYDFZ	- .00025	- .00025	- .00025

V = 40 mph

where,

FXGRAD ≡ gradient of μ_x with respect to slip in the high-slip region

T_F ≡ an assumed tire performance or wear factor indicating the ratio of the skid number for a given tire to that of the standard ASTM skid test tire on any surface

C_S ≡ longitudinal stiffness of tire

S_P ≡ value of slip at which μ_{xp} occurs

DUYDFZ ≡ variation of peak lateral friction coefficient with load $(lbs)^{-1}$.

Where appropriate, these terms are graphically defined on Figure B-10.
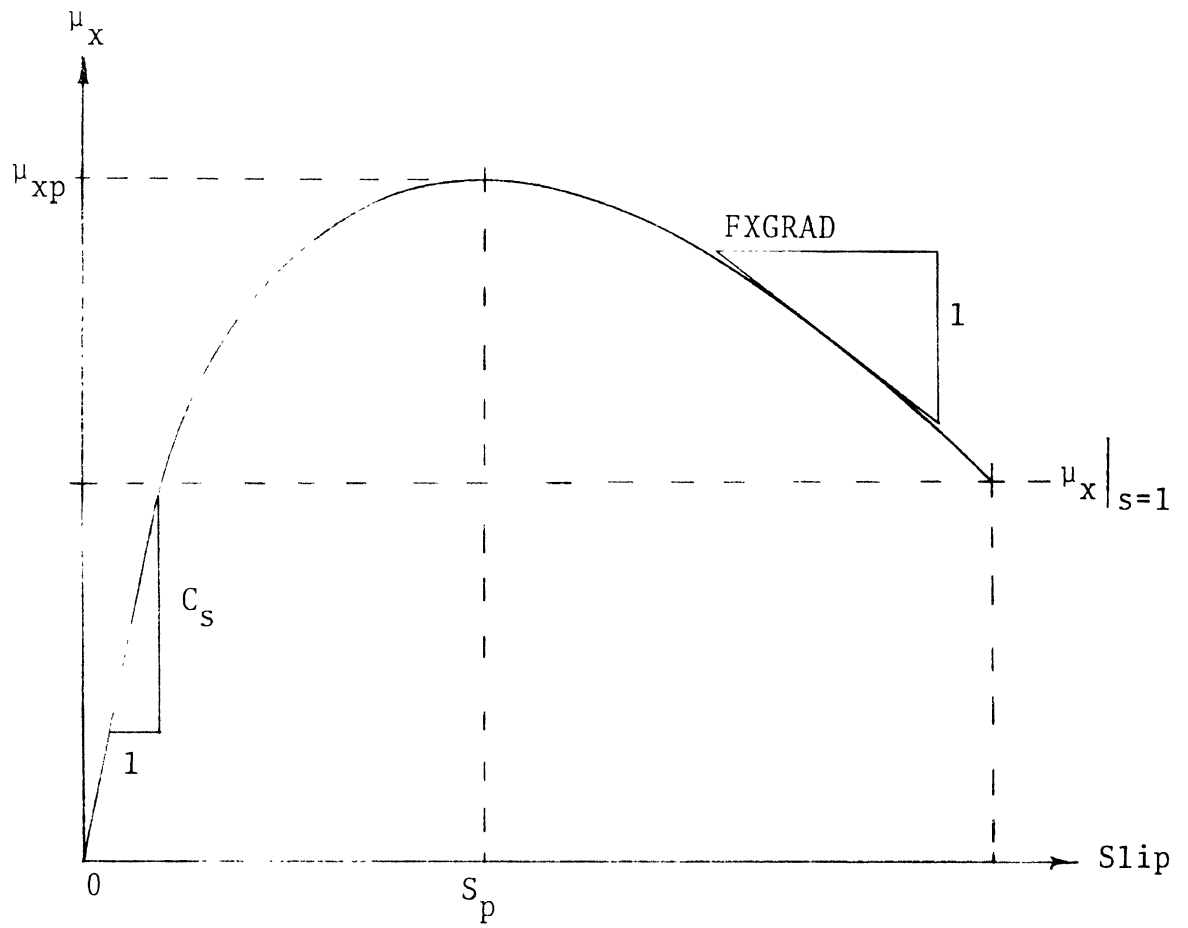
Figure B-10. Tire Parameter Term Definitions

In addition, it is assumed that the peak lateral coefficient of friction, μ_{yp}, saturates and that the value of μ_{yp} at this slip angle is equal to μ_{xp}. The saturation characteristics of μ_{yp} are shown on Figure B-11.

B.2.3 TERRAIN TABLE DATA GENERATION. The HVOSM simulation provides for a terrain or surface upon which the vehicle operates. Tabular input data for the program describes how the elevation varies with displacements in the two horizontal directions. It is the responsibility of the program user to provide this tabular input for each different terrain. Since in this study terrain geometrics were a principal interest, changes in terrain tables were frequent and would have required excessive amounts of time if prepared "by hand." Instead, an auxiliary program was written which assumed a general surface or terrain in the form of a "banked helical ramp," thus allowing for a constant radius path with downgrade or upgrade as well as superelevation. A sketch of a banked helical ramp is shown in Figure B-12.

The inputs to this auxiliary program are the radius of the curve (R_o), grade (G), and superelevation (e). The output is the tabular data in the form required by the HVOSM simulation. Thus a curved roadway of nominal radius R_o, grade G, and superelevation e, can be obtained by simply entering the three required parameters and allowing the program to generate the required table.
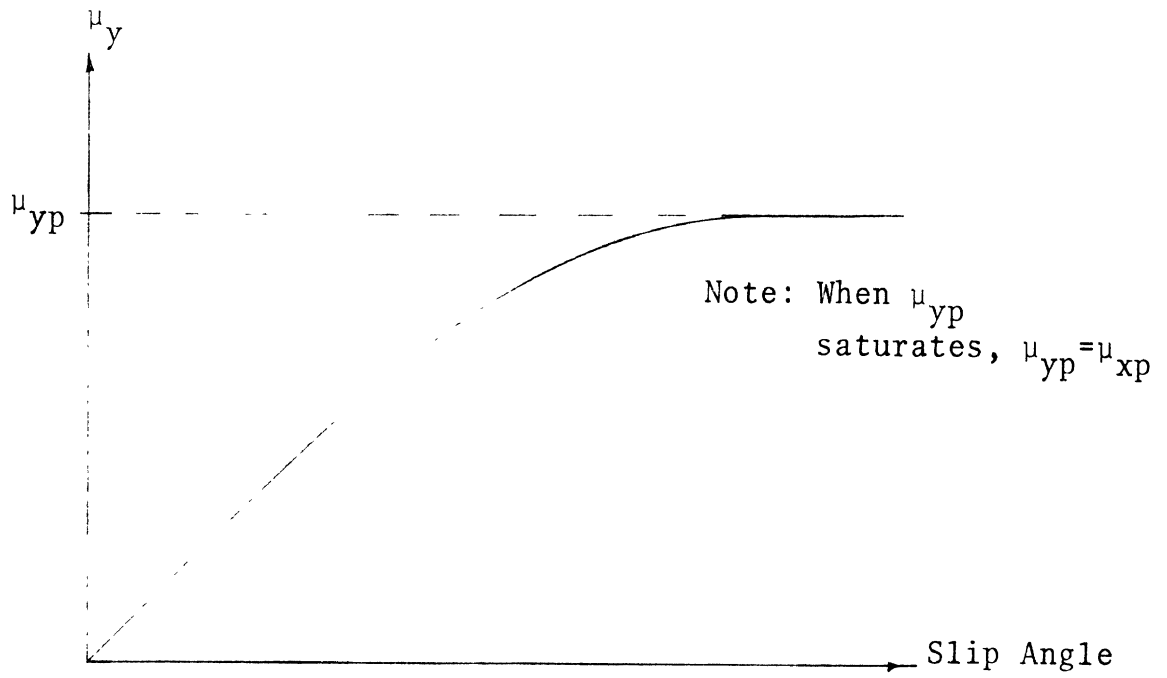
Figure B-11.   Saturation Characteristic of μ_y.
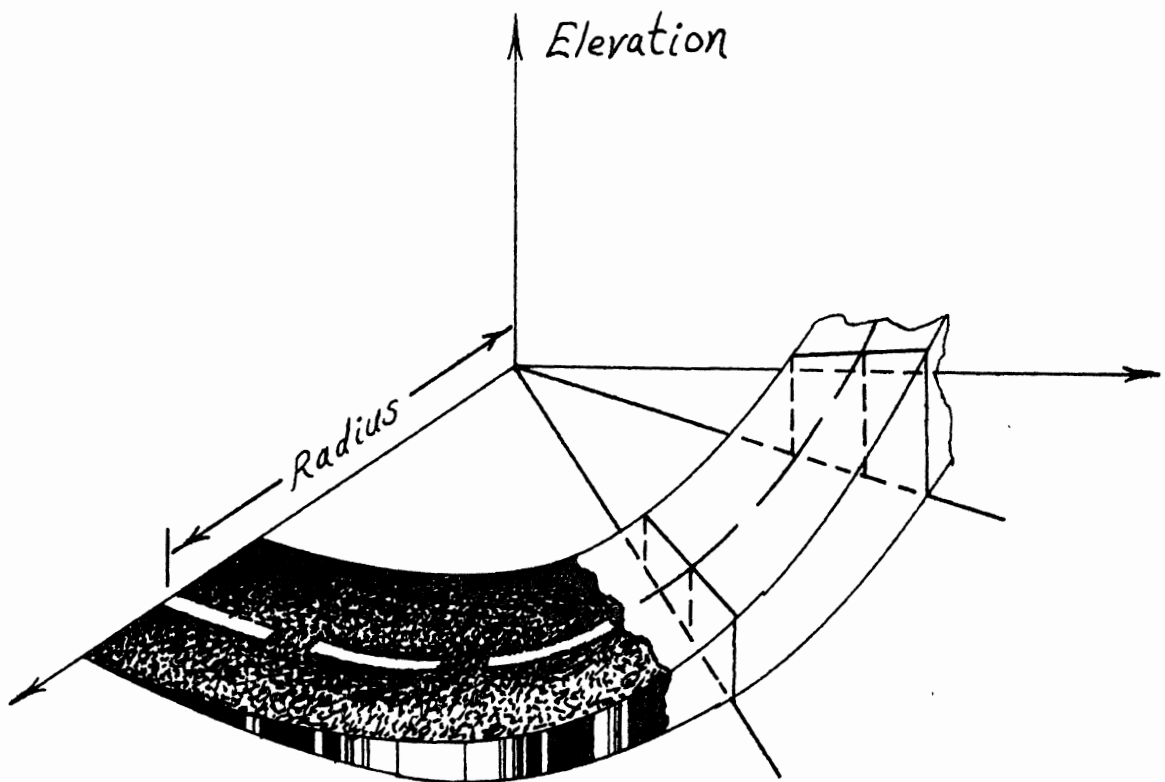
Figure B-12.   A Banked Helical Ramp

The relationship used for obtaining the elevation of points on the road is conveniently described in terms of the cylindrical coordinates (Z, R, and θ) shown in Figure B-13. First consider points on the centerline of the road. The elevation of points on the centerline of the road, illustrated in Figure B-13, is given by the equation:

$$Z = R_o \theta G \qquad (B.31)$$

where

Z is the elevation

R_o is the radius of the centerline of the road

θ is the angular position coordinate, and

G is the grade.

The elevation of all points on the road at any radii is given by

$$Z = R_o \theta G + (R-R_o)e \qquad (B.32)$$

where

R is the radial distance coordinate and

e is the superelevation.
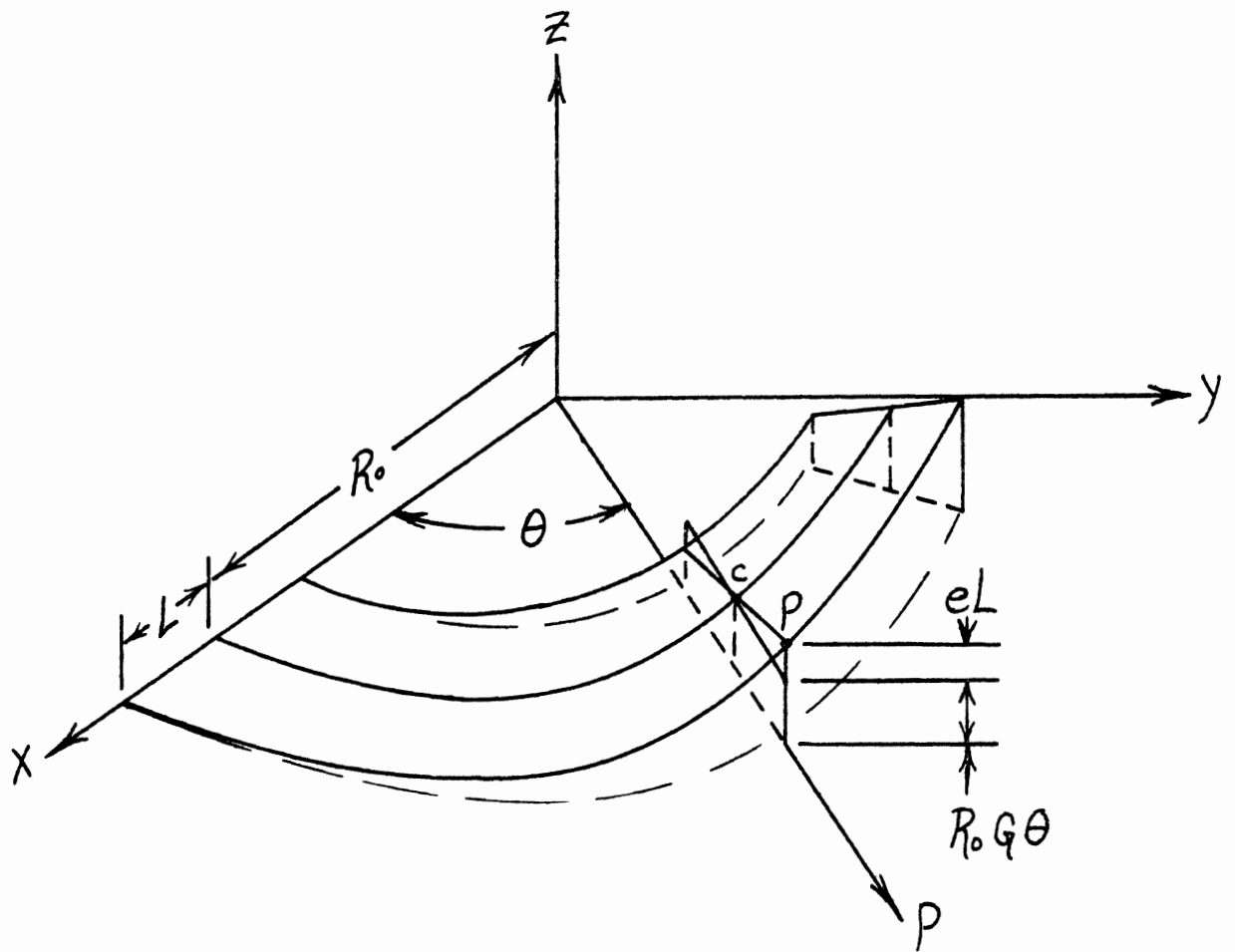
Figure B-13. Curve/Grade Geometry

Thus, as shown in Figure B-13, point P is at a higher elevation than point C. For a road with lane width L and superelevation e the point P on the outside edge of the road is higher than the point C on the centerline of the road by the amount, e · L.

For use in the HVOSM terrain tables the expression describing the road surface was converted from cylindrical coordinates to rectangular coordinates.

B.2.4 VEHICLE CONTROLLER.

B.2.4.1 General Description. It was apparent from the beginning of the study that a feedback control scheme would be required to guide a vehicle along circular paths while also being capable of performing lane changes about such paths. The basic requirements for such a control system are as follows:

1) Path deviation for a steady-state circular turn should be driven to near zero.

2) No highly oscillating or unusual control behavior during transient periods.

3) Good response, particularly during lane change or similar maneuvers.

No attempt was made to model or approximate human driver behavior by considering time delays and neuromuscular

272

dynamics. However, steer levels and rates which far exceeded those of human performance were not considered desirable.

After considering a number of different schemes, a general control system was developed. It is shown in Figure B-14. The appropriate variable relationships are shown in Figure B-15. The principal feedback variables are heading angle (ψ), sideslip angle (β), and yaw rate (r). Path angle error (λ) is the angular difference between the velocity vector direction ($\psi + \beta$) = γ or vehicle path angle and the desired path angle (ψ_p). As shown in Figure B-14, predicted path angle error, (λ'), is formed by the difference of the desired path angle (ψ_p) and vehicle path angle ($\psi + \beta$) predicted in time. λ' is fed forward with its integral forming y_p, which can be thought of as a predicted path deviation. This is then compared with the reference path deviation ΔR. The additional forward loop compensation and yaw rate damping is required for both stability and the performance requirements mentioned above. The output of the controller, front wheel angle (δ_{FW}), is the input to the vehicle dynamics block, thus clsoing the loop. The system as shown is basically single-loop and compensatory, with λ' as the primary error signal. ψ_p inputs as a function of time define the desired path to be followed, while the ΔR inputs define path variations superimposed about the path defined by ψ_p advanced in time.

$$Y = \psi + \beta$$

$$Y_p = 1 + C_4 p$$

$$Y_F = 1 + C_3 p$$

$$\Delta R = C_7$$
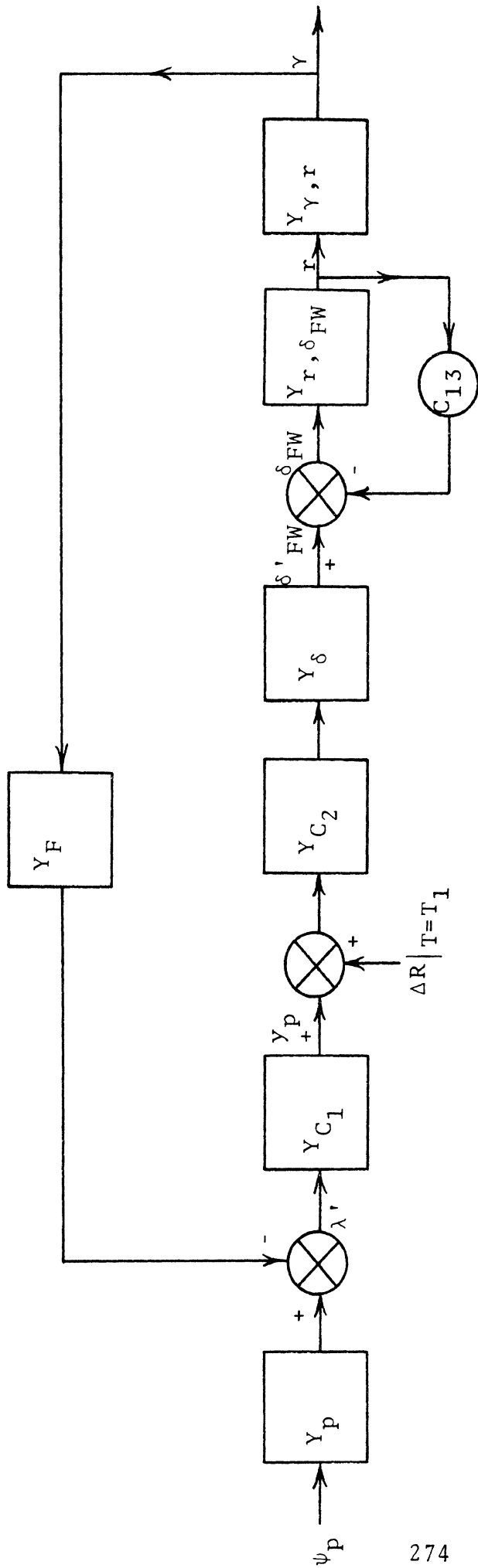
$$Y_{C_1} = C_5 + \frac{C_6}{p}$$

$$Y_{C_2} = K_1 (C_1 + \frac{C_2}{p}) \left(\frac{C_9 p + C_{10}}{p + C_{11}} \right)$$

$$Y_\delta = \frac{C_{12}}{p + C_{12}}$$

$$T_1 = C_8$$

$C_1 = 1.0$		$C_{10} = 3.0$
$C_2 = 3.0$		$C_{11} = 10.0$
$C_3 = 1.0$		$C_{12} = 20.0$
$C_4 = 1.0$		$C_{13} = .2$
$C_5 = 1.0$		$K_1 = 1.5$
$C_6 = 1.0$		
$C_7 = .1$		
$C_8 = 3.0$		
$C_9 = 1.0$		

Figure B-14. Vehicle Control System.

$\gamma = \psi + \beta$

ψ_p

$\lambda = \psi + \beta - \psi_p$
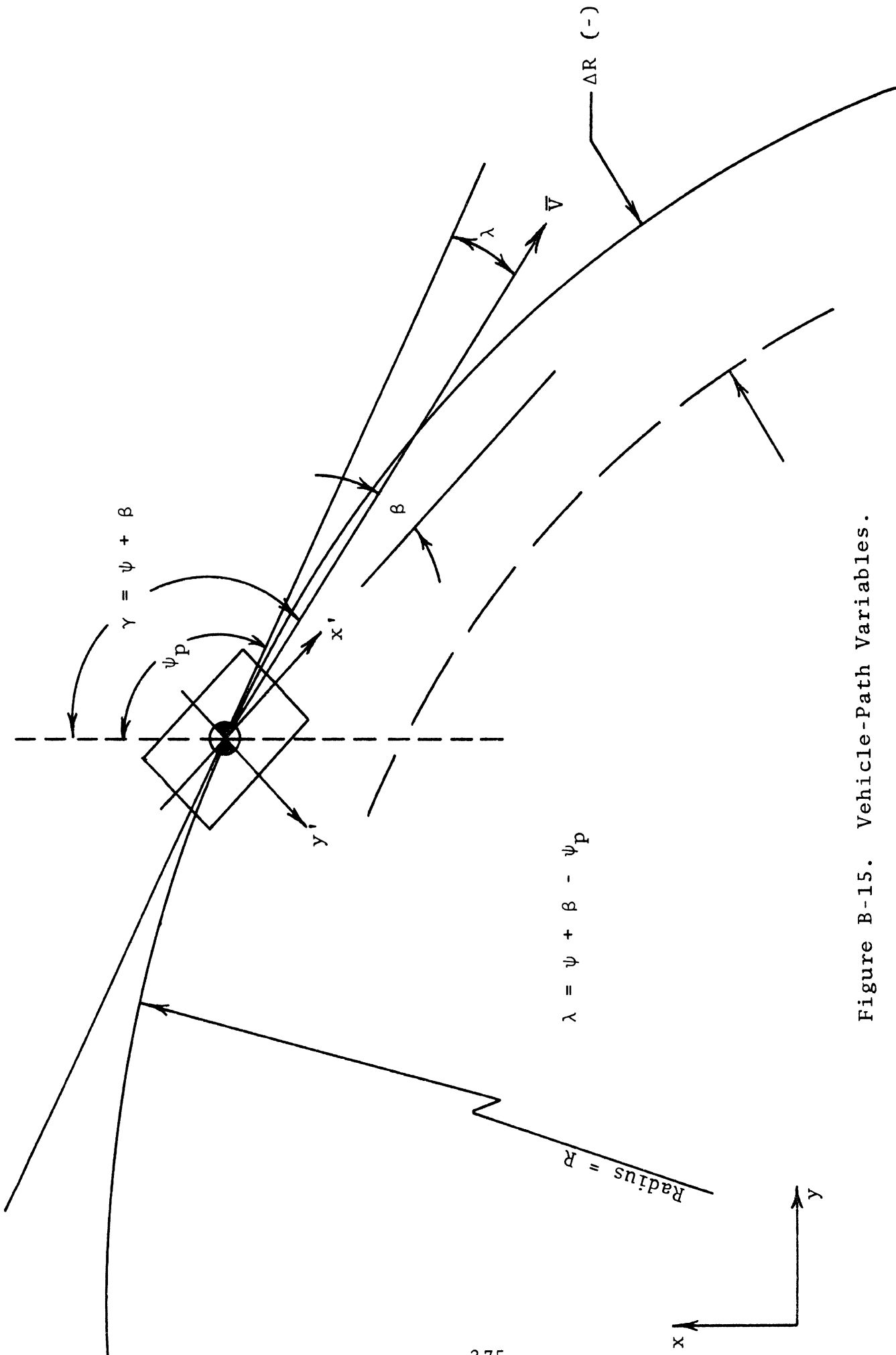
Figure B-15. Vehicle-Path Variables.

275

As an example, consider the circle-to-circle lane-change maneuver used in this study. The vehicle is required to follow a circular path for three seconds, at which time a 12-foot lane change to an inside concentric circle is to be performed. If the equation of the circle is

$$R^2 = x^2 + y^2 \tag{B.33}$$

then, by differentiating this expression, an equation for the desired path angle ψ_p can be obtained as follows: Performing the differentiation yields,

$$0 = 2x\dot{x} + 2y\dot{y} \tag{B.34}$$

or,

$$\frac{\dot{x}}{\dot{y}} = \frac{dx}{dy} = \frac{-y}{x} \tag{B.35}$$

Now observe that $\frac{dx}{dy}$, evaluated along the trajectory, is the tangent of the desired path angle along the trajectory. Thus,

$$\psi_p(T) = \tan^{-1}\left(\frac{-y}{x}\right) = \tan^{-1}\left[\frac{-y(T)}{x(T)}\right] \tag{B.36}$$

Therefore, the angular tangent to the circle (ψ_p) can be expressed in terms of simple path coordinates x and y, which are known as a function of time in the simulation.

276

At time T=0, with the vehicle at x = R, y = 0, and
oriented in the y-direction, the $\psi_p(T)$ input expressed
by Equation (B.36) will cause the vehicle to follow the
circle with radius R, provided the ΔR input is zero for
all time. These relationships are shown in Figure B-15.
If a lane change to a concentric inner circle is required
at T=3 seconds, then the time history for ΔR would be

$$\Delta R = 0 \quad , \quad \text{for } 0 \leq T < 3$$

$$\Delta R = C \quad , \quad \text{for } T \geq 3$$

where C is a constant equivalent to a 12-foot lane change.
Note that this step form of ΔR can cause an abrupt change
in steering to occur. Varying degrees of steering path
response can be obtained by ramping ΔR from 0 to C at the
desired rate, as shown in Figure B-16.
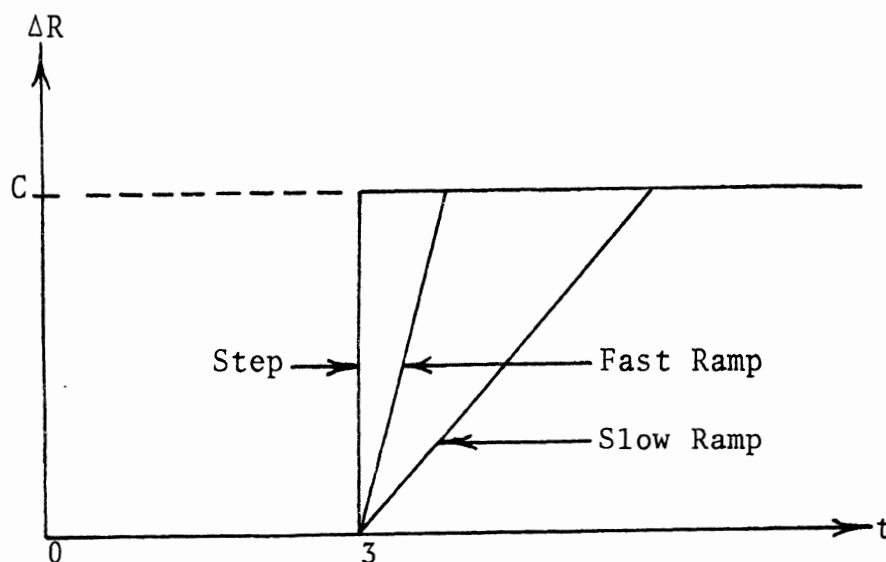
Figure B-16

B.2.4.2 <u>Vehicle Transfer Function Approximation</u>. Since

heading angle (ψ), sideslip angle (β), and yaw rate ($r=\dot{\psi}$)

are the principal feedback variables outlined in the

proposed control system, it is desirable from an analytical

and design viewpoint that a reasonably valid relationship

between these variables and front wheel angle is known.

The obvious approach is to write down the linear equations

of motion for a two-degree-of-freedom vehicle and then

form the required transfer functions:

$$\dot{v} = \left(\frac{-4C_\alpha}{Mu}\right) v + \left[\frac{2C_\alpha(b-a)}{Mu} - u\right] r + \left(\frac{2C_\alpha}{M}\right) \delta_{FW}$$

$$\dot{r} = \frac{2C_\alpha}{I} \left[(\frac{b-a}{u})v - (\frac{b^2+a^2}{u})r + (a)\delta_{FW}\right]$$

$$\dot{\psi} = r \qquad\qquad\qquad\qquad\qquad\qquad (B.37)$$

where

v = lateral velocity relative to vehicle body axis (ft/sec)

r = yaw rate (rad/sec)

ψ = yaw angle (rad)

δ_{FW} = front wheel angle (rad)

C_α = lateral stiffness of all tires (lb/rad)

M = vehicle mass (slugs)

u = forward velocity (ft/sec)

b = location of rear tires from c.g. (ft)

a = location of front tires from c.g. (ft)

I = vehicle yaw moment of inertia about vehicle vertical body axis (slug-ft^2)

The following values were chosen on the basis of the vehicle being simulated with a design speed of 100 ft/sec.

C_α = 10000

M = 120

u = 100

b = 5.5

a = 4.5

I = 2500

By appropriate substitutions and assuming $\beta \cong v/u$
(u = constant here), the two required transfer functions
are formed:

$$Y_{r,\delta_{FW}} \equiv \frac{r}{\delta_{FW}} = \frac{19(p + 1.8)}{p^2 + 3.6p + 7.3} \tag{B.38}$$

and

$$Y_{\psi+\beta,r} \equiv \frac{\psi+\beta}{r} = \frac{.0475(p^2 + p + 38.)}{p(p + 1.8)} \tag{B.39}$$

With yaw rate damping included (C_{13} = 0.2), the
$Y_{r,\delta_{FW}}$ transfer function becomes:

$$Y_{r,\delta_{FW}}' = \frac{Y_{r,\delta_{FW}}}{1 + C_{13} Y_{r,\delta_{FW}}} \tag{B.40}$$

or

$$Y_{r,\delta_{FW}}' = \frac{19(p + 1.8)}{p^2 + 7.4p + 14.1} \tag{B.41}$$

The effect of the yaw rate damper is to move the two
complex poles of the $Y_{r,\delta_{FW}}'$ denominator closer to and
farther out along the negative real axis in the complex
plane. This is desirable for reasons of response and
stability, as will be shown by some root loci plots.

B.2.4.3 <u>Forward Loop Gain</u>. The vehicle transfer functions $Y_{r,\delta_{FW}}{}'$ and $Y_{\psi+\beta,r}$ can now be combined with the controller transfer functions shown in Figure B-14 to form one forward loop transfer function Y_o. Using the values shown in Figure B-14, Y_o becomes:

$$Y_o = \frac{K_1(.9)(p^2 + 1.1p + 38)(p+1)(p+3)^2}{p^3(p^2 + 7.4p + 14.1)(p+10)} \qquad (B.42)$$

and therefore $H \equiv Y_o Y_F$ becomes

$$H = Y_o(p+1)$$

$$= \frac{K_1(.9)(p^2 + 1.1p + 38)(p+1)^2(p+3)^2}{p^3(p^2 + 7.4p + 14.1)(p+10)} \qquad (B.43)$$

A suitable value of forward loop gain (K_1) can now be chosen from a root locus plot of H for the particular set of controller values shown in Figure B-14. These controller values were chosen by generating root loci plots for different controller values to determine a suitable root locus plot. This plot was then used to choose K_1. Two root locus plots are shown in Figures B-17 and B-18, demonstrating the effect of yaw rate damping. Figure B-17 is the root locus for H shown above, which includes yaw rate damping. Figure B-18 is a root locus of a similar transfer function resulting from no-yaw-rate damping and slightly different controller values. The
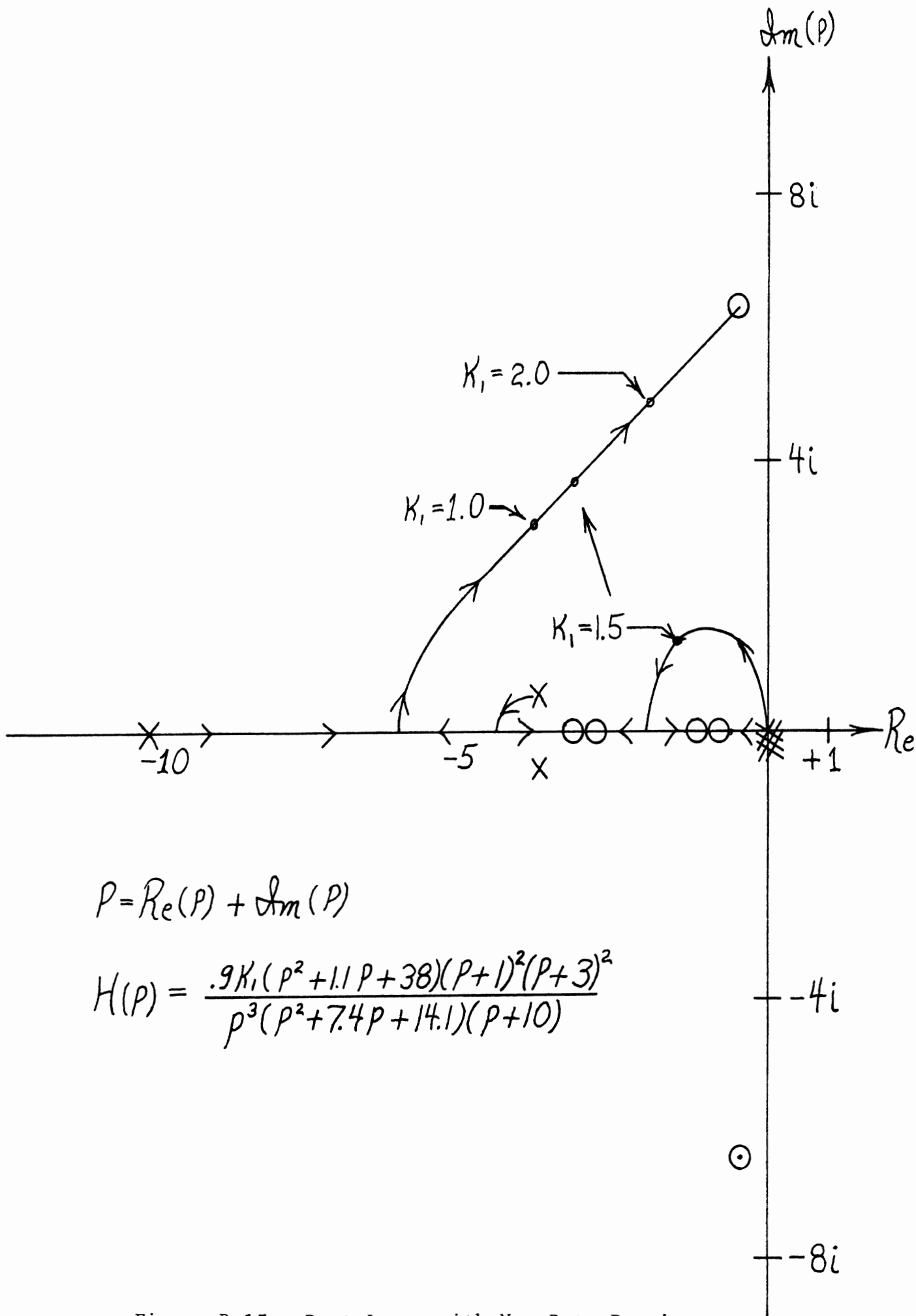
$$P = \mathcal{R}_e(P) + \mathcal{I}_m(P)$$

$$H(P) = \frac{.9K_1(P^2+1.1P+38)(P+1)^2(P+3)^2}{P^3(P^2+7.4P+14.1)(P+10)}$$

Figure B-17. Root Locus with Yaw Rate Damping

282

$$H(P) = \frac{.9K_1(P^2 + 1.1P + 38)(P+1)^2(P+2)^2}{P^3(P^2 + 3.6P + 7.3)(P+10)}$$
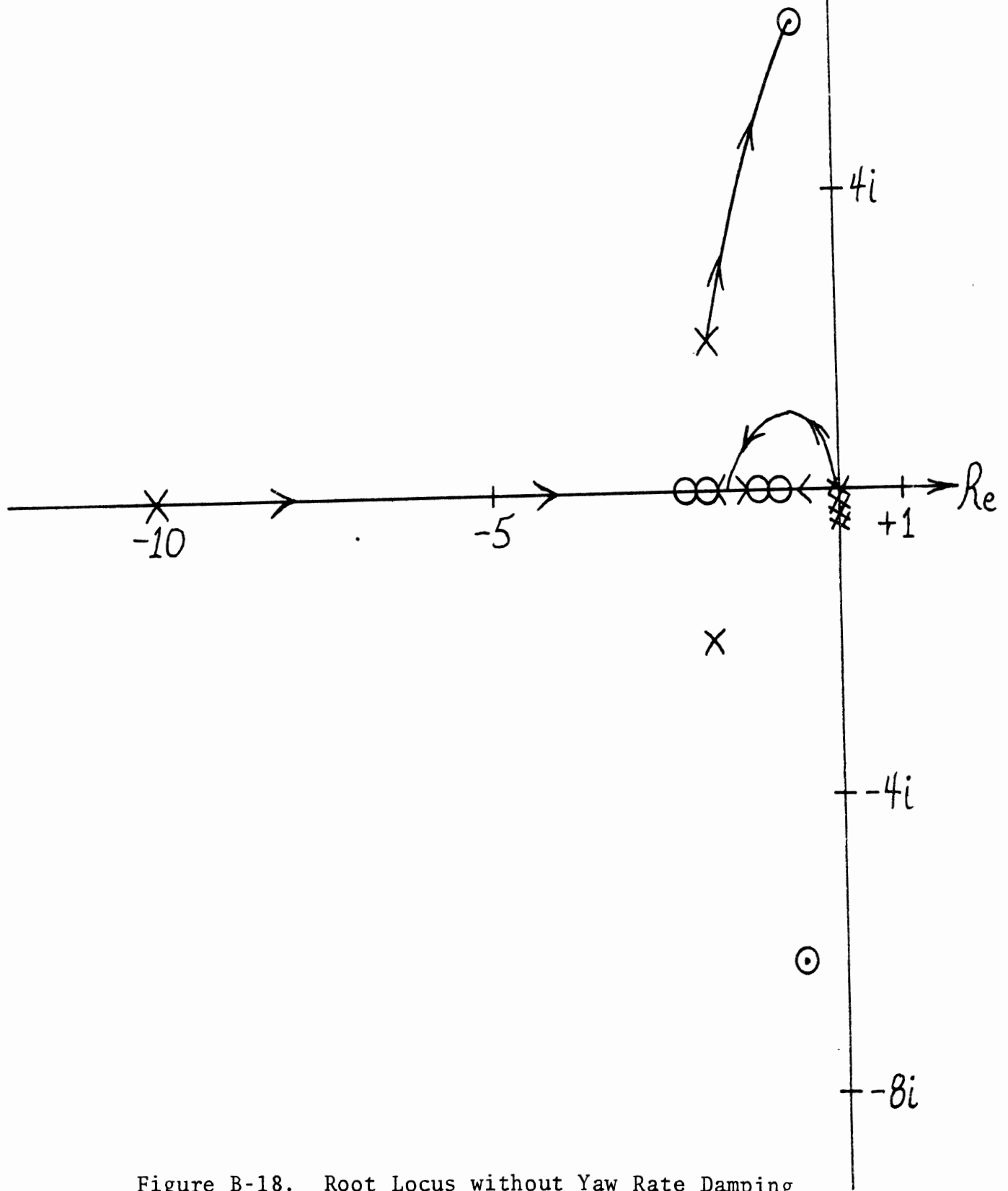
Figure B-18.   Root Locus without Yaw Rate Damping

283

difference in the nature of the plots is primarily the result of the yaw rate damping which moves the two complex poles to the left and toward the negative real axis.

A value of 1.5 was chosen for K_1 from the root locus of Figure B-17 and proved quite suitable in the computer simulation. Step changes in the ΔR input command provided responsive lane changes required for many of the maneuvers. Variable time histories shown in the next section demonstrate the effectiveness of the control scheme.

B.2.5 SIMULATION EXERCISES. Simulation exercises were carried out in two phases. In the first phase a pilot study was carried out to determine which parameters were most important in the vehicle interaction with the roadway. The second phase consisted of a more extensive examination of these important parameters.

The variables evaluated in the pilot study included:

1)   surface

2)   tires

3)   grade

4)   curvature

5)   superelevation

6)   vehicle type

7)   maneuver

8)   wind effects

9)   roadway perturbations

The results of the pilot study indicated that wind effects and roadway perturbations had a lesser influence on vehicle stability than some of the other parameters. Further examination of these parameters was therefore deferred as a means of limiting the scope of the study to manageable proportions. As a result, the primary study focused on the first seven parameters shown above. Table B-6 shows the range of variations considered for each of these parameters. (Also, the notation used to label the computer results is indicated in Table B-6.)

Table B-6

1. SURFACE

Notation	Meaning			
S_1	SN =	20	SN_{grad} =	$-.5(mph)^{-1}$
S_2	=	30	=	$-.5$
S_3	=	30	=	$-.2$
S_4	=	40	=	$-.75$
S_5	=	40	=	$-.5$

2. TIRE

Notation	Meaning
Tire A	New Tread
Tire B	Half-Worn Tread
Tire C	Fully-Worn Tread

3. GRADE

Notation	Meaning
G_1	-1%
G_2	-3%
G_3	-6%

4. CURVATURE

Notation	Meaning
D_1	1°
D_2	3°
D_3	6°

5. SUPERELEVATION

Notation	Meaning
e_1	3/16"/foot
e_2	9/16"/foot
e_3	1 1/8"/foot

6. VEHICLE TYPE

Notation	Meaning
C_1	Small Sedan
C_2	Intermediate Sedan
C_3	Station Wagon

7. MANEUVER

Notation	Meaning
V_{CR}	Cornering Under Traction
V_{LC}	Cornering and Lane Change
V_{LOC}	Cornering, Lane Change and Braking

Simulation runs were made for several of these parameter combinations at different velocities. Success or failure in performing a given maneuver at these different velocities therefore defined a safe region of operation with respect to that particular maneuver and operating conditions.

The results of the parameter study were described primarily in terms of so-called safe velocities. For each set of operating conditions (i.e., tire/surface friction, maneuver, roadway geometrics, etc.), there is ideally one velocity above which the vehicle would have difficulty performing the required maneuver due to various forms of instability that would result from insufficient friction. The amount of available friction from the tire/surface interface is highly dependent upon vehicle velocity under wet conditions, with lower friction available at higher vehicle velocities. These instabilities can be put into one of two categories:

1) loss of vehicle directional stability, and

2) loss of path or trajectory stability.

The former is commonly called a spin-out and results from loss of traction of the rear wheels. A spin-out is characterized by large vehicle sideslip angles, or the inability of the vehicle to maintain orientation in the approximate direction of the velocity vector. A path

instability is commonly called a plow-out and is the
result of loss of traction on the front wheels. A plow-
out is characterized by a large path error, or inability
of the vehicle to maintain a given path. Normally one or
both of these types of instabilities will begin to occur
above the so-called safe velocity for a given set of
operating conditions.

In this study, these safe velocities were classified
according to maneuver.

1) V-CRITICAL, or V_{CR}, is the safe velocity,
    subject to operating conditions, for a vehicle
    cornering under traction. The amount of
    traction necessary is that which will allow
    the vehicle to compensate for aerodynamic
    drag, road drag, and grade while maintaining
    constant velocity. No lane change or braking
    is involved.

2) V-LANE CHANGE, or V_{LC}, is the safe velocity
    for a vehicle cornering under traction that
    also performs a 9- to 12-foot lane change.

3) V-LOSS OF CONTROL, or V_{LOC}, is the safe velocity
    for a vehicle performing the V_{LC} maneuver but
    with traction removed and moderate braking

added at the time of the lane change. The
safe velocity in this case is defined as
that velocity the vehicle had at the very
start of the braking. Moderate braking
here is defined as 0.3g's deceleration.

In order to make clear the concept of stability for
each of the three chosen maneuvers, sets of typical time
history plots of appropriate variables will be presented
next with a discussion of each.

B.2.5.1 V_{LOC} - Lane Change and Braking. The V_{LOC}
maneuver is defined as follows: At time T=0, the vehicle
enters a curve of radius R and maintains that curve for
three seconds. At time T=3 seconds, the vehicle performs
a 9- to 12-foot lane change to the inside, via the feed-
back control scheme, and simultaneously applies braking
to maintain 0.3g's deceleration. The lane change should
be completed within four seconds of the time the maneuver
is initiated, or by time T=7 seconds. The purpose of this
maneuver is to demonstrate the effect of tire force loss
due to combined steering and braking in a typical highway
emergency maneuver without exceeding reasonable levels of
steer and braking. Figure B-19 shows the desired vehicle
trajectory. Figure B-20 contains time histories for a
typical stable maneuver.

ΔR Negative as Shown
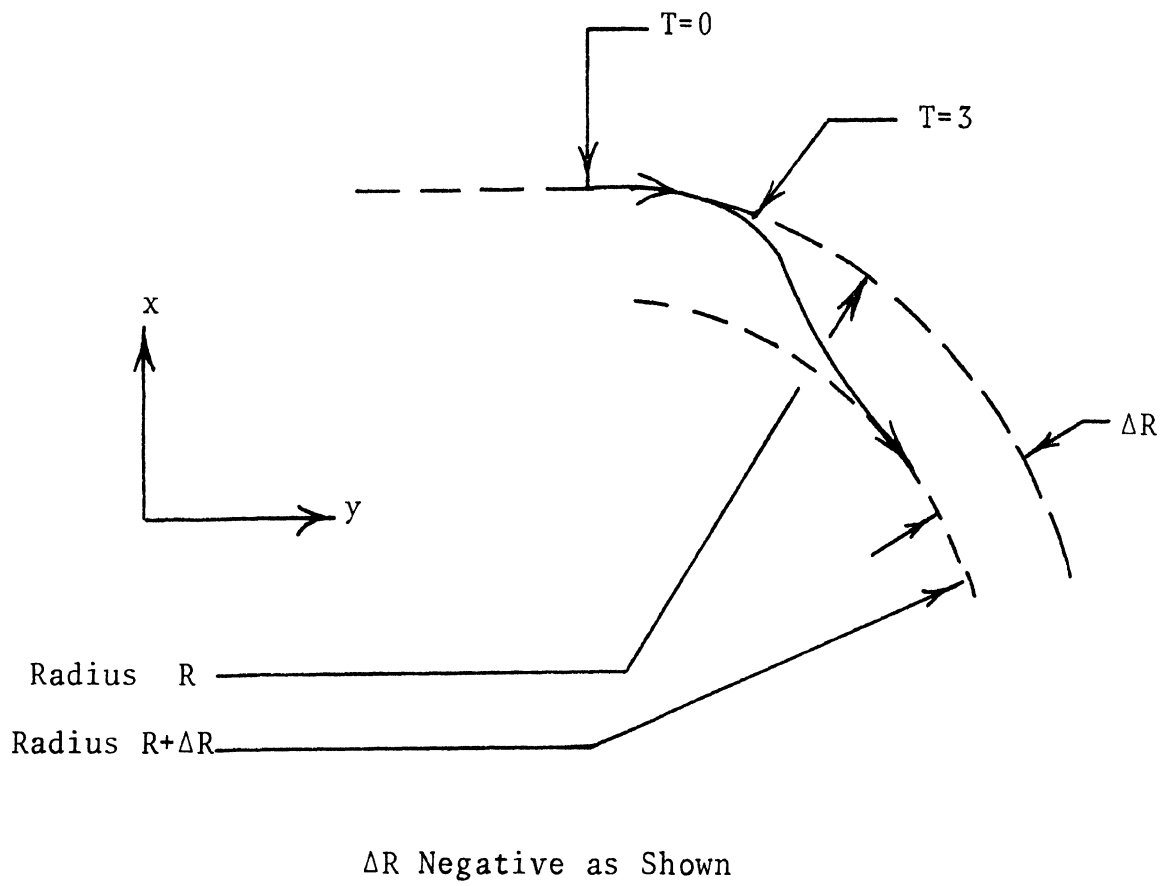
Figure B-19. Circle-to-Circle Lane Change, V_{LOC} and V_{LC}.
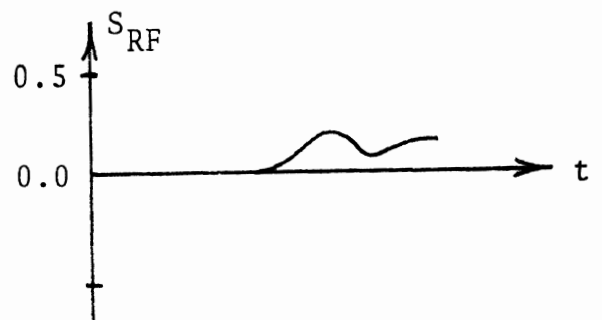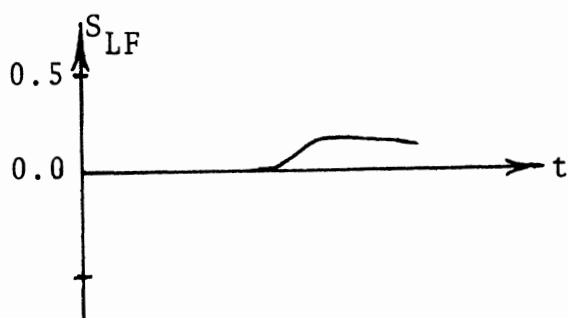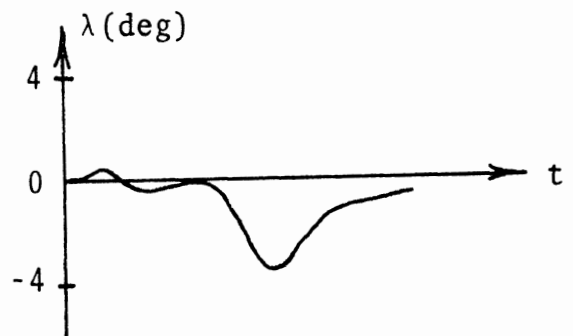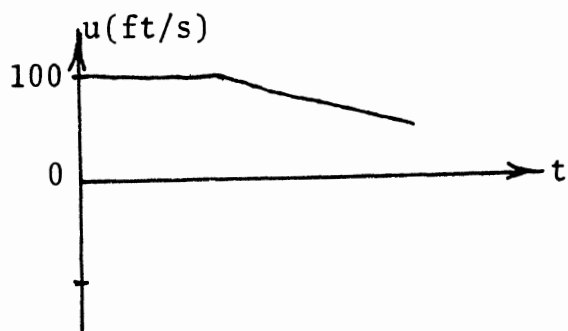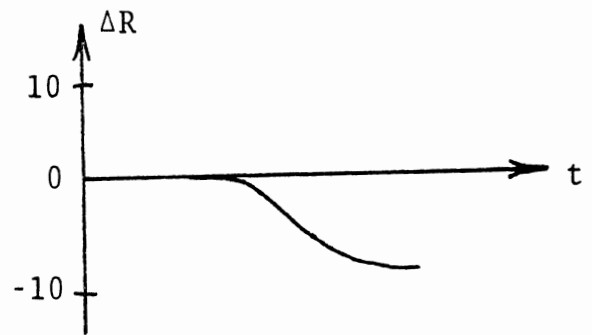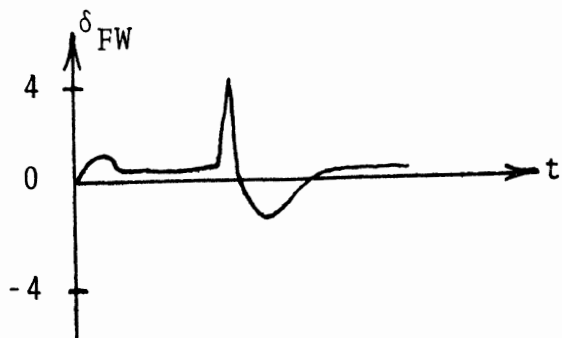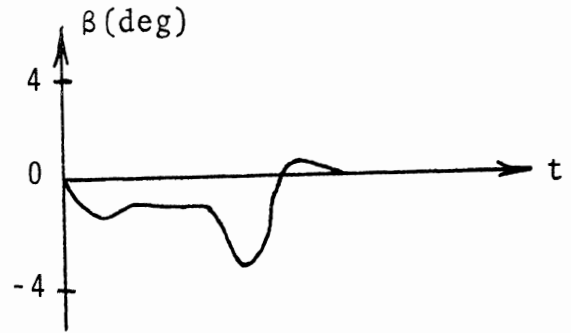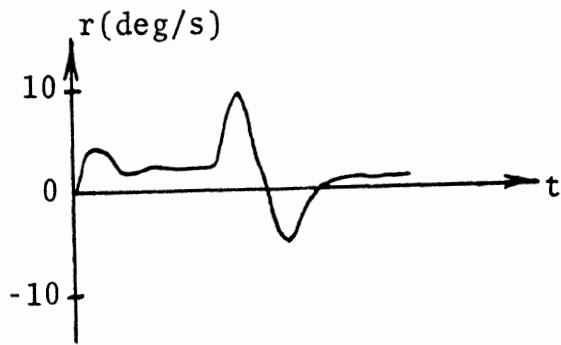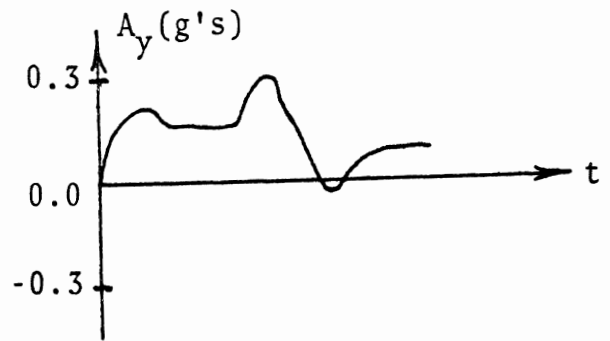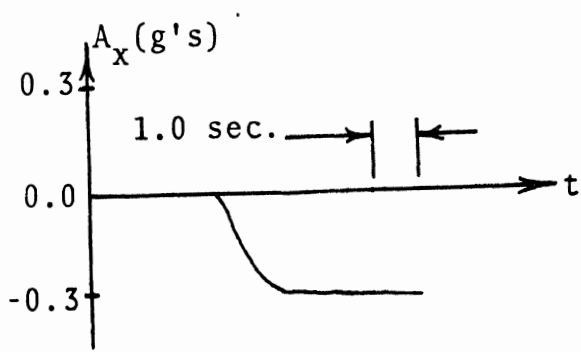
Figure B-20. Stable V_{LOC} Maneuver

Definitions for each of the variables shown in Figures
B-20 through B-28 are listed in Table B-7.

Table B-7
Plot Variable Definitions

A_x -   Longitudinal Acceleration

A_y -   Lateral Acceleration

r -   Yaw Rate

β -   Vehicle Sideslip Angle

δ_{sw} -   Steering Wheel Angle

ΔR -   Lateral Path Deviation from Initial Radius

u -   Forward Velocity

λ -   Path Angle Error, i.e., angular difference
between vehicle's velocity vector and
tangent to the prescribed path

S_{LF} -   Left Front Wheel Slip

S_{RF} -   Right Front Wheel Slip

S_{LR} -   Left Rear Wheel Slip

S_{RR} -   Right Rear Wheel Slip

A very common occurrence during moderate braking in low friction situations is wheel lockup. Due to the dramatic loss of tire side force with increased wheel slip, serious vehicle stability problems can arise. The type of instability is generally dependent upon which wheel or wheels have reached either a lockup or high-slip condition.

Front wheel lockup will result in a vehicle which is directionally stable but unstable in trajectory, i.e., a plow-out instability. That is, once the front wheels have locked, the vehicle will align itself with the velocity vector and acquire near zero sideslip, while its path from that point will be a straight line coincidental with the velocity vector at the time of the front wheel lockups. Front wheel steer has little or no effect as a result of the loss in tire side force from the locked wheel condition. This effect for the V_{LOC} maneuver is shown in Figure B-21. Note that the wheel lockups have occurred after the vehicle has started to the inside for the lane change. This situation results in the vehicle plowing off the road on the inside. If the front wheels had locked immediately before the vehicle had time to change directions to the inside for the lane change, then the result would be no lane change and a plow-out on the outside, as shown in Figure B-22.
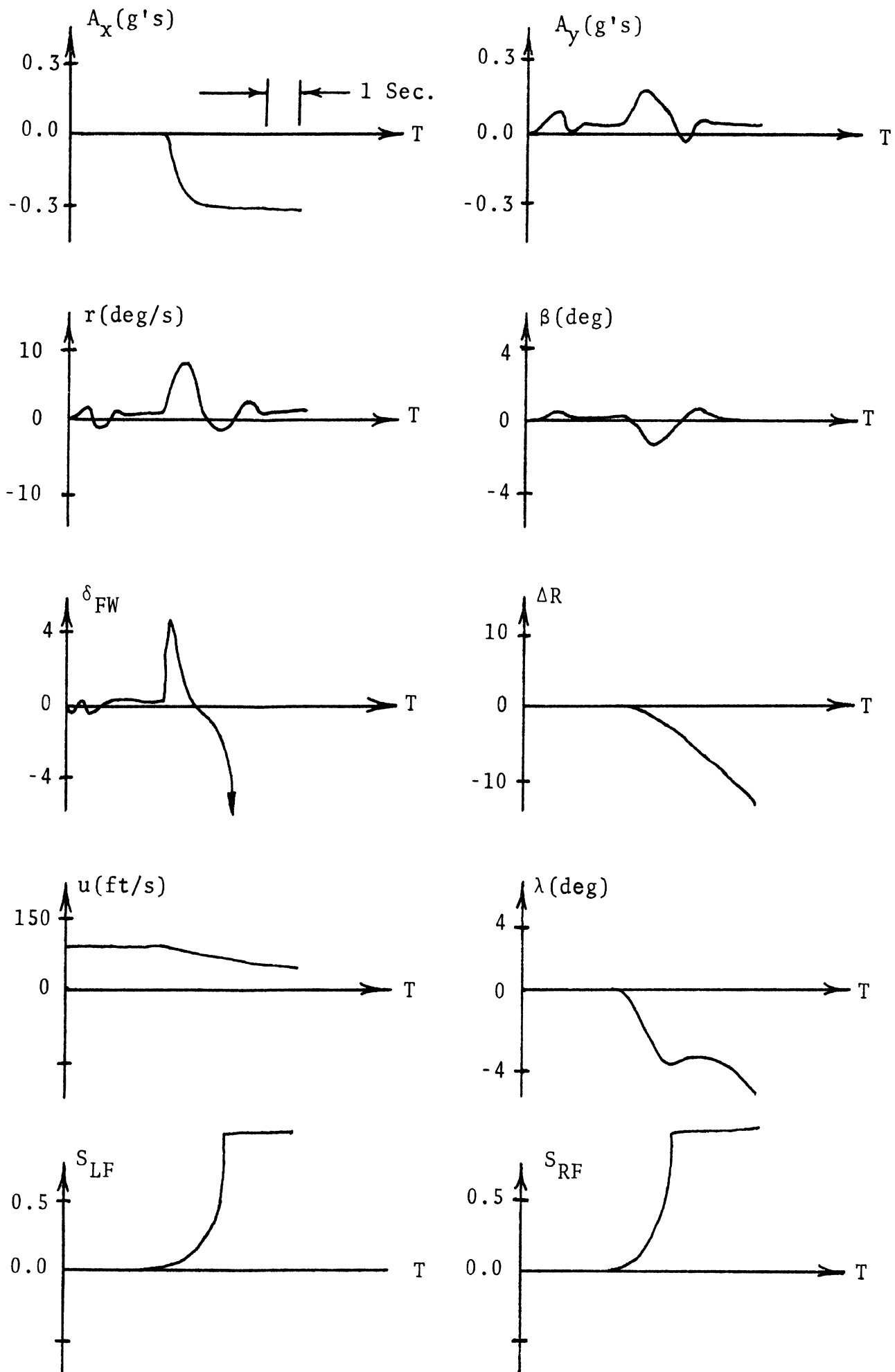
Figure B-21. V_{LOC} - Front Wheel Lockup

294
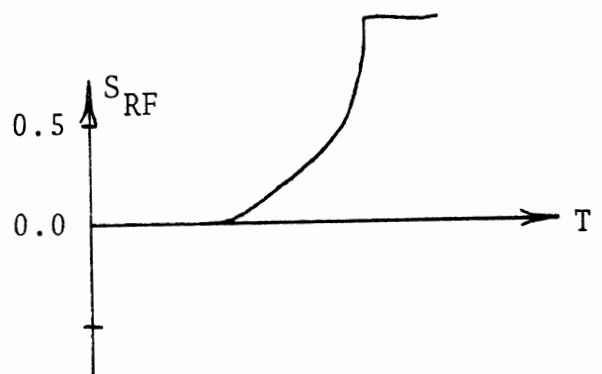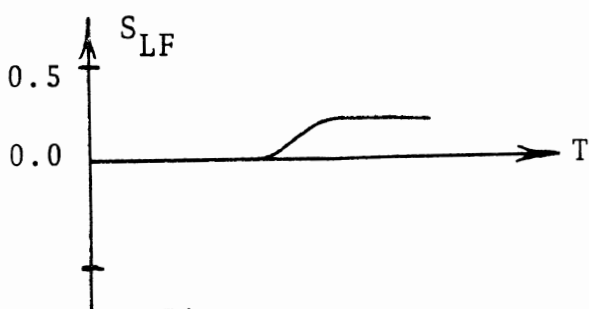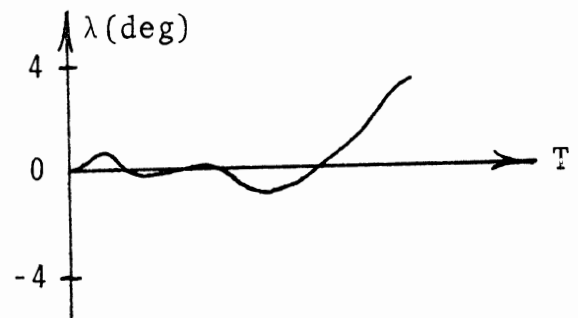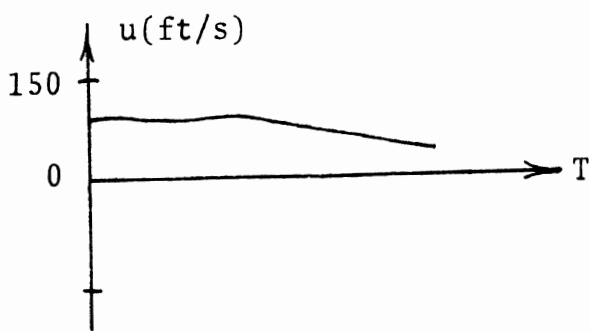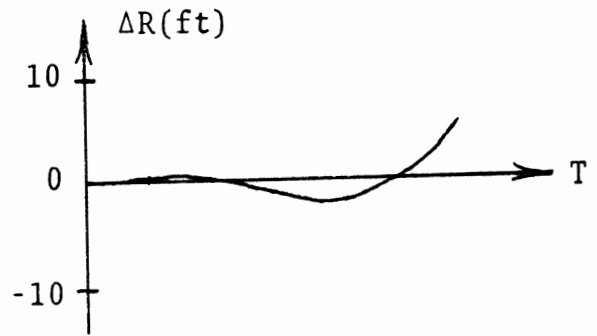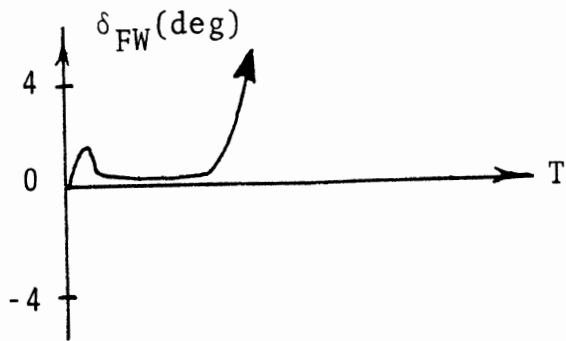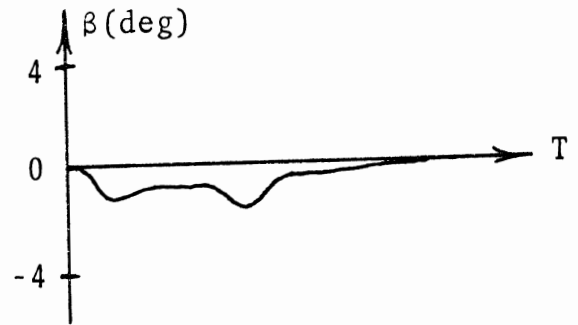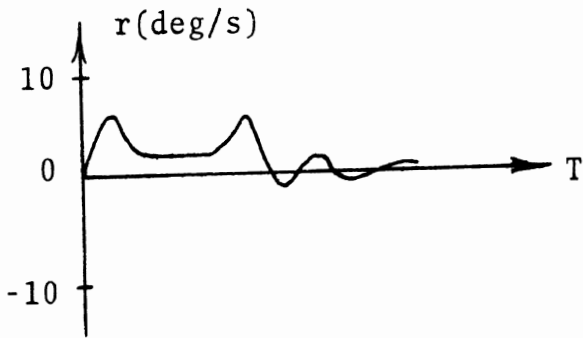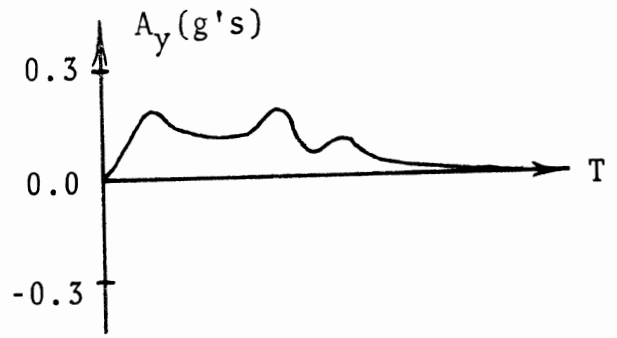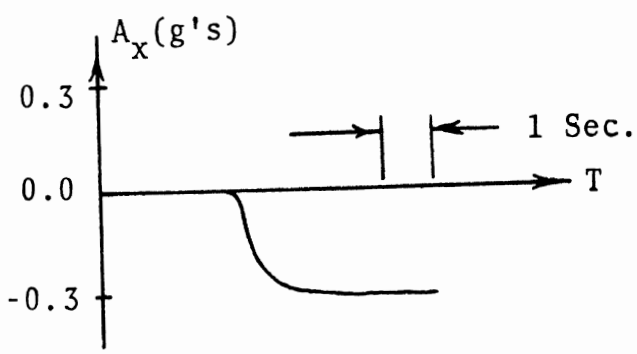
Figure B-22. V_{LOC} - Front Wheel Lockup

Cases in which rear wheel lockups occur result in vehicles unstable in both direction and trajectory. (Generally, the former implies the latter but not vice versa.) This always results in a spin-out or very large sideslip angles. An example of such a case in shown in Figure B-23.

Most vehicles, including those simulated in the study, have brake systems wherein the brake pressure is proportioned so that the front brakes are more effective. Hence, the front wheels will lock first during a braking maneuver. Load transfer will delay somewhat (or prevent in some cases) front wheel lockup and produce opposite effects on the rear. However, unless defective or smooth tires were on the rear, the cases studied produce primarily front-wheel lockups when lockups occurred at all. It should be noted that the V_{LOC} values obtained as a result of wheel lock instabilities are highly dependent on the amount of vehicle deceleration and hence brake line pressure that was chosen in the study (0.3 g's).

Maximum tire side force loss occurs when wheel lock occurs. However, very significant side force losses can occur even for low and intermediate wheel-slip values. Similar vehicle stability problems can arise as for the wheel lockup cases, but in a less dramatic manner. The most common problem resulting from such occurrences was
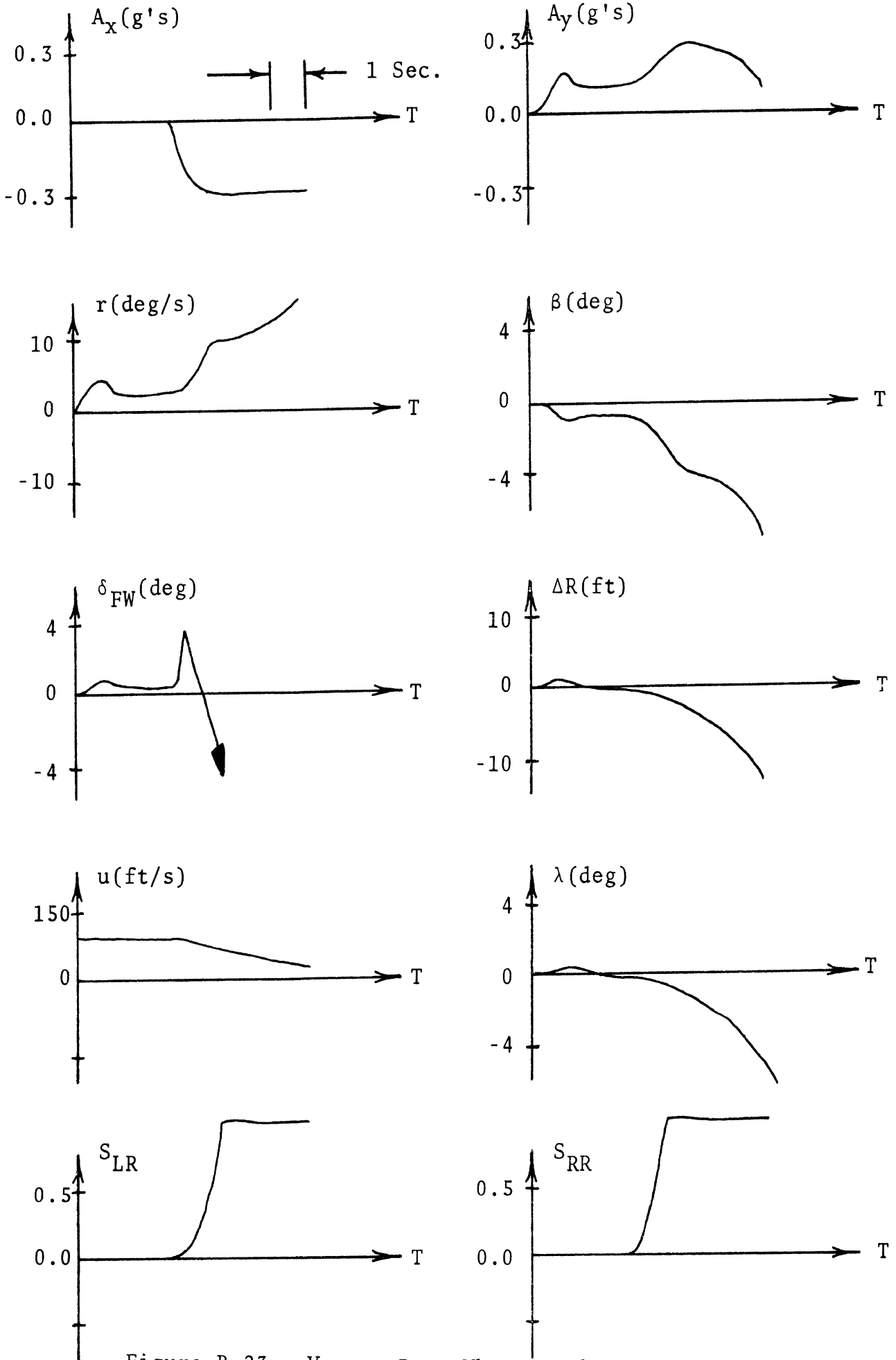
Figure B-23. V_{LOC} - Rear Wheel Lockup

297

diminished path stability. That is, when the vehicle was required to perform a 9- to 12-foot lane change under braking, the vehicle would remain directionally stable but be capable of performing a lane change of only 8 feet or less. The variable time histories shown in Figure B-24 demonstrate these reduced tire side force effects.

B.2.5.2 V_{LC} - Lane Change, No Braking. The V_{LC} maneuver is defined as the V_{LOC} maneuver but without braking. The primary problem encountered was one of directional stability during the lane-change maneuver above a certain velocity. The vehicle will begin to make the lane-change maneuver from the stable cornering maneuver. However as a result of higher sideslip angles necessary for the lane-change maneuver, the vehicle requires greater tire/surface friction than may be available. The result is directional instability of varying degree. For velocities near V_{LC} some temporary directional instability occurs, after which the vehicle is able to stabilize itself (using proper control) and complete the required lane change. This characteristic near V_{LC} has been used to define the V_{LC} velocities. Figure B-25 shows a successful V_{LC} maneuver performed below the critical V_{LC} value. Figure B-26 is the same run but performed at a velocity above the critical V_{LC} value. V_{LC} is 72 mph for the runs shown here.

298
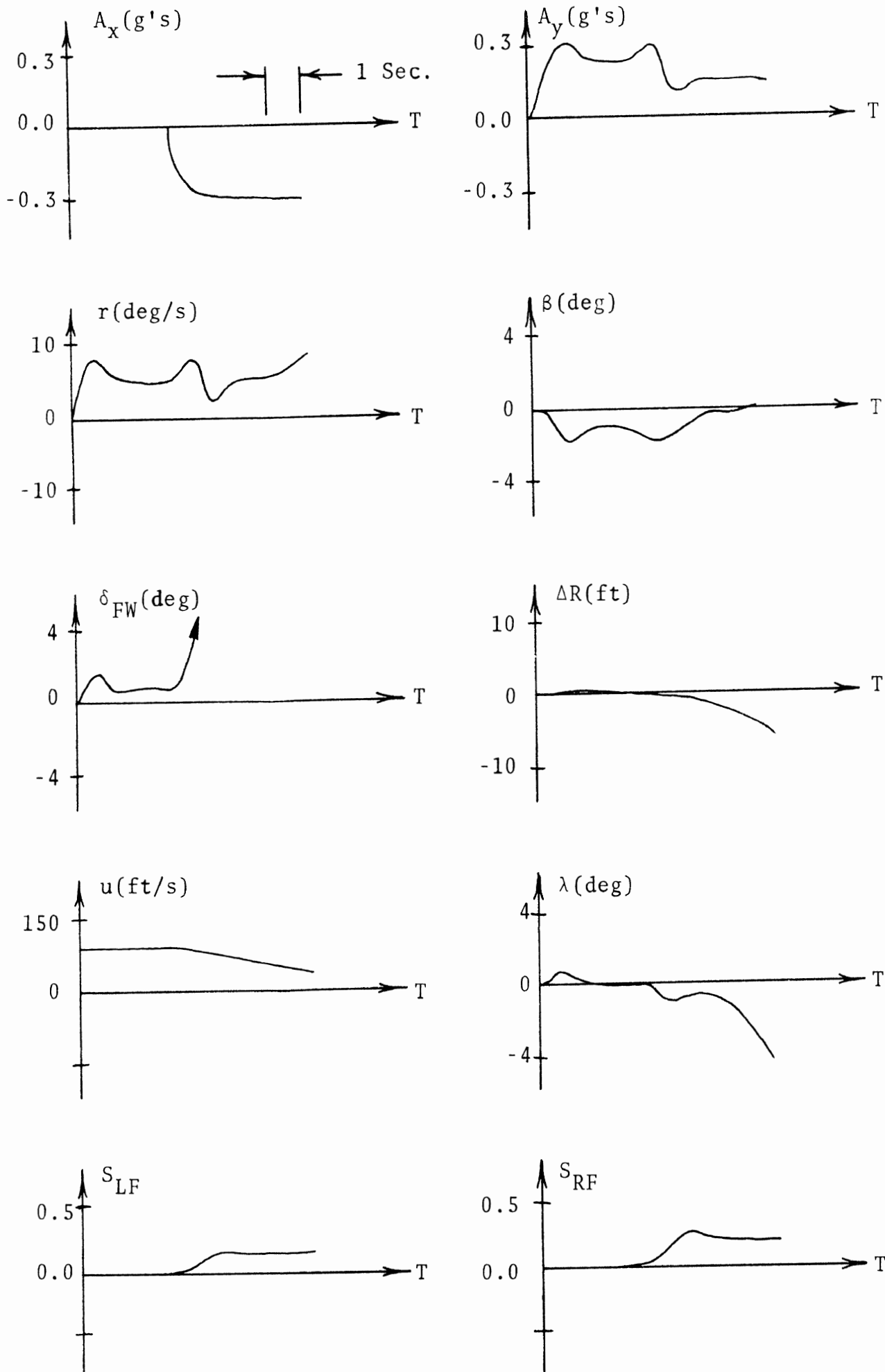
Figure B-24. V_{LOC} - Loss of Lateral Tire Forces,
No Wheel Lockups

299
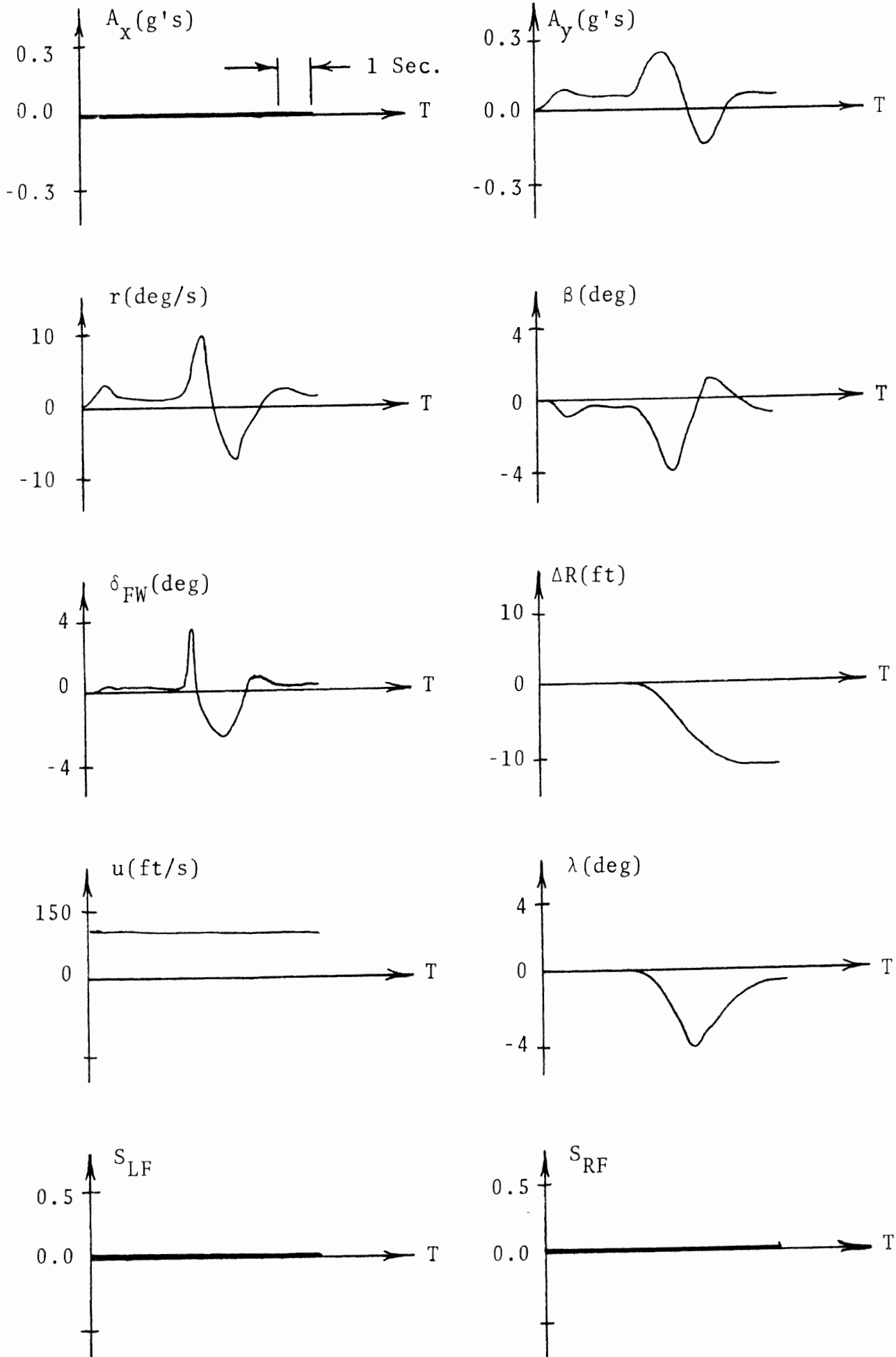
Figure B-25. Stable V_{LC} Maneuver
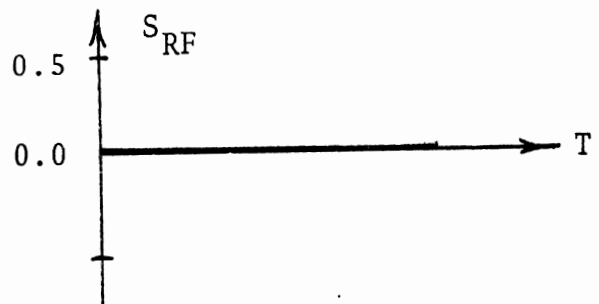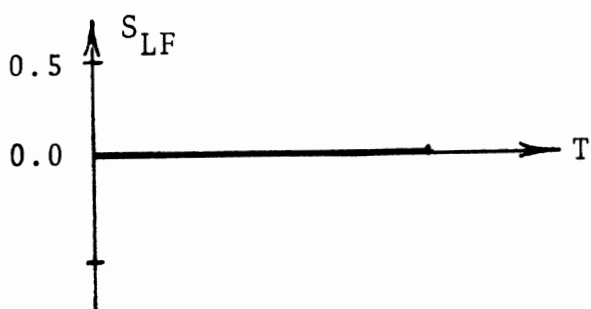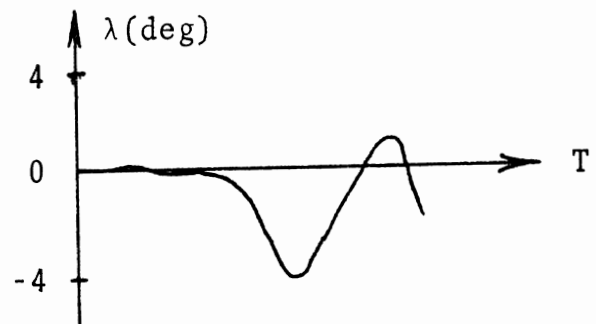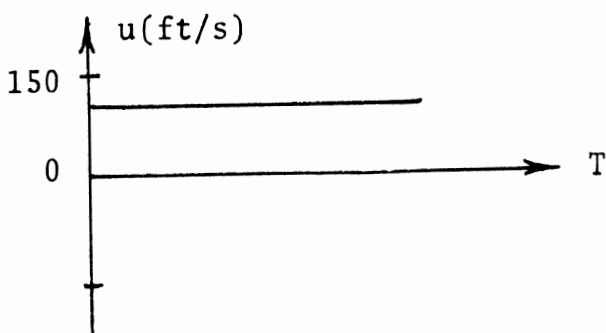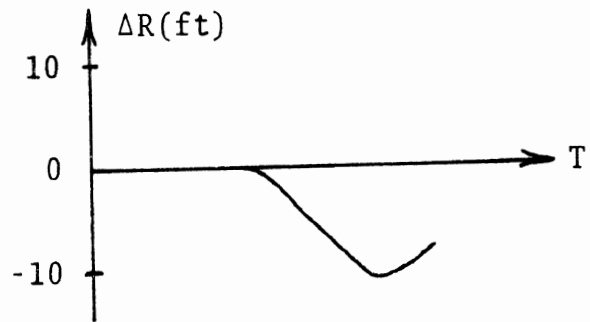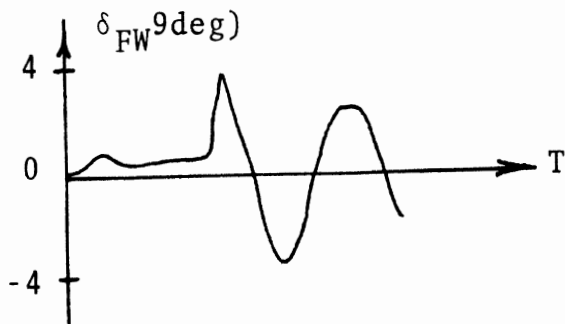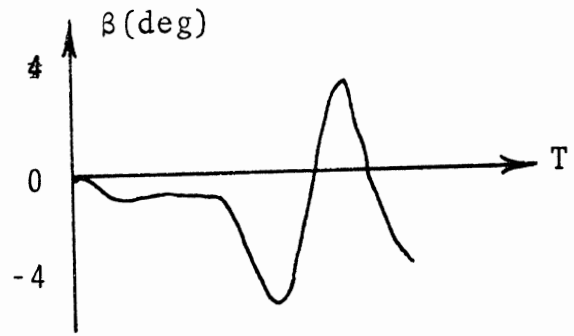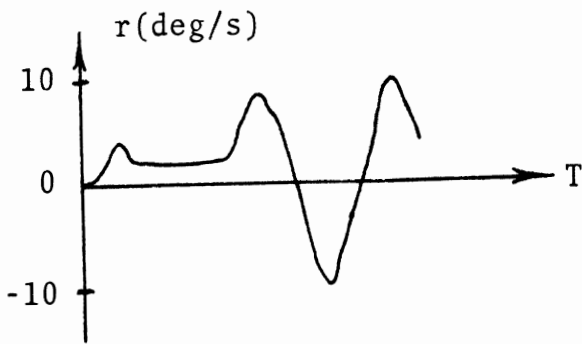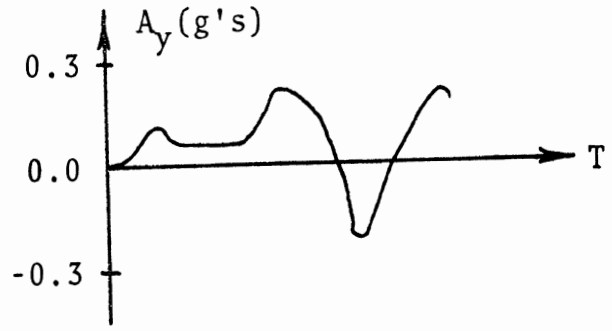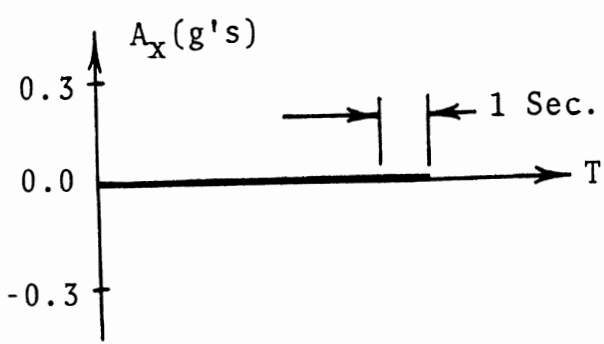
Figure B-26. V_{LC} - Directional Instability During Lane Change

301

The effect of different front-to-rear tire friction capabilities as reflected by tire wear was found to be very significant in the simulation study. For example, a vehicle having half-worn tires on both the front and rear and performing the V_{LC} maneuver had a critical V_{LC} value of 70 mph. The same runs were made but now with half-worn tires on the front and fully-worn tires on the rear. The effect was to reduce the maximum friction capability by 30% on the rear tires. The new critical V_{LC} value was found to be 55 mph. In light of this, it is not surprising that a large number of accident reports involving skidding indicate fully-worn rear tires.

B.2.5.3 V_{CR} - Cornering Under Traction, No Lane Change or Braking. The V_{CR} maneuver is defined simply as cornering with enough traction so as to overcome aerodynamic and rolling resistances and maintain constant forward velocity. The effect of traction under low friction conditions at high speeds has been the dominant factor in limiting the V_{CR} velocities. There is no doubt that considerably higher velocities could be achieved if aerodynamic and rolling resistance were ignored and hence no traction was necessary to maintain constant velocity. The effect of traction on tire side forces is similar to that of braking. Negative wheel slip, which is the case under traction, produces a loss of tire side force which is

similar to the side force loss that occurs under braking and positive wheel slip. The problem with traction on the rear wheels, in this context, is that tire side force losses here produce "fish-tailing" or directional stability problems at speeds considerably below those that would be limiting speeds for ideal cornering without traction. Figure B-27 shows a run at a velocity just below the V_{CR} velocity. Figure B-28 is the same run at a velocity above V_{CR}. V_{CR} is 106 mph for the runs shown here.

B.2.5.4 <u>Summary Plots</u>. The following plots summarize in concise form the results of the simulation study. Most plots are either V_{LOC}, V_{LC}, or V_{CR} versus D, where D represents the degree of curvature of the path followed. One degree of curvature corresponds to 5730 feet of radius. Six degrees corresponds to 955 feet of radius.

Figures B-29 through B-31 show the effects of super-elevation, surfaces, and tires on V_{CR} at different curvatures. Likewise, Figures B-32 through B-34 and Figures B-35 through B-37 demonstrate these same effects but for V_{LC} and V_{LOC}, respectively. Figure B-38 shows the effect grade has on V_{LOC}. The notation used in the plots is also defined in Table B-6.
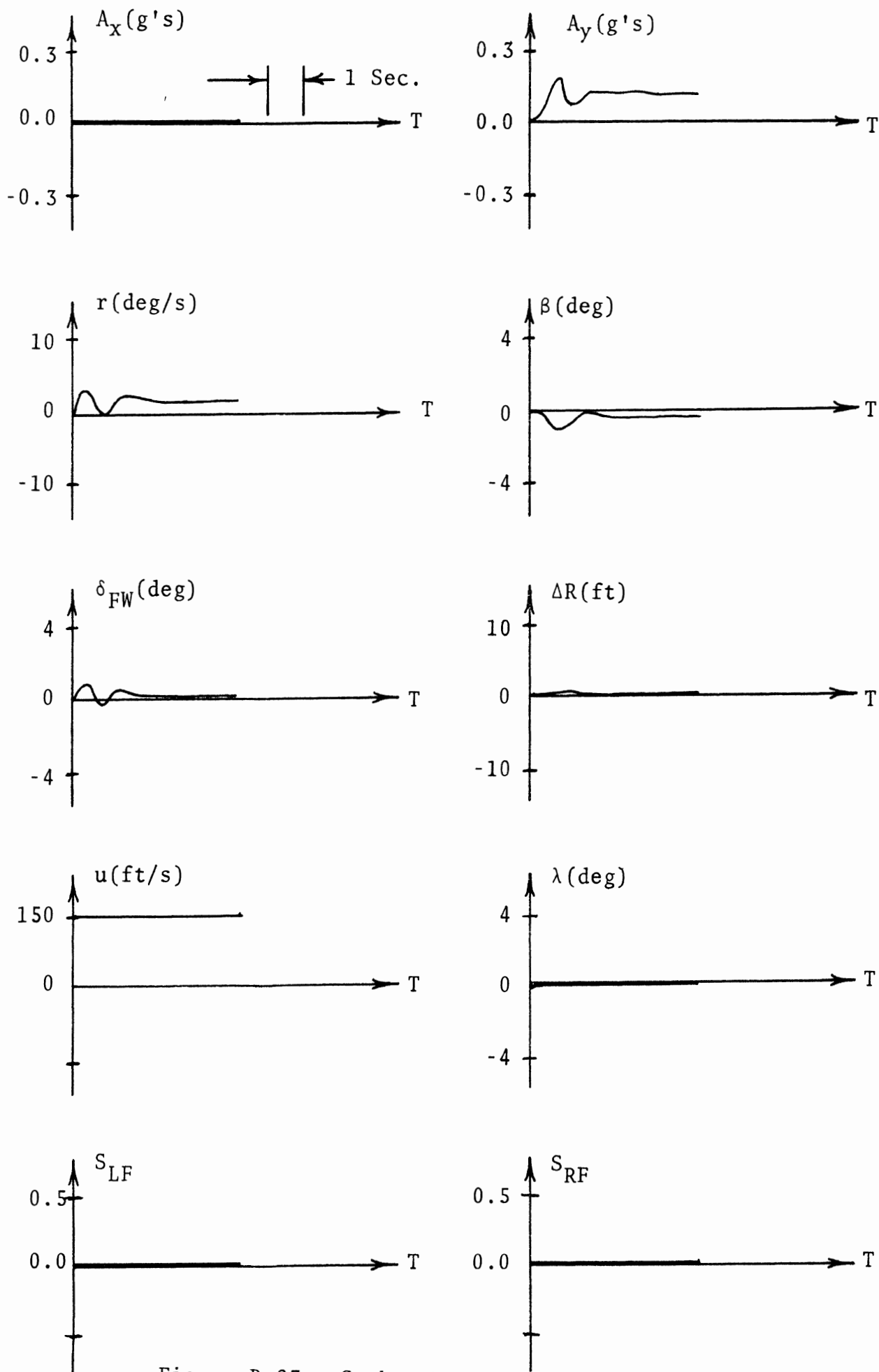
Figure B-27. Stable V_{CR} Maneuver
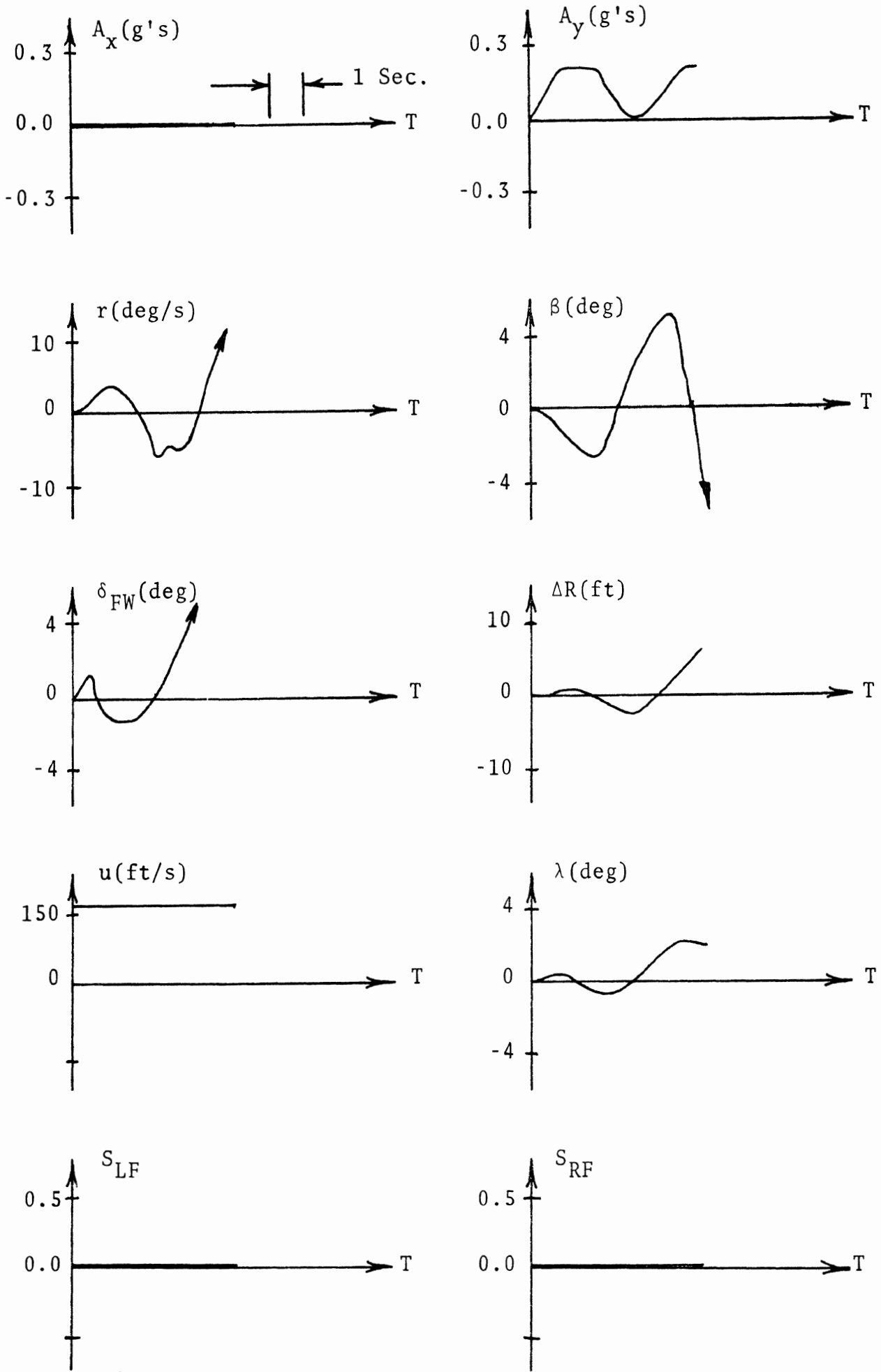
Figure B-28. V_{CR} - Loss of Directional Stability

305
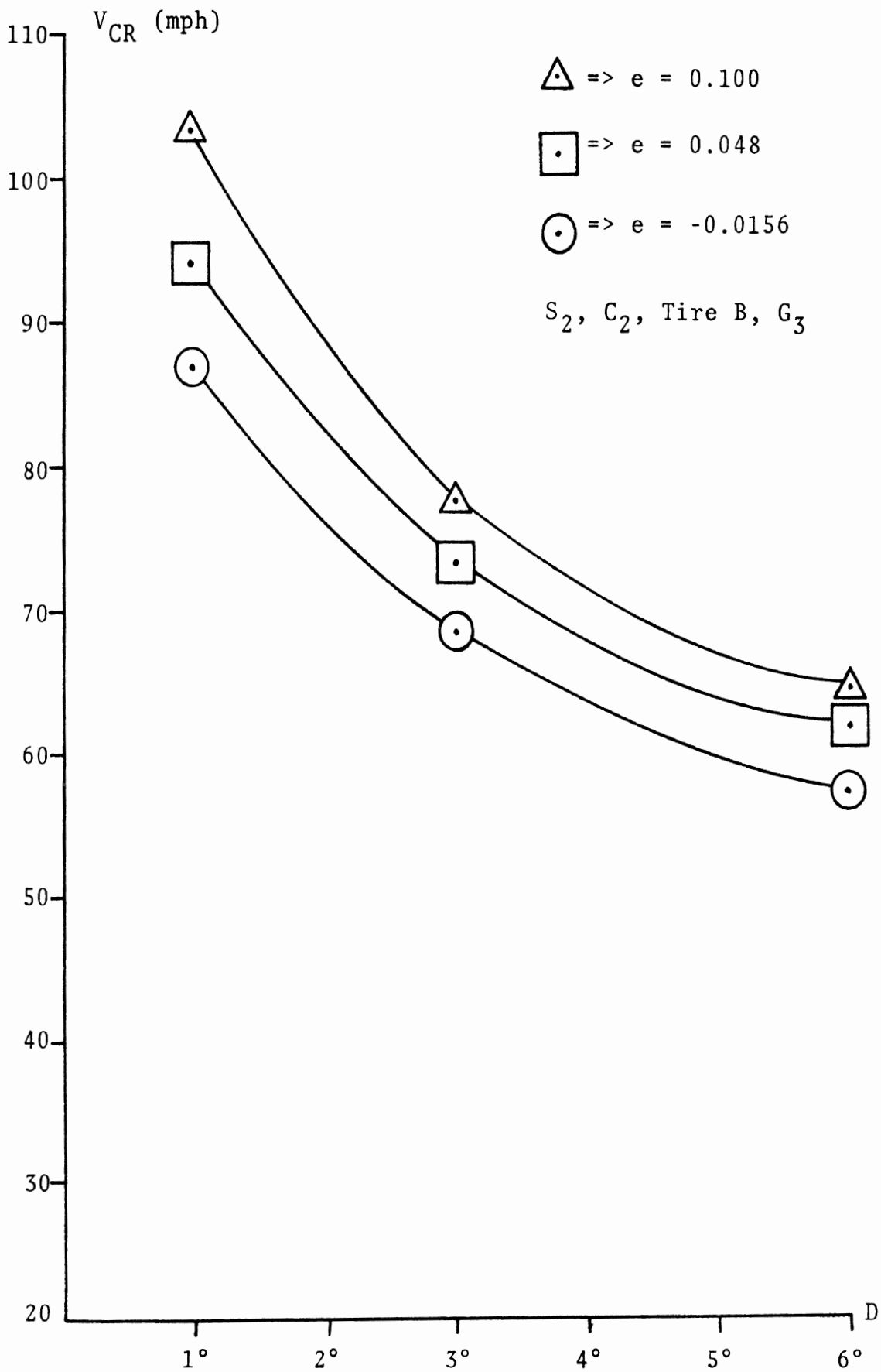
Figure B-29.   Effect of Superelevation on V_{CR}
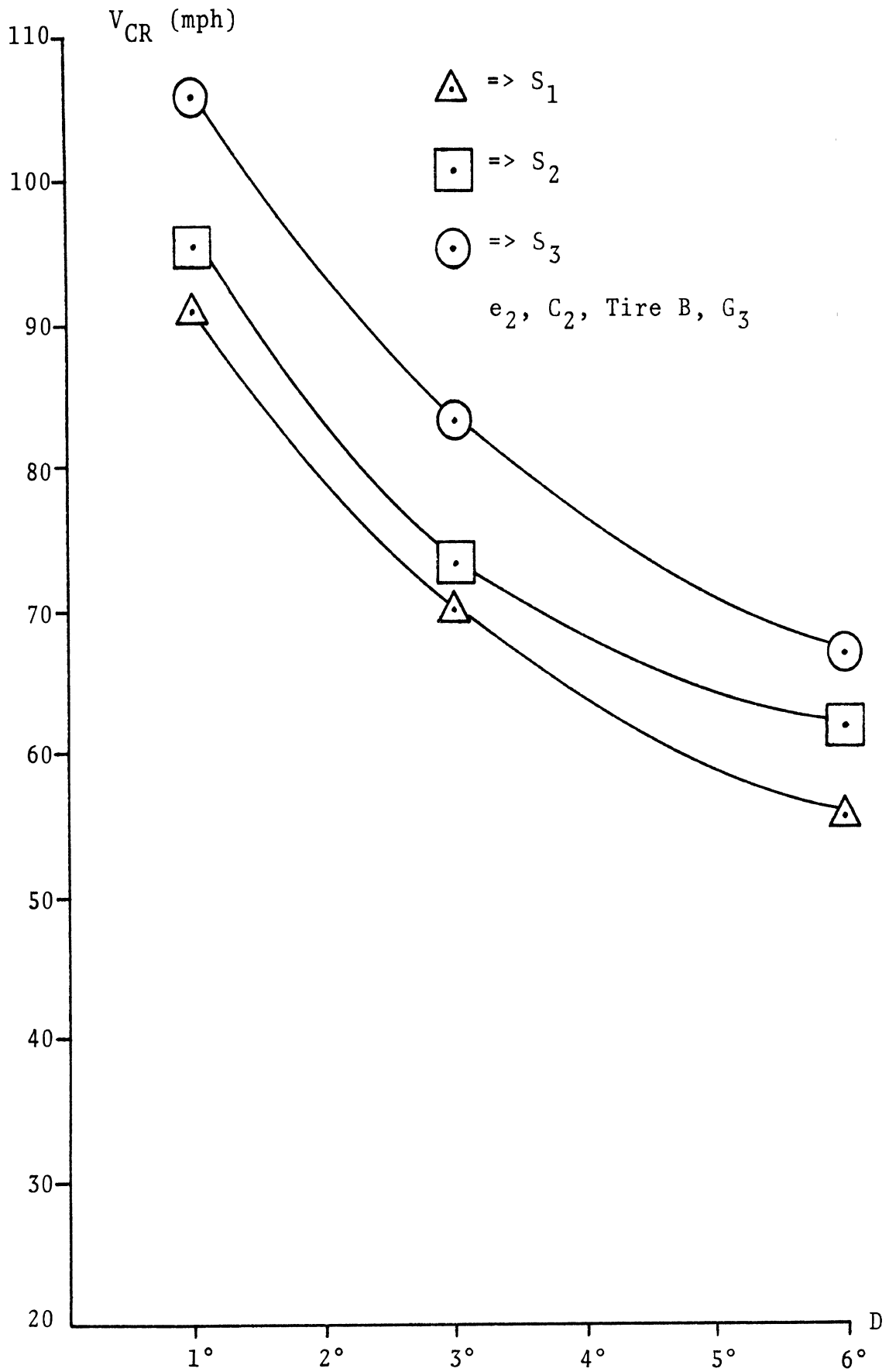
Figure B-30. Effect of Surface on V_{CR}
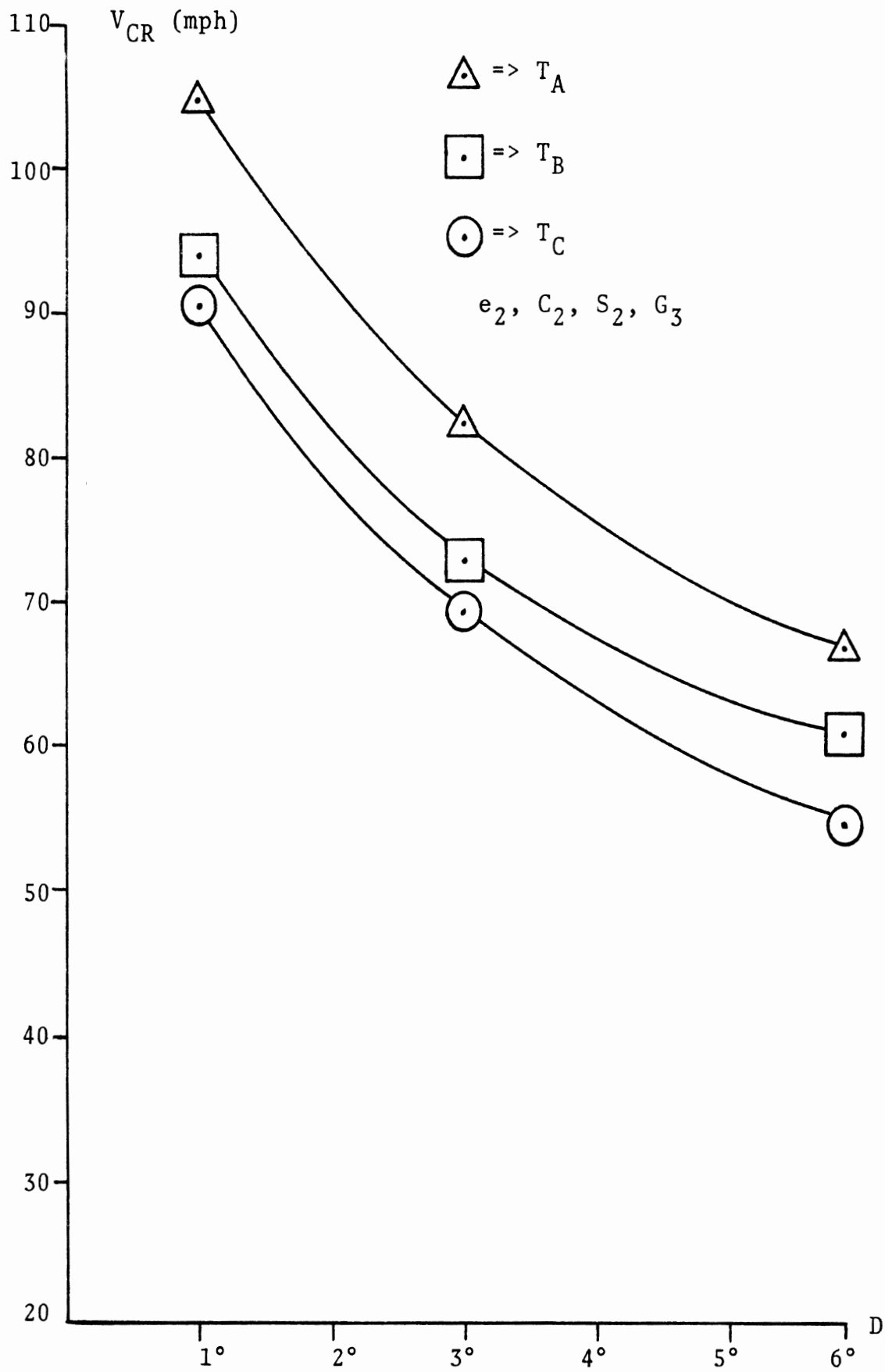
Figure B-31.   Effect of Tire Wear on V_{CR}
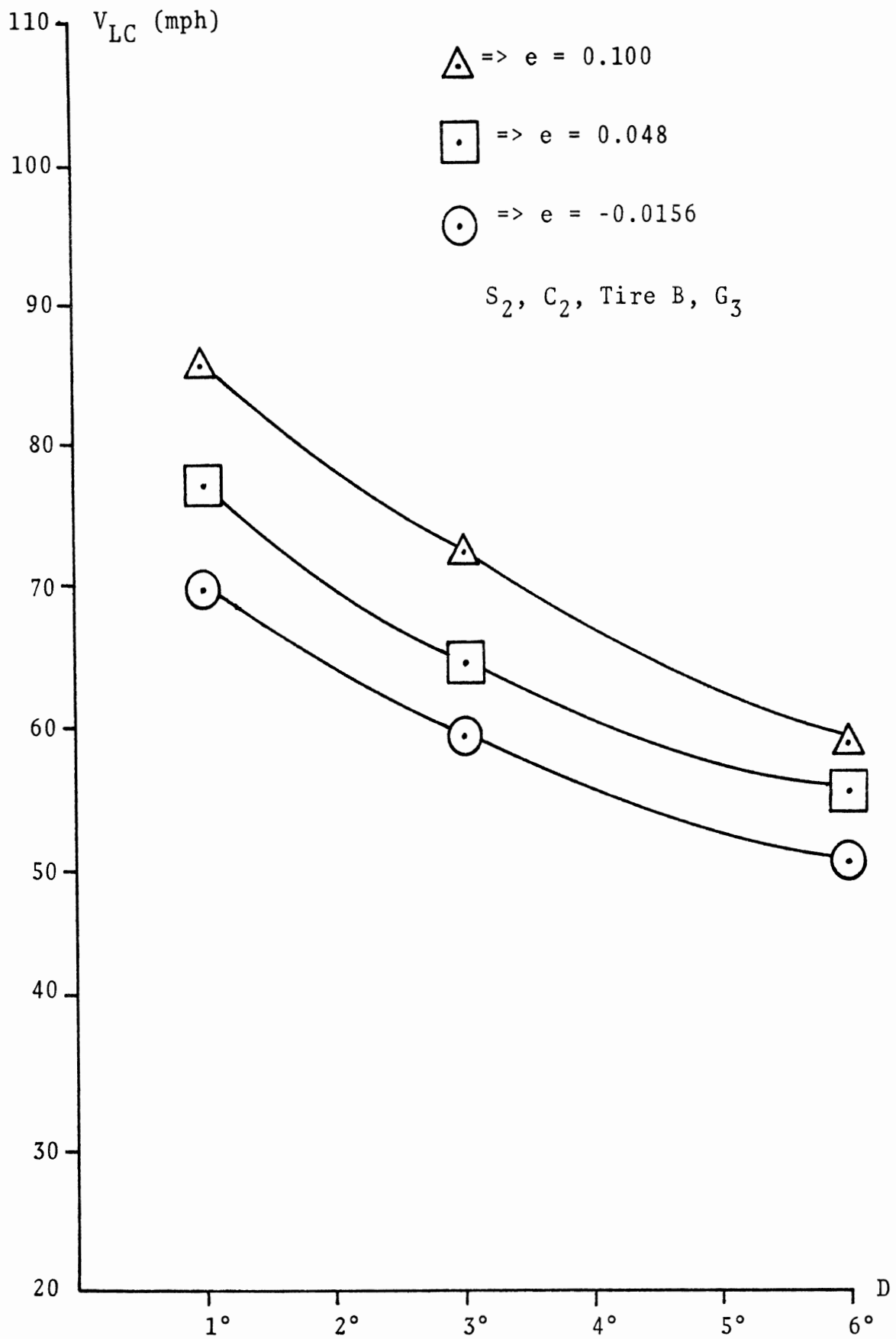
Figure B-32.   Effect of Superelevation on V_{LC}
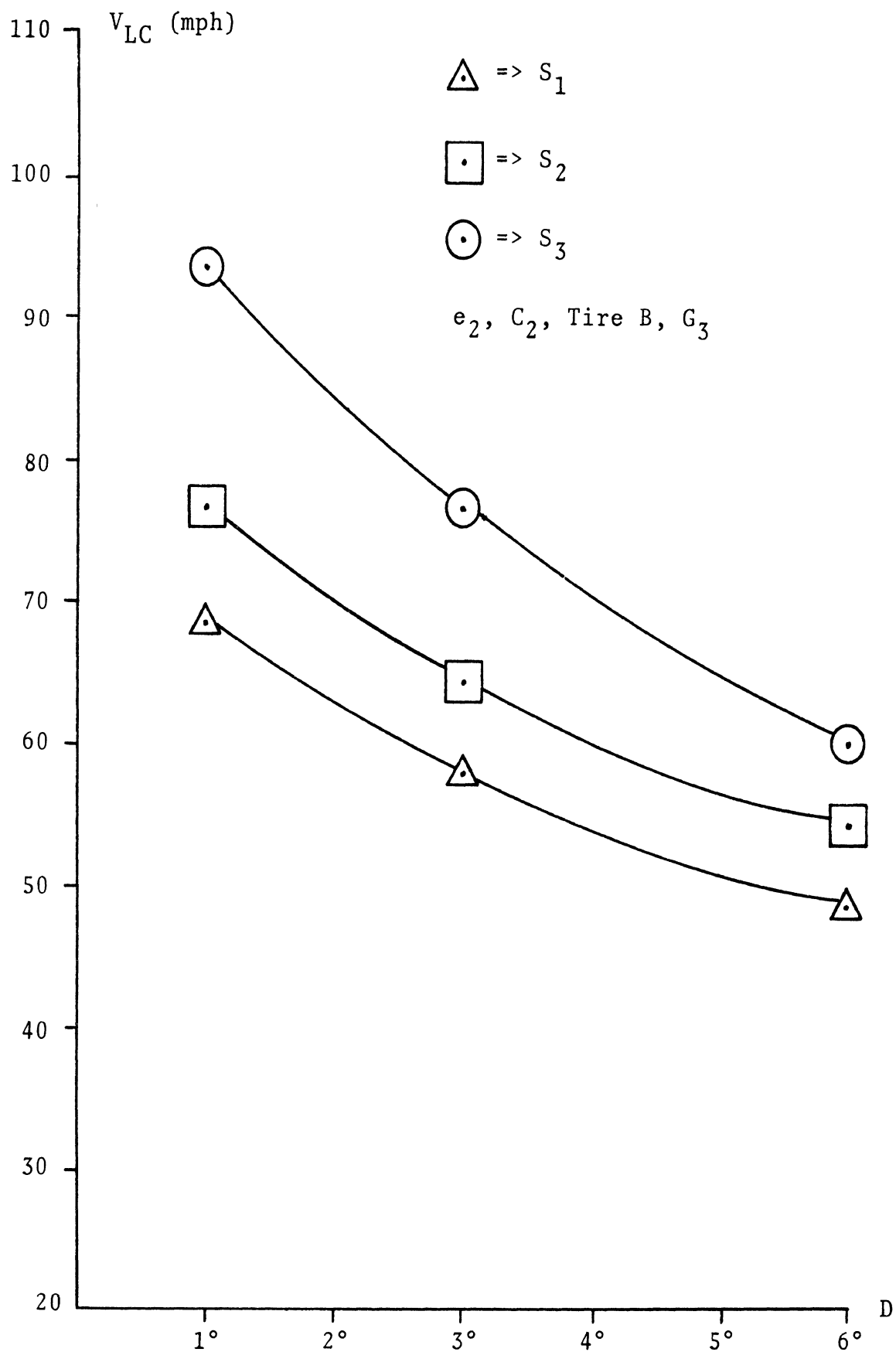
Figure B-33.   Effect of Surface on V_{LC}
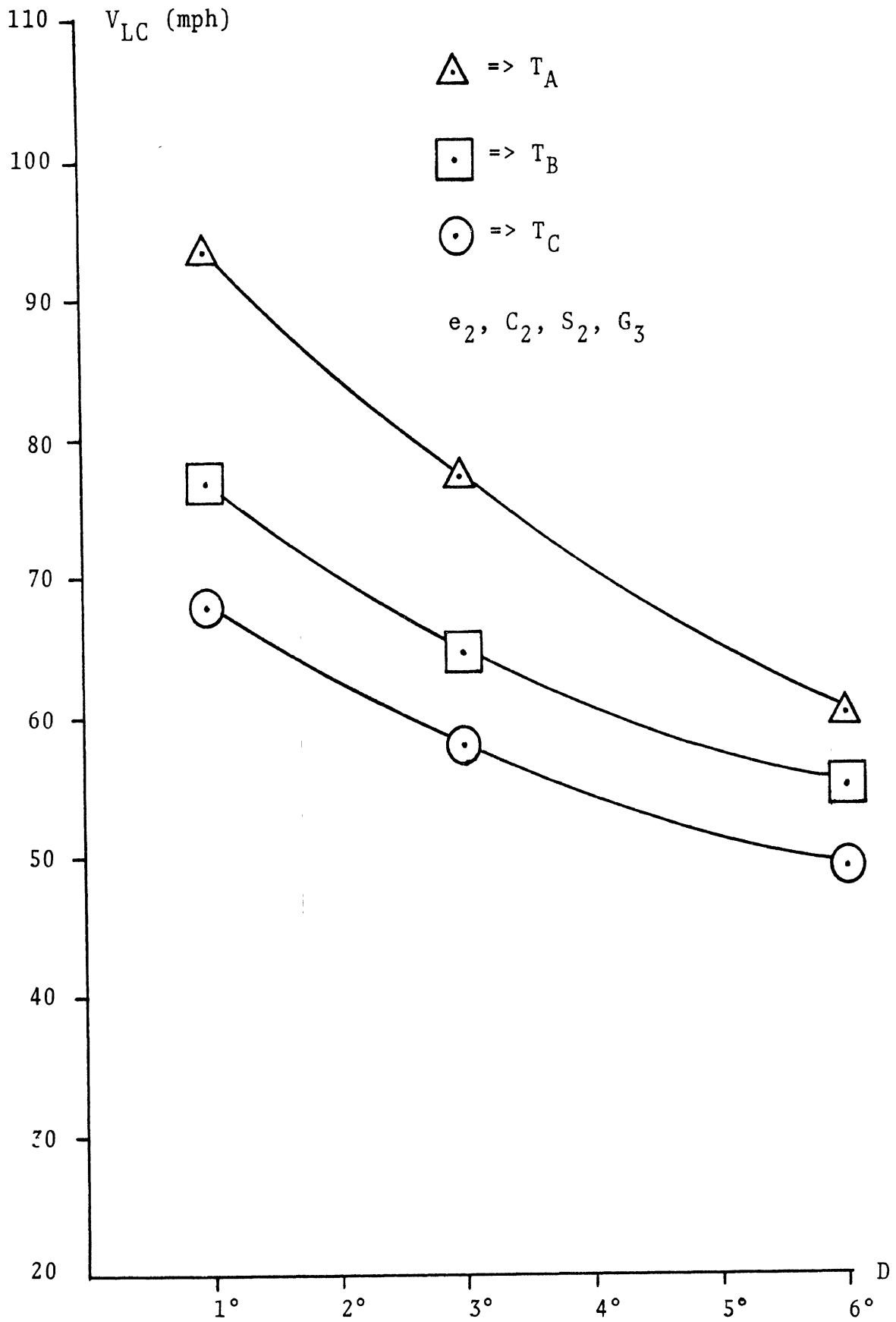
Figure B-34. Effect of Tire Wear on V_{LC}
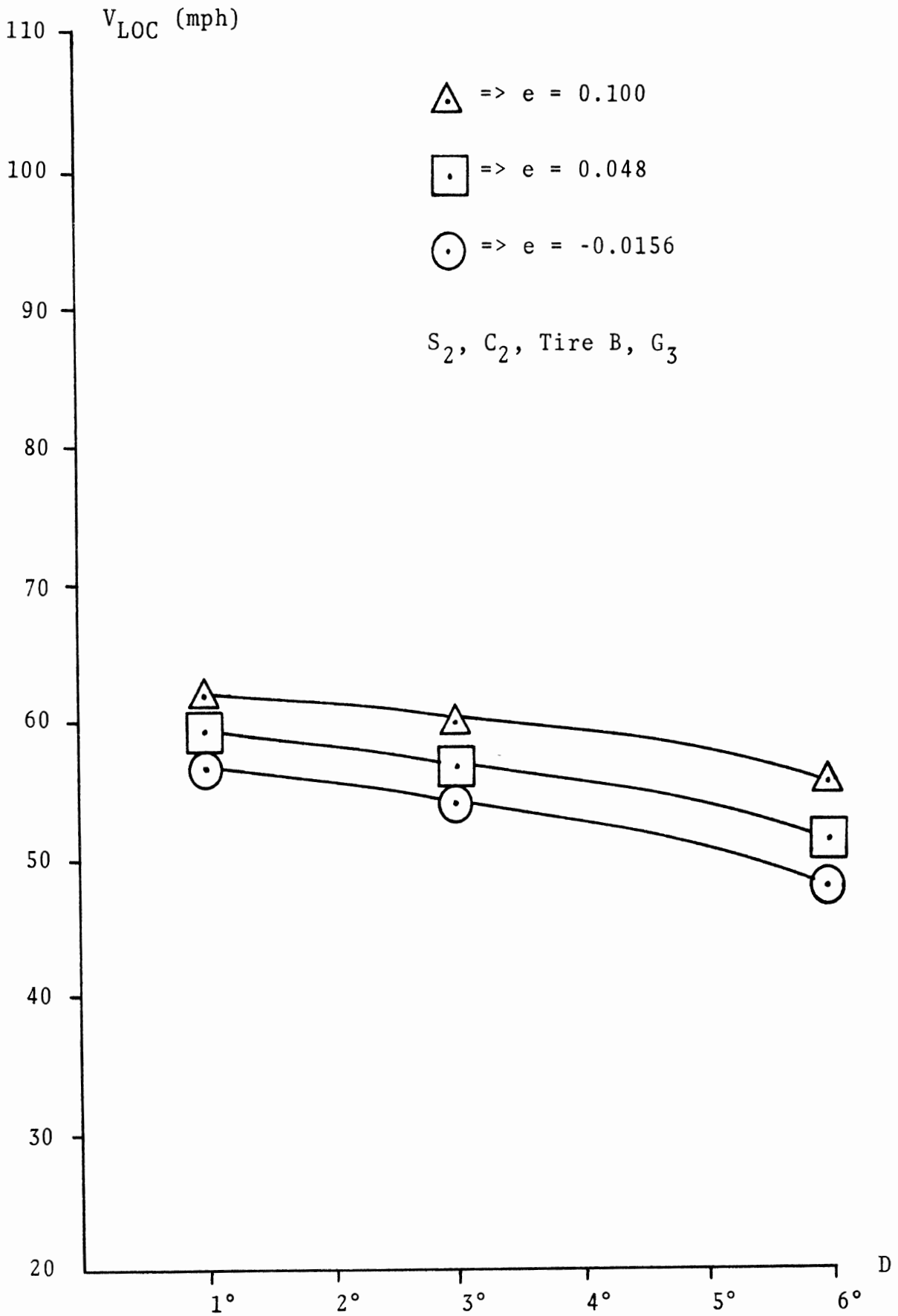
Figure B-35. Effect of Superelevation on V_{LOC}
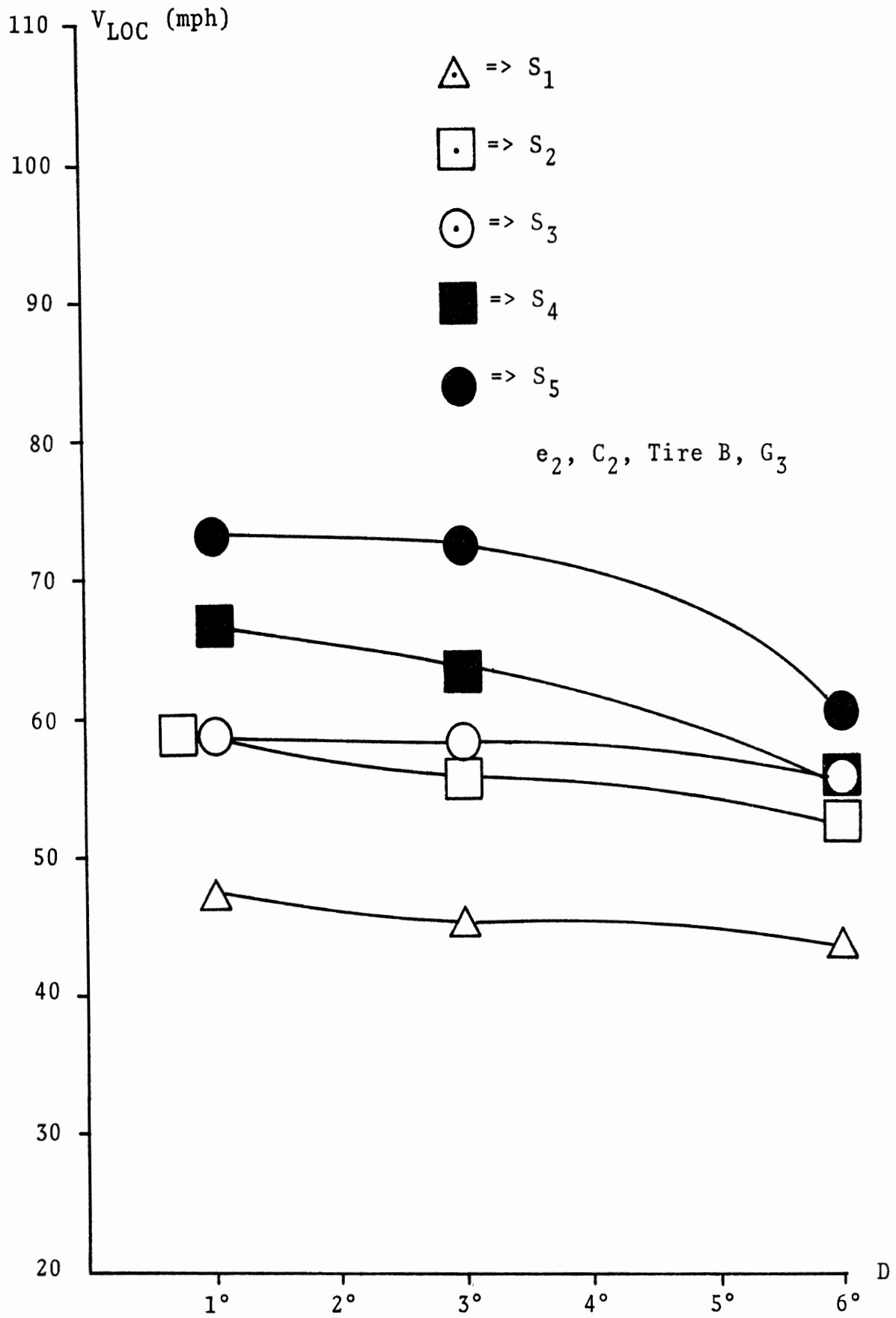
Figure B-36. Effect of Surface on V_{LOC}
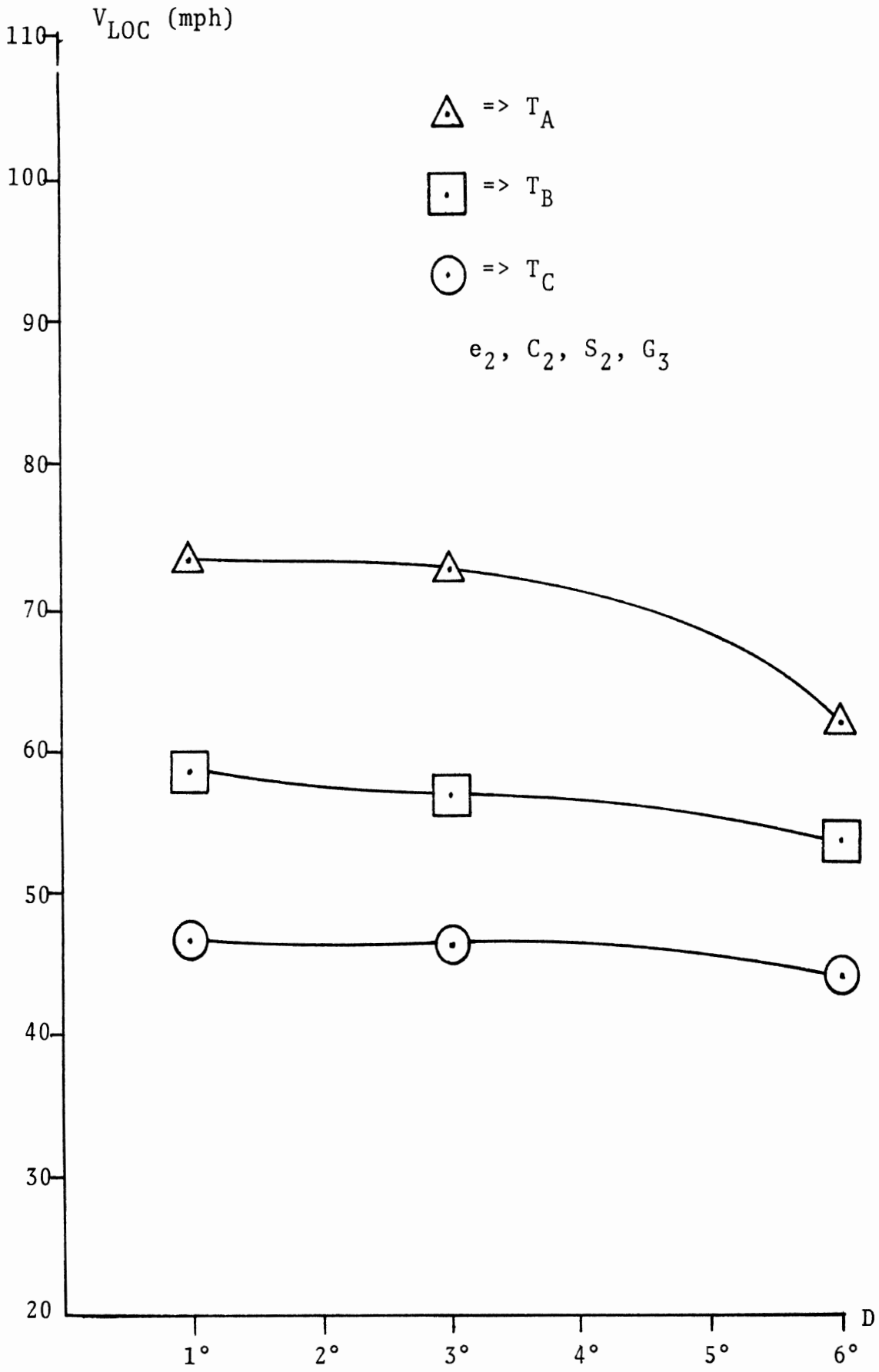
Figure B-37. Effect of Tire Wear on V_{LOC}
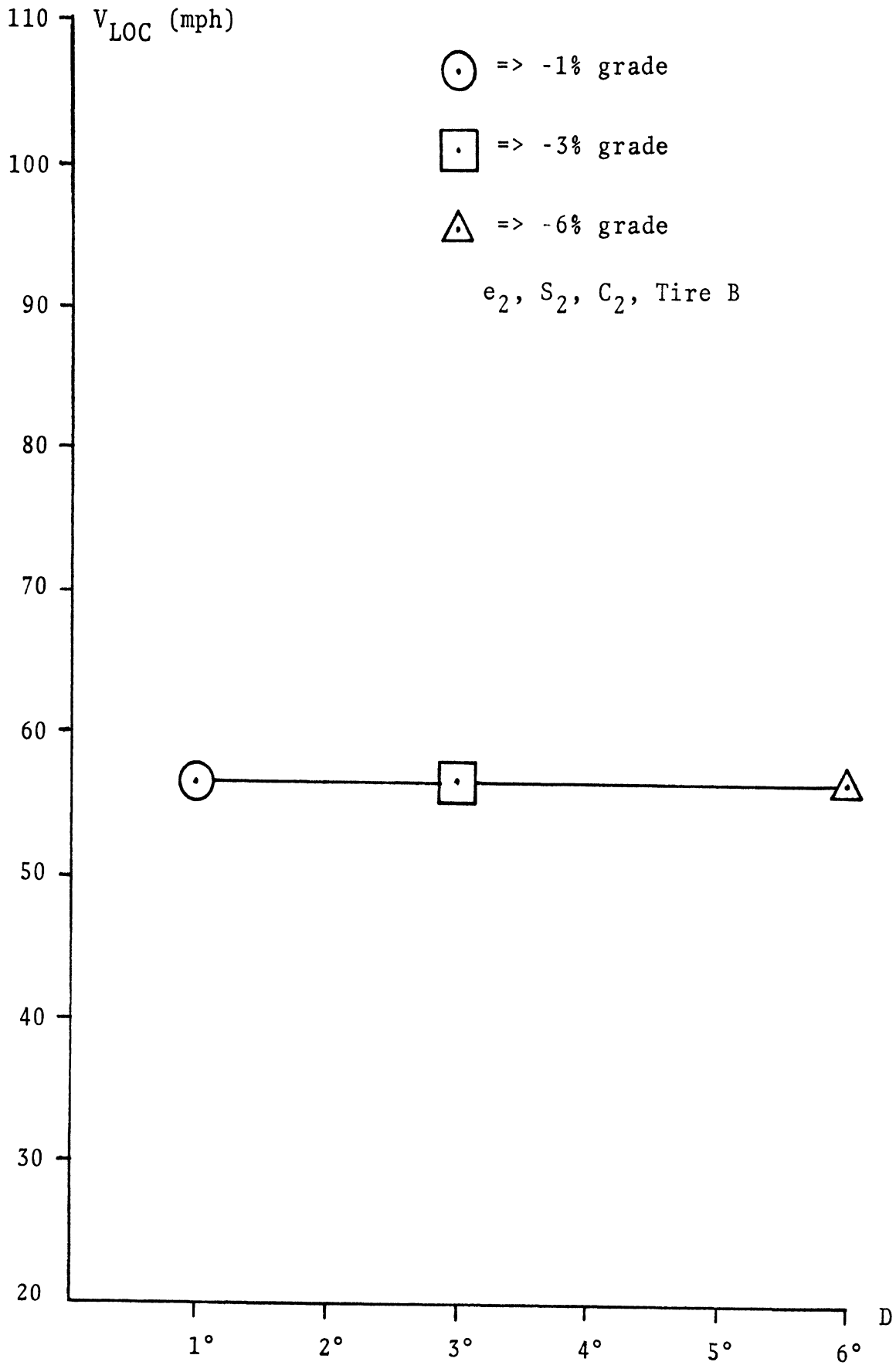
Figure B-38. Effect of Grade on V_{LOC}

The V_{CR} (steady turn) results shown in the first three figures indicate that V_{CR} is a sensitive function of the degree of path curvature. On 6° curves for vehicles operating on either heavily worn tires (TIRE C) or low skid number roads (SN_{40} = 20) V_{CR} can be less than 60 mph. For 3° curves, V_{CR} is greater than 70 mph in all the cases presented here. For 1° curves, V_{CR} is greater than 89 mph.

The V_{LC} results are significantly dependent upon highway geometrics. Even though the lane-change results were obtained from a mathematically complex set of non-linear differential equations in which the shear force characteristics of all four tires were computed using complicated empirical relationships, examination of the results given in Figures B-32, B-33, and B-34 indicates that V_{LC} can be approximated by a simple linear function of degree-of-curvature, superelevation, skid number, and tire factor for practical values of these variables for curves from 1° to 4° (possibly 5°). The approximate expression obtained is:

$$V_{LC} = 66 - 6.5(D-3) + 154(e-0.048) + 1.3(SN_{40}-30)$$
$$+ 37(T_F-0.85) \tag{B.44}$$

where all terms have been defined previously.

316

Clearly, this is a very simple formula for representing a host of complex factors. The tire factor, T_F, was taken as 1.2 for new tires (TIRE A), .85 for half-worn tires (TIRE B), and .6 for fully worn tires (TIRE C). The skid number gradient for this formula is -.5 skid numbers per mph. For surfaces with larger magnitude skid number gradients the results will not be conservatively safe. Also, water depth is not treated directly in this formula. Since the ASTM skid number is obtained at a water depth of approximately 0.02 inch, this equation may be applicable to weather conditions which result in about 0.02 inch of water on the road. For heavy rains or poor drainage conditions, the influence of water depth must be considered in determining the tire/road shear force potential.

Nevertheless, this formula is useful for

(1) predicting V_{LC} for a given set of roadway and tire conditions or

(2) estimating the skid number needed for a desired V_{LC} for a given set of roadway geometrics with a specified state of tire wear.

For estimating a skid number the Equation (B.44) can be written in the form:

$$SN_{40} = \frac{V_{LC} + 6.5D - 154e - 37T_F - 7.7}{1.3} \qquad (B.45)$$

It should be reemphasized that Equation (B.45) is an approximation to the computer results. The coefficients in (B.45) were chosen so that the region of greatest accuracy is centered around (1) highway curves in the range from 2° to 3° with AASHTO recommended levels of e; (2) 40 mph skid numbers in the range from 30 to 40; and (3) passenger cars with new to half-worn tires. Slightly different coefficients could be developed to obtain a more accurate expression for other ranges of the pertinent variables if desired.

Clearly V_{LC} is significantly less than V_{CR} under equivalent sets of operating conditions. For example, for a vehicle operating with fully worn tires on a 3° curve, $V_{LC} = 59$ mph (see Figure B-34), while under the same conditions, $V_{CR} = 71.5$ mph (see Figure B-31).

The V_{LOC} results presented here indicate that V_{LOC} is not significantly influenced by degree of curvature (see Figures B-34, B-36, and B-37) except for a few cases on 6° curves with either very good tires or good skid number road surfaces. Also, grade has no effect, as shown in Figure B-38. For normally superelevated roads with $SN_{40} = 30$ and vehicles with good (half-worn) tires, V_{LOC} is less than 60 mph. Clearly, V_{LOC} is a very sensitive

function of the friction potential available at the tire/ road interface. Thus it appears that if V_{LOC} is to be increased at curve/grade sites, the skid number must be increased and/or the quality of the tires used must be improved.

Very little difference in the V_{LOC} results was noted in various vehicles. This can be explained by the following: V_{LOC} values for any vehicle are determined primarily by the velocity at which front-wheel lockups first occur, hence reflecting the tire/surface friction characteristics. Since each vehicle was required to decelerate the same amount and the tire forces were normalized from vehicle to vehicle by weight, similar wheel slip values would be expected. See Figure B-39.

More noticeable differences from vehicle to vehicle were noted in the V_{LC} and V_{CR} results, although the differences were still small. Since these differences were small and normally occurred at velocities above 70 mph, the effects of vehicle-to-vehicle variations were not pursued. Consequently, the intermediate sedan (C_2) served as the baseline vehicle for the parameter variations in the simulation study.

Figure B-39

320
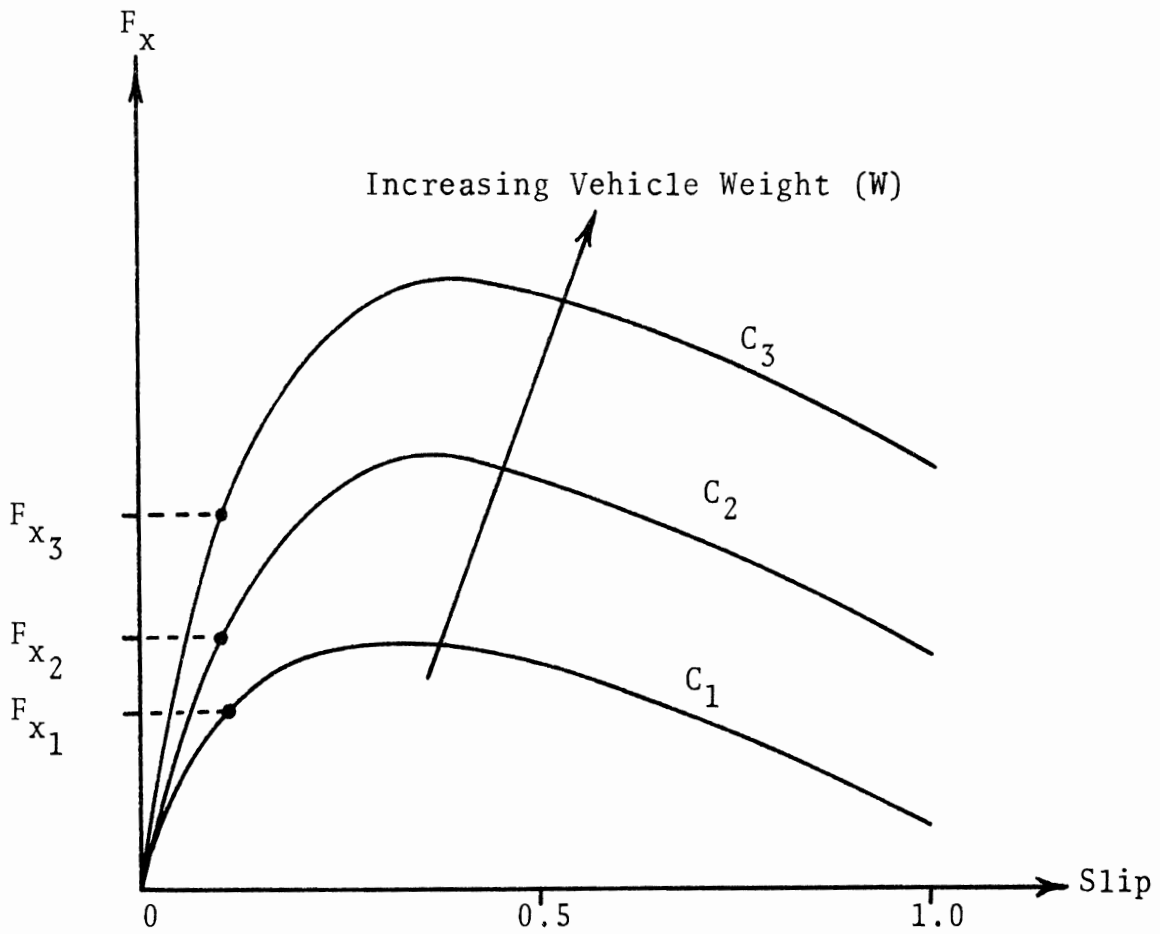
APPENDIX C

THE INFLUENCE OF GRADE AND CURVATURE ALIGNMENT
COMBINATIONS ON PAVEMENT DRAINAGE

Pavement water depth is an important factor in determining the available friction at the tire/road interface. At this writing, three research efforts have been carried out to determine the factors which influence pavement drainage and to predict water depth.

Gallaway et al. ([6]) at the Texas Transportation Institute have arrived at the following formula for relating water depth to its controlling factors:

$$d = [3.38 \times 10^{-3}(\tfrac{1}{T})^{-.11}(L_f)^{.43}(I)^{.59}(\tfrac{1}{S})^{.42}] - T \qquad \text{(C.1)}$$

where

d = average water depth above the texture, in.

T = average texture depth, in.

L_f = drainage path length, ft.

I = rainfall intensity, in/hr

S = cross slope, ft/ft

The formula was derived by using specially fabricated test surfaces which could be oriented as desired and subjected to controlled rainfall rates.

Ross and Russam ($\underline{7}$) at the Road Research Laboratory developed a similar expression which is given as follows:

$$d = \frac{0.0059(L_f I)^{.47}}{S^{0.2}} \qquad (C.2)$$

where the terms are defined as for Equation (C.1). This formula was developed in a manner similar to that used by Gallaway, although the surfaces were characterized by somewhat greater texture depths.

Similar work by Yeager and Miller ($\underline{8}$, $\underline{9}$) at the Goodyear Tire and Rubber Company has produced data which can be described by the formula:

$$d = 9.6 \times 10^{-4}(I)^{.44}(L_f)^{.55}(\tfrac{1}{S})^{.46} + 2.26 \times 10^{-3}(I)^{.49}(\tfrac{1}{S})^{.38}$$

$$(C.3)$$

Again, the data were derived by using a test surface which could be tilted and subjected to a controlled rainfall rate.

Equations (C.1), (C.2), and (C.3), although similar in form, give results which differ by as much as a factor of three. (See, for example, Figures D-3 and D-10 of Appendix D.) Although that fact should be noted, this appendix is concerned not with the quantitative levels of

water depths which the equations predict, but with the qualitative influence that curvature and grade combinations have on water depths. In this way, the important controlling factors can be identified and can be used to reduce water depths and thus increase driving safety.

In Equation (C.1), the roadway controlling factors are drainage length, slope, and texture depth. Only drainage length and slope appear in Equations (C.2) and C.3).

The slope is the angle between the horizontal and the plane of the road. In terms of grade and superelevation it can be shown that the slope can be written as:

$$\cos S \ = \ \cos e^* \ \cos G \qquad\qquad (C.4)$$

or,

$$S \ = \ \sqrt{G^2 + e^{*2}} \qquad\qquad (C.5)$$

where

$\quad G \ =$ roadway grade, %

$\quad e^* \ =$ true roadway superelevation (see Appendix F), ft/ft

The latter expression is an approximation based on small angle assumptions (a very good approximation in this case).

Similarly, it can be shown that the drainage path length, L_f, and the road width, L, are related by the expression:

$$L = L_f \cos \theta \qquad (C.6)$$

where θ is the drainage angle across the road as defined by Figure C-1. Further, it can be shown that

$$\tan \theta = \frac{\tan G}{\sin e^*} \qquad (C.7)$$

Using small angle approximations for G and e^*, Equation (C.6) can be rewritten with the aid of Equation (C.7) as:

$$L_f = \frac{L}{e^*} \sqrt{G^2 + e^{*2}}$$
$$= \frac{L\,S}{e^*} \qquad (C.8)$$

or that

$$\frac{L_f}{S} = \frac{L}{e^*} \qquad (C.9)$$

Referring back to Equation (C.1), now, the equation can be rewritten as follows:

324
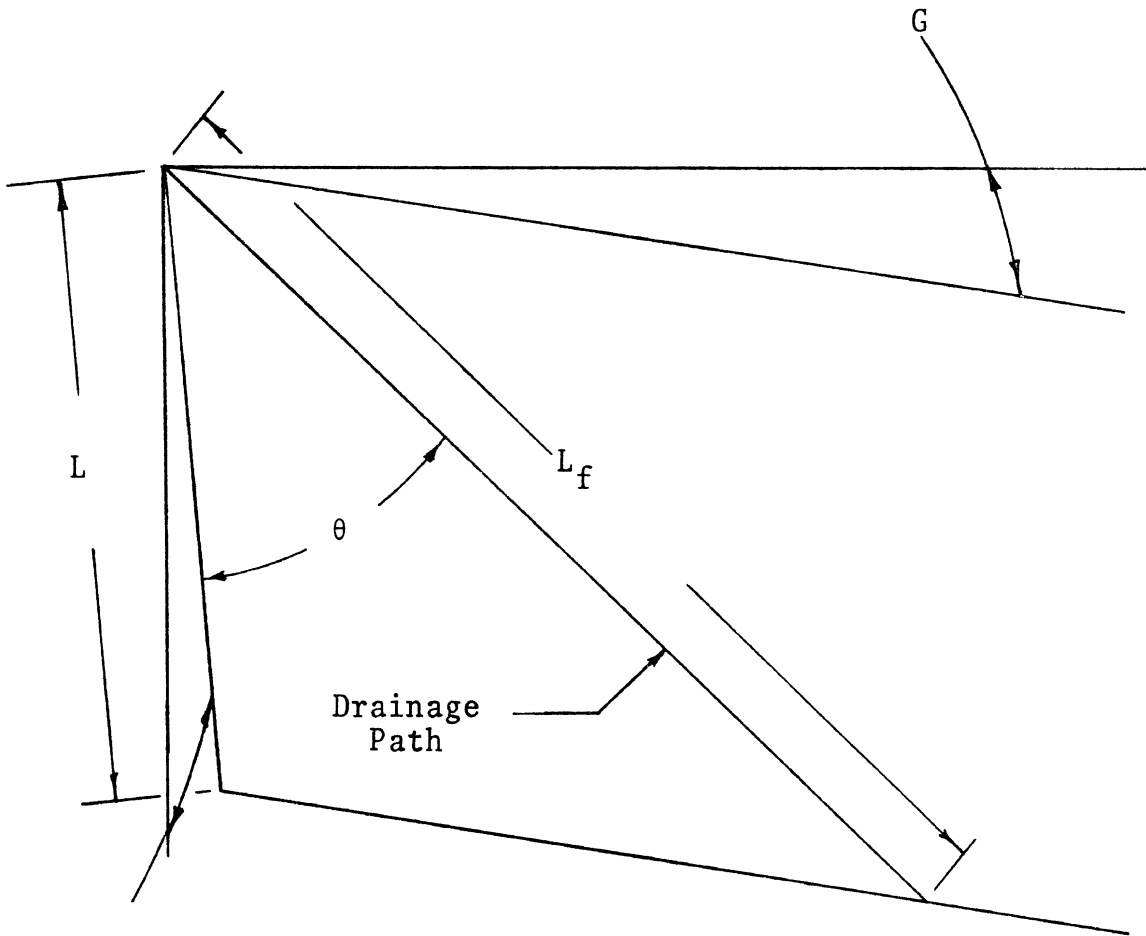
Figure C-1. Drainage Path Geometry

$$d = [3.38 \times 10^{-3}(\tfrac{1}{T})^{-.11} (\tfrac{L_f}{S})^{.425} (I)^{.59}] - T \qquad (C.10)$$

or with the aid of Equation (C.9)

$$d = [3.38 \times 10^{-3}(\tfrac{1}{T})^{-.11} (\tfrac{L}{e^*})^{.425} (I)^{.59}] - T \qquad (C.11)$$

Thus, if Equation (C.11) is to be believed, the primary roadway geometric factors influencing drainage are the pavement width and superelevation. Grade has virtually no influence. Increasing the grade simultaneously increases the pavement slope and the drainage path length. (For a fixed road width, increasing superelevation only increases the slope.) Increasing the pavement slope reduces the water depth, while increasing the drainage path length leads to an increased depth. The net effect is zero. Equation (C.11), then, indicates that water depth is independent of grade.

A similar conclusion can be drawn from Equation (C.2) and (C.3), although the result for Equation (C.2) is not as clear cut. Equation (C.2) is plotted on Figure C-2 to show the separate influences of grade and super-elevation on water depth. It can be noted on the upper plots that water depth is virtually independent of grade except at low values of superelevation. The same conclusion can be drawn from the lower plots, since the
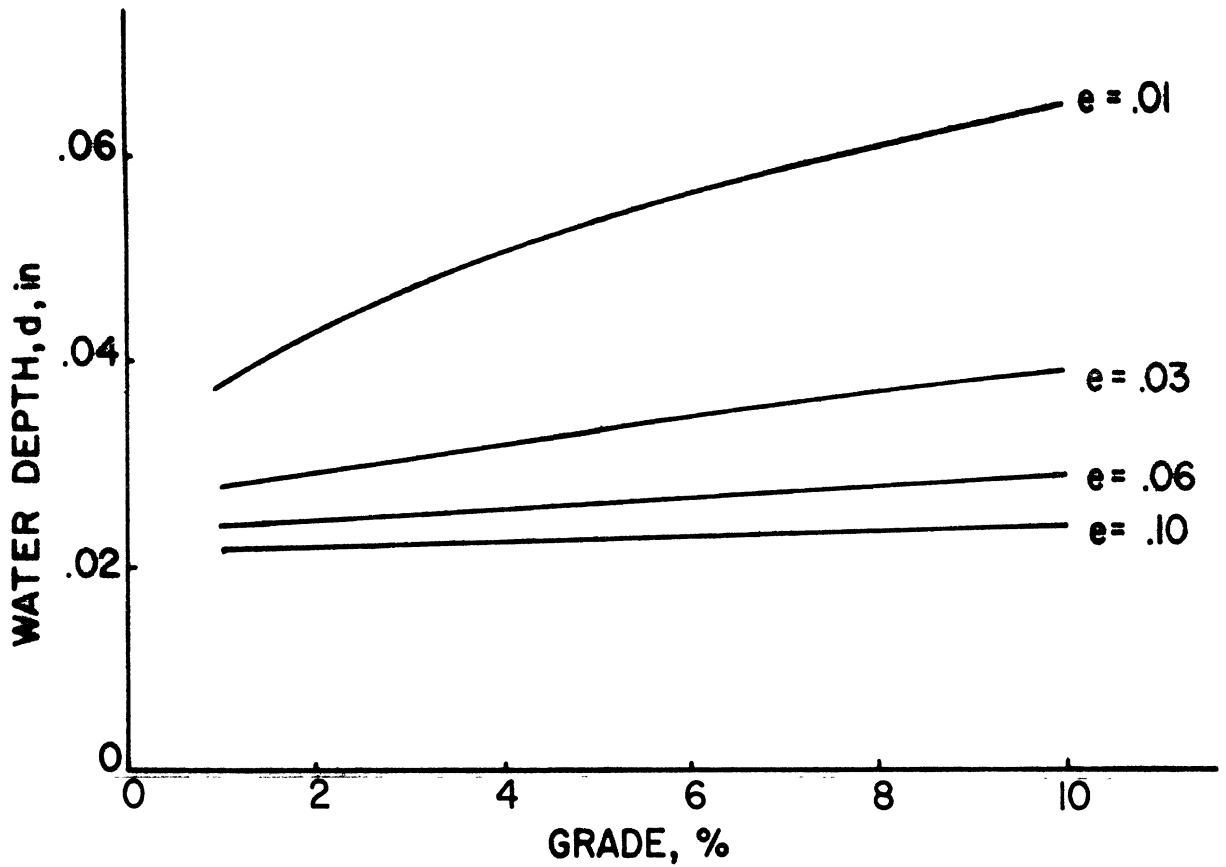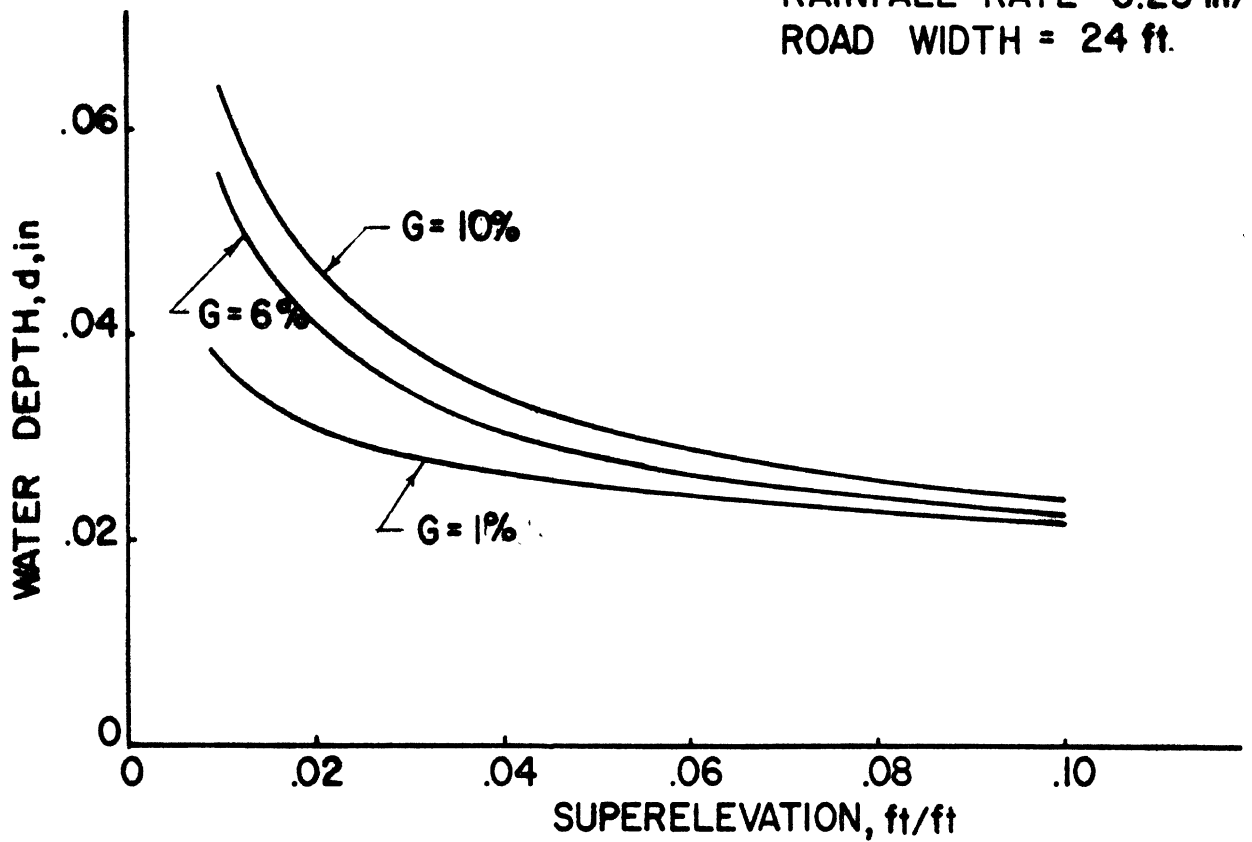
Figure C-2.   The Influence of Grade and Superelevation on
              Water Depth as Predicted by Equation (C.2)

327

plots of water depth versus superelevation tend to converge (i.e., become independent of grade) as superelevation increases.

Similar plots for Equation (C.3) are shown on Figure C-3. As before, it is evident that this equation also predicts small variation in water depth as the result of grade.

Equations (C.1), (C.2), and (C.3), although differing by as much as a factor of three in predictions of water depth, yield the conclusion that water depth is essentially independent of grade. Road width and super-elevation are the primary geometric factors influencing water depths. Therefore, for the most part, curvature and grade do not interact to produce greater water depths.
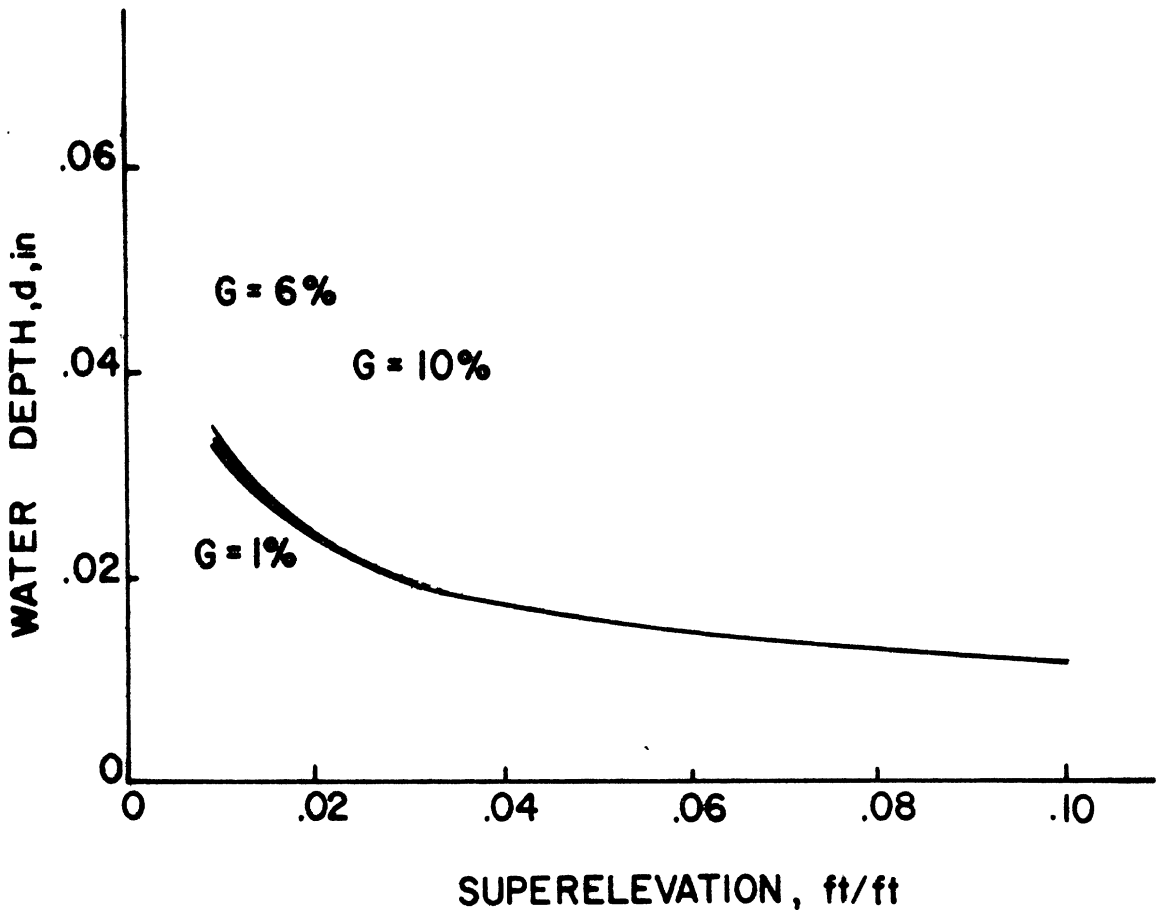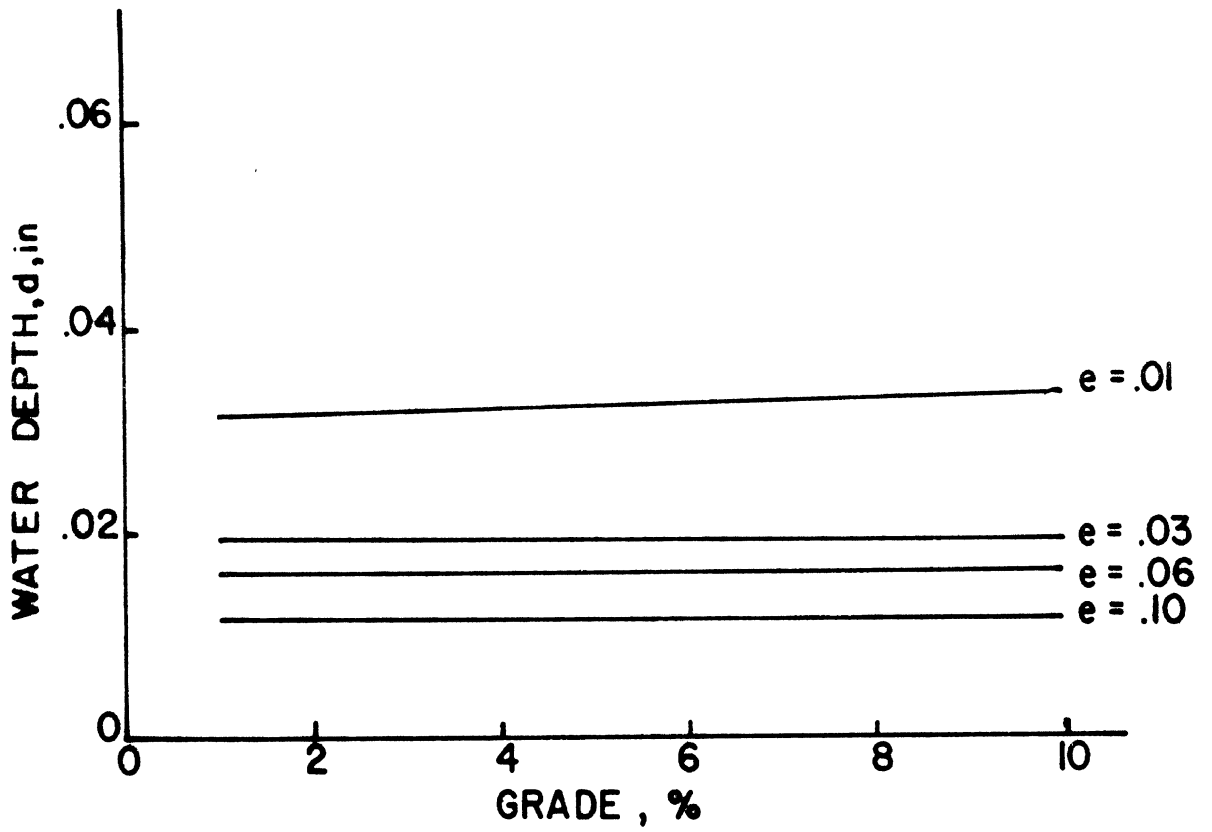
Figure C-3.   The Influence of Grade and Superelevation
on Water Depth as Predicted by Equation (C.3)

329

APPENDIX D

FIELD EVALUATION OF HIGHWAY SITES WITH HIGH ACCIDENT
RATES HAVING COMBINED GRADE AND HORIZONTAL CURVATURE

To determine the effect of combined grade and horizontal curvature as an accident causation factor, two highway sites were selected which have a history of high accident rates. Each site, in addition, exhibited an alignment geometry which combined vertical grade with horizontal curvature. In each case, the site curvature and grade could be classed as being relatively gentle and well within limitations set down by the AASHTO (2).

D.1 PRELIMINARY SITE SELECTION

The two sites selected were narrowed down from an initial group of six. The six initial sites were chosen on the basis of referrals from state highway officials and as a result of the turnpike accident data analyses described in Appendix A.

These six sites are described as follows:

1. Two right-angle curves located on I-75 in Troy, Michigan, approximately seven miles north of Detroit. The easternmost curve begins just north of the intersection of

I-75 and Maple Road and ends just east of
the interchange between I-75 and Rochester
Road. The westernmost curve begins just
west of the intersection between I-75 and
Livernois Road and ends just north of the
interchange between I-75 and Big Beaver Road.
The two curves are within about one mile of
each other. The curvature at each site is 3°,
with the eastern curve being superelevated at
a rate of 0.05 ft/ft and the western curve at
0.06 ft/ft. Traveling northbound, the grade
at the eastern site varies between a 2.00%
upgrade and a 1.50% downgrade, while the grade
at the western site varies similarly between
a 2.63% upgrade and 2.07% downgrade. Accident
data for 1971 indicate that 35 accidents were
reported on the eastern curve, with about 6%
of these occurring during wet weather. Thirty-
six accidents were reported on the westernmost
curve, and 39% of these were during wet weather.

2. A site on the Ohio Turnpike, just south of
Cleveland, between Exits 10 and 11. The site
is located in the westbound direction between
mileposts 166.4 and 166.6. The curvature at
the site is 1°00' and the downgrade varies

between -2.0% and -3.%. Two hundred and
fourteen accidents occurred between mile-
posts 166.4 and 166.6, and of these 34, 28
occurred during wet weather, two under snowy
conditions, and four during dry weather.
Twenty-seven of the 34 were single-vehicle
accidents. No interchange areas are within
four miles of the site.

3. A site on the westbound lane of the Pennsylvania
Turnpike between Interchanges 9 and 10 near
Edie, Pennsylvania. The site lies between
mileposts 105.5 and 105.8, with a 4° curve to
the left. With milepost numbers increasing in
the easterly direction, there is a downgrade of
3.0% for westbound traffic from mileposts 105.86
to 105.63. There is an upgrade of 2.84% from
mileposts 105.63 to 105.45. A total of 54
accidents were recorded in the segment 105.5
to 105.8 during the period January 1967 to
June 1969. Of these 54, 43 occurred in the west-
bound lane, and 34 of these 43 occurred under
wet surface conditions.

4. A site on I-80 near Brookville, Pennsylvania,
approximately one mile east of Exit 13 in the
eastbound lane. The site lies between mileposts
77/36 and 78/36, with a bridge located at

milepost 78/22. The curvature at the site is
1°30' with a superelevation rate of .042 ft/ft.
The downgrade is steadily increasing and
approaches 4.0% near the eastern edge of the
site. A total of 21 accidents were recorded
at the site from November 29, 1970, to
August 4, 1971. Fourteen of these occurred
during wet weather, and 10 of these wet-
weather accidents involved single vehicles. Of
the 21 total accidents, 11 involved tractor-
trailer semi rigs.

In October of 1971 a program was initiated to
reduce the accident-causing potential of the
site. A 150-foot section was grooved in the
transverse direction; a 1,300-foot section was
grooved longitudinally; 13 rumble strips were
installed (these have since been removed); a
berm in the median was cut back; the curve
shoulders were superelevated and paved; and a
wet-pavement warning light was installed which
triggered automatically under wet conditions.
Since these alterations were installed, there
have been no reported accidents at the site.

5. A site on I-95 at an interchange overpass with
   U.S. 1 just south of Fredericksburg, Virginia,

in the southbound lane. Traveling south, the curvature at the site is 1°0'56" to the right. The grade is downward at a rate varying between 2.64% and 3.06%, with a superelevation in both lanes of +0.0156 ft/ft. (This is the same as crown slope superelevation in Virginia.)

A total of 186 accidents were recorded at the site during the period of December 18, 1964, to June 26, 1972. Of these, 73 occurred under wet weather conditions. A 0.95-mile length of the site was longitudinally grooved on June 26, 1972. The grooving extends from 0.1 mile north of the exit to U.S. 1 to 0.36 mile south of the entrance from U.S. 1. In the period prior to grooving from June 27, 1971, to June 26, 1972, a total of 23 accidents were recorded in the 0.95 mile stretch—13 of these occurred during wet pavement conditions. After grooving, for a period between June 27, 1972, through June 26, 1973, 19 accidents were recorded—nine of these under wet conditions.

6.   A site on northbound I-95 near Woodbridge, Virginia, 1.68 miles in length, which lies between 150 feet south of the ramp to State Highway 123 and 150 feet north of the overpass

over County Highway 639. Traveling north,
the highway is three lanes wide with a curva-
ture of 1.29716° to the right. The grade at
the site is approximately 3.36% downward and
the superelevation rate is 0.0156 ft/ft. A
0.49-mile segment of the site was longitudinally
grooved on August 28, 1969.

During the period of August 28, 1966, to
August 27, 1969, a total of 80 accidents were
reported over the entire 1.68-mile segment.
Forty-five of these occurred in the area which
was later to be grooved. Of the 80 accidents
over the entire site, 45 occurred under wet
conditions and 32 of these occurred in the sec-
tion which was later grooved. After grooving,
79 accidents were reported over the entire site
for the period August 28, 1969 to August 27,
1972. Thirty-two of these 79 occurred during
wet weather conditions. In the grooved section,
35 accidents were reported and 14 of these
occurred under wet surface conditions.

D.2 PRELIMINARY SITE EVALUATIONS

Five of the six initial sites were subjected to a preliminary site evaluation. The Pennsylvania Turnpike site could not be included in this evaluation because of problems with high-density summer traffic.

The preliminary evaluation procedure is outlined as follows:

1. Make a motion picture record of each site while traveling through the site at the speed limit.

2. Using a British Portable Tester, measure the pavement friction properties at quarter-mile intervals at each site to be evaluated. Measurements are to be made in both lanes of two-lane highways and in the inside and outside lanes of three-lane highways. Measurements in each lane are to be made:

   a. between the inside wheel path and the lane edge,

   b. within the inside wheel path,

   c. between wheel paths,

   d. within the outside wheel path,

   e. between the outside wheel path and the lane edge.

At each measurement point, four replications
are to be made with the tester—one to smooth
the water layer on the surface, and three
others to be averaged for the surface friction
coefficient value.

3. Using the Silicone Putty method, measure the
pavement texture depth at each end and at the
midpoint of each site. Make measurements in
both lanes of a two-lane highway and in the
inside and outside lanes of a three-lane high-
way. At each measurement location, make
measurements across the lane, as was done under
Item 2 for the friction measurements. Two
putty impressions are to be made at each
measurement point and the results averaged.

4. Using the Schonfeld method (14), record the
pavement surface parameter values which can be
used to compute skid numbers. Estimate
parameter values at the points which were
measured under Item 2.

5. Note the following additional information at
each site in an appropriate log:

   a. the location of measurement points with
      respect to a station marker, mile post,
      bench mark, etc.,

b.   note the speed limit,

c.   on a hand-drawn sketch, indicate the
location of:

(1)   bridge decks

(2)   underpass locations

(3)   interchange ramps (particularly
those which appear to be hidden)

(4)   rock or hill cuts

(5)   lane drops

(6)   guardrail installations

(7)   pertinent signs

(8)   curbing

(9)   drainage facilities

(10)   grooving

(11)   weaving exit/entrance locations

(12)   relatively short acceleration or
deceleration lanes

(13)   pavement shoulders which are worn
away as the result of vehicles
running off the road edge.

6.   Record any additional pertinent information
on a tape recorder, as necessary.

D.3 FINAL SITE SELECTION

The two sites selected for indepth evaluation were chosen on the basis of the following criteria:

1. One site must be chosen from the Ohio or Pennsylvania Turnpikes so that the results of the turnpike accident data analysis can be utilized.

2. One site must be from Virginia or California so as to ensure interested local cooperation.

3. The two sites must exhibit somewhat different characteristics.

Using these criteria, the sites selected for indepth analysis were the Ohio Turnpike site and the I-95 site near Fredericksburg, Virginia. The Ohio Turnpike site is an uncomplicated curve grade with little traffic interaction and no apparent distracting features. The Virginia site, on the other hand, is at an interchange where weaving and decision-making are required. Each of these two sites are evaluated separately in terms of accident causation potential in the following two sections.

D.4 INDEPTH EVALUATION OF THE OHIO TURNPIKE SITE

A simplified plan and profile drawing of the Ohio Turnpike site is shown on Figure D-1 (15). In the
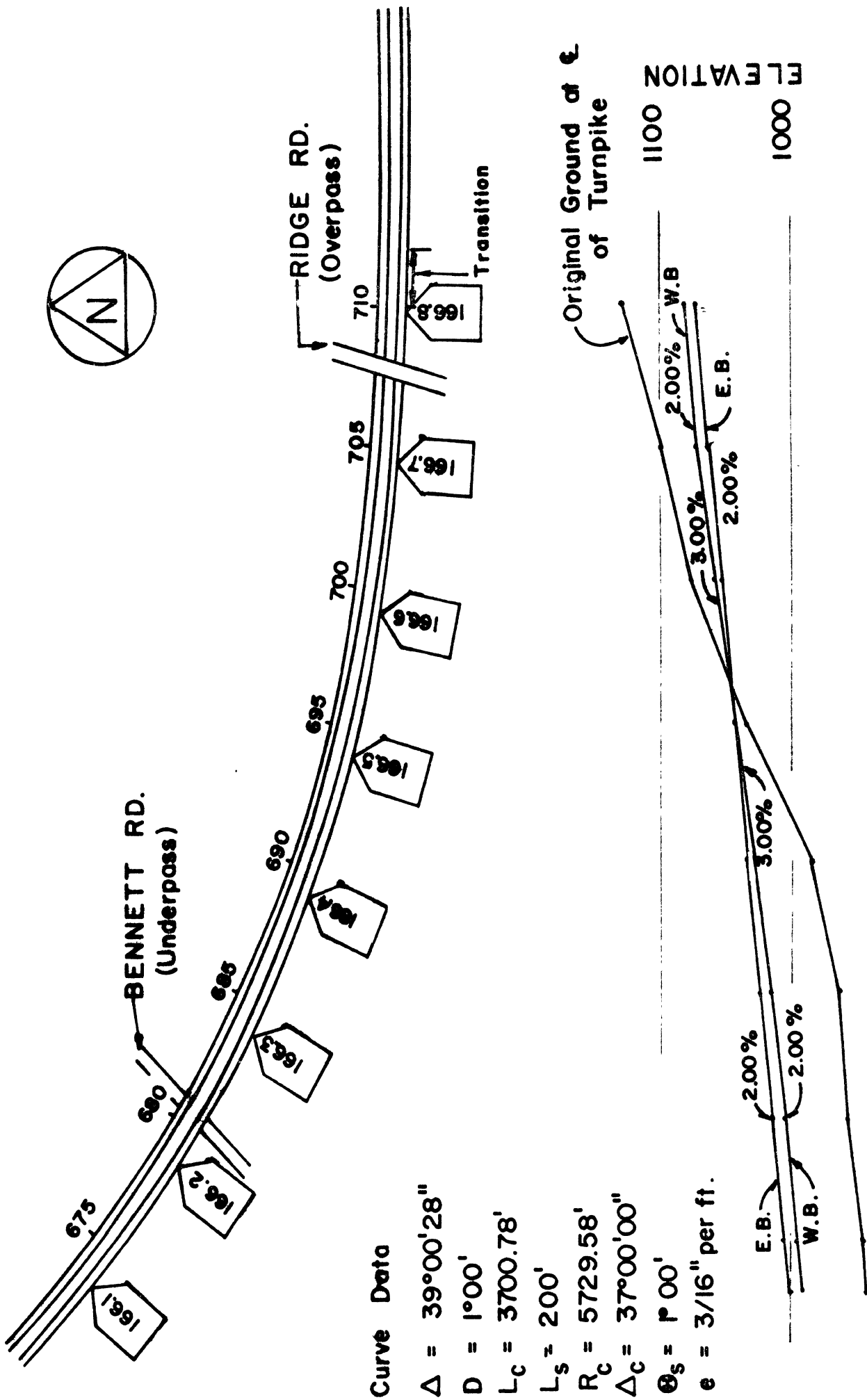
Figure D-1. Ohio Turnpike Site

Curve Data

$\Delta = 39°00'28''$

$D = 1°00'$

$L_c = 3700.78'$

$L_s = 200'$

$R_c = 5729.58'$

$\Delta_c = 37°00'00''$

$\Theta_s = 1°00'$

$e = 3/16''$ per ft.

westbound lane the roadway curves from a due west direction to a direction approximately 39° north of west. The curve data are shown on the figure. In the easterly direction from M.P. 166.6, the surrounding terrain gradually slopes upward from the roadbed until the roadbed is as much as 80 feet below the surroundings. In the region west of M.P. 166.6, the surroundings slope downward until the road is as much as 60 feet above the surroundings. The roadbed grade in the westbound lane is 2.0% downward east of M.P. 166.6. The grade is 3.0% downward between M.P.'s 166.6 and 166.4 and downward at 2.0% west of M.P. 166.4.

A typical cross-section of the roadway is shown on Figure D-2 (16). Note that there is a paved, ten-foot, superelevated shoulder on the outside, or high side of the curve. At the subject site the ten-foot shoulder is on the median side.

The road paving material as originally laid was P.C. concrete. A bituminous overlay was laid in June of 1970 (17).

There is a length of guardrail on the right shoulder of the westbound lane which begins near M.P. 166.5 and continues westward past the bridge over Bennett Road. The guardrail begins on the median or left side near M.P. 166.3 and also continues westward over the bridge. There
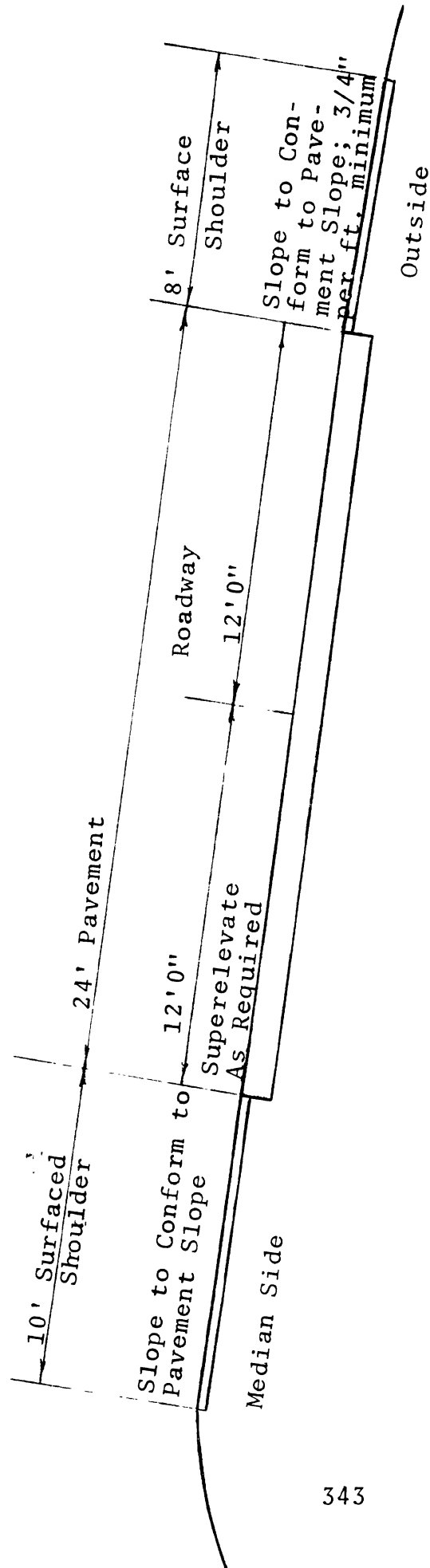
Figure D-2. Typical Roadway Curve Section - Ohio Turnpike

is also a section of guardrail on the median side which extends east from M.P. 166.6. There are no signs anywhere along the site segment.

D.4.1 OHIO TURNPIKE SITE ACCIDENT DATA ANALYSIS. A histogram of accidents on the Ohio Turnpike between mileposts 161.5 and 170.5 is shown on Table D-1. The data are for the period of January 1, 1966, to June 30, 1970. The numbers of accidents between mileposts 166.3 and 167.0 are the highest for any section of the turnpike which does not include an interchange or a service plaza. Note particularly the numbers of accidents in the westbound direction. The largest group of accidents in any three consecutive mileposts has occurred at mileposts 166.4, 166.5, and 166.6.

Specific data concerning each of the 54 accidents that occurred at these mileposts from January 1, 1966 to May 1, 1973 is shown on Table D-2. The data include mention of the general circumstances of the accident, contributing factors, and climatic data.

Climatic data were obtained from the weather station at Cleveland Hopkins Airport, which is approximately nine miles northwest of the site. Hourly rainfall accumulations at the airport during the hours before, during, and after the hours of the accident are given. These are

Table D-1

A Histogram of Ohio Turnpike Accidents Between Mileposts 161.4 and 170.5 During the Period 1/1/66 to 6/30/70

Milepost	Total	Eastbound	Westbound	Off Line
161.4	1 +X	1 +X	0 +	0 +
161.5	5 +XXXXX	2 +XX	3 +XXX	0 +
161.6	1 +X	0 +	1 +X	1 +X
161.7	3 +XXX	1 +X	2 +XX	0 +
161.8	7 +XXXXXXX	5 +XXXXX	2 +XX	3 +XXX
161.9	4 +XXXX	3 +XXX	1 +X	3 +XXX
162.0	7 +XXXXXXX	1 +X	6 +XXXXXX	23 +XXXXXXXXXXXXXXXXXXXXXXX
162.1	2 +XX	1 +X	1 +X	2 +XX
162.2	2 +XX	0 +	2 +XX	1 +X
162.3	4 +XXXX	0 +	4 +XXXX	0 +
162.4	1 +X	0 +	1 +X	0 +
162.5	7 +XXXXXXX	1 +X	6 +XXXXXX	1 +X
162.6	2 +XX	0 +	2 +XX	0 +
162.7	2 +XX	0 +	2 +XX	0 +
162.8	4 +XXXX	1 +X	3 +XXX	0 +
162.9	2 +XX	1 +X	1 +X	0 +
163.0	0 +	0 +	0 +	0 +
163.1	1 +X	1 +X	0 +	0 +
163.2	4 +XXXX	2 +XX	2 +XX	0 +
163.3	2 +XX	1 +X	1 +X	0 +
163.4	2 +XX	2 +XX	0 +	0 +
163.5	5 +XXXXX	1 +X	4 +XXXX	0 +
163.6	2 +XX	1 +X	1 +X	0 +
163.7	1 +X	1 +X	0 +	0 +
163.8	2 +XX	1 +X	1 +X	0 +
163.9	0 +	0 +	0 +	0 +
164.0	1 +X	0 +	1 +X	0 +
164.1	1 +X	0 +	1 +X	0 +
164.2	2 +XX	2 +XX	0 +	0 +
164.3	0 +	0 +	0 +	0 +
164.4	2 +XX	0 +	2 +XX	0 +
164.5	1 +X	1 +X	0 +	0 +
164.6	2 +XX	2 +XX	0 +	0 +
164.7	2 +XX	1 +X	1 +X	0 +
164.8	3 +XXX	2 +XX	1 +X	0 +
164.9	4 +XXXX	2 +XX	2 +XX	0 +
165.0	3 +XXX	0 +	3 +XXX	0 +
165.1	0 +	0 +	0 +	0 +
165.2	6 +XXXXXX	4 +XXXX	2 +XX	0 +
165.3	4 +XXXX	2 +XX	2 +XX	0 +
165.4	6 +XXXXXX	4 +XXXX	2 +XX	0 +
165.5	8 +XXXXXXXX	5 +XXXXX	3 +XXX	0 +
165.6	4 +XXXX	4 +XXXX	0 +	0 +
165.7	3 +XXX	2 +XX	1 +X	0 +
165.8	4 +XXXX	3 +XXX	1 +X	0 +
165.9	2 +XX	2 +XX	0 +	0 +
166.0	4 +XXXX	2 +XX	2 +XX	0 +
166.1	1 +X	1 +X	0 +	0 +
166.2	4 +XXXX	2 +XX	2 +XX	0 +
166.3	6 +XXXXXX	3 +XXX	3 +XXX	0 +
166.4	16 +XXXXXXXXXXXXXXXX	5 +XXXXX	11 +XXXXXXXXXXX	0 +
166.5	21 +XXXXXXXXXXXXXXXXXXXXX	4 +XXXX	17 +XXXXXXXXXXXXXXXXX	0 +
166.6	8 +XXXXXXXX	2 +XX	6 +XXXXXX	0 +
166.7	16 +XXXXXXXXXXXXXXXX	3 +XXX	13 +XXXXXXXXXXXXX	0 +
166.8	21 +XXXXXXXXXXXXXXXXXXXXX	11 +XXXXXXXXXXX	10 +XXXXXXXXXX	0 +
166.9	14 +XXXXXXXXXXXXXX	9 +XXXXXXXXX	5 +XXXXX	0 +
167.0	7 +XXXXXXX	3 +XXX	4 +XXXX	0 +
167.1	2 +XX	1 +X	1 +X	0 +
167.2	7 +XXXXXXX	5 +XXXXX	2 +XX	0 +
167.3	8 +XXXXXXXX	5 +XXXXX	3 +XXX	1 +X
167.4	2 +XX	0 +	2 +XX	0 +
167.5	2 +XX	1 +X	1 +X	0 +
167.6	12 +XXXXXXXXXXXX	6 +XXXXXX	6 +XXXXXX	0 +
167.7	6 +XXXXXX	2 +XX	4 +XXXX	0 +
167.8	8 +XXXXXXXX	3 +XXX	5 +XXXXX	0 +
167.9	9 +XXXXXXXXX	3 +XXX	6 +XXXXXX	0 +
168.0	0 +	0 +	0 +	0 +
168.1	1 +X	1 +X	0 +	0 +
168.2	0 +	0 +	0 +	0 +
168.3	0 +	0 +	0 +	0 +
168.4	0 +	0 +	0 +	0 +
168.5	12 +XXXXXXXXXXXX	7 +XXXXXXX	5 +XXXXX	0 +
168.6	0 +	0 +	0 +	0 +
168.7	3 +XXX	1 +X	2 +XX	0 +
168.8	5 +XXXXX	4 +XXXX	1 +X	0 +
168.9	2 +XX	2 +XX	0 +	0 +
169.0	0 +	0 +	0 +	0 +
169.1	0 +	0 +	0 +	0 +
169.2	1 +X	1 +X	0 +	0 +
169.3	2 +XX	0 +	2 +XX	0 +
169.4	2 +XX	1 +X	1 +X	0 +
169.5	8 +XXXXXXXX	4 +XXXX	4 +XXXX	0 +
169.6	4 +XXXX	2 +XX	2 +XX	0 +
169.7	3 +XXX	0 +	3 +XXX	0 +
169.8	3 +XXX	1 +X	2 +XX	0 +
169.9	3 +XXX	0 +	3 +XXX	1 +X
170.0	5 +XXXXX	4 +XXXX	1 +X	14 +XXXXXXXXXXXXXX
170.1	5 +XXXXX	2 +XX	3 +XXX	5 +XXXXX
170.2	1 +X	1 +X	0 +	0 +
170.3	5 +XXXXX	4 +XXXX	1 +X	3 +XXX
170.4	4 +XXXX	1 +X	3 +XXX	1 +X
170.5	2 +XX	1 +X	1 +X	0 +

Table D-2

ACCIDENT DATA - WESTBOUND OHIO TURNPIKE

M.P. 166.4 to 166.6

January 1, 1966 to May 1, 1973

Date	Hour	Speed	Road Condition	Driver Condition	Vehicle Condition	Vehicle #1	Vehicle #2	Accumulated Precip. One Hour Prior To Accident	Accumulated Precip. During Hour of Accident	Accumulated Precip. One Hour After Accident	Wind Vel. (kn.)	Wind Dir.	
2/25/66	1800-1900	30	Snowy	Satisfactory	Satisfactory	Hit a Stopped Vehicle	Illegally Stopped or Parked	.02" rain	.04" rain 1.2" snow	.02" rain	4-6	S	Both Passenger Cars
4/2/66	0800-0900	60	Wet	Satisfactory	Defective Tires	Hit Guardrail in Median	None	Trace rain	Trace rain	Trace rain	7-9	NW	Passenger Car, Skidding
4/27/66	1300-1400	60	Wet	Satisfactory	Satisfactory	Ran Into Median	None	.05" rain	.08" rain	.12" rain	11-15	E	Passenger Car, Skidding
5/21/66	1200-1300	65	Wet	Satisfactory	Satisfactory	Ran Into Median	None	.06" rain	.09" rain	.06" rain	4-6	S	Passenger Car, Skidding
8/10/66	2100-2200	65	Wet	Satisfactory	Satisfactory	Hit Guardrail on Right	None	.16" rain	.04" rain	.23" rain	11-14	S	Passenger Car, Skidding
8/14/66	0200-0300	65	Wet	Unpracticed or Unskilled	Satisfactory	Hit Guardrail on Right	None	Trace rain	.01" rain	Trace rain	8	SE	Passenger Car, Skidding
9/3/66	2000-2100	60	Wet	Driver Inattention or Carelessness	Defective Tires	Hit Guardrail on Right	None	.27" rain	.13" rain	.02" rain	10-14	S	Passenger Car, Skidding
9/20/66	0600-0700	55	Wet	Satisfactory	Satisfactory	Hit Guardrail on Right	None	.16" rain	.08" rain	.11" rain	14	E	Passenger Car, Skidding
10/15/66	1300-1400	65	Wet	Satisfactory	Satisfactory	Ran off Road on Right	None	.01" rain	.22" rain	.12" rain	15-16	S	Passenger Car, Skidding
11/2/66	1400-1500	63	Wet	Satisfactory	Satisfactory	Hit Guardrail on Right	None	.08" rain	.10" rain	.07" rain	21	N	Passenger Car, Skidding
6/22/67	0600	45	Wet	Satisfactory	Satisfactory	Ran Into Median	None	.01" rain	Trace rain	None	5-8	NW	Passenger Car, Skidding

Date	Hour	Speed	Road Condition	Driver Condition	Vehicle Condition	Vehicle #1	Vehicle #2	Accumulated Precip. One Hour Prior To Accident	Accumulated Precip. During Hour of Accident	Accumulated Precip. One Hour After Accident	Wind Vel. (kn.)	Wind Dir.	
6/30/ 67	1910	50	Dry	Satisfactory	Satisfactory	Hit Object in Roadway	None	Trace rain	None	None	5-6	SW	Tractor-Trailer
7/20/ 67	1730	55	Dry	Satisfactory	Satisfactory	Hit Guardrail on Right and Then Into Median	None	None	None	None	5-7	N	Passenger Car Towing House Trailer
8/26/ 67	1745	50	Wet	Satisfactory	Unknown	Hit Guardrail in Median	None	.03" rain	None	None	7-14	S	Passenger Car, Skidding
9/9/ 67	1920	60	Wet	Satisfactory	Satisfactory	Hit Guardrail on Right	None	Trace rain	None	None	8-12	N	Passenger Car, Skidding
3/15/ 68	1730	65	Wet	Satisfactory - Both Drivers	Defective Tires #1 Satisfactory #2	Hit Stopped Vehicle	Stopped Due to Prior Accident	.02" rain	.01" rain Trace snow	.02" rain	6-7	S	Both Passenger Cars; Skidding for Vehicle #1
5/11/ 68	1305	60-65	Wet	Satisfactory	Satisfactory	Hit Guardrail on Right	None	.12" rain	.11" rain	.05" rain	3-4	NE	Passenger Car, Skidding
5/11/ 68	1810	70	Wet	Satisfactory	Unknown	Hit Guardrail on Right	None	.02" rain	.04" rain	.01" rain	6-9	NE	Passenger Car, Skidding
5/29/ 68	2255	70	Wet	Satisfactory	Defective Tires	Ran Into Median	None	Trace rain	Trace rain	.02" rain	3-4	N	Passenger Car, Skidding; Rear Tires Had 1/32" of Tread
6/25/ 68	1426	40	Wet	Satisfactory	Unknown	Ran Into Median	None	.05" rain	None	Trace rain	7-13	SE	Tractor-Trailer; Skidding; Overturned
7/23/ 68	1855	40	Wet	Satisfactory	Defective Tires	Hit Guardrail on Right	None	None	None	None	3-6	NE	Passenger Car, Skidding
8/4/ 68	1340	55	Dry	Satisfactory	Satisfactory	Hit Guardrail on Right	None	None	None	None	4-9	SW	Passenger Car Towing Trailer

347

Table D-2 (Continued)

Date	Hour	Speed	Road Condition	Driver Condition	Vehicle Condition	Vehicle #1	Vehicle #2	Accumulated Precip. One Hour Prior To Accident	Accumulated Precip. During Hour of Accident	Accumulated Precip. One Hour After Accident	Wind Vel. (kn.)	Wind Dir.	
1/29/69	1640	#1-70 #2-55	Wet	Satisfactory - Both Drivers	Defective Tires on Vehicle #1	Hit Guardrail on Right	Ran Into Vehicle #1	Trace rain	.05" rain	.05" rain	8-9	S	Passneger Car; Skidding; Ran Into Path of Tractor-Trailer
1/29/69	1651	10-15	Wet	Satisfactory - Both Drivers	Satisfactory - Both Vehicles	Hit a Stopped Vehicle	Parked to Help at Accident	Trace rain	.05" rain	.05" rain	8-9	S	Both Vehicles Tractor-Trailers
5/18/69	1050	65	Wet	Satisfactory	Defective Tires	Ran Into Median	None	.08" rain	.04" rain	.06" rain	11-15	S	Passenger Car; Skidding; Insufficient Tread Depth on Rear Tires
6/13/69	0540	60	Wet	Satisfactory	Defective Tires	Ran Into Median	None	.05" rain	Trace rain	None	8-12	S	Passenger Car; Skidding; Rear Tires Bald
9/27/69	1410	55-60	Wet	Satisfactory	Satisfactory	Trailer Broke Loose	None	.05" rain	.01" rain	Trace rain	7-8	SW	Passenger Car Towing Trailer
11/1/69	0840	50-55	Wet	Satisfactory	Defective Tires	Hit Guardrail on Right	None	.02" rain	.04" rain	.04" rain	8-10	S	Passenger Car; Skidding; R.R. Tire 2/32" Tread; L.R. Bald
11/1/69	1935	70	Wet	Satisfactory	Satisfactory	Hit Guardrail on Right	None	.01" rain	.05" rain	.02" rain	6-10	SE	Passenger Car; Skidding
11/20/69	0635	65	Wet	Satisfactory	Satisfactory	Hit Guardrail in Median	None	Trace rain	No rain 0.7" snow	Trace rain	7-11	W	Passenger Car; Skidding
12/18/69	1115	65	Wet	Satisfactory - Both Drivers	Satisfactory - Both Vehicles	Hit Vehicle #2 in Rear	No Apparent Fault	Trace rain	.02" rain	.02" rain 0.4" snow	16-19	S	Both Passenger Cars
12/31/69	0745	#1-35 #2-30	Snowy Icy	Satisfactory - Both Drivers	Satisfactory - Both Vehicles	Hit Vehicle #2 on Side	No Apparent Fault	.01" rain 3.4" snow	.02" rain	Trace rain	16-17	N	Both Passenger Cars; Skidding for Vehicle #1

348

Table D-2 (Continued)

Date	Hour	Speed	Road Condition	Driver Condition	Vehicle Condition	Vehicle #1	Vehicle #2	Accumulated Precip. One Hour Prior To Accident	Accumulated Precip. During Hour of Accident	Accumulated Precip. One Hour After Accident	Wind Vel. (kn.)	Wind Dir.	
5/5/70	1240	50	Dry	Satisfactory	Satisfactory	Trailer Jackknifed	None	None	Trace rain	Trace rain	16-19	W	Passenger Car Towing Trailer; Trailer Jackknifed at Construction Cross-Over
6/25/70	0407	#1-45 #2-30 -35	Dry	Satisfactory - Both Drivers	Satisfactory - Both Vehicles	Hit Vehicle #2 in Rear	Improper Slowing	None	None	None	7-10	N	Tractor-Trailer Ran Into Passenger Car
7/9/70	0740	50-60	Wet	Satisfactory	Satisfactory	Hit Embankment on Right	None	.03" rain	.01" rain	None	7-10	SE	Passenger Car; Skidding
7/29/70	1517	55	Wet	Satisfactory	Defective Tires	Hit Guardrail on Right	None	Trace rain	1.26" rain About 3.75 in/hr	Trace rain	10-14	SW	Passenger Car; Skidding; R.R. Tire-Bald; L.R. 1/32" Tread
10/10/70	1515	55	Dry	Satisfactory	Fire in Vehicle	Fire	None	None	None	None	5-8	W	Tractor-Trailer
11/2/70	1440	50-55	Wet	Satisfactory	Defective Tires	Hit Guardrail in Median	None	.03" rain	.04" rain	.01" rain	10-15	E	Passenger Car; Skidding; R.R. Tire 2/32" Tread; L.R.-Bald
2/8/71	1050	#1-40 -50 #2-40	Snowy Icy	Satisfactory - Both Drivers	Satisfactory - Both Vehicles	Hit Guardrail on Right	Ran Into Vehicle #1	.03" rain	.02" rain	.05" rain 1.5" snow	14	N	Vehicle #1 - Passenger Car Which Skidded; Vehicle #2 - Tractor-Trailer
2/17/71	2040	65-70	Icy	Satisfactory	Satisfactory	Hit Guardrail on Right	None	None	None	None	10-13	SW	Passenger Car (VW) Hit Icy Spot on Road
2/17/71	2105	65	Icy	Satisfactory	Satisfactory	Hit Guardrail on Right Then on Left	None	None	None	None	12-13	SW	Passenger Car Hit Icy Spot on Road
5/1/71	1545	40	Wet	Satisfactory	Satisfactory	Hit Guardrail on Right	None	Trace rain	Trace rain	Trace rain	12-16	SW	Pickup Truck Towing Trailer; Skidding

349

Table D-2 (Continued).

Date	Hour	Speed	Road Condition	Driver Condition	Vehicle Condition	Vehicle #1	Vehicle #2	Accumulated Precip. One Hour Prior To Accident	Accumulated Precip. During Hour of Accident	Accumulated Precip. One Hour After Accident	Wind Vel. (kn.)	Wind Dir.	
5/24/71	1930	65-70	Wet	Satisfactory	Satisfactory	Ran Into Ditch on Right	None						Passenger Car; Skidding
7/9/71	1925	55	Dry	Satisfactory	Unknown	Hit Guardrail on Right	None	None	None	None	4	N	Passenger Car; Skidding; Failing to Regain Control After Passing
2/13/72	1201	55	Snowy Icy	Satisfactory	Defective Tires	Hit Guardrail on Right Then Into Median	None	.02" rain	.04" rain 1.8" snow	.05" rain	10-12	N	Passenger Car; Skidded on Ice; L.F., R.R., L.R Tires Bald
3/28/72	1350	60-65	Dry	Satisfactory	Satisfactory	Hit Guardrail in Median	None	None	None	None	11-16	NE	Passenger Car; Skidding; Tires Satisfactory
4/15/72	1110	70-80	Dry	Satisfactory	Defective Tires	Flipped Over Guardrail on Right	None	None	None	None	14-17	SW	Passenger Car; Skidding; L.R. Tire Blew Out; Other Tires Satisfactory
5/30/72	1315	60	Wet	Satisfactory	Defective Tires	Hit Guardrail on Right Then One In Median	None	.05" rain	.03" rain	.05" rain	7-8	SW	Passenger Car; Skidding; Rear Tires Less Than 2/32" Tread
5/30/72	1510	60	Wet	Satisfactory	Satisfactory	Hit Guardrail on Right Then One In Median	None	.05" rain	Trace rain	None	7-9	S	Passenger Car; Skidding
6/14/72	1530	50	Wet	Satisfactory	Satisfactory	Hit Two Parked Vehicles	Stopped Due to Heavy Rain	.01" rain	None	None	10-14	S	Passenger Car; Skidding
8/6/72	1835	55-70	Wet	Satisfactory	Satisfactory	Ran Into Median	None	.15" rain	.03" rain	Trace rain	6-9	SW	Passenger Car; Skidding

350

Table D-2 (Continued)

Date	Hour	Speed	Road Condition	Driver Condition	Vehicle Condition	Vehicle #1	Vehicle #2	Accumulated Precip. One Hour Prior To Accident	Accumulated Precip. During Hour of Accident	Accumulated Precip. One Hour After Accident	Wind Vel. (kn.)	Wind Dir.	
9/17/72	1655	35	Wet	Satisfactory - Both Drivers	Defective Tires on #1	Hit Vehicle #2 in Rear	No Apparent Fault	None	.17" rain	.19" rain	19-22	S	Both Passenger Cars; Tires on #1, LF 2/32" Tread, RF 1/32" Heavy Rain Storm
9/17/72	1720	65	Wet	Satisfactory	Satisfactory	Ran Into Median	None	.17" rain	.19" rain	.04" rain	3-7	SW	Passenger Car; Skidding
9/27/72	1205	65	Wet	Satisfactory	Defective Tires	Hit Guardrail in Median	None	Trace rain	None	None	11-13	NE	Passenger Car; Skidding
4/27/73	1015	50-55	Wet	Satisfactory	Satisfactory	Ran Into Median; Rolled Over	None	.05" rain	.05" rain	.08" rain	17-18	N	Passenger Car; Skidding; Heavy Rain; Wind Hit Vehicle

351

included to account for possible variances due to the location of the weather station. The wind data also represents an average over the three-hour period within which the accident occurred. Wind velocity is probably the least accurate information given, since the local terrain around the accident site is undoubtedly somewhat different than at the airport. It should be remembered that, traveling west, the roadway emerges from a deep hill cut (up to 80 feet below the surrounding terrain) at M.P. 166.6, and then progresses into a heavily filled area where the roadway is as much as 60 feet above the surrounding terrain.

The data on Table D-2 are summarized in Table D-3. It can be noted that of the 55 accidents occurring at the site, 40, or 73%, occurred during wet weather. In addition, 16 of the 55 involved defective tires as a contributing factor, although tire condition was not always examined or reported in each case.

Rainfall rate ranges are also recorded on Table D-3, due to the fact that a large majority of the accidents occurred during wet weather. Rainfall rate influences the water depth on the pavement, and water depth, in turn, influences tire traction. The indicated rainfall rates represent accumulation during the hour of the accident

TABLE D-3

ACCIDENT DATA SUMMARY
WESTBOUND OHIO TURNPIKE
M.P. 166.4-166.6
January 1, 1966 to May 1, 1973

Year	Total	Pavement Condition			Smooth Tires	Skidding L.O.C. Wet Surface	Other Cause	Hourly Rainfall Accumulation		
		Wet	Dry	Snow/Ice				<.10 in/hr	.10-.25 in/hr	>.25 in/hr
1966	10	9	0	1	2	9	1	7	3	0
1967	5	3	2	0	0	3	2	3	0	0
1968	7	6	1	0	3	6	1	5	1	0
1969	10	9	0	1	4	6	4	10	0	0
1970	6	3	2	0	2	3	3	3	0	1
1971	6	2	1	3	0	2	4	2	0	0
1972	10	7	2	1	5	7	3	4	2	0
1973	1	1	0	0	0	1	0	1	0	0
Total	55	40	8	6	16	37	18	38	6	1
Percent		73	15	11	29	67	33	69	11	2

353

at a point nine miles northwest of the site. Therefore, actual rainfall rates at the time of the accident are probably different due to (1) the distance factor, and (2) the fact that the rates indicated are averaged over an hour. The latter would suggest that instantaneous rainfall rates at the time of the accident could be much higher, or much lower, than the indicated hourly average rates.

During June of 1970 the pavement at the subject site was resurfaced with a bituminous overlay. Prior to that time, the pavement surface was P.C. concrete. Table D-4 shows a comparison of the percentage of wet surface accidents to total accidents for each of the years before and after resurfacing. As indicated, before repaving 79% of the accidents occurred during wet weather; afterward, 62%. Apparently repaving had some beneficial effect, but not a large effect.

D.4.2 ACCIDENT CAUSATION ANALYSIS. It is apparent that wet weather is a controlling factor relative to accident causation at the Ohio Turnpike site. Other factors may also be involved. In the discussions that follow, the degradation of pavement surface friction during wet weather will be considered first. Next will follow a discussion of other possible accident-causation factors.

TABLE D-4

A COMPARISON OF THE PERCENTAGE OF WET WEATHER ACCIDENTS,
BY YEAR, BEFORE AND AFTER RESURFACING

Year	Total	Wet	% Wet Weather Accidents / Total Accidents
1966	10	9	90
1967	5	3	60
1968	7	6	86
1969	10	9	90
1970	2	0	0
PAVEMENT RESURFACED			
1970	4	3	75
1971	6	2	33
1972	10	7	70
1973	1	1	100

Cumulative Percentage Before Repaving $\dfrac{27 \times 100}{34} = 79\%$

Cumulative Percentage After Repaving $\dfrac{13 \times 100}{21} = 62\%$

355

D.4.2.1 Wet Weather Effects. Wet weather accident-causation effects are primarily the result of a wet pavement surface. (Visibility may also be a factor, but poor visibility usually causes the traffic to slow down, or stop, whereas wet pavement per se usually does not.) In this section, the measurements of pavement skid resistance made at the site are described first. Next follows a discussion of pavement drainage characteristics. Finally, the probable traction characteristics of the site are predicted, as such traction properties can be estimated by skid resistance measurements and by surface drainage properties.

D.4.2.1.1 Measurements of pavement friction. Measurements of pavement friction properties, made at or near the site by the Ohio Department of Transportation, are given in Table D-5. Unfortunately, a skid test measurement program was not begun in Ohio until the latter part of 1969. Because of this, no skid tests were made at the subject site prior to the time the site was resurfaced in June, 1970. Friction properties prior to this time must therefore be inferred from measurements made at other sections of the Turnpike. During October of 1969 some unresurfaced sections of the Turnpike were subjected to skid tests as a means of checking out newly acquired skid

TABLE D-5

AVAILABLE MEASURED SKID TRAILER DATA

Date	Measurement Device	M.P.	Lane	Measurements	Range	Average
10/2/69 Before Resurfacing	Locked Wheel Skid Trailer at 40 mph Test Speed	101-109	Traveling	34, 30, 28, 28, 30, 25, 30, 29, 36	25-36	30.0
		109-114	Passing	38, 38, 48, 34, 34	34-48	38.2
		114-118	Traveling	25, 25, 25, 26	25-26	25.3
		127-132	Traveling	38, 38, 44, 34	34-44	38.5
11/15/71 After Resurfacing	Locked Wheel Skid Trailer at 40 mph Test Speed	166	Traveling			40
		167	Passing			53

testing apparatus (19). The results of these tests are shown on the upper part of Table D-5. It can be inferred from these results that prior to resurfacing, the site between M.P. 166.4-166.6 had a skid number in the range of 25 to 44 in the traveling lane and 34 to 48 in the passing lane. After resurfacing, tests at the site, made in November of 1971, show skid numbers of 40 and 53 in the traveling and passing lanes, respectively (19). These are listed on the lower line of Table D-5.

As a part of the present program, additional tests were made at the site to determine pavement friction properties. Surface friction was measured with a British Portable Tester (20, 21) and by means of the Schonfeld photo-interpretation method (14). In addition, the average texture depth of the pavement was measured by means of the putty impression method (22). Measurements were made at mileposts 166.00, 166.25, 166.50, 166.75, and 167.00. The results of the measurements, as averaged across the four mileposts, are given in Table D-6. Note that ten measurements were made across the roadway, five each in both the traveling and passing lanes.

The data obtained with the British Portable Tester were collected with sliders made of the same rubber compound used to make the ASTM standard test tire as per ASTM Designation E249-66 (11). The sliders were made

TABLE D-6

OHIO TURNPIKE SURFACE MEASUREMENTS

Position	British Portable Number (BPN)[1]	Schonfeld Method Estimates			Estimated Skid Trailer $SN_{40}T_r$		Measured Skid Trailer $SN_{40}T_r$[4]	Average Texture Depth-in[1]
		$SN_{30}S$	$SN_{40}S$	$SN_{60}S$	Based On BPN[2]	Based On BPN[3]		
Right Road Edge Traveling Lane	75	47	43	35	68	49		.0041
Right Wheel Path Traveling Lane	67	43	40	33	56	46		.0089
Middle Traveling Lane	79	47	43	35	74	49	40	.0065
Left Wheel Path Traveling Lane	74	43	40	33	66	46		.0048
Left Lane Edge Traveling Lane	76	47	43	35	69	49		.0098
Right Lane Edge Passing Lane	79	47	43	35	74	49		.0047
Right Wheel Path Passing Lane	75	43	40	33	68	46		.0052
Middle Passing Lane	84	47	43	35	81	49	53	.0041
Left Wheel Path Passing Lane	81	43	40	33	76	46		.0027
Left Lane Edge Passing Lane	84	47	43	35	81	49		.0068

1. Averaged over five sites between M.P. 166-167, three measurements being taken at each site.
2. Adjusted with Equation $SN_{40}T_r = -41 + 1.45$ BPN (23)
3. Adjusted with Equation $SN_{40}T_r = 6 + SN_{40}S$ (24)
4. See Table D-5

from a single batch and were obtained from the General Tire and Rubber Company. In carrying out the measurements, the slider contact length was adjusted between 4-7/8 and 5 inches.

In examining the skid number data it can be noted that the BPN values are generally higher than those determined by both the Schonfeld photo-interpretation method and by skid trailer measurements. This result is probably caused by the sliders which were used on the British Portable Tester. In a limited test series conducted during the project, other "standard" sliders have yielded skid number values as much as 30 units below the values indicated on Table D-6. Since the program was not aimed at correlating skid testing measurements, however, no attempt has been made to "adjust" the measured BPN values.

The Schonfeld and skid trailer data are probably the most representative measures of pavement friction characteristics, although the respective measurements were made almost 20 months apart. These data indicate that the current SN_{40} values at the site are probably somewhere between 40 and 50.

Pavement texture values averaged less than 0.01 in., indicating a relatively smooth surface.

D.4.2.1.2 <u>Pavement drainage characteristics</u>. Prior

to resurfacing, the skid number data given on Table D-5

suggests that the subject site may have had a sub-

standard friction surface. There were no actual tests

made at the site, however, and this conclusion must be

inferred from data taken at other similar sites. After

resurfacing, the surface would appear to be adequate

according to currently accepted criteria. It is apparent,

then, that some other factor is very probably responsible

for the high incidence of wet-weather accidents at the

site.

The most likely causative factor relates to the

drainage characteristics of the site. As indicated in

Appendix C, pavement surface drainage is a function of

the drainage path length, surface slope, rainfall intensity,

and probably texture depth. The three equations that were

developed to relate water depth to the above variables

are repeated as follows:

$$d = [3.38 \times 10^{-3})(\tfrac{1}{T})^{-0.11}(L_f)^{0.43}(I)^{0.59}(\tfrac{1}{S})^{0.42}] - T$$

(D.1)

$$d = \frac{0.0059(L_fI)^{0.47}}{S^{0.20}}$$

(D.2)

$$d = (9.6 \times 10^{-4})(I)^{0.44}(L_f)^{0.55}(\tfrac{1}{S})^{0.46}$$
$$+ (2.26 \times 10^{-3})(I)^{0.49}(\tfrac{1}{S})^{0.38}$$

(D.3)

where

     T = average surface texture depth, in.

     L_f = length of flow path, ft.

     I = rainfall intensity, in/hr

     S = pavement slope

Equation (D.1) was developed at the Texas Transportation Institute (6), Equation (D.2) at the Road Research Laboratory (7), and Equation (D.3) at the Goodyear Tire and Rubber Company (8, 9). As indicated in Chapter 2, Equation (D.1) predicts water depths which are as much as a factor of three less than those predicted by Equation (D.2). The predictions from Equation (D.3) fall somewhere in between. Since Equations (D.1) and (D.2) bracket expected results, however, the remaining discussions will be primarily concerned with these two. Where design policy is concerned, the worst-case predictions represented by Equation (D.2) will be used.

Equations (D.1) and (D.2) are plotted on Figure D-3 in terms of water depth versus road width. Separate curves are shown for rainfall intensities of 0.10, 0.25, and 0.50 in/hr. These values were chosen to reflect the hourly rainfall accumulations recorded at Cleveland Hopkins Airport and to account for higher rainfall rates that undoubtedly occur for shorter periods than would be reflected in an average hourly rate. (For example, on
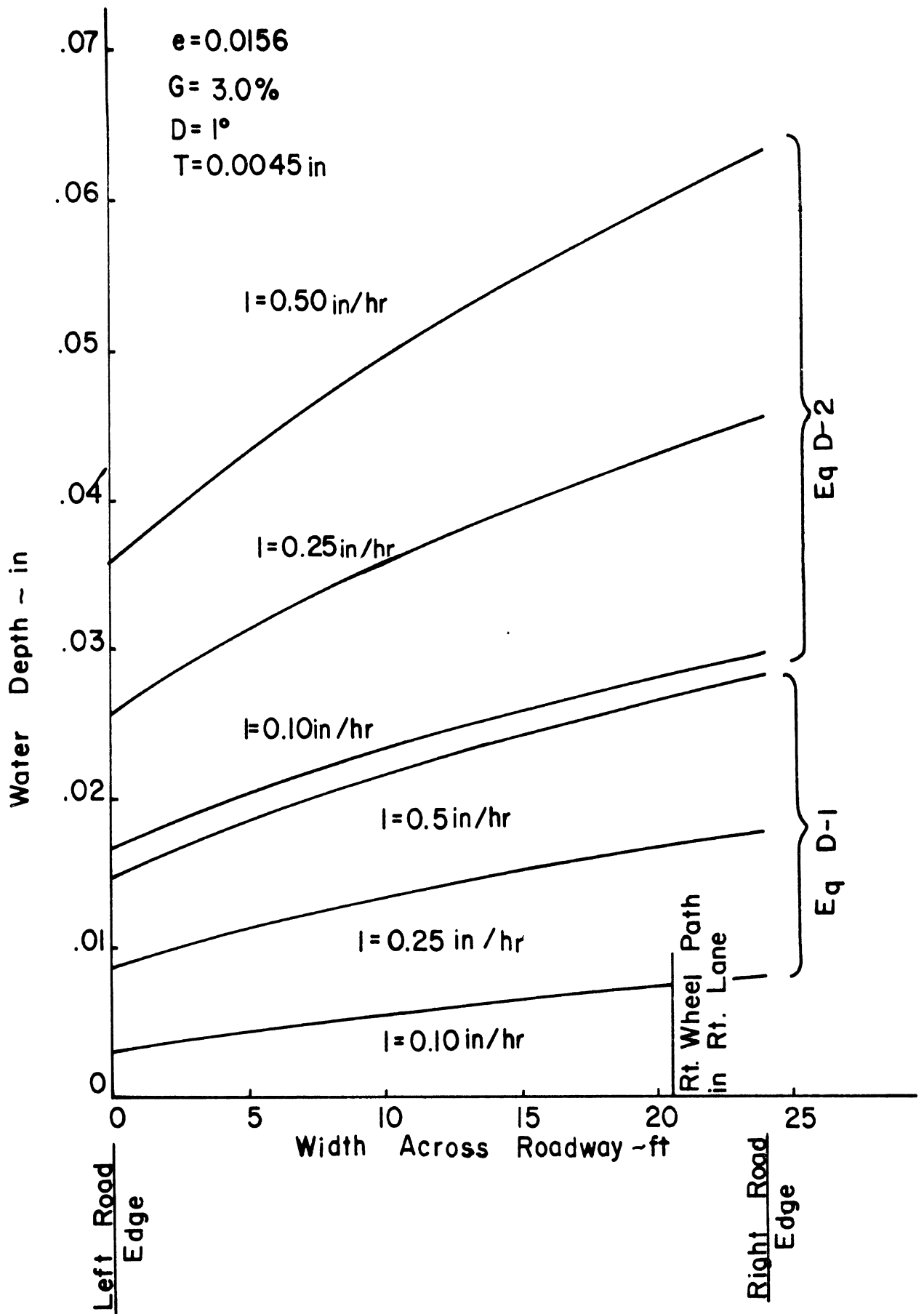
Figure D-3. Water Depth vs. Road Width for Various Rainfall
Rates Between M.P. 166.4-166.6 on Existing
Westbound Ohio Turnpike.

363

July 29, 1970, a thunderstorm occurred between 1505 and 1525 EDT. The total precipitation accumulated during the period from 1500 to 1600 EDT was 1.26 inches of rain. The rainfall rate during the twenty-minute interval of the storm, therefore, was roughly three times this value or about 3.75 in/hr.) It can be noted on Table D-3 that hourly rainfall accumulations of less than 0.1 inch are the most frequent during the accident events that have occurred at the site. There is only one case where the accumulation was greater than 0.25 inch, and in that case the accumulation was 1.26 inch.

Rainfall intensity classifications, typical yearly duration, and visibility restrictions are given in Table D-7 (5, 25, 26). Note that rainfall rates on the order of one inch per hour and above are very uncommon. Further, for rainfall rates of 0.8 in/hr and below, there is little impairment to driving in terms of visibility restrictions. Drivers would not be expected to reduce speed, therefore, on the basis of visibility alone.

Returning now to Figure D-3, the specific site parameters used in Equations (D.1) and (D.2) are listed as follows:

$$G = -3.0\%$$
$$e = 0.0156$$
$$T = 0.0045 \text{ in.}$$

Table D-7

Rainfall Intensity Experience

Condition	Intensity (in/hr)	Typical Yearly Duration (hr/yr)	Restrictions to Driving
Drizzle	<0.01 (Trace)	32	None
Light Rain	0.04 - 0.20	20	None
Moderate Rain	0.25 - 0.50	16	Very slight visibility reduction
Heavy Rain	0.60 - 0.80	13	Slight visibility reduction
Heavy Downpour	1	1.1	Moderate visibility reduction
Very Heavy Storm	4	0.4	Greatly reduced visibility

It is evident that the two separate equations yield results which are different by an approximate factor of two or three—Equation (D.2) predicting the deeper water depths. (The reason for the water depths not starting at zero at the left road edge is that there is a paved, ten-foot superelevated shoulder on the left, or median, side of the road.) The effect that these water depths have on driving safety can be examined by considering the reduction in tire traction at the site as a function of water depth.

D.4.2.1.3 <u>Pavement traction characteristics in</u> <u>wet weather</u>. Figure D-4 consists of several curves of velocity versus water depth for fixed values of brake force coefficient, BFC (<u>5</u>). The data are for a 5.20 x 10 cross-ply tire which has been worn smooth and for a "smooth" concrete surface. In terms of surface texture, the surface is very much like that at the subject site. The curve at the upper right represents the hydroplaning characteristics of the tire on the surface. Note that complete hydroplaning—the situation where the tire lifts off the surface and spins down (i.e., stops rotation)— does not occur for water depths of less than about 0.13 inch at typical highway speeds. At 60 mph, however, the water depth need only be 0.02 inch to produce a BFC of 0.10—a value well below that which is needed for safe driving. To produce a BFC of 0.4, the water depth must
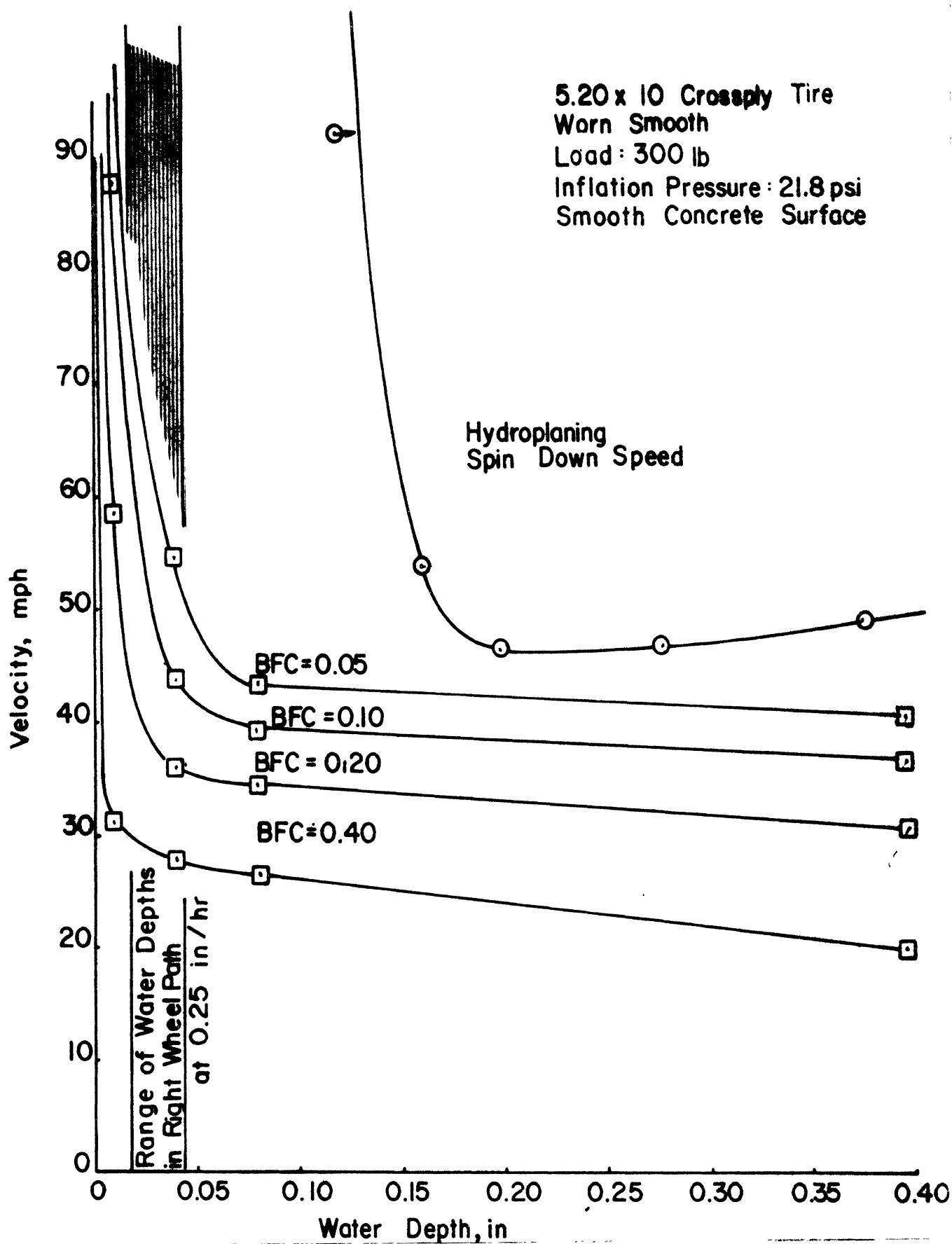
Figure D-4. Smooth Tire Traction Characteristics

367

be well below 0.005 inch at ordinary turnpike speeds. It is clear from this isolated case of a particular worn tire, then, that dangerously low friction levels can occur at the subject site under relatively common rainfall conditions. Complete dynamic hydroplaning is not very likely, however, unless uneven surface undulations create water depths somewhat deeper than the average values.

Similar data for a fully treaded tire of the same construction and tested under the same conditions are shown on Figure D-5. This tire will not hydroplane for water depths less than 0.17 inch. Further, a BFC of at least 0.2 can be realized at 70 mph for a water depth of 0.04 inch. Water depths must still be below 0.01 inch, however, to produce a BFC value of 0.4 at ordinary turnpike speeds.

It is interesting to compare the traction properties of the subject site with a tangent section on the Turnpike. Whereas on crowned tangents the drainage path length is at most twelve feet, this length is a maximum of 34 feet at the subject curve. Further, since the pavement is super-elevated at a rate which is the same as that of the crown slope, water depths during commonly occurring rain showers are roughly double those which occur on tangent sections. Since water depth is a critical factor in tire traction, it is clear that the friction available for emergency
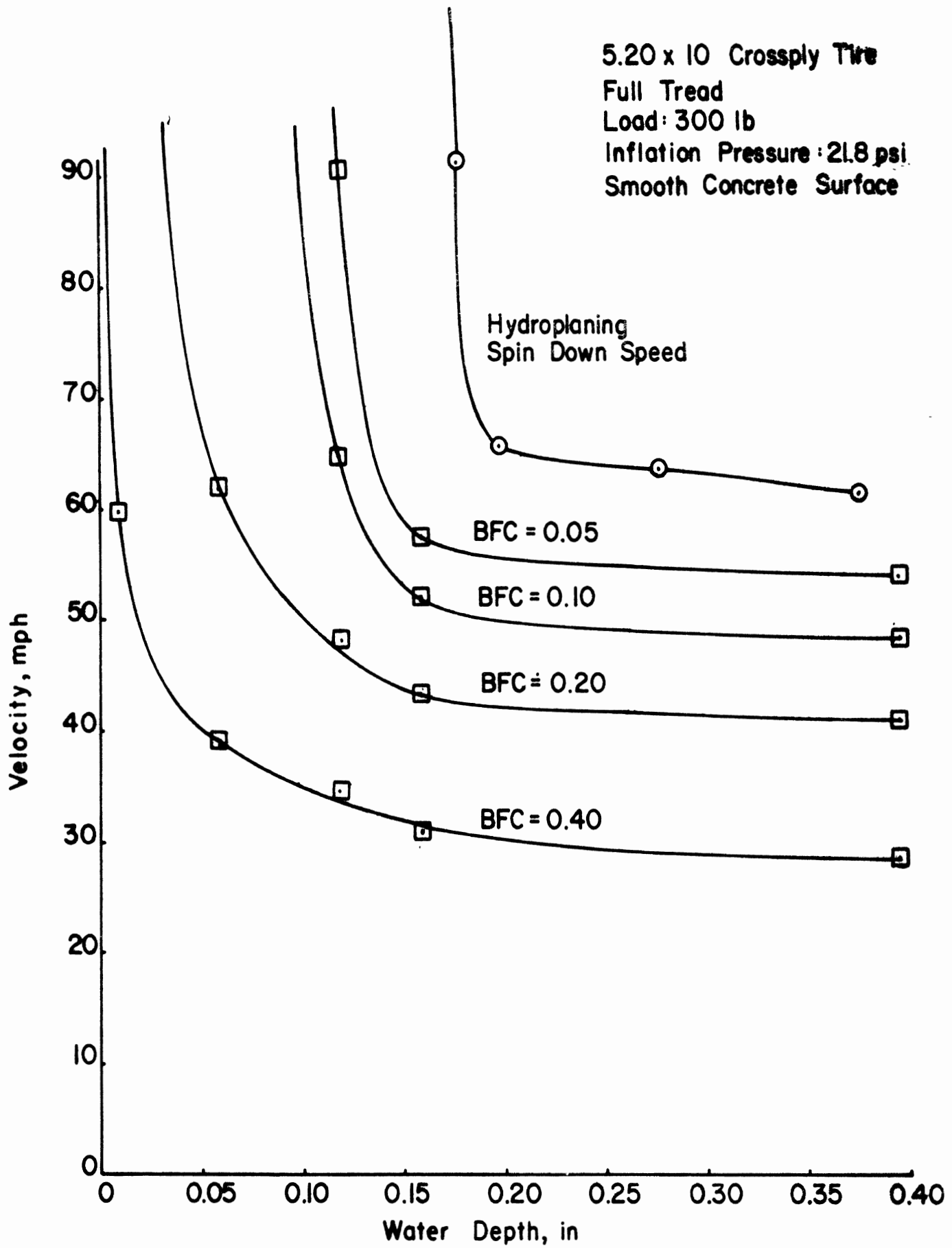
Figure D-5. Full-Tread Tire Traction Characteristics

369

maneuvers at the site is somewhat below that available on a corresponding tangent section. The comparative situation can be easily demonstrated by referring to Figures D-3 and D-5. Using the experimental data that were used to construct Figure D-5, BFC values versus water depth are replotted on Figure D-6 for constant values of velocity. The data on Figure D-6 are for a fully-treaded tire. Similar data for a smooth tire are plotted on Figure D-7. With Figures D-3, D-6, and D-7, then, a comparison between traction losses at the subject site as compared to that available on a tangent are given in Table D-8. For vehicles traveling at ordinary highway speeds with fully-treaded tires, there is a loss of .05 or 0.6 in BFC on the subject curve. Since the BFC values were measured with a skid trailer (5), the numbers can be equated to a skid number loss of 5 or 6. The loss for smooth treaded tires is not as great, but it should be kept in mind that the operating levels of skid resistance are already well below safe levels.

The tire data used in this subsection obviously do not include all tires in common use on the Ohio Turnpike. Comprehensive tire data showing the relationship between traction, water depth, and surface characteristics do not exist and if available would constitute an entire report in itself. However, the data used are believed to be
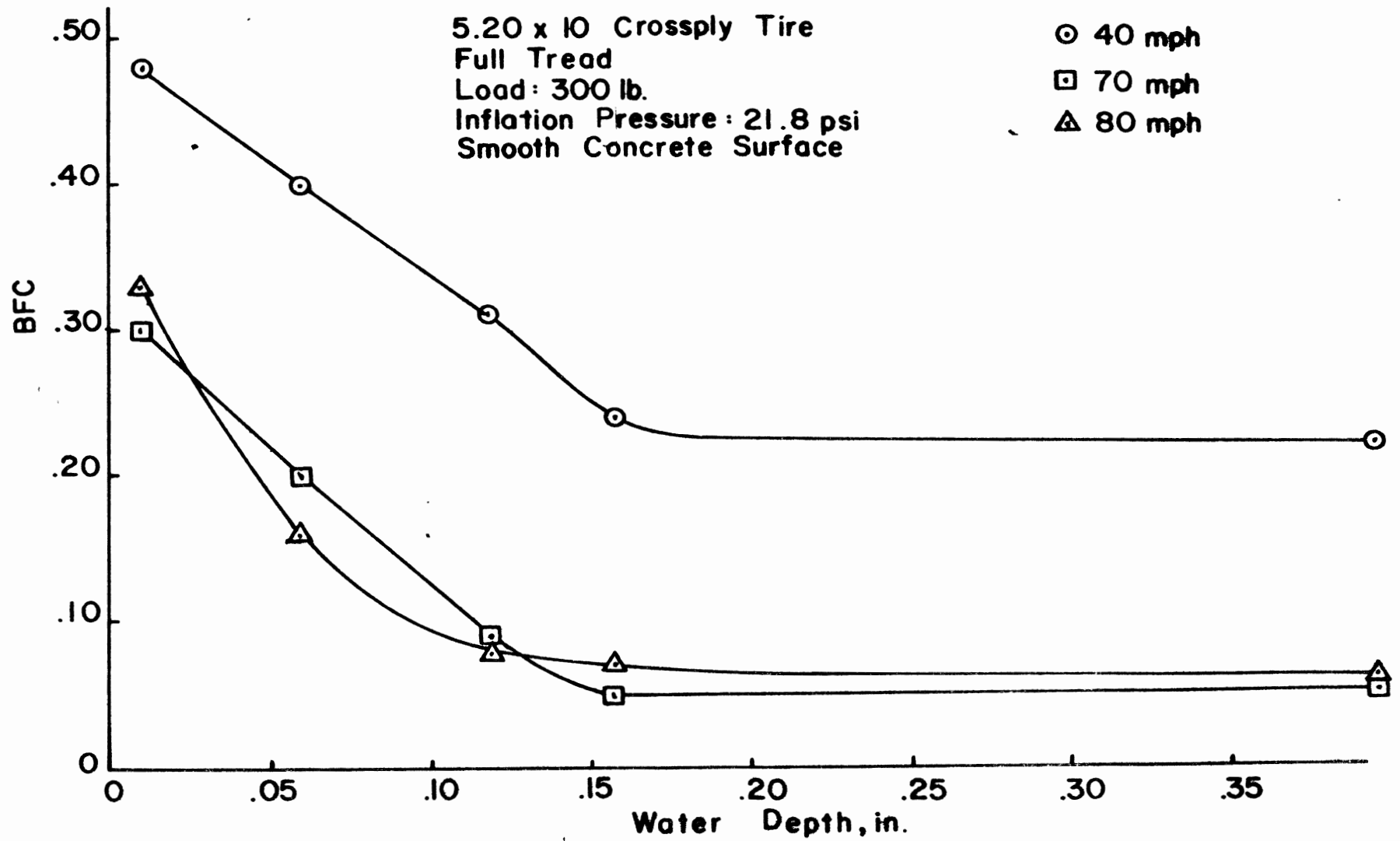
Figure D-6.   Brake Force Coefficient as a Function of Water Depth - Fully Treaded Tires
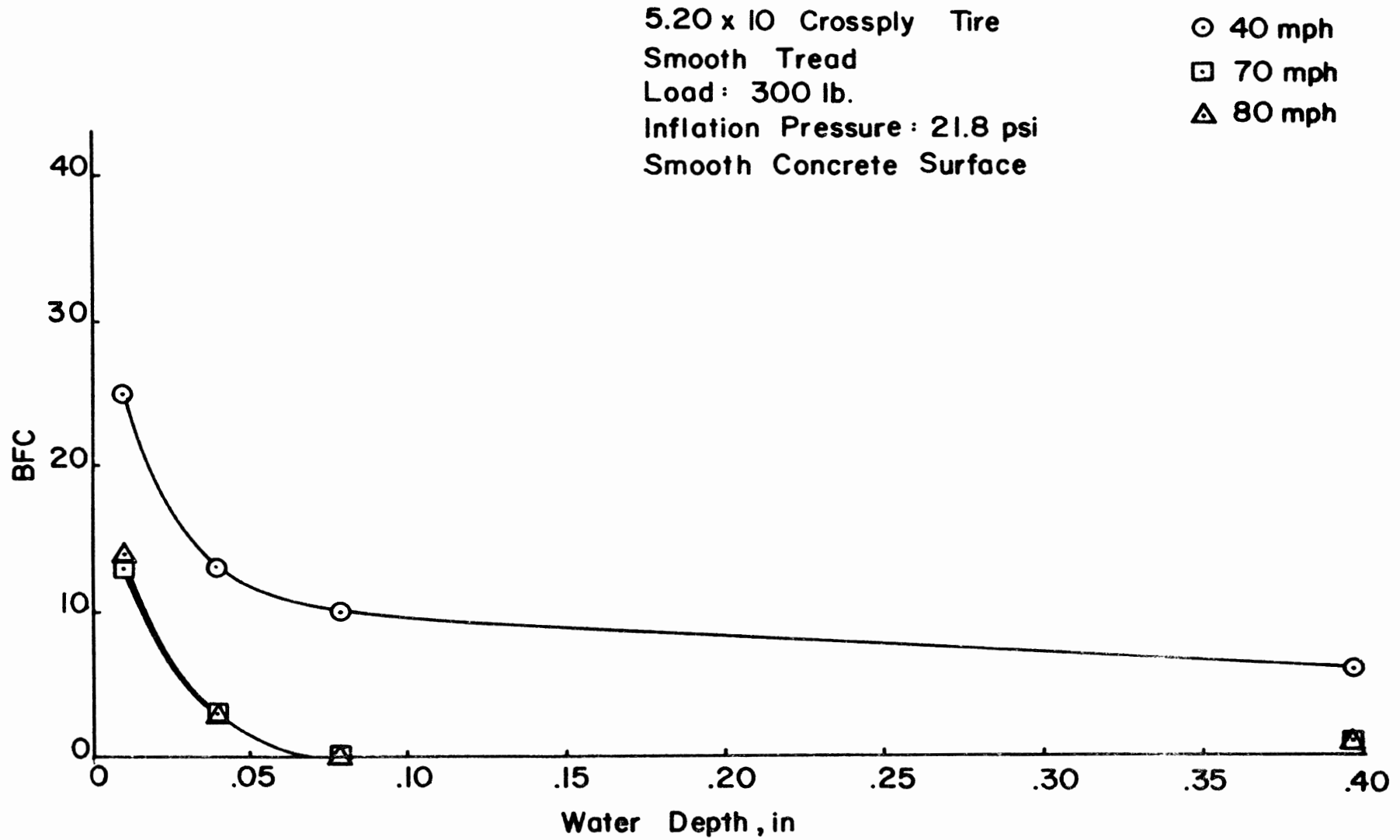
Figure D-7.   Brake Force Coefficient as a Function of Water Depth –
Smooth Treaded Tires

Table D-8

Ohio Turnpike Site Friction Losses Due to Water Depth
As Compared to a Tangent Section

Velocity mph	Water Depth-Tangent, in.[1]	Water Depth Curve Site, in.[2]	BFC Tangent		BFC Curve		Δ BFC	
			Full Tread[3]	Smooth Tread[4]	Full Tread[3]	Smooth Tread[4]	Full Tread	Smooth Tread
40	.028	.046	.45	.157	.42	.119	.03	.038
70	.028	.046	.27	.052	.23	.018	.05	.034
80	.028	.046	.26	.056	.20	.018	.06	.038

[1]Data taken from Figure D-3 for an 0.25 in/hr rainfall rate as predicted by Equation (D.2), for a road width of twelve feet (two feet on the abscissa of Figure D-3, since a ten-foot paved shoulder is assumed on the Figure).

[2]Same as 1, except that road width is 34 feet (24 feet on the abscissa of Figure D-3).

[3]Taken from Figure D-6.

[4]Taken from Figure D-7.

representative of traction conditions that exist at the subject site during wet weather. Additional data showing the influence of water depth, tire load, tire construction, tread width, tread depth, and surface characteristics can be found in References 5, 26-30. The material given in these references supports the remarks presented here.

D.4.2.2 Other Accident Causation Factors. Other possible accident causation factors at the site include wind effects, signing, geometrics, and sight distance. These additional causation factors can be generally dismissed with the possible exception of wind effects. Beyond the Ridge Road overpass at M.P. 167.77 the site is essentially free of sight distance obstructions, with the minimum sight distance no less than 900 feet. As mentioned earlier, there are no signs in the region of the site and none are evidently needed. Geometrics are of little concern, since the site consists of a gentle one-degree curve ranging through an increment of 39° with 200-foot spiral transitions at each end. Wind effects, on the other hand, may be a contributing causation factor.

Accident reports from the site list only one case where wind was listed as a factor. Nevertheless, the site is located in an area where the roadbed is some 60 feet above the surrounding terrain and the terrain is generally

hilly and uneven. Although wind records at Cleveland
Hopkins Airport (some nine miles distant) indicate winds
above 15 kn. are infrequent, winds at the site could be
substantially different—both in direction and velocity.
Further, automobile aerodynamic data, as shown on Figure
D-8, indicate a consistent tendency for the lift on a
vehicle to increase as the direction of the relative
wind varies from head-on to an approximate 30° yaw angle
(31, 32). The net increase in lift due to a cross-wind

Figure D-8. Variation of Aerodynamic Lift Coefficient
with Yaw Angle, Ψ

can be greater by as much as a factor of four. For a passenger car, this increase in lift can reduce the downward force—exerted by the vehicle on the road—by as much as 400 lb. for a vehicle traveling at 80 mph in a 25-knot cross-wind. These conclusions are illustrated on Figure D-9, which is a plot of change in lift versus cross-wind velocity for traveling speeds of 40 mph and 80 mph. A lift force of 400 lb. can reduce the effective coefficient of friction at the tire/road interface by as much as 0.1. Adverse cross-wind conditions, then, could substantially reduce the available traction at the site as the result of aerodynamic lift.

In addition to aerodynamic lift, the side force on the vehicle is also substantially affected by cross-winds. For most automobiles, the aerodynamic side force increases linearly with the angle of the relative wind (31) (see Figure D-10). A typical relationship between side force and cross-wind velocity for vehicle speeds of 40 mph and 80 mph is shown on Figure D-11. Clearly, a side force resulting from a cross-wind may either help or hinder a vehicle in a cornering maneuver. The wind-produced side forces indicated on Figure D-10 may require an increment in friction coefficient as large as 0.08 to compensate for wind effects.

376
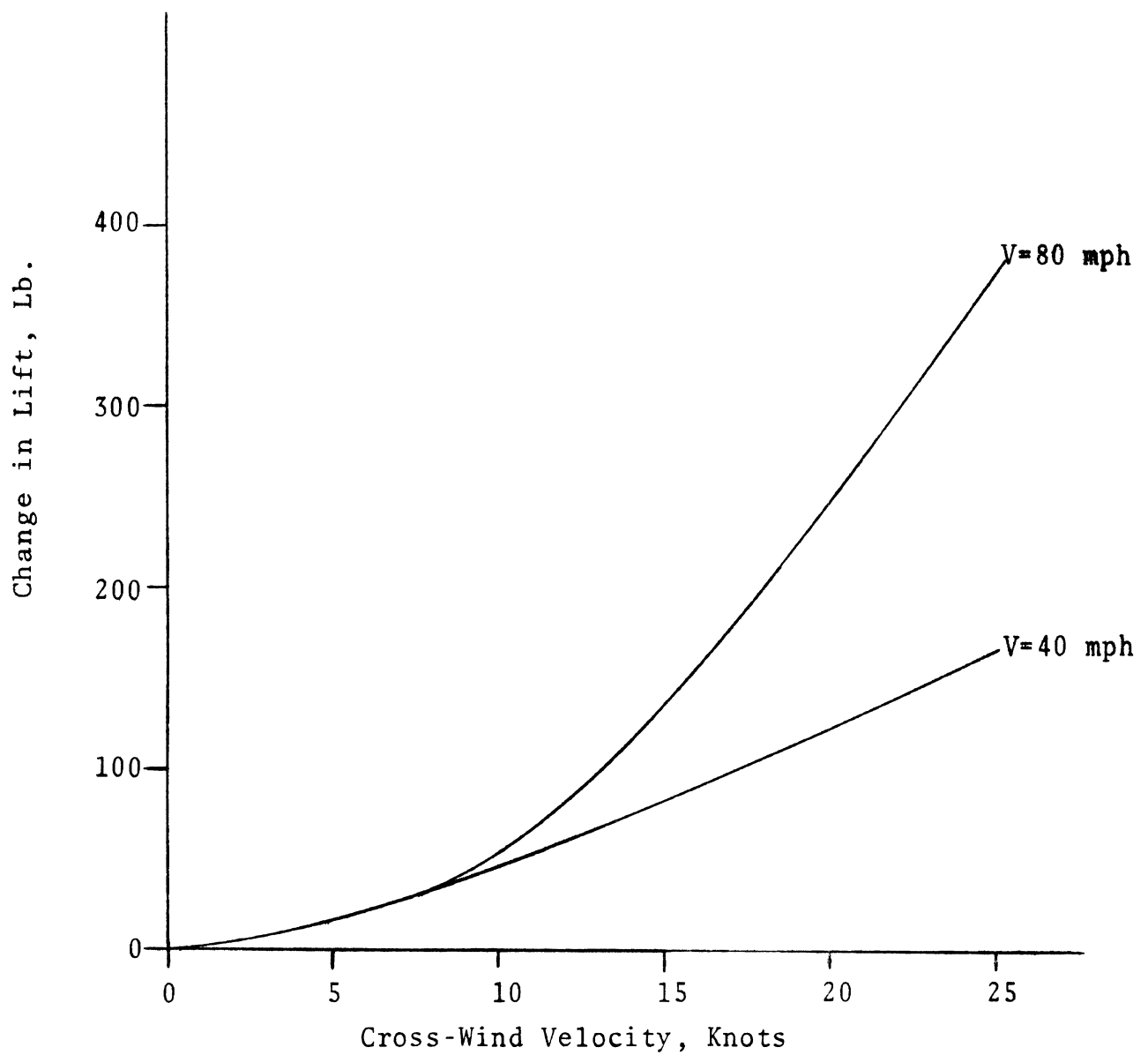
Figure D-9. The Influence of Cross-Wind on Aerodynamic Lift
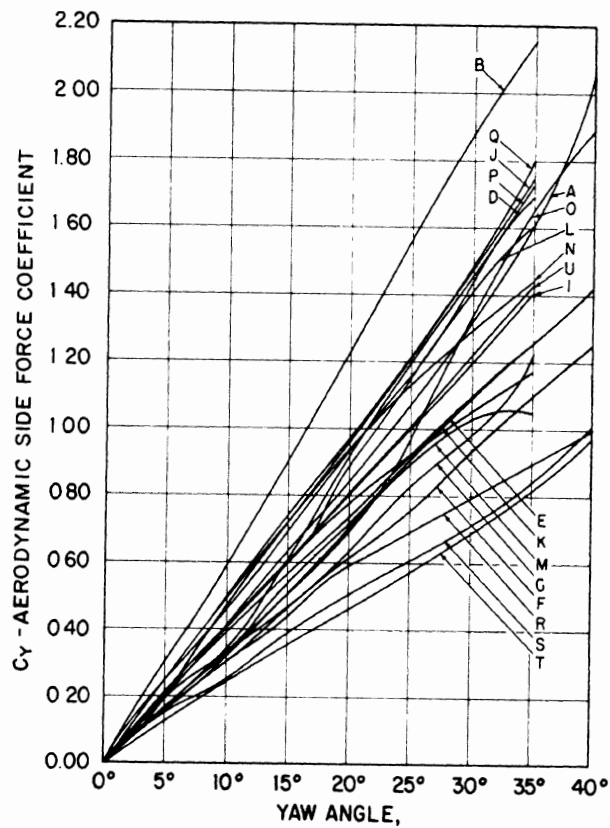
Figure D-10. Variation of Aerodynamic Side Force
Coefficient, C_Y, with Yaw Angle, Ψ

Aerodynamic lift and side force effects, then, can
have a substantial effect on the cornering performance of
a vehicle. Aerodynamic forces can also produce yawing,
rolling, and pitching moments on a vehicle, and in this
way can affect general handling performance. Aerodynamic
effects are not large, however, unless the cross-winds are
on the order of 15 knots or greater.

378
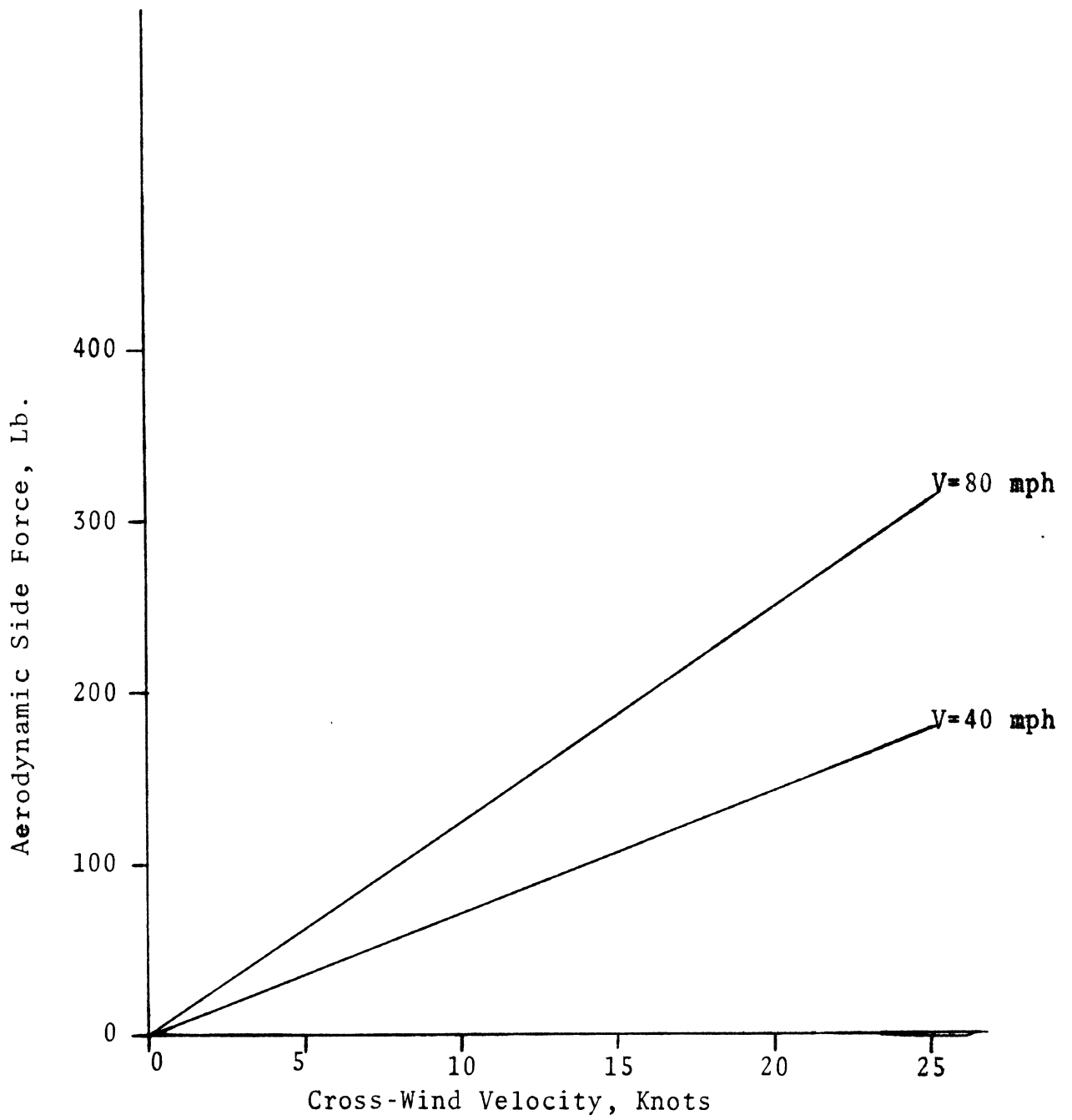
Figure D-11.   The Influence of Cross-Wind on Aerodynamic
Side Force

The wind data given in Table D-2, as measured at Cleveland Hopkins Airport at the time of the accident, is summarized on Table D-9. Of the 54 accident cases where wind data was available, nine (17%) had winds in excess of 15 kn. Twenty-five of the 54 were cross-winds—sixteen from the south and nine from the north. Five of the 25 cross-winds were greater than 15 kn. Nineteen of the accidents occurred in the presence of both cross-winds and wet pavement. This number is just under one-half of all of the wet pavement accidents. For the one accident where wind was listed as a contributing factor, the wind was recorded as being from the north at a velocity of 17-18 kn.

Although there is little indication from the accident records that wind is a major accident-causation factor at this site, the high frequency of occurrence of combinations of cross-winds and wet pavement suggests that wind is a possible aggravating effect. However, the wind data from Cleveland Hopkins Airport can only be considered as an indication of wind conditions at the site. The irregular nature of the local terrain, the nine-mile distance from the Airport to the site, and the 60-foot elevation of the roadway above the surrounding land would all tend to alter the wind patterns at the site as compared to those at the airport. Much better wind data is needed at the site, then, before specific conclusions can be

Table D-9

Wind Statistics as Recorded at the Time of the
Accident—Ohio Turnpike Site

		Wind Velocity[1], Kn.					
		0-5	6-10	11-15	16-20	21-25	Totals
All Winds		3	23	19	7	2	54
Cross[2] Winds Only	North	2	2	3	1	1	9
	South	0	7	6	2	1	16
Cross Winds + Wet Pavement	North	1	0	1	1[3]	1	4
	South	0	6	6	2	1	15

[1]Wind velocities and directions as measured at Cleveland Hopkins Airport.

[2]The roadway at the Ohio Turnpike site so that cross-winds are taken to be in the north or south direction.

[3]The accident corresponding to this wind condition was the only one noted to be influenced by wind.

drawn concerning the need for remedial measures.
Recommendations for obtaining such data are given in
Section D.4.4 and in Chapter 4.

D.4.3 SUGGESTED SITE MODIFICATIONS. The major
problem which can be clearly identified at the Ohio Turn-
pike site is inadequate wet-weather traction. There are
several controlling factors which can be altered to achieve
better traction. Some of these are:

1. Regulate the tire tread depth of vehicles
    using the freeway during wet weather and
    refuse access to those vehicles with
    insufficient tread.

2. Enforce reduced speed regulations at the
    site.

3. Improve the pavement drainage.

4. Roughen the surface to achieve a higher
    level of surface friction.

The results achievable by implementing Items 1 and 2 can
be ascertained from Figures D-4 and D-5 and need no
further discussion. The safety implications involved in
applying Items 3 and 4 are discussed in the following
subsections.

D.4.3.1 <u>Improving the Pavement Drainage</u>. Pavement
drainage at the Ohio Turnpike site can be improved by:

1.   Increasing the superelevation rate.

2.   Reducing the drainage path length.

3.   Providing additional drainage paths which
     reduce surface water accumulation.

As indicated in Appendix C the major roadway geometric
factors that influence drainage on an impervious surface
are road width and superelevation. The influence of grade
is not large, since increasing grade increases both the
overall slope and the drainage path length. The former
tends to decrease the water depth, while the latter
tends to increase it, with the overall result that the
two tend to cancel. In summary, then, superelevation
and pavement width are the major geometric factors con-
trolling water depth, while other factors such as grade
and surface texture have a minor influence.

The reduction in water depth at the site which can
be realized by increasing the superelevation rate is
illustrated on Figure D-12. On this figure, the water
depth in the right wheel path in the traveling lane is
plotted versus superelevation rate for a rainfall rate
of 0.25 in/hr. (Based on the hourly rainfall accumulations
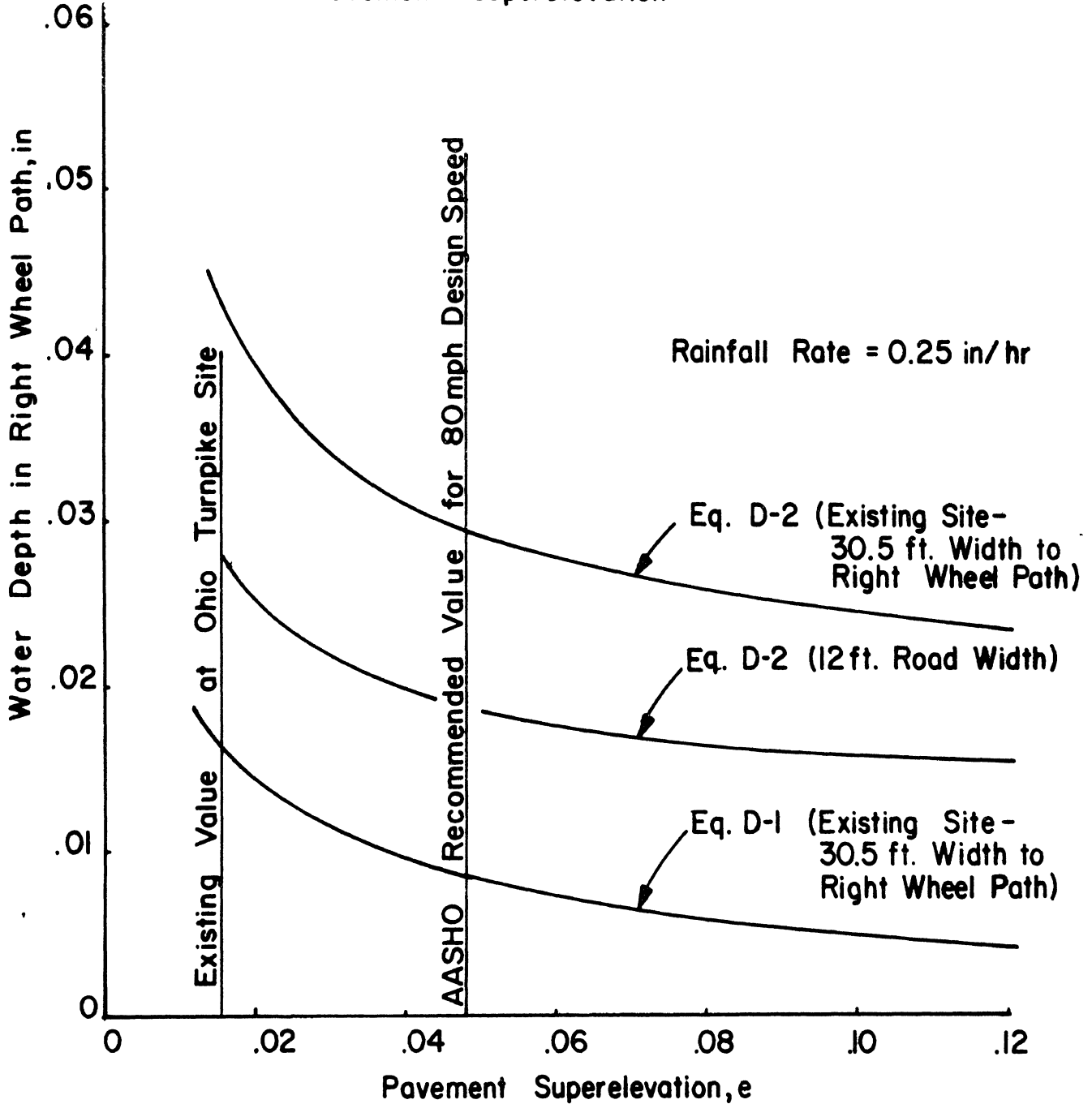
Figure D-12.   The Variation in Water Depth with Superelevation

given in Tables D-2 and D-3, a rainfall rate of 0.25 in/hr seems to be a reasonable design value for short-term conditions.) It is evident that increasing super-elevation to reduce water depths is most effective when the superelevation rates are small. This countermeasure becomes less and less effective with an increasing super-elevation rate. From Figures D-4 and D-5, it is evident that water depths must be reduced to a range of .01-.02 inch if pavement traction is to be maintained at a level approximating safe conditions. Clearly, these reduced water depths cannot be achieved by altering superelevation alone if the results from Equation (D.2) are to be believed.

An alternative solution is to combine an increase in superelevation with a reduction in drainage path length. This could be accomplished by providing longitudinal drains, flush with the pavement surface, at both the middle and left edge (high side of the curve) of the road. If this were done, the water depth at these locations would be effectively zero. Thus, the maximum drainage path length in either traffic lane would be twelve feet, or 8.5 feet in the right wheel path. Equation (D.2) is replotted on Figure D-12 for a twelve-foot drainage path length. Using a depth of between .01 and .02 as acceptable, a superelevation rate of .06 combined with

385

flush longitudinal drains in the middle and left edge of the pavement would represent an effective means of reducing water depths (and thus improving traction) without resorting to other remedies.

A second set of alternatives, which does not involve the use of special drains, is to provide some means of ensuring that rainfall runoff flow takes place at a level below that of the tire surface contact. Three methods might be used for this purpose:

1. Add an open textured weaving course with fairly large, sharp aggregate such that water can drain between the surface asperities. The large, sharp aggregate will increase pavement friction as well as improve drainage.

2. Add a porous wearing course such that surface water can drain down through the pavement itself (33).

3. Groove the pavement in a cross-hatched pattern to allow water to drain off below the ungrooved surface (34). The transverse grooves will enhance sideward runoff flow and improve braking friction, while the longitudinal grooves will increase sideward friction properties.

Of these three methods, adding a wearing course with large, sharp aggregate is probably the most practical. A porous pavement overlay would probably act effectively for a time, but such surfaces have been found to wear excessibly and to be susceptible to freeze-thaw degradation. Grooving in a cross-hatched manner is an attractive alternative if it can be done on an overlay surface at the site. Currently, the surface material is a bituminous type which makes grooving difficult. Further, although grooving would very likely reduce surface water depths, at the present time no data is known to exist on the subject. If one of these methods is used such that a new wearing course is added at the site, care should be taken to ensure that the pavement is superelevated at as high a rate above 0.06 as is considered practical.

D.4.3.2 Improving Pavement Friction. If it is assumed that 80 mph is a reasonable design speed for the subject curve, the average steady-state side force factor, f, which must be generated by vehicles traveling the curve can be determined from the AASHTO curve design equation (2):

$$f + e = \frac{V^2 D}{85,944} \tag{D.4}$$

where

$$V = \text{vehicle speed, mph}$$

$$D = \text{degree of circular curvature, deg.}$$

For D = 1°0', e = 0.0156 and V = 80 mph, the side friction factor is 0.059. As discussed in Appendix B, it would be erroneous to assume that a value of f of .059 is all that is needed to negotiate the curve.

Much evidence has shown that vehicles often follow a path of much greater curvature than that of the roadway (35). Further, no consideration is being given to the fact that a vehicle may be required to make a non-steady-state maneuver. If, for example, a vehicle were following a 3° curved path while making a lane-change passing maneuver at the site, then the required value of f would be about .21. For other kinds of maneuvers which are occasionally necessary, the friction requirements can be far greater. These considerations are thoroughly discussed in Appendix B.

It might be argued that lane changes and other kinds of emergency maneuvers are relatively common and that these maneuvers are as frequently required on tangents as on curves. This is very probably true. With standard AASHTO curve design practices, however, the friction available on a tangent, given that the surface friction is the same in each case. On a curve, a portion of the available friction—the f term in Equation (D.4)—must

be used for steady-state cornering and is thus not available in emergency conditions.

It is clear, then, that a surface of greater friction is needed on highway curves when the centrifugal force is not balanced by the superelevation. Complicating this requirement is the fact that the friction surface on a curve tends to wear away faster because of the required vehicle cornering forces. Further, drainage is less efficient due to a longer run-off length and thus traction is reduced still more.

Equation (15) (see Chapter 3) can be used to compute the required SN_{40} value for the site as it now exists. Using the following information:

$$SN_{40T} = 34 \qquad\qquad e = 0.0156$$

$$V = 80 \text{ mph} \qquad SN_{grad} = -0.5 \text{ SN units/mph}$$

$$G = 3\% \qquad\qquad \text{Tire Tread Depth} = 2/32 \text{ in.}$$

$$D = 1° \qquad\qquad L = 30.5 \text{ ft}$$

$$I_D = 0.25 \text{ in/hr}$$

then,

$$S = 0.0338 \qquad K(\frac{L}{e}) = 2,460$$

$$K = 1.26 \qquad\qquad SN_D = 7$$

$$T_F = 0.50$$

and the equation gives a required SN_{40} value of 92. Thus, the site as it presently exists would require an impractically large value of skid resistance to be made safe for wet-weather travel. If a pavement overlay is added at the site, such that the superelevation is made to be 0.060, then the SN_{40} value need only be 65. Further, if tire tread depth is regulated to be 3/32 in. rather than 2/32 in., then the required SN_{40} value can be reduced further to 57. The long drainage length at the site frustrates any attempt to make the skid number requirement anywhere near what is needed on a tangent section, however. Thus, if a paved superelevated shoulder is to be used at the site (and there is good evidence to support the use of such shoulders), then an additional increment in skid resistance will be required.

D.4.3.3 <u>Wind-Related Improvements</u>. As suggested earlier, wind may also be an accident-causation factor at the site. It may be necessary to provide wind screens at the site to shield the traffic from effects of cross-winds. Before these measures are implemented, however, a program should be undertaken to measure the wind profiles at the site.

D.4.4 SUMMARY OF ANALYSIS OF OHIO TURNPIKE SITE. The most clearly identifiable factor responsible for the high incidence of wet-weather accidents at the Ohio

Turnpike is that of poor water drainage. The drainage
path length on the curve at the site is roughly three
times that of crowned tangent sections. Water depths
during wet weather are about twice as deep. If it is
assumed that the brake force and cornering force coeffi-
cients are affected similarly by water depth, approximately
5 or 6 skid number units are lost at the site during
rainfall rates of 0.25 in/hr at typical turnpike speeds.
An additional 5 or 6 units are needed just to negotiate
the curve in a steady-state manner in order to balance
the centrifugal forces produced during cornering. The
result is that 10 to 12 skid number units are needed to
negotiate the curve during wet weather over and above
that needed on tangent sections. Since the SN_{40} value at
the site is very probably no more than 40, the skid
number at turnpike speeds is likely to be less than 20.
Thus, almost <u>half</u> of the available friction is being used
just to travel the curve in a steady-state manner—if
a vehicle is equipped with fully treaded tires. If
something other than steady-state cornering is required—
e.g., a lane change is required, or gusting cross-winds
are present—it is readily apparent that the available
friction can be exceeded and skidding will result. The
situation is yet worsened if mild surface unevenness is

present at the site, since local undulations can produce water depths at least twice as deep as the average values shown on Figure D-3.

With worn tires the friction margin is very probably non-existent. During wet weather, then, vehicles with smooth tires, traveling at the speed limit, are likely to be confronted with loss-of-control problems while routinely negotiating the curve. Loss of control with fully treaded tires is more likely the result of braking, lane changing, wind gusts, or combinations thereof.

Suggested remedies include (1) enforcing a lower speed limit at the site; (2) restricting turnpike access during wet weather to vehicles with tires of adequate tread depth; (3) adding a pavement overlay to increase the curve superelevation to .06; (4) grooving the pavement in a cross-hatched manner to improve drainage, or if this is impractical, adding a pavement overlay with large, sharp, exposed aggregate; (5) ensuring that the surface friction at the site is compatible with site geometry, site drainage conditions, and existing tire regulations.

D.5 INDEPTH EVALUATION OF THE I-95 SITE NEAR FREDERICKSBURG, VIRGINIA

A simplified plan and profile drawing of the I-95 site near Fredericksburg, Virginia is shown on Figure D-13 (36). In the southbound lane the roadway curves from an
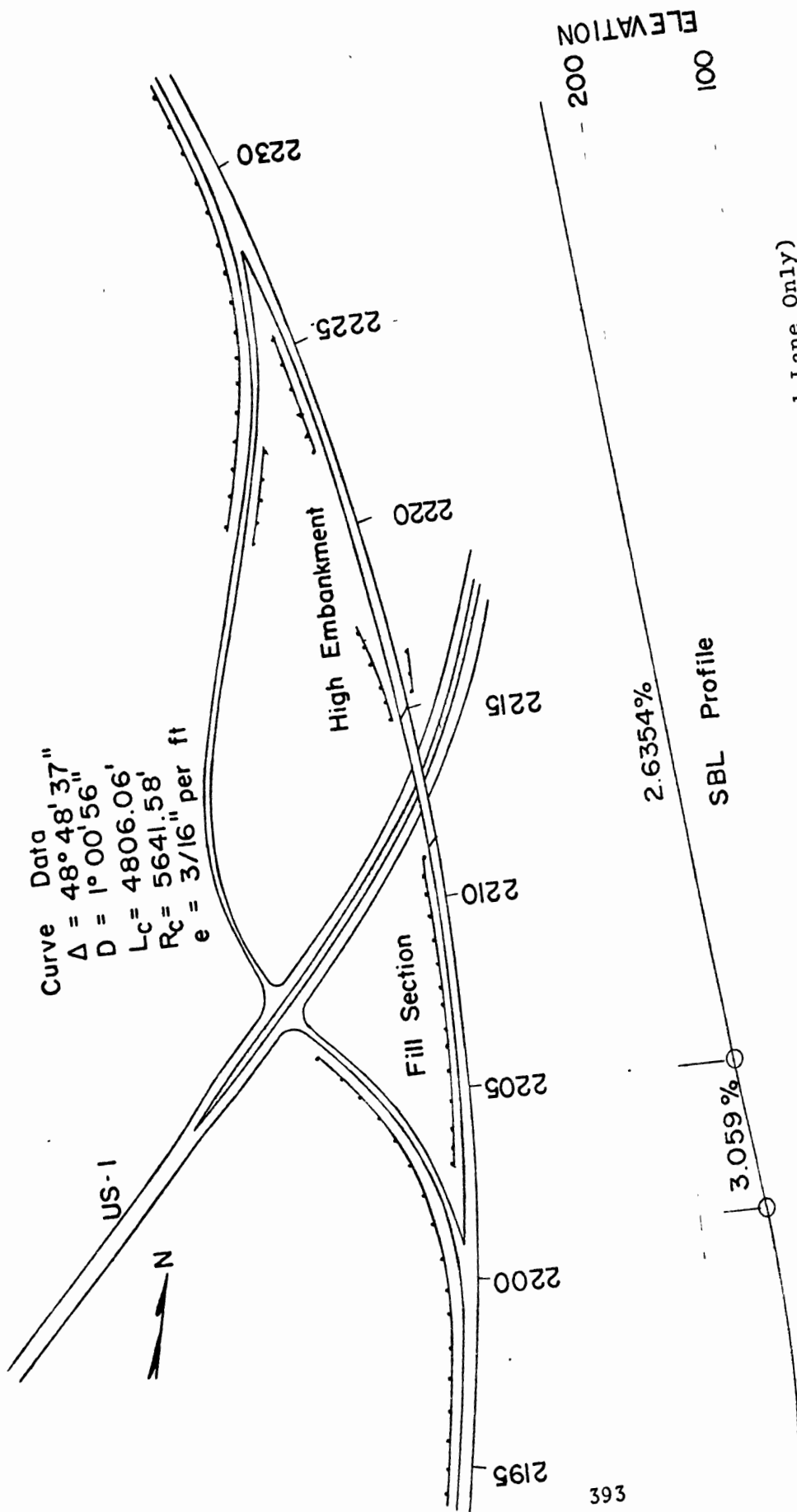
Figure D-13. I-95 Site Near Fredericksburg, Virginia (Southbound Lane Only)

Curve Data
Δ = 48° 48' 37"
D = 1° 00' 56'
L_c = 4806.06'
R_c = 5641.58'
e = 3/16" per ft

High Embankment

Fill Section

US-1

N

ELEVATION

200

100

2.6354%

3.059%

SBL Profile

2230
2225
2220
2215
2210
2205
2200
2195

393

approximate southeasterly direction to a direction approximately due south. Data for the curve are shown on the figure. (Note that there are no transition curves.) In the general area of the site, the natural terrain gradually slopes downward from north to south. There are embankments along the western edge of the southbound lane between Station 2234 and the exit to U.S. 1 (about Station 2224) and between the exit gore (about Station 2223) and the north end of the bridge (Station 2215). I-95 is elevated about 20 to 25 feet above the surrounding terrain from the south end of the bridge (Station 2211) to the entrance ramp (Station 2200).

The roadbed grade is about 2.6% downward from Station 2240 south to Station 2210. There is a grade transition beyond this to Station 2206 which is just south of the bridge. The grade then becomes about 3.1%. The grade remains downward at 3.1% until Station 2201, where a sag curve begins and the grade turns upward. The change from 2.6% slope to 3.1% slope occurs about 600 feet north of the entrance ramp from U.S. 1.

A typical cross-section of the road is shown on Figure D-14. Note that the paved shoulder on the high side of the curve is not superelevated, as was true at the Ohio Turnpike site.
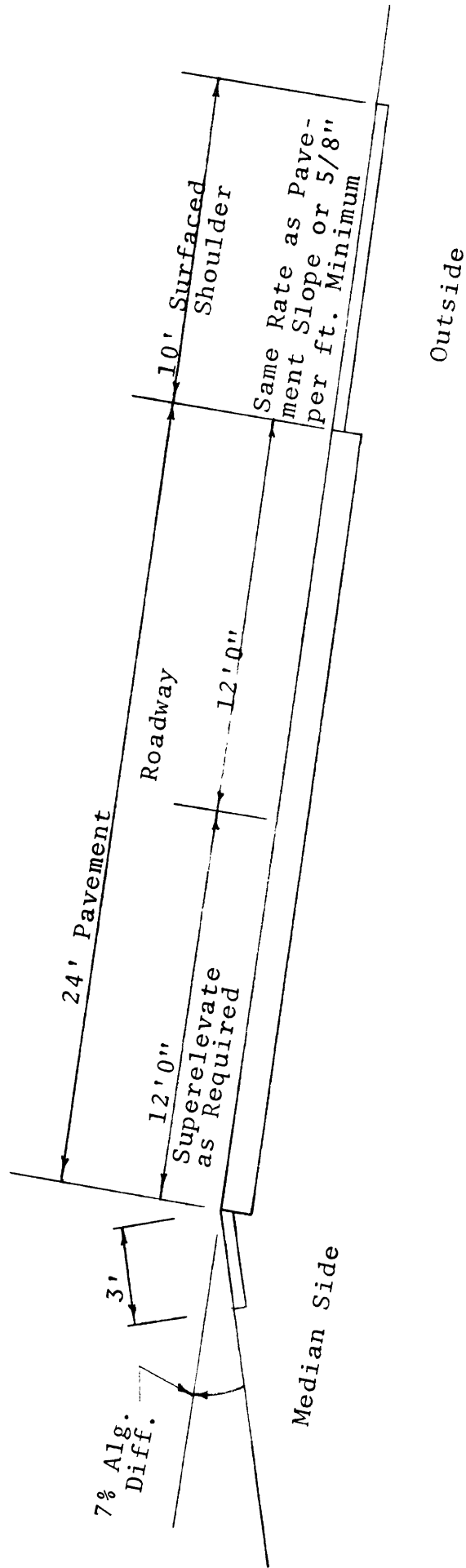
Figure D-14. Typical Roadway Curve Cross-Section – I-95 , Virginia

The road paving material is P.C. concrete. The site was grooved June 27, 1972, between Stations 2176 + 14 and 2238 + 44. The grooves are 1/8" x 1/8" on 3/4" centers.

Guardrail installations along the site are indicated on Figure D-13.

There are approximately fifteen signs of various types along I-95 at the interchange. These will be discussed as appropriate in later subsections.

D.5.1 I-95 SITE ACCIDENT DATA ANALYSIS. A summary of the accident data statistics at the I-95 site is given on Table D-10. The accidents listed are only those which occurred on I-95 itself. Of the 133 accidents occurring at the site, 51 or 38% occurred during wet weather. Seventy-four or 59% of the accidents involved vehicles running off the road and hitting fixed objects. Forty-four or 33% involved rear-end or side-swipe accidents.

The effects of worn tires on wet-weather accident causation cannot clearly be ascertained. The data indicated were obtained from accident reports for those specific accidents which occurred during wet weather. (Only the wet-weather accident reports were obtained due to the large total number of reports involved.) The tire

TABLE D-10

ACCIDENT DATA SUMMARY

SOUTHBOUND I-95 NEAR FREDERICKSBURG, VIRGINIA
1000 FEET BEYOND BEGINNING AND ENDING OF SPEED CHANGE LANES
AT INTERCHANGE WITH U.S. 1
December 18, 1964 to June 26, 1972

Year	Total	Wet	Pavement Condition Dry	Snow/Ice	Smooth Tires	Skidding L.O.C. Wet Surface	Side Swipes	Rear Ends	Fixed Object	Other Causes	Hourly Rainfall Accumulation <.10 in/hr	.10-.25 in/hr	>.25 in/hr	Accident Location on I-95 Before Exit	Between Exit & Bridge	At Bridge	Between Bridge and Entrance Ramp	After Entrance Ramp
1964	2	1	0	1	0	1	0	0	1	1	1	0	0	0	1	0	1	0
1965	10	3	7	0	1	0	1	2	7	10	3	0	0	3	1	0	5	1
1966	22	2	5	15	0	2	0	11	11	20	2	0	0	4	6	5	6	1
1967	14	8	6	0	2	6	0	2	9	8	7	1	0	3	4	1	4	2
1968	22	7	9	6	1	6	3	5	13	16	6	1	0	3	7	4	4	4
1969	16	3	11	2	0	3	1	5	9	13	3	0	0	5	2	0	6	3
1970	23	14	8	1	4	14	1	4	16	9	10	3	1	2	7	7	4	3
1971	13	7	6	0	0	7	2	3	6	6	3	3	1	3	5	1	0	4
1972	11	6	5	0	1	6	1	3	7	5	4	2	0	0	3	5	2	1
Total	133	51	57	25	9	45	9	35	79	88	39	10	2	23	36	23	32	19
%		38	43	19	7	34	7	26	59	66	29	8	1	17	27	17	24	15

condition data are inconclusive, since it is not clear whether tire condition was always reported on the accident records.

The hourly rainfall data for the day of each of the wet-weather accidents were obtained from the Marine Corps Air Station at Quantico, Virginia. The Air Station is located approximately 22 miles from the site. The pattern of rainfall accomulations in terms of expected rainfall rates is similar to that found at the Ohio Turnpike site. (See Table D-3.)

The majority of accidents occurred between the exit and entrance ramps, with the numbers being almost equally distributed in the areas before and after the bridge. A review of the "Collision Diagrams" (10) reveals that many of the accidents suggest indecision in weaving, merging, exiting, and entering situations.

A special study was conducted to evaluate the effectiveness of the pavement grooving project. The results of the study are shown on Table D-11. The table indicates that the total number of accidents at the site was reduced by 17% after grooving. The proportion of accidents which occurred on wet pavement was reduced from 57% before grooving to 47% after grooving, while the proportion of accidents which were loss-of-control

Table D-11

Accident Data Before and After Grooving

0.25 mi. North of Ramp to U.S. 1
0.47 mi. South of Ramp from U.S. 1
Total Length of Grooving - 0.95 mi.

Period	Total	Pavement Condition			Skidding L.O.C. Wet Surface	Other Cause	Side-Swipes	Rear[1] Ends	Fixed Object
		Wet	Dry	Snow/Ice					
Before 6/27/71-6/26/72	10	13 57%	10 43%	0	10-12 43%-52%	11-13 48%-57%	4 17%	5(7) 22%	11 48%
After 6/27/72-6/26/73	19	9 47%	10 53%	0	6-9 32%-47%	10-13 53%-68%	3 16%	7(12) 37%	4 21%

[1]Numbers in parentheses represent the total number of rear-end events. Some accident cases involved more than one rear-end collision. The percentages are given only in terms of the total number of accident cases, i.e., the numbers not in parentheses.

skidding crashes on a wet pavement went from 43-52% down
to 32-47%. The above results are all consistent with
benefits that might be expected from the grooving project.
However, none of the reductions are statistically signi-
ficant at even the 0.10 confidence level. That is, the
apparent improvements might have resulted from chance.
This failure to statistically support the hypothesis that
grooving reduced wet-surface accidents may result from
the rather low power of the test, i.e., the low numbers of
accidents available for drawing inferences.

D.5.2 ACCIDENT CAUSATION ANALYSIS. It is apparent
that wet weather is a controlling factor relative to
accident causation at the I-95 site, but not to the extent
that was true at the Ohio Turnpike site. Again, however,
pavement traction characteristics must be examined. In
addition, such factors as vertical alignment, interchange
layout, site distance, and signing are also apparently
involved. Wind may also be a factor. These matters will
be discussed, in turn, in the following subsections.

D.5.2.1 Pavement Traction Characteristics. Measure-
ments of pavement skid number made at the site with a
skid trailer (37, 38) are as follows:

Date	Pavement Condition	Traveling Lane	Passing Lane
March 1970	Prior to Grooving	54	61
9/27/73	North of Grooving Area	52	55
9/27/73	Grooved Area	53	60
9/27/73	Grooved Bridge Deck	55	62

There appears to be little difference between the grooved and ungrooved sections. Since skid trailer measurements generally represent braking efficiency, these values are not necessarily indicative of differences in cornering capability.

Surface measurements made during the present program are given in Table D-12. Discrepancies are again apparent in the various methods used to measure surface friction. A best guess is that the SN_{40} value is between 45 and 60 parallel to the grooves and between 60 and 80 transverse to the grooving.

Pavement texture depth averages between 0.010 and 0.013 in. with the results being confused by the grooving.

Pavement drainage characteristics at the I-95 site can be determined using the same methods presented in Section D.4.2.1, although the calculations are less certain because of the pavement grooving. Water drainage tests at the site, however, have shown that water does drain across the grooves on the superelevated curve and not

TABLE D-12

I-95 SURFACE MEASUREMENTS

Position	British Portable Number (BPN)[1]		Schonfeld Method Estimates			Estimated Skid Trailer SN40T			Measured Skid Trailer SN40T Parallel to Grooves		Average Texture Depth - in[1]
	Parallel to Grooves	Transverse to Grooves	SN30S	SN40S	SN50S	Based On BPN[2]		Based On SN40S	March '70	Sept. 27, '73	
						Par.	Trans.				
Right Road Edge Traveling Lane	60	83	44	40	26	46	79	46			.0117
Right Wheel Path Traveling Lane	53	71	52	48	37	36	62	54			.0104
Middle Traveling Lane	55	81	40	35	31	39	76	41	54	53-55	.0125
Left Wheel Path Traveling Lane	55	72	52	49	37	39	63	55			.0090
Left Lane Edge Traveling Lane	57	82	44	40	26	41	78	46			.0135
Right Lane Edge Passing Lane	59	83	44	40	26	45	79	46			.0132
Right Wheel Path Passing Lane	55	72	52	49	37	39	63	55			.0106
Middle Passing Lane	59	81	40	35	31	45	76	41	61	60-62	.0118
Left Wheel Path Passing Lane	55	72	52	49	37	39	63	55			.0109
Left Lane Edge Passing Lane	58	86	44	40	26	43	84	46			.0132

[1] Averaged over five sites between Stations 2195 and 2230 (See Figure D-13)

[2] Adjusted with equation $SN_{40T_r} = -41 + 1.45 \, BPN$ (23).

[3] Adjusted with equation $SN_{40T_r} = 6 + SN_{40S}$ (24)

along the grooves as might be expected. Therefore there is reason to believe that water depths as predicted by Equations (D.1) and (D.2), if nothing else, will bracket the drainage characteristics of the site.

Predicted water depths at the site are plotted on Figure D-15 for the following site parameters:

$$G = -3.059\%$$

$$e = 0.0156$$

$$T = 0.0117 \text{ in.}$$

Again, discrepancies between the predicted results from the two equations are apparent, with Equation (D.2) predicting the deeper depths. The fact that Equation (D.1) predicts negative water depths on the left road edge results from the predicted water depth being below the tops of the surface asperities.

The effect that the predicted water depths have on tire traction can be examined by referring to Figures D-4, D-5, D-6, and D-7. (The data plotted on these figures are not necessarily applicable to grooved pavement. No data for grooved pavement, of the type shown on these figures, are known to exist. Inasmuch as the water expulsion properties of grooved surfaces are better than that of ungrooved, smooth concrete, the conclusions derived through the use of the smooth pavement data will be conservative in terms of predicting degraded tire
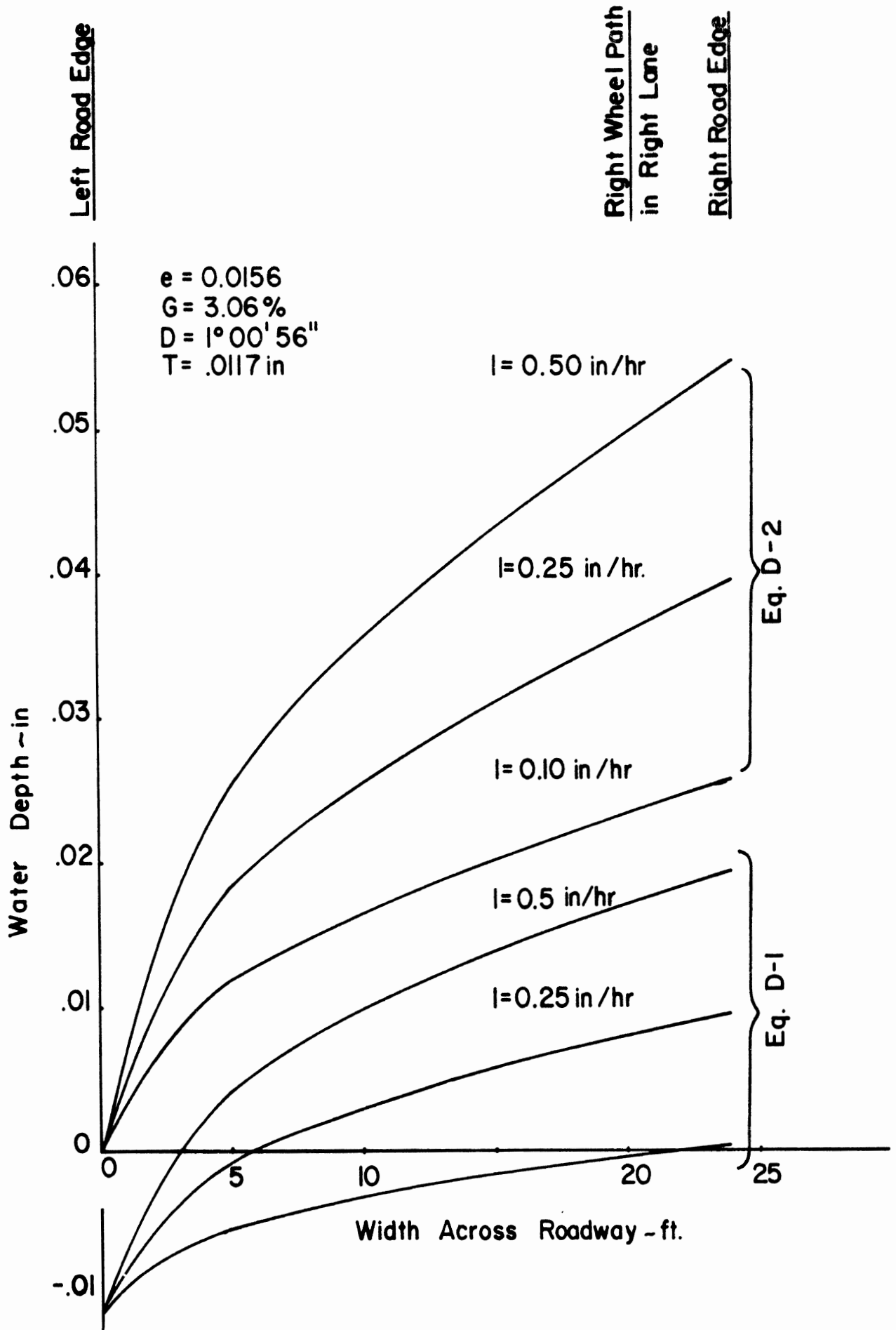
Figure D-15. Water Depth vs. Road Width for Various Rainfall
Rates for Southbound I-95 at Interchange with
U.S. 1. 404

traction due to water depth.) A comparison between traction losses at the subject site with traction available on a tangent is given on Table D-13. At typical freeway speeds there is a loss of .03 or .04 in BFC. These numbers equate to a skid number loss of 3 or 4. With uneven pavement undulations at the site (a very probable condition) the losses could easily be double these values.

D.5.2.2 Site Geometry and Signing. Many of the accidents at the I-95 site appear to result from the location of the exit and entrance ramps. Both the exit and entrance ramps are on the inside of the curve and are somewhat obscured by embankments, shrubbery, bridge railings, and crest curves. The situation in the southbound lane can be contrasted with the northbound lane, where the exit and entrance ramps are on the outside of the curve and are thus more visible. Accordingly, accident experience in the northbound lane is lower. The probable effects of signing and geometrics are discussed in order, proceeding from the exit ramp southward.

Geometrically there is a vertical curve which ends at the approximate point where the deceleration lane for the exit ramp begins. The crest of the curve is about 1,700 feet in advance of the deceleration lane. Using

Table D-13

I-95 Site Friction Losses Due to
Water Depth as Compared to a Tangent Section

Velocity mph	Water Depth Tangent, in.[1]	Water Depth Curve Site, in.[2]	BFC Tangent	BFC Curve[3]	ΔBFC
40	.028	.040	.45	.43	.02
70			.27	.24	.03
80			.26	.22	.04

[1]Data taken from Figure D-15 for an 0.25 in/hr rainfall rate as predicted from Equation (D.2), for a road width of twelve feet.

[2]Same as 1 except road width is 24 feet.

[3]Taken from Figure D-6

the AASHTO value of 3.75 feet for a driver's eye height and an object of zero height (2), the deceleration lane would theoretically come into view about 670 feet in front of the vehicle. (An object of zero height was chosen instead of the standard six-inch AASHTO object because of the tangential aspect of the exit pavement at maximum sight distance. In addition, vegetation growing along the inside of the curve makes it difficult to discern a break in the pavement edge.) This means a driver has five or six seconds in which to act from the time the exit is first sighted until the exit must be initiated. Without signing it would be difficult to easily use the exit ramp due to this short sight distance.

Signing at the site can be confusing, however. Starting from the north and proceeding south, the various signs at the site are listed on Table D-14. There are five guide signs preceding the exit. The first sign, approximately one mile ahead, is an advance warning sign which indicates that the next exit will be for U.S. 1 and the city of Massaponax. Next, approximately 4,000 feet ahead, is a sign indicating that the next exit will lead to the south bypass of U.S. 17. Some 150 feet from the beginning of the deceleration lane follows a trail- blazer assembly showing again that the exit is to south bypass U.S. 17. At the beginning of the deceleration lane

SIGN INVENTORY AT I-95 SITE
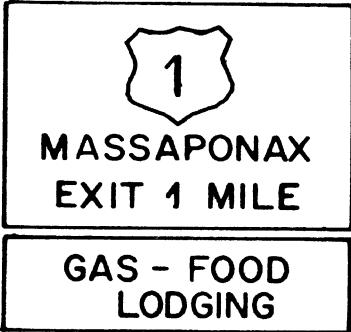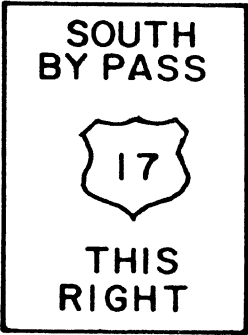
Station	Sign No.	Illustrative Drawing	Message Type	Colors		Sign Type
				Letters or Symbols	Background	
2278	15	(1) MASSAPONAX EXIT 1 MILE GAS - FOOD LODGING	Permanent	Black	White	Advance Guide Sign
				White	Green	
				White	Blue	Service Sign
2238	14	SOUTH BY PASS (17) THIS RIGHT	Permanent	White	Green	Exit Direction Sign

TABLE D-14 (Continued)
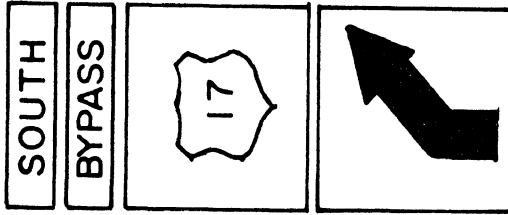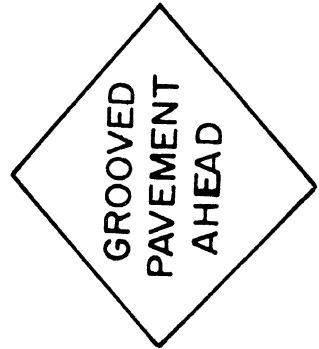
Station	Sign No.	Illustrative Drawing	Message Type	Colors Letters or Symbols	Colors Background	Sign Type
2235 +50	15	SOUTH BYPASS 17 (arrow)	Permanent	Black	White	Guide Trailblazer Assembly
2234 +90	12	GROOVED PAVEMENT AHEAD	Permanent	Black	Yellow	Warning Sign

TABLE D-14 (Continued)
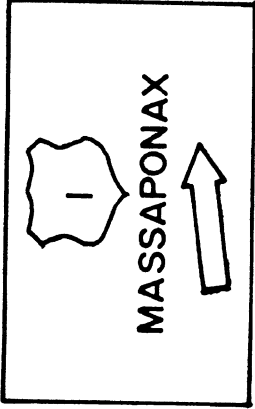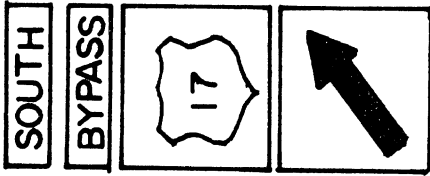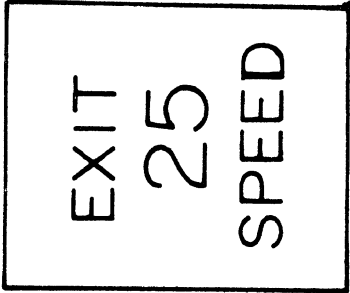
Station	Sign No.	Illustrative Drawing	Message Type	Colors — Letters or Symbols	Colors — Background	Sign Type
2234	11	MASSAPONAX	Permanent	Black / White	White / Green	Exit Direction Guide Sign
2231	10	SOUTH BYPASS 17	Permanent	Black	Yellow	Guide Trailblazer Assembly
2227	9	EXIT 25 SPEED	Permanent	Black	Yellow	Advisory Exit Speed Sign

TABLE D-14 (Continued)
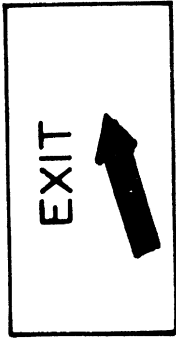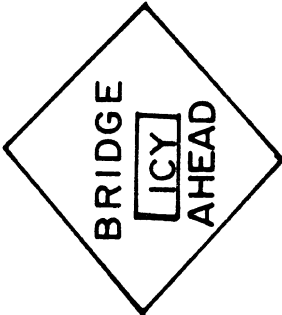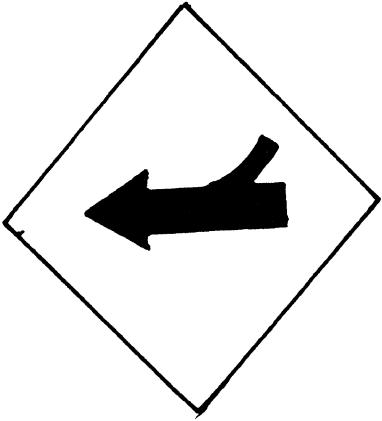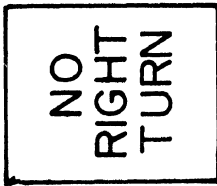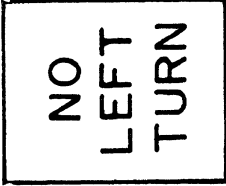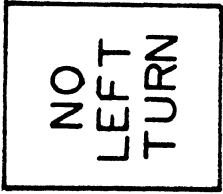
| Station | Sign No. | Illustrative Drawing | Message Type | Colors | | Sign Type |
				Letters or Symbols	Background	
2227	8	EXIT	Permanent	White	Green	Gore Sign
2224	7	NO HITCH HIKING	Permanent	Black	White	Regulatory Sign
2223	6	BRIDGE ICY AHEAD	Permanent and Manually Variable	Black	Yellow	Warning Sign

411

TABLE D-14 (Continued)

Station	Sign No.	Illustrative Drawing	Message Type	Colors Letters or Symbols	Colors Background	Sign Type
2207	5	[diamond sign with left-pointing arrow]	Permanent	Black	Yellow	Merge Sign
2203	4	NO RIGHT TURN	Permanent	Black	White	Turn Pro-hibition Sign
2203	3	NO LEFT TURN	Permanent	Black	White	Turn Pro-hibition Sign
2198	2	NO LEFT TURN	Permanent	Black	White	Turn Pro-hibition Sign

is a sign indicating that the exit is also for U.S. 1
and the city of Massaponax. Some 300 feet farther down,
midway in the deceleration lane, is a second guide trail-
blazer assembly to U.S. 17 south bypass. This is much
the same as the first assembly. There are three signs,
then, indicating that the exit is for U.S. 17 south bypass,
and two separate signs indicating that the exit is also
for U.S. 1 and Massaponax. Unfortunately, however, the
U.S. 1/Massaponax sign nearest the exit is almost entirely
obscured by the Grooved Pavement Ahead sign and by the
first trailblazer assembly. The situation was first
noticed on the motion pictures taken at the site during
the preliminary site evaluation. A photograph illustrating
the condition is shown on Figure D-16. The unobscured
U.S. 1/Massaponax sign is shown on Figure D-17. It is
evident, then, that drivers seeking to exit to U.S. 1 or
Massaponax, not being familiar with the area, could be
confused by the obscured sign and be indecisive.

Given that a driver has successfully made the decision
to exit and has entered the deceleration lane, a second
problem arises. The deceleration lane at the exit consists
of a 250-foot taper section plus a 250-foot tangent leading
into the exit curve, for a total length of 500 feet. This
length is well above the AASHTO minimum recommended length
of 450 feet for the exit ramp conditions existing at the
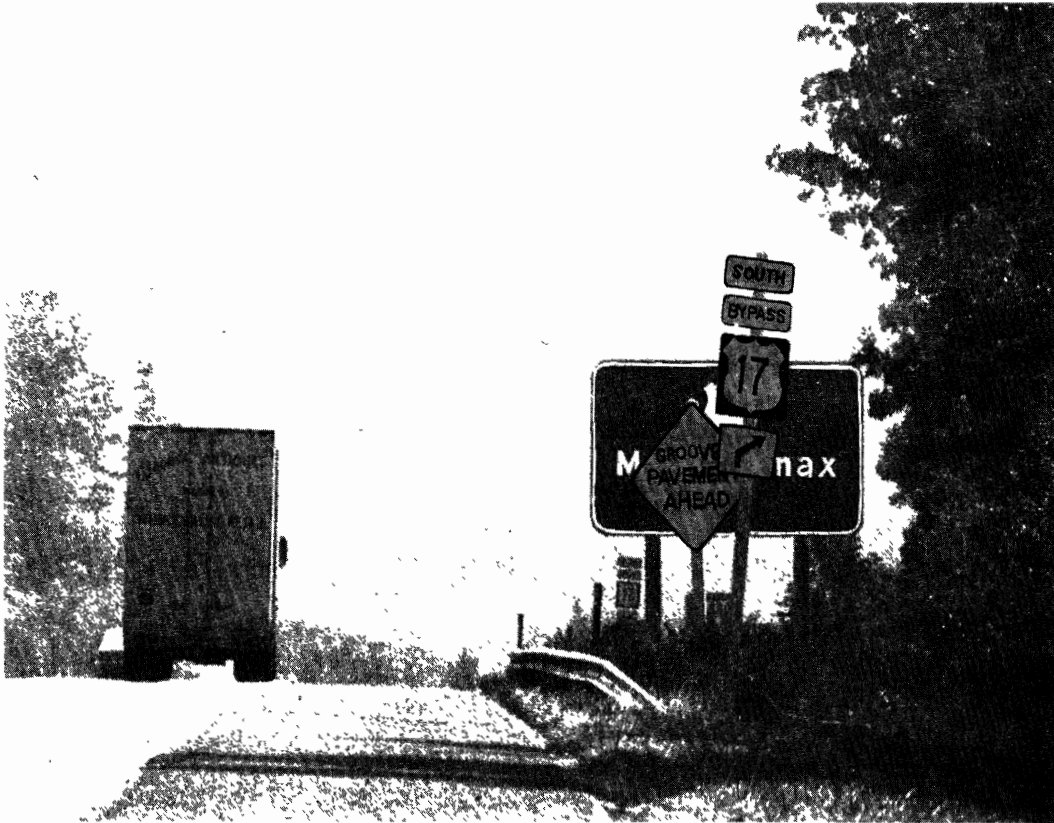
Figure D-16.   An Obscured View of the U.S. 1/
Massaponax Sign.
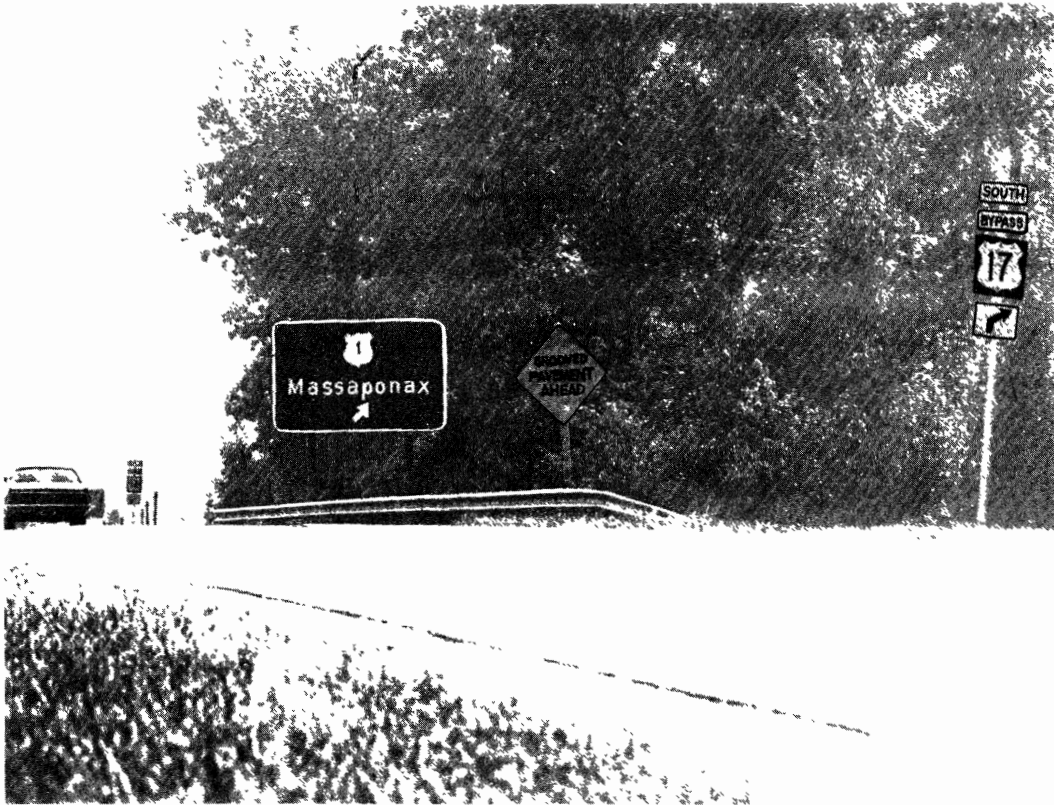
Figure D-17.   An Open View of the Sign

site (2). Briefly, AASHTO recommends that for exit ramp radii of curvature greater than 690 feet (the value is 1162 feet or 4.9° at the exit ramp curve) freeway speeds up to 80 mph, and the freeway grade no more than 2%, the minimum deceleration lane length is 450 feet. For freeway grades greater than 3 to 4% downgrade, this length should be multiplied by 1.2. Since the freeway grade is between 2 and 3%, the present ramp length exceeds recommended limits. Not taken into account, however, is the fact that the ramp itself is on a steep downgrade (-6.5% at some points). Further proceeding down the exit ramp, the ramp curvature reverses (see Figure D-13) to a radius of 723 feet, or 7.9°. Thus, although the exit ramp deceleration lane is already beyond minimum AASHTO recommendations, it would seem worthwhile to consider the subject ramp as an unusual case.

Indeed, the fact that the advisory exit speed has been set at 25 mph would suggest that the curvature and grade geometry at the site has already been considered unusual. It should be noted that the ramp radius of curvature of 690 feet corresponds to a ramp design speed of 50 mph. Thus, if the actual practical ramp speed is only 25 mph, and not 50 mph, then the minimum deceleration lane length recommended by AASHTO is 650 feet. On the basis of the advisory ramp speed, then, the exit

deceleration lane is at least 150 feet shorter than current AASHTO recommendations.

The position of the advisory exit speed sign should be noted. The sign is located just beyond the deceleration lane and around the curve at the head of the exit ramp. In this location, the sign cannot be seen until the vehicle is in the exit curve. Thus, the advisory speed is of small value in terms of advising the driver to use the deceleration lane as a means of slowing to a safe exit speed.

Proceeding past the exit ramp now, the next section of interest lies between the exit and the bridge. Approaching the bridge on the right, there is a variable message sign which is used to warn motorists of an icy bridge deck. Just in front of this warning sign is a regulatory sign which states that hitchhiking is not allowed. Unfortunately, however, the no-hitchhiking sign obscures the icy bridge sign over much of the approach road to the sign. The condition is illustrated on Figure D-18. The unobscured sign is shown on Figure D-19.

It can also be noted on these photographs that the high embankment and vegetation on the inside of the curve hide the bridge from oncoming motorists. The situation is probably most acute when traffic is heavy, since the traffic itself contributes to loss of visibility (see Figure D-19).

Figure D-18.   An Obscured View of the Icy Bridge Sign.

Figure D-19.   An Open View of the Sign.

417

As the motorist approaches the bridge, the bridge railings, being relatively high and within three feet of the road edge, contribute further to the loss of sight distance. Since the bridge is both on a curve and at the top of a crest (the road grade changes from -2.64% to -3.1% just beyond the bridge) the road ahead cannot be seen until the driver is on top of the bridge deck. Even when on and well beyond the bridge, however, a driver has little inkling of an upcoming entrance ramp, except for the merge arrow sign (sign number 5). The condition is shown on Figures D-20 and D-21. Since the entrance ramp merges on the inside of the curve, the vegetation, the road crest, road curvature, and the bridge railings tend to hide the entrance from the motorist. The result is that accidents involving weaving, sudden slowing, failure to yield the right of way, etc., commonly occur in the accident statistics. The situation is further aggravated by the fact that the entrance ramp design is such that vehicles entering the freeway are frequently moving at slow speed relative to freeway traffic.

The entrance ramp is a curving upgrade of some 800 feet in length. Curvature is 8.1° (710-foot radius) and the upgrade is about 3.4% maximum. Following the exit ramp there is an acceleration lane adjacent to the freeway which is 500 feet in length, including a 250-foot taper
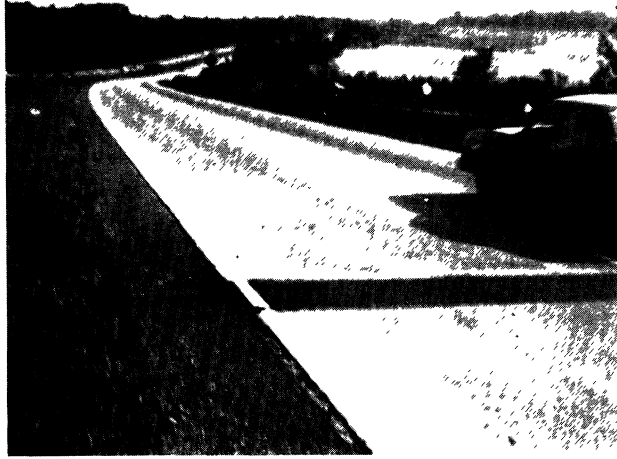
Figure D-20. A View of the Entrance Ramp from
Just South of the Bridge

Figure D-21. A Closer View of the Entrance Ramp.

section. For a freeway of 2% grade or less, and for a ramp radius of curvature of 690 feet, the AASHTO recommendation for acceleration lane length is 575 feet. This length includes a 300-foot taper. (The indicated values are for a 70-mph freeway design speed.) This length is based on the premise that traffic entering the acceleration lane is traveling at 50 mph. Short-term observations at the entrance ramp, however, have shown that most drivers are traveling less than 20 mph at the beginning of the acceleration lane. The reason for this behavior is evident from an examination of the sight distance conditions on the ramp. Three views of the scene as it would be viewed by a driver traveling up the entrance ramp are shown on Figure D-22. It is evident that visibility of the scene ahead is extremely poor until the vehicle is virtually upon the acceleration lane. In addition, the perspective of the relatively short acceleration lane is clearly indicated.

Using a more realistic speed of 20 mph at the point of entry into the acceleration lane, the AASHTO-recommended length for the lane is 1,500 feet x 1.5. = 2,250 feet. The 1.5 factor is used to account for the fact that the freeway upgrade is almost 3% in the area where the acceleration lane is required. The entrance ramp then is approximately 1,750 feet too short for the prevailing conditions.
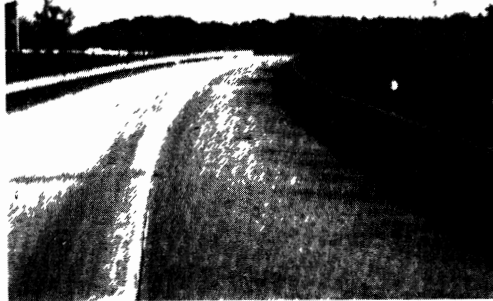
Figure D-22. Three Views of the Entrance Ramp as a Vehicle
Proceeds Up the Ramp to the Acceleration Lane.

421

D.5.3 SUGGESTED MODIFICATIONS. Roadway-induced accidents at the I-95 site are apparently the result of several factors. These include:

1. Traffic speed

2. Pavement drainage

3. Pavement friction

4. Signing

5. Sight Distance

6. Interchange ramps

Suggested improvements, with the exception of reduced vehicle speeds, which can be expected to redress the accident causation potential associated with these factors are discussed in the following subsections. The benefits of speed reduction are more or less self-evident and need no discussion.

D.5.3.1 Improving the Pavement Drainage. Much of the material given in Section D.4.3.1 with respect to the Ohio Turnpike site is equally applicable to the I-95 site. Curvature and superelevation at the two sites are virtually identical. The fact that the pavement has been grooved at the I-95 site and that the shoulders are not superelevated would suggest that drainage is not as great a problem. Even with these differences, however, the data given in Table D-10 show that skid number losses of 3 or

4 can be expected solely as the result of water build-up on the I-95 curve. These losses again are compared to the skid resistance available on a tangent section.

As fully discussed in Section D.4.3.1, the primary methods which can be used to improve drainage are to increase the superelevation rate and to provide additional drainage paths so as to reduce surface water accumulations. Reference to Figure D-7 suggests that a superelevation of 0.06 would be a value which would produce a substantial reduction in water depth. (The road width at the I-95 site is 24 feet. The water depth versus e characteristics for a 24-foot road width can be inferred from the 24- and 30.5-foot curves on Figure D-7.) Larger values of super-elevation produce a decreasingly smaller percentage of improvement. A suggested means of achieving the super-elevation is to add a pavement overlay.

Suggested methods for ensuring that water runoff occurs below the tire contact surface are either to ensure that the pavement overlay has a wearing course of large, sharp aggregate, or to groove the overlay in a cross-hatched pattern. The longitudinal grooves currently at the site do not enhance transverse water drainage. Such grooves, however, do improve wet-weather traction by providing water escape paths in the tire/road contact patch.

D.5.3.2 <u>Improving Pavement Friction</u>. Although
friction measurements at the site indicate a comparatively
good friction surface (see Table D-11), the discussions
in Appendix B have indicated that an even better surface
is needed. Given that six skid numbers are needed just
to negotiate the curve in a steady-state manner (the
analysis in Section D.4.3.2 is completely applicable here),
as much as 9 or 10 skid numbers are needed during wet
weather, over and above that needed on a tangent—the
additional 3 or 4 skid numbers being needed to overcome
the increased water depth levels on the curve. For non-
steady-state maneuvers, of course, the requirements are
far greater. The point, however, is that the emergency
friction margin on a tangent is somewhat greater than for
a curve, since a part of the available friction is needed
just to negotiate the curve.

Again using Equation (15) of Chapter 3, the required
SN_{40} value for the site, as it now exists, can be computed
from the following site data:

SN_{40T} = 34 e = 0.0156

V = 80 mph SN_{grad} = -0.5 SN units/mph

G = 2.64% Tire Tread Depth = 2/32 in

D = 1°0'56" L = 20.5 ft

I_D = 0.25 in/hr

Using this information

$$S = 0.0298 \qquad K(\frac{L}{e}) = 1{,}790 \text{ feet}$$

$$K = 1.36 \qquad SN_D = 13$$

$$T_F = 0.50$$

and Equation (15) gives a required SN_{40} value of 91. Thus, even though the drainage length is ten feet less than that for the Ohio Turnpike site, the skid number requirement is virtually the same. Therefore, the same arguments hold for increasing the superelevation of the cross-section and restricting worn tire use, along with increasing surface skid resistance.

D.5.3.3 Improving Signing. Major signing suggestions pertain to the following signs:

1. Sign 11, the U.S. 1/Massaponax exit sign.

2. Sign 9, the advisory exit speed sign.

3. Sign 6, the icy bridge sign.

4. Sign 5, the merge sign.

The only indication that the exit can be used for U.S. 1 is on signs 15 and 11. Sign 15 is approximately one mile in advance of the exit while sign 11 is virtually at the beginning of the exit deceleration sign. Since sign 11 is obscured by other signs, however, the fact

that the exit is for U.S. 1 as well as U.S. 17 may not
be clearly apparent.

Obviously, then, sign 11—the U.S. 1/Massaponax
sign—should be made more visible. This can be accomp-
lished by moving both the grooved-pavement (sign 12) and
the U.S. 1 guide trailblazer assembly (sign 13) from in
front of sign 11. The grooved-pavement sign could be
moved further from the road edge or removed altogether.
The trailblazer assembly could also be moved laterally
or advanced further ahead. Whatever the method, care
should be taken to check that there is a clear view of
sign 11.

Although the exit speed advisory sign (sign 9) has
apparently been installed according to the "Manual on
Uniform Traffic Control Devices" (13), it is suggested
that this sign be moved to a point midway in the decelera-
tion lane. This will allow the sign to be seen by
motorists prior to entering the exit lane.

Since the icy bridge sign (sign 6) can be a very
important warning device, it is suggested that every
effort be made to ensure that the sign is clearly visible
to oncoming motorists. It is recommended, therefore,
that the no-hitchhiking sign either be removed altogether
or that the icy bridge sign be advanced in front of the

no-hitchhiking sign. The latter course seems preferable since it will provide an additional increment of advance warning.

The only modification suggested at the merge sign, sign 5, is to add the additional message "MERGE" below the merge arrow. This alteration should further clarify the fact that an entrance ramp is ahead and will put the sign installation in compliance with the standard in Reference 13.

These sign alterations should be beneficial in clarifying the information available to freeway users and should reduce some of the uncertainty and indecision at the interchange ramps.

D.5.3.4 _Improving Sight Distance_. If it is presumed that the basic curve-grade geometry of the site should not be altered, then the major means of improving sight distance is through clearing away sight obstructions on the inside of the curve. Prior to the exit ramp this can be accomplished by removing part of the roadside embankment and by removing excess foliage and vegetation. The same can be done between the exit and the bridge.

On the bridge itself, consideration should be given to widening the bridge deck so that a minimum shoulder width of ten feet is available—particularly on the

inside of the curve. A better solution during the design phase might have been to eliminate the median gap between the northbound and southbound bridge so that bridge rails on the median side would not be required. Although this design is admitted to be initially more expensive, overall costs would very probably be less because of reduced accident severity.

Since neither the exit or entrance ramps can be easily seen due to crest vertical curves, it is suggested that:

1. The grass in advance of these ramps be faithfully removed.

2. Curbs be added on the far side of each ramp and that these be painted yellow.

3. The pavement in the speed-change lanes be made to contrast with the freeway pavement.

Each of these suggestions should improve ramp visibility without altering basic roadway geometrics.

D.5.3.5 <u>Improving Interchange Ramps</u>. Without drastically modifying the site, the major improvements in the interchange ramps can be made by lengthening the speed-change lanes.

At the exit ramp, the deceleration lane is longer than needed to satisfy recommended AASHTO minimums, but not long enough to satisfy the 25-mph exit advisory speed. Because of this 25-mph ramp speed—the speed reflecting both the steep grade and sharp curve on the ramp—and because of the lack of sight distance prior to the exit, it is suggested that the ramp be made 300 feet longer. In addition, it is suggested that a channelizing curb some 200 feet in length be added at the end of the deceleration lane. In this way vehicles once committed to the exit lane will not be able to re-enter the freeway at the last second and cause traffic conflicts. (Vehicles exiting erroneously are not unduly penalized, since the southbound exit ramp is easily accessible at the junction with U.S. 1.)

The acceleration lane at the end of the entrance ramp is substantially shorter than the minimum AASHTO-recommended length for a ramp speed of 20 mph. It is suggested that this lane be extended at least 1,800 feet beyond the present length. A channelizing curb 500 feet in length is also recommended here so as to prevent slow-moving vehicles from entering the freeway before having achieved a minimum level of speed. The curb should extend from the beginning of the acceleration lane southward along the right road edge of the freeway.

D.5.4 SUMMARY OF ANALYSIS OF I-95 SITE. The basic
factors responsible for the high accident rate at the
I-95 site are poor water drainage, inadequate sight dis-
tance, unclear signing, and inadequate interchange speed-
change lanes. Water depth accumulations during wet
weather and steady-state cornering requirements are enough
to reduce the available skid number as much as 9 or 10
units below what is available on tangent sections. Verti-
cal crest curves are present just in front of both the
exit and entrance ramps. These, along with roadside
embankments, roadside foliage, and road edge bridge rail-
ings tend to limit sight distance. Signs for the exit
ramp and for warning motorists of icy bridge conditions
are obscured by other signs. The exit deceleration lane,
although longer than minimum AASHTO recommendations, is
inadequate for the unusually steep grade and sharp curva-
ture of the exit ramp. These are reflected in the exit
ramp advisory speed of 25 mph. The entrance ramp
deceleration lane is substantially shorter than AASHTO
recommendations.

Suggested remedies include (1) adding a pavement over-
lay of large, sharp exposed aggregate to increase curve
superelevation to 0.06 and improve wet-surface friction;
(2) cutting back the embankment and foliage along the

inside of the curve and widening the bridge deck so as to improve sight distance; (3) moving, rearranging, or altering critical signs; and (4) extending the length of both the exit and entrance speed-change lanes.

APPENDIX E

THE INFLUENCE OF GRADE ON THE AASHTO CURVE DESIGN FORMULA

The AASHTO curve design formula is as follows ($\underline{2}$):

$$e + f = \frac{V^2}{15R} \tag{E.1}$$

The derivation of this equation rests on the following assumptions:

1. The vehicle can be considered as a point mass.

2. Highway curvature and superelevation values are small enough to be within the range of small angle approximations, i.e., $\sin \alpha \cong \tan \alpha \cong \alpha$, $\cos \alpha \cong 1$.

3. Highway upgrade or downgrade vertical alignment can be neglected.

The purpose of this analysis is to derive the curve design formula in its exact form, assuming only that the vehicle is a point mass, and compare this with the AASHTO formula of Equation (E.1).

E.1   DERIVATION OF THE EXACT CURVE DESIGN FORMULA

The exact curve design formula can be derived by considering the forces acting on a vehicle (considered to be a point mass) which is traveling on a section of

433

highway having combined grade and horizontal curvature.
In traveling along the curve/grade, the vehicle is assumed
to be traversing the curve on a circular path and not
skidding. The derivation is initiated by defining the
road surface in terms of its orientation with respect to
the horizontal.

In Figure E-1, the i coordinate system is defined such
that the unit vectors, $\bar{i}_1$ and $\bar{i}_2$, lie in the horizontal
plane with

$\bar{i}_1$ in the nominal direction of the radius of
        curvature of the roadway,

$\bar{i}_2$ in the nominal direction of travel along
        the roadway, and

$\bar{i}_3$ in the direction of the gravity vector.

The k coordinate system is defined by rotating the i system
through an angle G about the $\bar{i}_1$ axis. G is the grade of
the roadway (+ for upgrade). The m coordinate system
is defined by rotating the k system through an angle e*
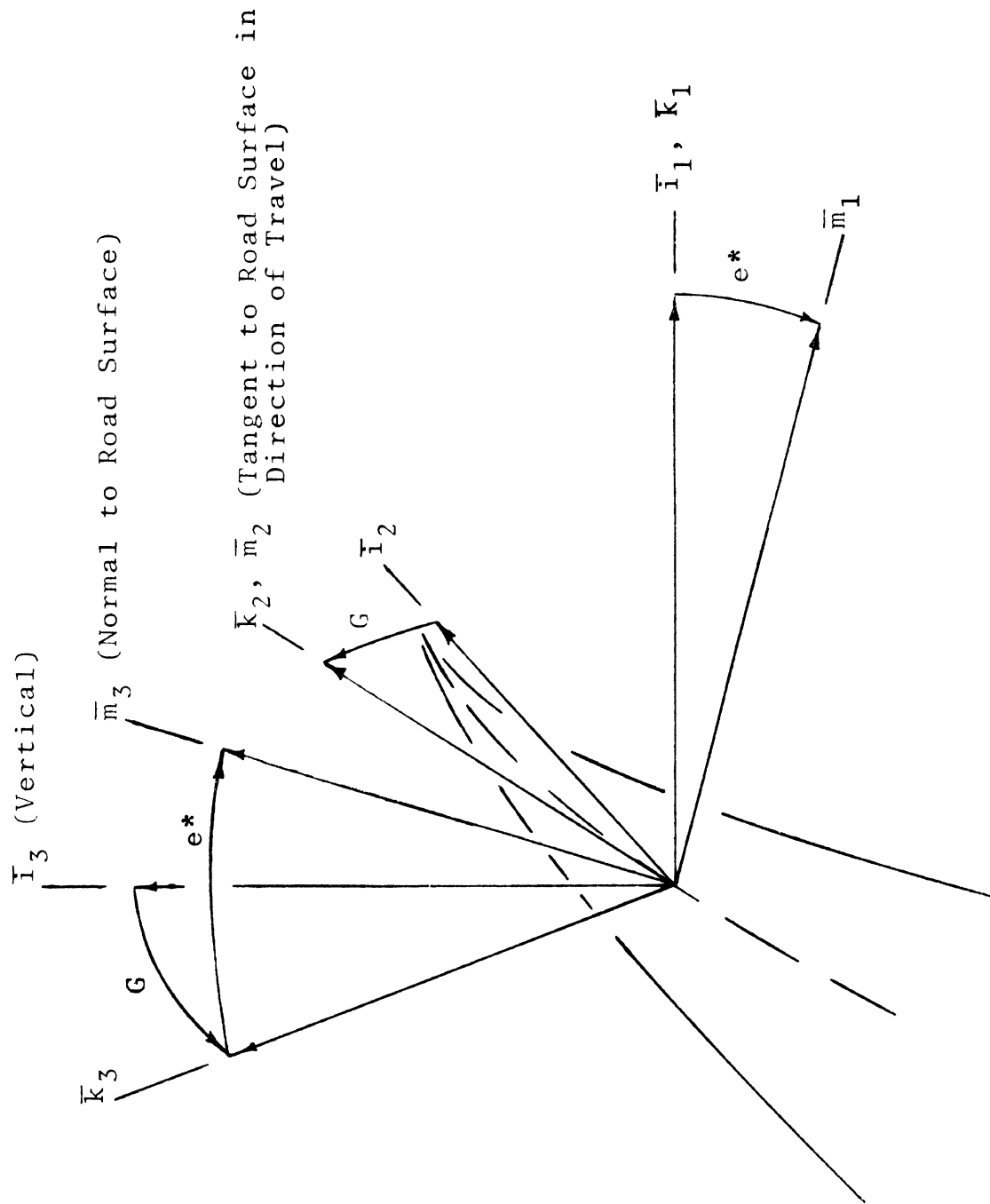
Figure E-1. Coordinate Conventions

$\bar{i}_3$ (Vertical)

$\bar{m}_3$ (Normal to Road Surface)

$\bar{k}_2$, $\bar{m}_2$ (Tangent to Road Surface in Direction of Travel)

$\bar{i}_2$

$\bar{i}_1$, $\bar{k}_1$

$\bar{m}_1$

$\bar{k}_3$

e*

G

about the $\bar{k}_2$ axis. e* corresponds to the superelevation of the pavement.[1]

The orientation of the m coordinate system is such that the unit vectors, $\bar{m}_1$ and $\bar{m}_2$, lie in the plane of the road surface with:

$\bar{m}_1$ in the direction of the radius of curvature of the roadway,

$\bar{m}_2$ in the direction of travel along the roadway, and

$\bar{m}_3$ normal to the road surface.

---

[1] e* is the superelevation angle built into a road when the road is constructed on a grade. When forms for the pavement surface are laid out, the superelevation is measured in a plane which is normal to the roadbed. Therefore, e* is not the true superelevation. The true superelevation, e, is measured in a vertical plane. e* is measured in a plane which is canted from the vertical by the grade angle G. e* is related to e by the following equation:

$$\tan e = \tan e^* \cos G \qquad (E.2)$$

In actuality, then, the true value of superelevation is slightly less than the specified value when a curve is constructed on a grade. For grades up to 12%, however, the error is less than 0.8%.

The forces acting on the vehicle as it traverses a curve/grade without skidding are depicted in Figure E-2. In terms of the previously defined coordinate systems, these forces are summed as follows:

$$F\bar{m}_1 - W\bar{i}_3 - \frac{WV^2}{g\,R}\ \bar{i}_1 + \frac{W}{g}\ \dot{V}\ \bar{m}_2 + N\ \bar{m}_3 = 0 \qquad (E.3)$$

Now

$$F = fW \qquad (E.4)$$

and by the angular transformations which define the m coordinate system in terms of the i system:

$$
\begin{bmatrix} \bar{i}_1 \\ \bar{i}_2 \\ \bar{i}_3 \end{bmatrix}
=
\begin{bmatrix}
\cos e* & 0 & \sin e* \\
\sin e*\ \sin G & \cos G & -\cos e*\ \sin G \\
-\sin e*\ \cos G & \sin G & \cos e*\ \cos G
\end{bmatrix}
\begin{bmatrix} \bar{m}_1 \\ \bar{m}_2 \\ \bar{m}_3 \end{bmatrix}
$$

Therefore, Equation (E.3) can be rewritten as:

$$fW\bar{m}_1 - W(-\sin e*\ \cos G\ \bar{m}_1 + \sin G\ \bar{m}_2 + \cos e*\ \cos G\ \bar{m}_3)$$

$$\frac{-WV^2}{gR}\ (\cos e*\ \bar{m}_1 + \sin e*\ \bar{m}_3) + \frac{W}{g}\ \dot{V}\ \bar{m}_2 + N\ \bar{m}_3 = 0$$

$$(E.5)$$
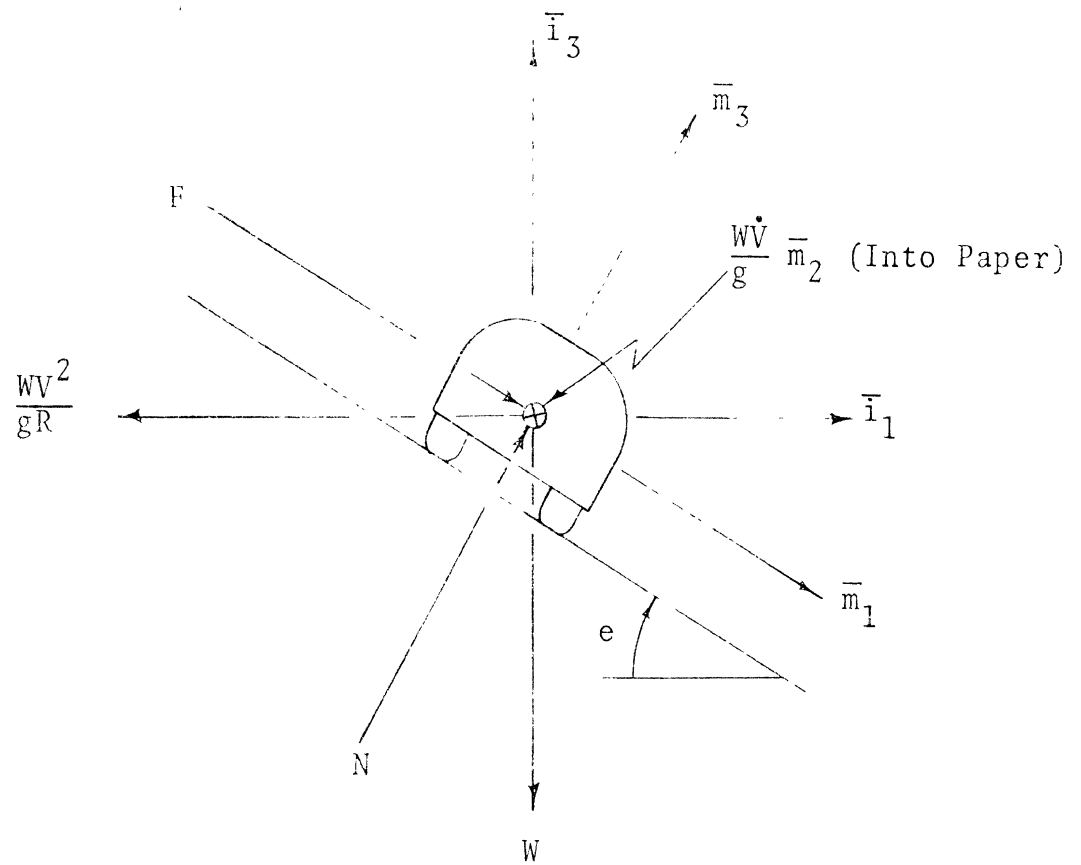
Figure E-2. Forces Acting on Vehicle

or

$$(f + sine* \cos G - \frac{WV^2}{gR} \cos e*)\overline{m}_1 + (\frac{\dot{V}}{g} - sinG)\overline{m}_2$$

$$+ (\frac{N}{W} - \cos e* \cos G - \frac{V^2}{gR} sine*)\overline{m}_3 = 0 \qquad (E.6)$$

The three components of this equation represent the summation of forces acting on the vehicle along the three axes of the m coordinate system. The $\overline{m}_1$ component is the <u>cornering</u> term, the $\overline{m}_2$ component the <u>longitudinal acceleration</u> term, and the $\overline{m}_3$ component the term <u>normal</u> to the road surface. Only the $\overline{m}_1$ component is of interest here.

Since the magnitude of the vector represented by Equation (E.6) is zero, each of its components must be zero. Thus the $\overline{m}_1$ component can be written in scalar form as:

$$f + sine* \cos G = \frac{V^2}{gR} \cos e* \qquad (E.7)$$

Equation (E.7) is the exact form of the AASHTO curve design formula as given by Equation (E.1). (With V in mph, the term on the right becomes $\frac{V^2}{14.97R} \cos e* \cong \frac{V^2}{15R} \cos e*$.)

439

E.2   ERROR ANALYSIS

The error resulting from the use of the AASHTO curve
design formula in the presence of upgrade or downgrade
vertical alignment can be determined by comparing Equations
(E.1) and (E.7). These equations are written as follows:

$$f \; = \; \frac{V^2}{gR} \; - \; e \tag{E.1}$$

$$f' \; = \; \frac{V^2}{gR} \; \cos e* \; - \; \sin e* \; \cos G \tag{E.8}$$

where f' in Equation (E.8) signifies the fact that the
exact value of the side friction factor is different than
that which is assumed when the AASHTO formula is applied.

The error then is:

$$\text{ERROR} \; = \; \frac{100 \left| f - f' \right|}{f'} \tag{E.9}$$

The expression is plotted on Figure E-3 as a func-
tion of superelevation rate for fixed values of velocity,
grade, and curvature. It can be noted that the maximum
error is 0.73%, and that this error occurs at a super-
elevation rate of 0.12. Additional plots of the error
expression (Equation (E.9)) are shown on Figure E-4.
These plots show the variation in error as a function of
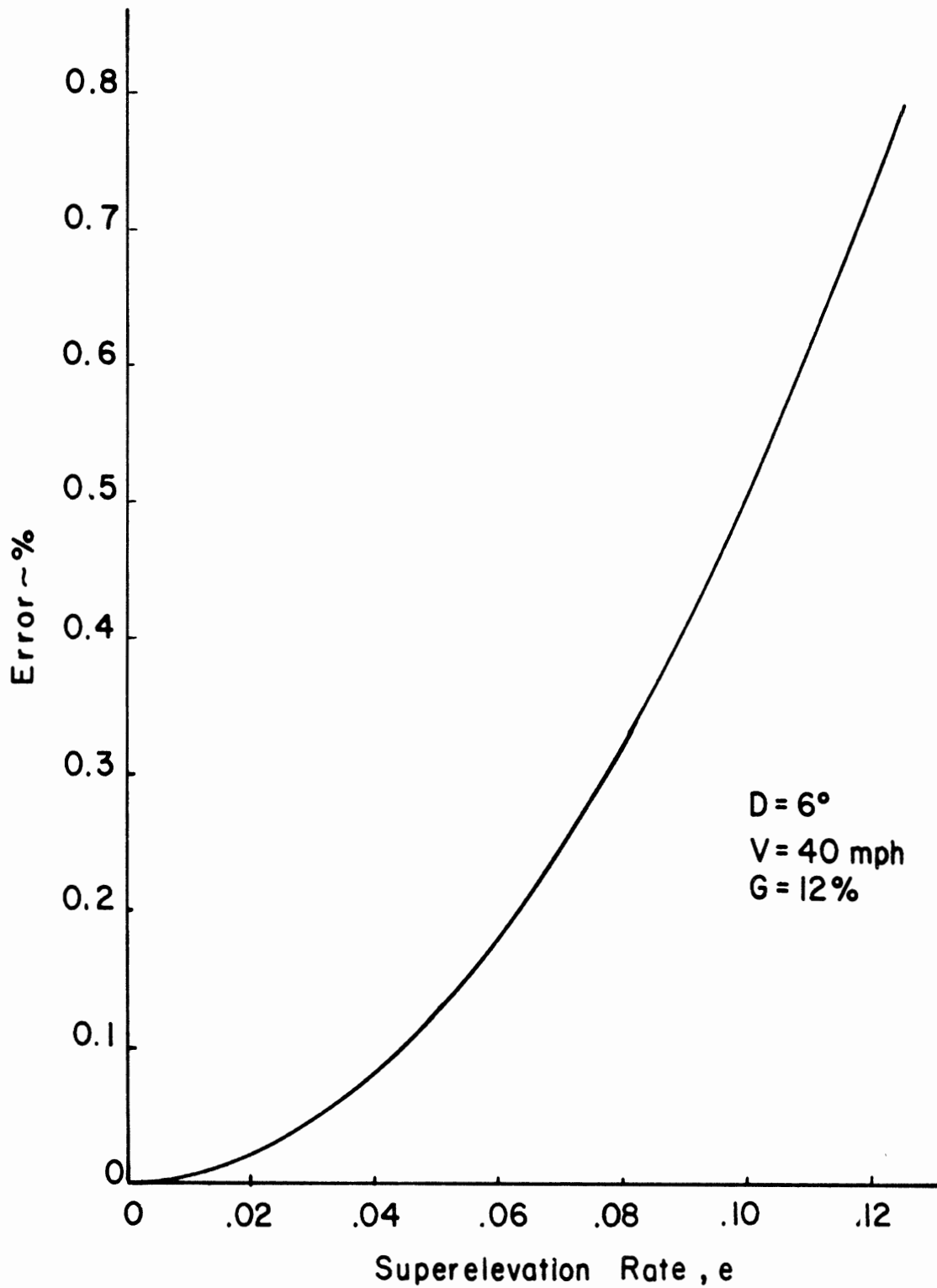curvature, velocity, and grade near maximum error
conditions.

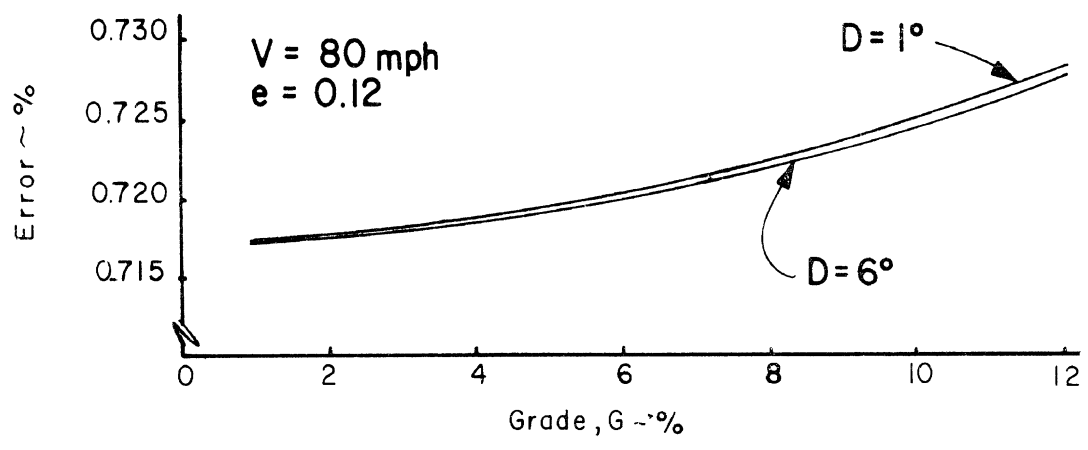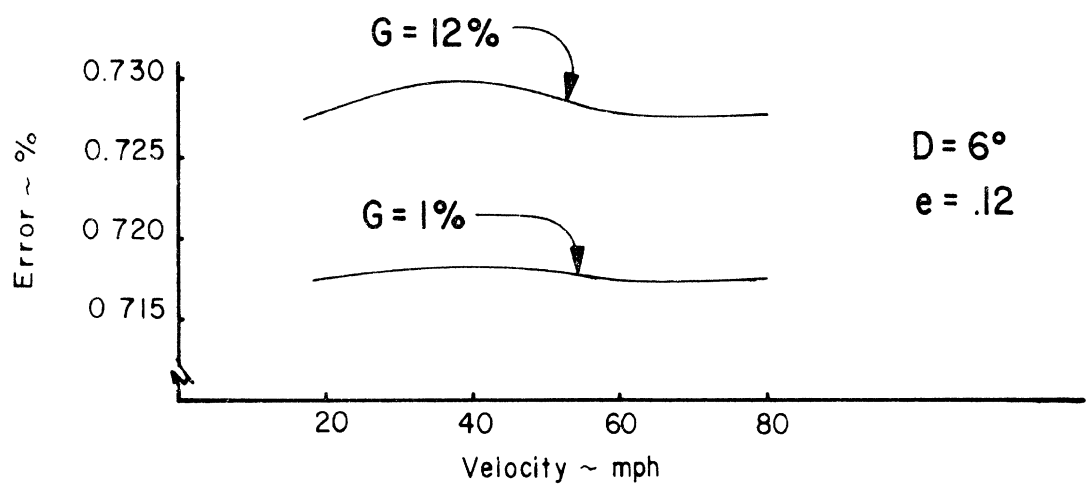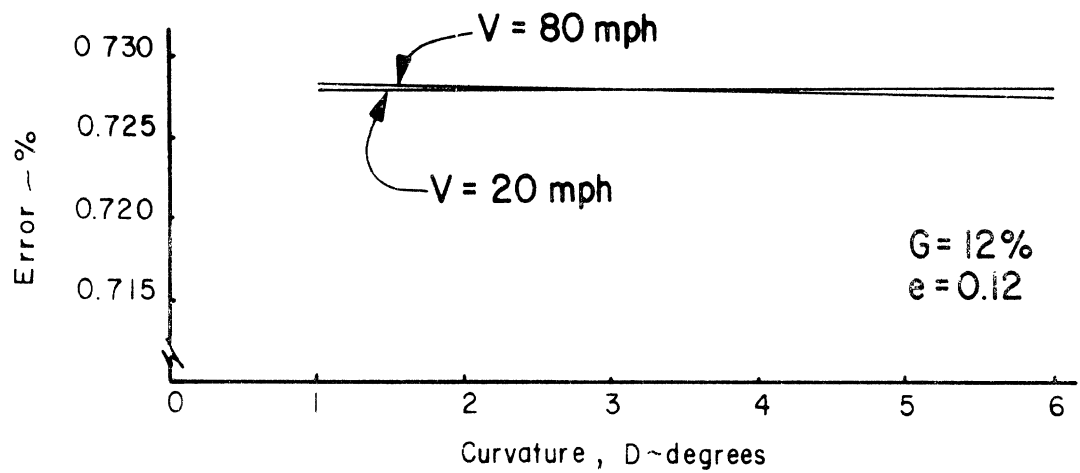Figure E-3. Error Versus Superelevation Rate

Figure E-4. Error Versus Curvature, Velocity, and Grade

It is clear from the plots on Figures E-3 and E-4 that the error is primarily a function of superelevation rate. Grade is a secondary factor, while velocity and curvature have essentially no influence. It is additionally clear that within the ranges of V, D, e, and G common to highway practice, <u>the AASHTO curve design formula is virtually equivalent to the exact formula and is essentially independent of grade</u>.

E.3 CONCLUSION

It has been shown that the AASHTO curve design formula is equally applicable to horizontal curves alone as well as curves constructed on upgrade and downgrade vertical alignments. Lest the wrong impression be given, however, it must be made clear that these remarks do not constitute an endorsement of the AASHTO curve design formula. The equation is based on steady-state cornering performance and does not take into account the actual dynamic characteristics of a vehicle as it executes a cornering maneuver or a combined maneuver such as cornering plus braking or cornering plus lane change.

APPENDIX F

TENTATIVE METHODS FOR ANALYSIS OF ACCIDENT-CAUSATION FACTORS AT HIGHWAY SITES WITH HIGH ACCIDENT RATES

Highway sites with high accident rates can be pin-pointed through the analysis of accident data. Classes of accidents at these sites can also be identified through such data. However, accident causation factors, particularly those associated with the site, are not always so easily identified. This appendix consists of a tentative form which can be used to identify such site deficiencies. Obviously, each item in the form is not applicable to every site. Neither does the existence of a particular feature at a site presuppose that that feature is an accident-causation factor. Single features as well as combinations of features acting together may be accident-causation factors.

In identifying the accident-causation factors at an existing site, the form is meant to be used in conjunction with accident data. When used as an aid in design, the checklist can be used to identify potentially bad design practice.

Accident-causation factors other than highway site factors, i.e., those related to the vehicle or driver, are not considered here.

The form is divided into two parts. The first part consists of a Site Description form. The second part is a Site Evaluation Checklist wherein the possible accident-causation features of the site can be checked off.

F.1 SITE DESCRIPTION FORM

1. Route Number:_____

2. Geographic Location:_____

_____

_____

_____

3. Type of Road

    a. Freeway   _____

    b. Expressway   _____

    c. Conventional Road _____

4. Type of Area

		Rural	Urban
a.	Residential	_____	_____
b.	Commercial	_____	_____
c.	Industrial	_____	_____
d.	Agricultural	_____	_____
e.	Institutional	_____	_____
f.	Undeveloped	_____	_____
g.	Other _____	_____	_____

5. AADT_____

6. Posted Speed Limit_____

7. Site Characteristics

    a. Right of Way Width   _____

    b. Number of Lanes One Direction_____

    c. Sight Distance (Minimum) _____

d. Lane Types   Width   Check if applicable

    (1) Through   _____   _____

    (2) Auxiliary   _____   _____

    (3) Speed-
        Change   _____   _____

    (4) Storage   _____   _____

    (5) Weaving   _____   _____

    (6) Truck   _____   _____

    (7) Climbing   _____   _____

    (8) Other_____   _____   _____

e. Interchange

    (1) N/A   _____

    (2) Freeway   _____

    (3) Expressway   _____

    (4) Arterial Highway   _____

    (5) Parkway   _____

    (6) Major Street   _____

    (7) Through Street   _____

    (8) Local Street   _____

    (9) Other_____   _____

f. Horizontal Alignment

    (1) Tangent   _____

    (2) Transition Curve   _____

    (3) Circular Curve   _____

        (a) $<0°30'$ Curvature   _____

        (b) $0°30' - 1°29'$ Curvature_____

        (c) $1°30' - 3°00'$ Curvature_____

        (d) $> 3°$ Curvature   _____

    (4) Other_____   _____

g. Vertical Alignment

    (1) Level   _____

    (2) Upgrade   _____

    (3) Downgrade   _____

    (4) V. C. Summit   _____

    (5) V. C. Sag   _____

    (6) Roller Coaster   _____

    (7) Other_____   _____

h. Roadway Cross-Section

    (1) Curbing   _____

    (2) Median   _____

        (a) Width_____   _____

        (b) Paved   _____

        (c) Unpaved   _____

        (d) With Median Barrier _____

        (e) None   _____

        (f) Other_____   _____

    (3) Shoulders   _____

        (a) Paved   _____

        (b) Sodded   _____

        (c) Gravel   _____

        (d) Bare   _____

        (e) Other_____   _____

    (4) Clear Roadside Width at
            Site (Min.)   _____

i. Road Surface Cross-Section   Sta. to Sta.

Superelevation Rate

(1)   _____   _____to_____

(2)   _____   _____to_____

(3)   _____   _____to_____

(4)   _____to_____

(5) Variable   _____to_____

(6) In Superelevation Transition   _____to_____

(7) Other (Draw Below)

j. Surface Type

   (1) Asphaltic Concrete   _____

   (2) Other Bituminous   _____

   (3) Portland Cement Concrete   _____

   (4) Portland Cement Concrete -
        Longitudinal Grooving   _____

   (5) Portland Cement Concrete -
        Lateral Grooving   _____

   (6) Other_____   _____

k. Surface Skid Resistance

   (1) SN_{40} Value   _____

   (2) $SN_{grad.}$ _____

   (3) Avg. Texture Depth _____

1. Artificial Illumination

    (1) None   _____

    (2) Tungsten   _____

    (3) Florescent   _____

    (4) Mercury Vapor   _____

    (5) Sodium Vapor   _____

    (6) Other_____   _____

PLAN VIEW ILLUSTRATIVE DRAWING OF SITE

F.2 SITE EVALUATION CHECKLIST

The Site Evaluation Checklist is divided into eight parts:

1. Ambience Factors

2. Geometric Factors

3. Traffic Barrier Factors

4. Illumination Factors

5. Roadway Maintenance Factors

6. Marking Factors

7. Unguarded Hazard Factors

8. Signing Factors

Most sections of the checklist are provided with two columns on the right-hand side which are labeled "Presence" and "Accident Causation Factor." These columns are to be coded as follows:

PRESENCE

0 - The item, even though present at the site, is not an accident-causation factor

1 - The item is most likely an accident-causation factor

— Accident-causation effect is unknown

In filling out the form, the "Accident-Causation Factor" column need only be filled in when there is a 1 in the

"Presence" column. Additionally, the "Accident-Causation Factor" column is placed at the extreme right to facilitate a rapid review of the checklist.

Under the topic labeled <u>Ambience Factors</u>, the "Presence" column is replaced by one labeled "Occurrence." The "Occurrence" column is to be coded as follows:

OCCURRENCE

1. Frequent   > 50 times/yr.

2. Occasional 10 - 50 times/yr.

3. Seldom   1 - 10 times/yr.

4. Almost Never < 1 time/yr.

Finally, under the topic of <u>Signing Factors</u>, a completely different format is employed. The coding key for this area is given as follows:

SIGNING KEY

MESSAGE TYPE

1. Permanent

2. Manually Variable

3. Automatically Variable

4. N/A

5. Other_____

ILLUMINATION

1. Unlighted

2. Externally Lighted

3. Luminescent Panels

4. Luminous Tube Message

5. Other_____

454

CONTENT, OR ARRANGEMENT

1. Sign Too Small

2. Sign Letters Too Small or Too Narrow

3. Sign Legend Components Confusing

4. Sign Too Wordy to be Read Quickly

5. Confusion Caused by Too Many Signs

6. Insufficient Differentiation Between Major and Minor Signs

7. N/Z

8. Other_____

VISIBILITY

1. Sign Down

2. Sign Frequently Obscured by Dirt, Snow, or Ice

3. Sign Obscured by Foliage

4. Sign Obscured by Roadside Structure

5. Sign Obscured by Other Sign

6. Sign Leaning - Difficult to Read

7. Sign Too Low - Difficult to Read

8. Sign Not Reflectorized

9. Sign Not Lit or Inadequately Lighted

10. Other_____

ADVANCE WARNING

1. Inadequate Advance Warning of Interchange Ahead

2. Inadequate Advance Warning of Curve Ahead

3. Inadequate Advance Warning of Bridge Ahead

4. Inadequate Advance Warning of Change from Divided to Undivided Highway

5. Inadequate Advance Warning of Change in Number of Lanes

6. Inadequate Advance Warning of Low Underpass or Tunnel Clearance

7. Inadequate Advance Warning of Steep Grade

8. Other_____

SITE EVALUATION CHECK LIST

Item	Occurrence	Accident Causation Relevance
I. AMBIENCE FACTORS		
A. Visibility Limitations		
1. Smoke		
2. Smog		
3. Natural Haze		
4. Dust Storms		
B. Wind and Wind Gusts		
1. > 50 mph		
2. 20-50 mph		
3. 0-20 mph		
C. Rain		
1. Drizzle ~0.01 in/hr		
2. Light Rain 0.04-0.20 in/hr		
3. Heavy Rain 0.60-0.80 in/hr		
4. Heavy Downpour 1.0 in/hr		
5. Very Heavy Storm 4.0 in/hr		
D. Other Precipitation		
1. Snow		
2. Sleet		
E. Sun		
1. Seasonal or Daily Direct Glare		
2. Seasonal or Daily Reflected Glare		

Item	Presence	Accident Causation Factor

II. GEOMETRIC FACTORS

    A.   Site Distance Limitations

        1. Hillcrest

        2. Blind Curve

        3. Combined Crest Curve

        4. Dip

        5. Embankments

        6. Piled Snow

        7. Guardrail

        8. Bridge Rail or Abutment

        9. Foliage

      10. Highway Sign

      11. Commercial Sign

      12. Building

      13. Fence

      14. Other_____

    B.   Interchange Design Deficiencies

        1. Inadequate Maneuvering Distance Between Successive Exits

        2. Inadequate Maneuvering Distance Between Entry and Exit Ramps

        3. Entry Lane Too Short for Safe Merging with Traffic

        4. Exit Lane Too Short Requiring Slow Down on Roadway

        5. Entry Ramp Curve Not Fitted to Roadway

        6. Exit Ramp Curve Not Fitted to Roadway

        7. Entry Ramp Grade Too Steep

        8. Exit Ramp Grade Too Steep

        9. View of Traffic From Entry Lane Inadequate

	Presence	Accident Causation Factor
Item		

10. Exit and Entry Ramps Too Narrow for Traffic Volume

11. Ramp Shoulders Too Narrow

12. Inadequate Warning Distance in Front of Interchange Such That Weaving Length is Too Short

13. Other_____

C. Curve/Grade Deficiencies

   1. Superelevation Inadequate

      a. Below AASHO recommended policy

      b. Water drainage inadequate in wet weather

      c. Inner and outer lanes superelevated at different rates

      d.

      e. Other_____

   2. Grade Excessive

   3. Sharp Curve at Bottom of Grade

   4. Sharp Curve at Top of Grade

   5. Approach Angle at Bridge, Tunnel, or Underpass Too Acute for Safe Turn

   6.

   7. Other_____

D. Cross-Section Deficiencies

   1. Inadequate Lane Width

   2. Shoulders Too Narrow for Emergency Use

   3. Median Geometry

      a. Visibility ahead obscured by elevated median

      b. Median too narrow to prevent cross-median accidents

      c. Median too narrow and too low to prevent headlight glare

Item	Presence	Accident Causation Factors

4. No Traffic Island Where Needed to Channelize Traffic

5. Curve Shoulders Not Superelevated

6. Lateral Clearance at Bridge Abutment Inadequate

7. Bridge, Tunnel, or Underpass Too Narrow

8. Shoulder Lower Than Pavement

9.

10. Other_____

III. TRAFFIC BARRIER FACTORS

A. Guardrail Deficiencies

1. Not Present Where Warranted

2. Present Where Not Warranted

3. Configuration Inadequate

    a. Too low

    b. Insufficient lateral strength

    c. Hazardous end treatment

    d. Too close to road edge

    e. Causes excessive passenger injury

    f. Causes excessive vehicle damage

    g. Causes large angle redirection back into traffic stream

    h. Causes wheel snagging

    i. Causes Pocketing

    j. Other_____

Item	Presence	Accident Causation Factor
B. Median Barrier Deficiencies		
1. Not Present Where Warranted		
2. Present Where Not Warranted		
3. Configuration Inadequate		
a. Too low		
b. Insufficient lateral strength		
c. Hazardous end treatment		
d. Too close to road edge		
e. Causes excessive passenger injury		
f. Causes excessive vehicle damage		
g. Causes large angle redirection back into traffic stream		
h. Causes wheel snagging		
i. Causes pocketing		
j. Other_____		
C. Bridge Rail Deficiencies		
1. Not Present Where Warranted		
2. Present Where Not Warranted		
3. Configuration Inadequate		
a. Too low		
b. Insufficient lateral strength		
c. Hazardous end treatment		
d. Too close to road edge		
e. Causes excessive passenger injury		
f. Causes excessive vehicle damage		
g. Causes large angle redirection back into traffic stream		
h. Causes wheel snagging		
i. Causes pocketing		
j. Other_____		

Item	Presence	Accident Causation Factor

D. Barrier Curb Inadequacies

    1. Not Present Where Warranted

    2. Present Where Not Warranted

    3. Configuration Inadequate

        a. Too low

        b. Too high

        c. Too close to road edge

        d. Encourages mounting rather than redirection

        e. Encourages spin-out

        f. Causes excessive vehicle damage

        g. Causes large angle redirection back into traffic stream

        h. Other_____

E. Impact Attenuator Deficiencies

    1. Not Present Where Warranted

    2. Present Where Not Warranted

    3. Configuration Inadequate

        a. Too short in length

        b. Too low in height

        c. Causes excessive passenger injury

        d. Causes excessive vehicle damage

        e. Inadequate side impact performance

        f.

        g. Other_____

Item	Presence	Accident Causation Factor

IV. ILLUMINATION FACTORS

    A.   Overhead Illumination Inadequate or Missing on High-Density Curve

    B.   Overhead Illumination Inadequate or Missing at Intersection or Interchange

    C.   Other_____

V. ROADWAY MAINTENANCE FACTORS

    A.   Surface Deficiencies
        1.   Smooth/Even
            a.   Slick/Polished
            b.   Oily/Greasy
            c.   Bleeding Patches
            d.   Abrasive
            e.   Other_____

        2.   Rough
            a.   Pot holes in surface
            b.   Bumps in surface
            c.   Map cracks
            d.   Eroded
            e.   Studded tire ruts
            f.   Lane joints open, rough, or uneven
            g.   Patched
            h.   Other_____

        3.   Loose Stones, Sand or Dirt on Surface

        4.   Other_____

Item

    B. Shoulder Deficiencies

        1. Shoulder Rough, Soft, Muddy, or Rutted

        2. Shoulder Poorly Aligned Due to Wear

        3. Other_____

VI. MARKING FACTORS

    A. Markings Inadequate

        1. Markings Insufficient to Warn of Approaching Interchange Exit

        2. Markings Insufficient to Warn of Approaching Interchange Entry Lane

        3. Inadequate Channeling of Traffic in Advance of Interchange

        4. Markings Not Reflectorized Where Needed

        5. Other_____

    B. Markings Omitted

        1. No Lane Markings

        2. No Nose or Funnel Markings at Exit or Entry Ramps

        3. No Pavement-Width Transition Markings Where Needed

        4. No Diagonal Markings to Warn of Approach to Fixed Obstruction

        5. No Diagonal Markings on Underpass Piers, Abutments, Culvert Headwalls, etc.

        6. No Road Edge Delineators

        7. No Object Markings on Curb or Island

        8. Other_____

    C. Markings Worn or Obscured

        1. Markings Worn Away

        2. Markings Frequently Covered by Snow, Ice or Mud

        3. Other_____

	Presence	Accident Causation Factor
Item		
VII. UNGUARDED HAZARD FACTORS		
A. Utility Poles		
B. Sign Poles		
C. Trees		
D. Buildings		
E. Fencing		
F. Embankments		
G. Ditches		
H. Median Piers		
I. Roadside Bridge Piers		
J. Culvert Abutments		
K. Other_____		

VIII. SIGNING FACTORS Sign No.	Illustrative Drawing	Message Type	Illumination	Content or Arrangement	Visibility	Advance Warning	Remarks	Accident Causation Factor
1								
2								
3								
4								
5								
6								
7								

466

APPENDIX G

RELATIONSHIP BETWEEN TIRE SHEAR FORCE AND TIRE CONDITION AND CONSTRUCTION FACTORS

A tire traction field is a comprehensive description of the shear force generated between tire and road over a wide range of operating conditions. The shear stresses generated in the tire footprint combine to produce a longitudinal force, F_{xw}, a lateral force, F_{yw}, and an aligning moment, M_{zw}. These forces and moments are functions of many operating variables. The most important variables are:

α' , lateral slip angle

s' , longitudinal slip

F_z , vertical load on the tire

V , translational velocity of the wheel

γ' , inclination (camber) angle of the wheel

(Note that the rates of change of some of these variables may be important in drastic vehicle maneuvers.)

Conceptually, it is convenient to symbolize the shear force vector as follows:

$$(F_{xw}, F_{yw}) = \vec{f}(\alpha', s', F_z, V, \gamma') \tag{G.1}$$

(Clearly, the aligning torque, M_z, is also a function of these same variables.) Equation (G.1), however, is not complete, in that the shear force is also highly dependent upon road surface factors, and tire construction and condition factors. On extending Equation (G.1) to contain parameters r_1 through r_m, representing the road (and its state of contamination), and parameters t_1 through t_n, representing tire construction and condition factors, the following expression is obtained:

$$(F_{xw}, \ F_{yw}) = f(\alpha', \ s', \ F_z, \ V, \ \vec{\gamma'}; \ r_1 \ldots r_m; \ t_1 \ldots t_n)$$

(G.2)

Tire traction research has identified some of the more important road surface parameters, viz,

- water depth
- macro-texture
- micro-texture
- type of construction material
- type of aggregate

Nevertheless, the research performed to date does not enable us to predict (quantitatively) the influence of the above parameters on the tire traction field generated by a particular tire. It follows that actual tire measurements, as collected on a road surface, are needed

468

to quantify tire shear force performance if one desires to predict the limit maneuvering behavior of a motor vehicle operating on that very same road surface.

The emphasis in this appendix centers upon the influence exercised by tire factors (which may change through use, lack of maintenance, or replacement) on motor vehicle performance. The major factors of interest are:

t_1 - shoulder wear

t_2 - tread wear

t_3 - construction (radial, bias, or bias belted)

t_4 - inflation pressure

t_5 - tread type (highway, snow, or studded snow)

The above "tire-in-use" factors are known to have a large influence on the tire traction field. To the degree that these factors are variable around the vehicle (side-to-side and front-to-rear) the maneuvering behavior of the vehicle is altered as these factors change. Thus, on a given road surface, R, the shear forces generated by a given tire, should be represented by the following functional relationship:

$$(F_{xw}, F_{yw}) = \vec{f}_R(\alpha', s', F_z, V, \gamma'; t_1 \ldots t_5) \qquad (G.3)$$

Recently, a number of mathematical models employing empirically determined parameters have been developed for describing the tire traction field ($\underline{39}$, $\underline{40}$, $\underline{41}$). Without exception, these models require that shear force measurements be made to determine traction parameters such as cornering stiffness, C_α, longitudinal stiffness, C_s, camber stiffness, C_γ, peak longitudinal shear force, peak lateral shear force, sliding friction, and the rate of change of friction with velocity. It appears that semi-empirical models can serve to describe the influence of tire-in-use factors t_1 through t_5 on the tire traction field by measuring the influence of the tire-in-use factors on the various traction parameters of the tire.

G.1 SHOULDER WEAR

A limited number of tire tests ($\underline{42}$, $\underline{43}$) have indicated that a small amount of shoulder wear can cause a significant increase in the peak lateral force that can be generated by pneumatic tires on dry surfaces. Figure G-1 shows test results that have been obtained with an L78-15 tire. These data were procured with the HSRI mobile tire tester, a device that serves to (1) provide, in a controlled fashion, a vertical load and slip angle to the tire such that it is worn in a manner analogous to the wear produced in vehicle testing and (2) gather side force data concurrent with the wearing process. The wear
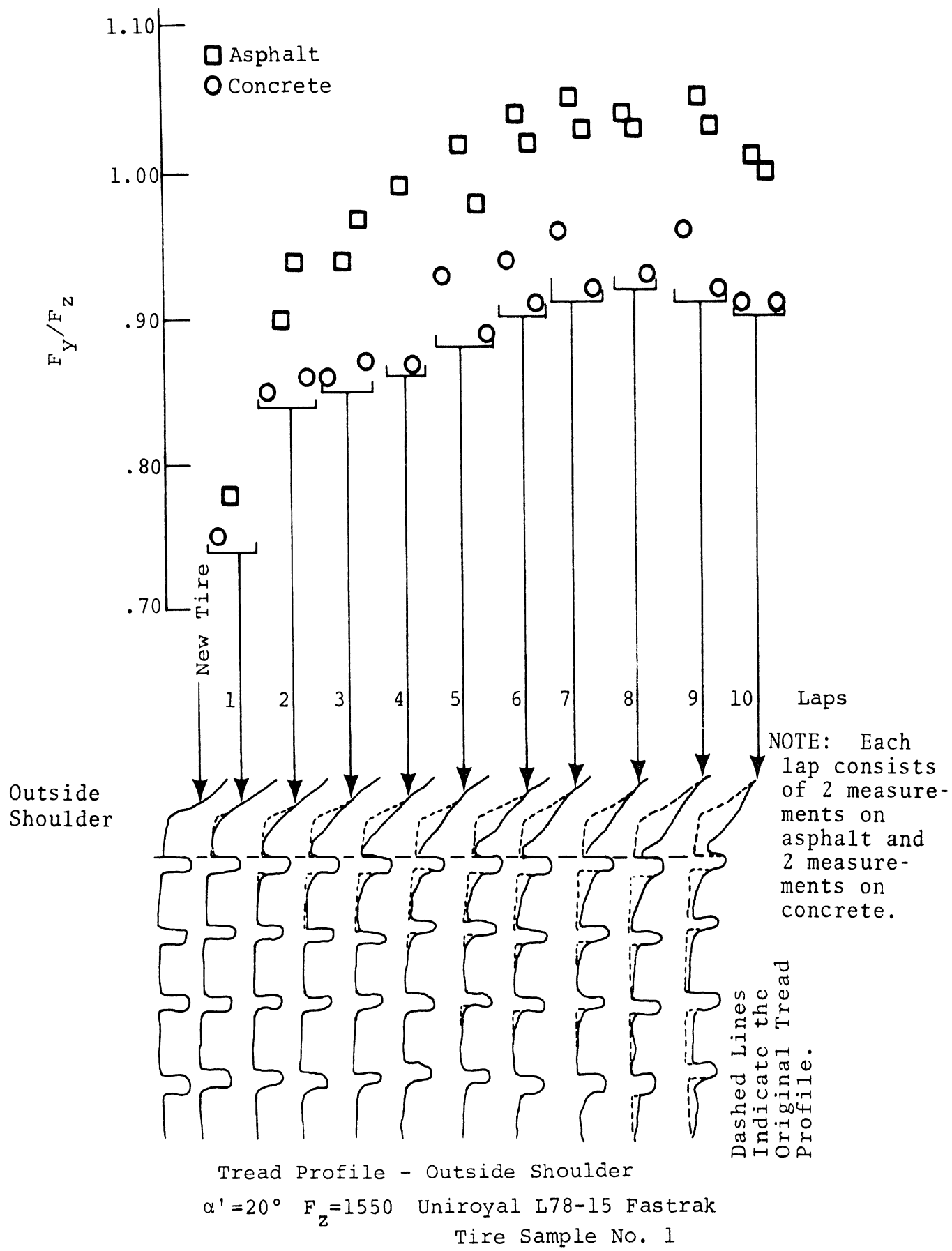
Figure G-1

471

pattern achieved at the end of a specified "lap," consisting of a test run across both asphalt and concrete surfaces, is displayed along the bottom of Figure G-1, and the average normalized lateral shear force obtained on each surface is plotted on the ordinate scale. Examination of this figure shows that a small amount of wear on the outside shoulder of the tire produces a dramatic increase in lateral force.

Similar results have been obtained for a number of tires (42), and data corraborating these shoulder wear findings have been obtained on flatbed tire test machines (43). For example, flatbed tests were made on tires which had 1/2 the tread artifically removed in two different patterns: (1) an 8-inch crown radius and (2) a 6-inch crown radius. The test results, obtained at 1200-lb. load and 20° slip angle, were as follows:

Tread Condition	Lateral Force, Lbs.
New tire (broken in)	1100
1/2 worn, 8" crown radius	1300
1/2 worn, 6" crown radius	1400

Note that the smaller radius crown is a profile analogous to that produced by shoulder wear.

It is clear that differential shoulder wear, front
and rear, as produced by emergency maneuvers and as fur-
ther influenced by the partial replacement of worn tires
can induce changes in the limit turning behavior of a
motor vehicle. For example, a "plow-out" response in a
J-turn maneuver may change to a "spin-out" response.

G.2   AVERAGE TREAD WEAR

Tire tests have shown that, in general, a decrease
in tread depth results in larger lateral forces being
produced on dry surfaces. However, the opposite is true
on wet surfaces. Clearly, tire-shear-force capability
on wet road surfaces is a critical safety item wherein
tread depth is very important. Figure G-2 shows the
influence of the state of tread wear on the peak braking
force obtained for three tire constructions (bias, belted
bias, and radial ply) (44). The influence of the type
of surface and the velocity of the test is also shown in
Figure G-2. These data show that the new tires produce
higher braking forces on wet surfaces than the worn tires.
The data also show that the velocity at which the test
is performed is a highly significant variable, particularly
on the concrete and jennite surfaces. (The asphalt sur-
face used in these tests had a coarse macrotexture. If,
however, tests had been performed on an asphalt surface
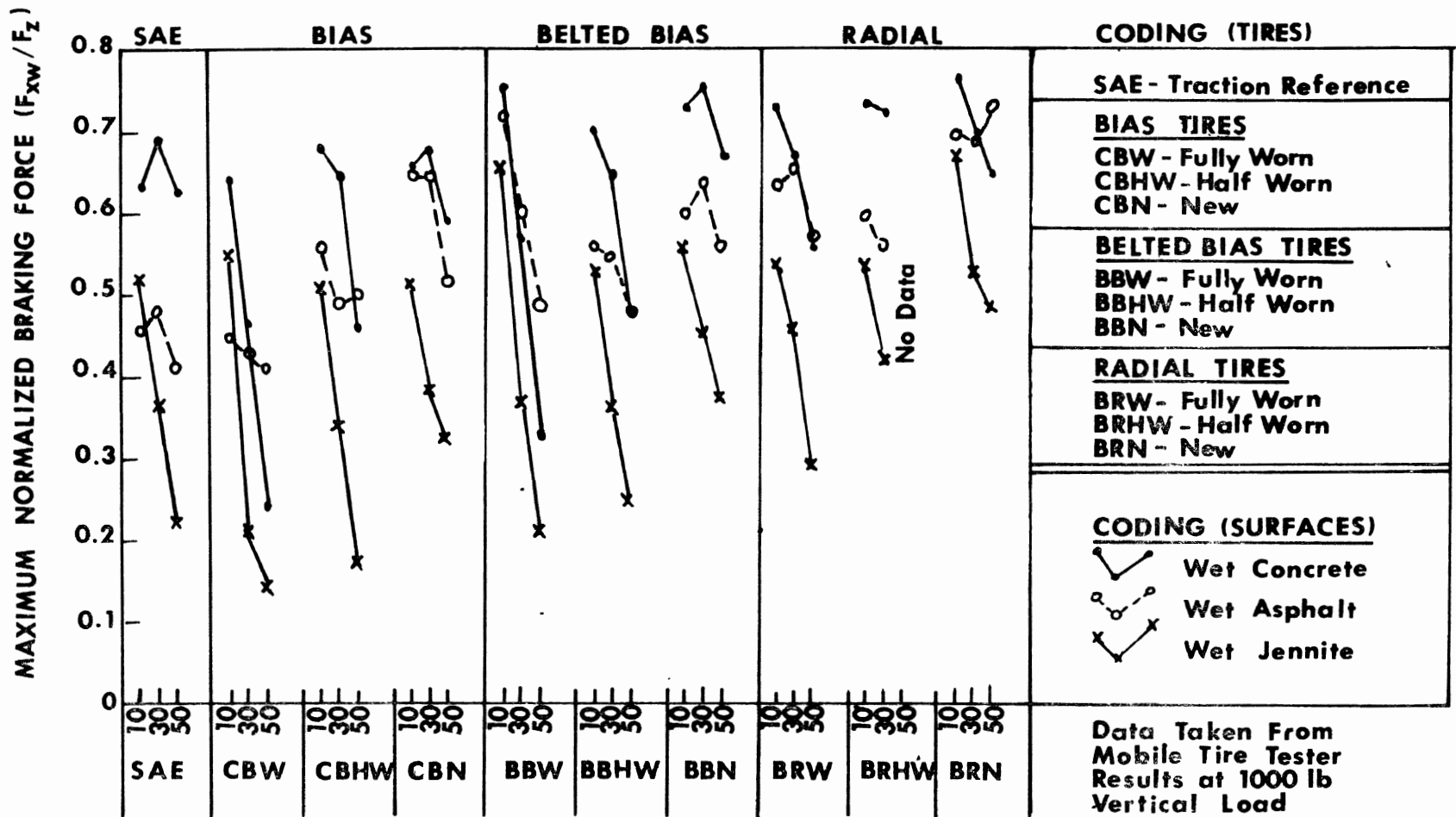with a smooth macrotexture, then, in all likelihood, the

Figure G-2. Influence of Tread Wear at 3 Velocities (10, 30, and 50 mph) on 3 Surfaces for 3 Types of Tire Construction

474

longitudinal force would have been highly dependent upon test velocity.)

Results similar to those presented in Figure G-2 have been obtained for both maximum lateral force and the 100% slip (locked-wheel) braking force (44). It was observed that tread wear causes little or no degradation in peak forces at low velocities (around 10 mph) on smooth wet surfaces with macrotexture, but that read wear causes losses in shear force performance to show up at 30 and 50 mph on all three surfaces.

G.3   BIAS, BIAS-BELTED, OR RADIAL CONSTRUCTION

The radial tire is generally stiffer than the bias or the bias-belted tire, in that radial tires usually have a higher cornering stiffness and a higher longitudinal (braking) stiffness. The belted-bias tire is usually stiffer than the bias ply tire. When the tires on one axle of a vehicle are changed from bias or belted-bias to radial tires, the normal driving performance of the vehicle can be noticeably changed if the radial tires have a much larger cornering stiffness than the original tires. (Of course, significant changes in front-to-rear cornering stiffness can also be caused by front-to-rear differences in inflation pressure or tread depth.) Much of the current interest in the tire mix problem stems from

the safety concerns of vehicle fleet managers and of average citizens who are thinking of replacing worn original equipment tires which longer-wearing radial tires. There is a need for guidance in this area.

The stiffness and the peak force capability of a tire is a function of other design variables besides carcass construction. For instance, it is possible that differences in tread compounding and tread pattern design can produce bias and/or bias-belted tires which have larger cornering stiffnesses and peak force capabilities than some radial tires. Thus, tire construction alone does not necessarily serve as an indicator of stiffness and peak shear force performance.

G.4   INFLATION PRESSURE

Studies of vehicles in use show that wide ranges of tire inflation pressure exist in practice (45). Since the shear-force performance of a tire is highly dependent upon inflation pressure, the directional maneuvering characteristics of a vehicle can be altered by using inflation pressures that depart from the recommended values. Specifically, reduced inflation pressures result in lower cornering stiffnesses and lower values of the peak lateral force at large slip angles. The latter

effect is demonstrated graphically in Figure G-3 where data are given for a conventional passenger car tire operated at a slip angle of 15 degrees. At 18 psi, the maximum lateral force is 1120 lbs., while, at 24 psi, the maximum lateral force is 1390 lbs. At 30 psi, the peak lateral force is more than 1575 lbs. Clearly, inflation pressure is the tire-in-use factor which has the most influence on the shear-force performance attained on dry road surfaces.

G.5   TREAD TYPE (HIGHWAY, SNOW, OR STUDDED SNOW)

The directional instability resulting (in part) from snow tires mounted on the rear axle of a station wagon has been reported in the literature (46). Among the other factors causing this behavior is the comparatively low cornering stiffness exhibited by some snow tires that possess a very deep open tread.

In a recent HSRI study (47) measurements were made to compare (a) the peak longitudinal force, (b) the locked-wheel longitudinal force, and (c) the lateral force produced at eight degrees of slip and for the same type of tire with a highway tread, a snow tread, and a studded snow tread. The measurements were made on a wet concrete surface. For this particular tire, it can be seen (see
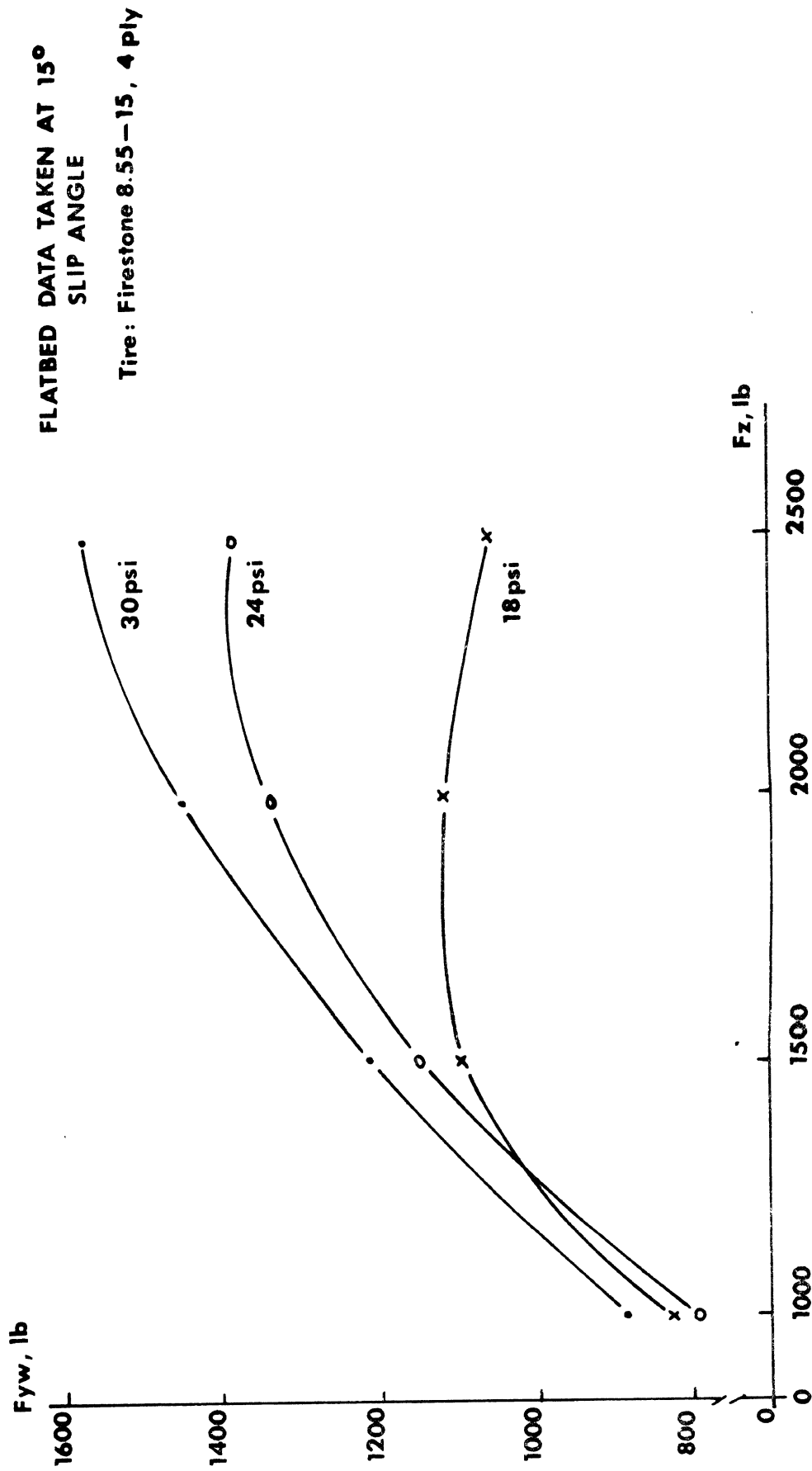
Figure G-3.   The Influence of Inflation Pressure on Maximum Lateral Force at 15° Slip Angle

Table G-1) that both the studded snow tire and the non-studded snow tire produce lower normalized peak forces than the tire with the highway tread.

TABLE G-1

COMPARISON* OF A STUDDED AND NON-STUDDED SNOW TIRE
AND A HIGHWAY TREAD TIRE ON WET CONCRETE
(Goodyear Polyglas G78-15)

	Maximum Longitudinal μ_{xp}	Locked Wheel Braking μ_{xs}	8° Slip Angle μ_{yp}
Studded Snow	.60 ± .01	.50 ± .01	.62 ± .01
Non-Studded Snow	.61 ± .02	.50 ± .01	.65 ± .02
Highway Tread	.70 ± .03	.51 ± .02	.70 ± .03

*Mobile tire tester data, water depth .02",
40 mph.

G.6   SUMMARY

In this Appendix, example shear force data have been presented to illustrate the influence of tire shoulder wear, tread wear, construction, tread type, and inflation pressure.

REFERENCES

1. McHenry, R.R. and DeLeys, N.J., Automobile Dyanmics
    - A Computer Simulation of Three-Dimensional Motions
    for Use in Studies of Braking Systems and of the
    Driving Task. Cornell Aeronautical Laboratory, Inc.,
    Report No. VJ-2251-V-7, Aug. 1970.

2. A Policy of Geometric Design of Rural Highways, The
    American Association of State Highway Officials, 1965.

3. A Policy on Design of Urban Highways and Arterial
    Streets, The American Association of State Highway
    and Transportation Officials, 1973.

4. Zuk, W., "Instability Analysis of a Vehicle Negotiating
    a Curve With Downgrade Superelevation," Paper presented
    at the Annual Meeting of the Highway Research Board,
    Washington, D.C., Jan. 1972.

5. Staughton, G.C. and Williams, T., Tyre Performance in
    Wet Surface Conditions, RRL Report LR 355, Road Research
    Laboratory, Crowthorne, England, 1970.

6. Galloway, B.M., Schiller, R.E., Jr., and Rose, J.D.,
    The Effects of Rainfall Intensity, Pavement Cross Slope,
    Surface Texture, and Drainage Length on Pavement Water
    Depths, Texas Transportation Institute, Research
    Report Number 138-5, May 1971.

7. Ross, N.F. and Russam, K., The Depth of Rain Water on
    Road Surfaces, Road Research Laboratory, RRL Report
    236, 1968.

8. Yeager, R.W., and Miller, J.D., Actual Water Depths
    on Roadways and Its Relationship to Tire Testing,
    Unpublished Report, Goodyear Tire & Rubber Co.,
    January 5, 1971.

9. Yeager, R.W., The Depth of Rain Water on Road Surfaces,
    Unpublished Report, The Goodyear Tire & Rubber Co.,
    Sept. 1971.

10. "Collision Diagram, Interstate Route 95 Interchange
    with Route 1", December 18, 1964 - March 31, 1968;
    April 1, 1968 - September 30, 1970; October 1, 1970
    - June 26, 1972.

11. "Standard Specification for Standard Tire for Pavement Tests", ASTM Designation: E249-66, American Society for Testing and Materials.

12. Fancher, P.S., Jr. and Segel, L., "Tire Traction Assessed by Shear Force and Vehicle Performance," Tire Science and Technology, Vol. 1, Number 4, (November 1973).

13. Manual on Uniform Traffic Control Devices for Streets and Highways, U.S. Department Transportation, 1971.

14. Shonfeld, R., "Photo-Interpretation of Skid Resistance," Highway Research Record 311, 1970.

15. "Plan and Profile - As Built Plans," Sta. 650+00 to Sta. 675+00; Sta. 675+00 to Sta. 700+00; Sta. 700+00 to Sta. 725+00, Ohio Turnpike Commission, July 9, 1953.

16. "Typical Roadway Sections," Ohio Turnpike Commission, September 26, 1952.

17. Letter from C. Radyk, Superintendent of Traffic and Safety, Ohio Trunpike Commission, to D.F. Dunlap, Highway Safety Research Institute, on August 14, 1973.

18. Informal memo from Mr. Fred E. Behn, Ohio Department of Transportation, September 25, 1973.

19. Tests 5530 and 5531 conducted by Ohio Department of Transportation, November 15, 1971.

20. Instructions for Using the Portable Skid-Resistance Tester, Road Note No. 27, Road Research Laboratory, 1960.

21. Giles, C.G., Sabey, B.E., and Cardew, K.H.F., "Development and Performance of the Portable Skid-Resistance Tester," Road Research Technical Paper No. 66, Road Research Laboratory, 1964, Also AST, Special Technical Publication No. 326, Symposium on Skid Resistance (1962), American Society for Testing and Materials.

22. Gallaway, B.M., Epps, J.A., and Tomita, H., Effects of Pavement Surface Characteristics and Textures on Skid Resistance, Texas Transportation Institute, Research Report 138-4, March, 1971.

23. Stocker, A. J., Gallaway, B.M., Ivey, D.L., Swift, G., and Darroch, J.G., *Frictional Characteristics of Automobile Tires*, Texas Transportation Institute, November, 1968.

24. Britton, S.C., A dissertation on the comparison of road surface friction measurement methods, Texas A & M University.

25. Lucas, J., "Measurement of Geometric Roughness and Drainage of Water from Road Surfaces," International Colloquium on the Interrelation of Skidding Resistance and Traffic Safety on Wet Roads, Berlin, June 1968.

26. Yeager, R.W., and Tuttle, J.L. "Testing and Analysis of Tire Hydroplaning," SAE Preprint 720471, Society of Automotive Engineers, May, 1972.

27. Horne, W.B., and Dreher, R.C., *Phenomena of Pneumatic Tire Hydroplaning*, NASA TN-D-2056. National Aeronautics and Space Administration, Langley Research Center. November, 1963.

28. Horne, W.B., and Joyner, U.T., "Pneumatic Tire Hydro-planing and Some Effects on Vehicle Performance". SAE-970C, 1965.

29. Gengenbach, W., "Experimental Investigation Into the Aquaplaning of Vehicle Tyres on Wet Roads." *Automobil-Industrie*, Vol. 12, No. 4, (November 1967), pp.74-79.

30. Besse, J., *Water Film Thickness Effects on the Friction Between Tire and Pavement*, NCHRP Project 1-12 (2), Pennsylvania State University, June 1972.

31. Bowman, W.D., "Generalizations on the Aerodynamic Characteristics of Sedan Type Automobile Bodies," SAE paper 660389, June, 1966.

32. Potthoff, J., "Drag and Lift of Modern Vehicles," *MIRA* Translation 40/71, November 1969.

33. Horne, W.B., "Tire Hydroplaning and Its Effects on Tire Traction," *Highway Research Record* 214, 1968.

34. Weller, D.E., and Maynard, D.P., *Treatments to Retexture a Worn Concrete Surface of a High-Speed Road*, RRL Report LR250, Road Research Laboratory, 1969.

35. Glennon, J.C., and Weaver, G.D., *The Relationship of Vehicle Paths to Highway Curve Design*, Texas Transportation Institute, Research Report 134-5, May 1971.

36. "Plan and Profile of Proposed State Highway," Sta.
     2162+00 to Sta. 2194+00; Sta. 2194+00 to 2226+00;
     2226 to 2240+00, Commonwealth of Virginia Department
     of Highways, January, 1959.

37. Letter from D.C. Mahone to D.F. Dunlap dated October 4,
     1973.

38. Cook, L.M. and Dancy, W.H., Jr., "Development and
     Fabrication of the Virginia Skid-Resistance Measurement
     Vehicle (Model 2)," Virginia Highway Research Council,
     October, 1970.

39. Dugoff, H., Fancher, P.S., Segel, L., Tire Performance
     Characteristics Affecting Vehicle Response to Steering
     and Braking Control Inputs, Final Report, National
     Bureau of Standards Contract CST-460, August 1969.

40. Sakai, H., "Theoretical Study of the Effect of Tractive
     and Braking Forces on Cornering Characteristics of
     Tires," Paper No. 4, JSAE Safety Tour in U.S.A.,
     October-November 1969.

41. Livingston, D., Brown, J., "Physics of the Slipping
     Wheel II. Slip Under Both Tractive and Lateral Forces,"
     presented to the Division of Rubber Chemistry, American
     Chemical Society, Buffalo, N.Y., October 14-17, 1969.

42. Ervin, R.D., Grote, P., Fancher, P.S., MacAdam, C.C.,
     Segel, L., Vehicle Handling Performance, Research
     Study, Vol. 1, Highway Safety Research Institute,
     The University of Michigan, November 1972.

43. Rasmussen, R.E., Cortese, A.D., The Effect of Certain
     Tire-Road Interface Parameters on Force and Moment
     Performance, General Motors Proving Ground Report A-
     2526, July, 1969.

44. Fancher, P.S., Segel, L., MacAdam, C., Pacejka, H.B.,
     Tire Traction Grading Procedures as Derived from the
     Maneuvering Characteristics of a Tire-Vehicle System,
     Final Report, Contract No. NBS-1-35715, DOT-HS-800
     813, September 1973.

45. Harvey, J.L., Brenner, F.C., "Tire Use Survey, the
     Physical Condition, Use and Performance of Passenger
     Car Tires in the United States of America," NBS
     Technical Note 528, May 1970.

46. Rice, R.S., Jr., Milliken, W.F., Jr., "The Effects of
     Loadings and Tire Characteristics on the Steering
     Behavior of an Automobile," First International
     Conference on Vehicle Mechanics, July 16-18, 1968.

47. Wild, R.E., _Wet Traction Test Program_, Final Report, Highway Safety Research Institue, The University of Michigan, February 1973.